DETERMINANTS OF SENSITIVITY TO BH3 MIMETICS IN DIFFUSE LARGE B-CELL LYMPHOMA

Thesis is submitted for the degree of

Doctor of Philosophy

at the University of Leicester

By

Victoria May Smith BSc

Molecular Cell Biology

College of Life Sciences

University of Leicester

February 2020

Abstract

Determinants of sensitivity to BH3 mimetics in diffuse large B-cell lymphoma

Victoria Smith

Diffuse large B-cell lymphoma (DLBCL) is an aggressive B-cell malignancy, with immuno-chemotherapy relapsed/refractory patients dying within months if left untreated. The inhibition of BCL2 by ABT-199 monotherapy has shown spectacular activity in chronic lymphocytic leukaemia (CLL). In contrast, ABT-199 monotherapy in DLBCL has been less successful despite high level expression of BCL2 in over 40% of cases. Thus, there is a requirement to identify biomarkers to allow the stratification of patients for sensitivity to BH3 mimetics.

The data presented here identifies subgroups of DLBCL which exhibited either specific BCL2/ $BCLX_L$/ MCL1 dependence, dual dependence or dependence on none of these proteins. Dependence could not be determined accurately *via* protein expression or using the functional assay BH3 profiling. However, anti-apoptotic protein dependence was associated with the direct sequestration of BAK, BAX and BIM.

Although primary resistance is a major barrier to overcome before the widespread use of BH3 mimetics in DLBCL is possible, acquired resistance will likely also become a significant problem. DLBCL cell lines with acquired resistance to BH3 mimetics have been developed to investigate mechanisms of resistance. RCK8 was uniquely sensitive to $BCLX_L$ inhibition by A1331852 and was sensitive to ABT-737.The derived resistant cell lines are over 4000 times more resistant to their respective mimetics. The resistant cell lines displayed an upregulation of BCL2 and interestingly RCK8-A133R became 40 times more sensitive to ABT-199, indicating a switch in dependence to BCL2. Conversely, RCK8-737R response to ABT-199 did not change. RIVA was remarkably sensitive to ABT-199 and ABT-737 and the derived resistant cell lines were over 1000 times resistant to their respective compounds. Despite an increase in $BCLX_L$ mRNA expression, the cell lines did not become more sensitive to either $BCLX_L$ or MCL1 inhibition, indicating that the cell lines have not become more functionally dependent on these proteins.

Acknowledgements

I would firstly like to thank my supervisors **Dr. Salvador Macip** and **Professor Martin Dyer** for providing me with the opportunity to undertake a PhD in their laboratories. Their invaluable knowledge and passion for research has stimulated thought-provoking discussions, leading to greater data analysis and inspired new experiments. Their support and guidance has been unwavering and they have almost convinced me that there are indeed 'no silly questions'.

I am also very grateful for the continued support and advice from **Dr. Meike Vogler** (Goethe-University, Germany) who provided the preliminary data and original proposal for this project. I am extremely delighted that she has since remained a close collaborator.

I would also like to thank all of the members of the MOCAA lab, past and present who have helped me throughout my studies and shared their expertise in the lab. Our cake filled lab meetings have allowed me to greatly improve my critical analysis of data. I would like to give special thanks to **Mrs Antonella Tabasso-Smith** and **Miss Marta Poblocka** with whom I have built great friendships that have been especially appreciated on days which were more stressful.

I would also like to acknowledge the members of the Dyer lab, past and present who have welcomed me to an extent that I feel as though I am part of their lab. Special recognition to **Dr. Sandrine Jayne** whose co-ordination of primary samples and the lab in general has been instrumental. I would also like to thank **Mr. Ross Jackson** whose help and discussions have led to greater understanding and interpretations of data. Special thanks to **Mr. Christopher Trethewey** and **Mr. Gethin Thomas** who have helped process patient samples, often at inconvenient times between their own experiments.

I am indebted to the patients who have donated samples that have been used in this thesis. I would also like to thank the clinical team at the Hope Clinical Trials facility.

Thank you to all of the friends and colleagues on the third floor of the Henry Wellcome building, of whom there are too many to mention but have all contributed to a fun work

environment. In particular I appreciate the coffee trips with **Gethin** and surprise chocolate from **Marta**. I would also like to give special thanks to **Ross** and **Antonella**, who started their PhDs at the same time as myself. Since then we have been on this journey together and our friendship has provided endless support and without whom the last three years would be unthinkable, thanks Sneks δ!

Finally I would like to thank my **parents** who have always supported me, had faith in me and made me believe I could do anything I wanted. Without whom I would not have the confidence, patience and determination to find out the answers I want to know… although maybe I would be quieter and a bit less stubborn, but where would be the fun in that!

Thank you.

Contents

List of Figures

List of Tables

Abbreviations

aa	Amino acid
ABC	Activated B-cell
AID	Activation-induced cytidine deaminase
AIF	Apoptosis inducing factor
AML	Acute myeloid leukeamia
APAF-1	Apoptotic protease activating factor-1
APS	Ammonium persulfate
ATP	Adenosine triphosphate
AUC	Area under the curve
BAK	BCL2 antagonist/ killer
BAX	BCL2 associated X
BCL2	B-cell lymphoma 2
BCL2A1	BCL2-related protein A1
BCL2L1	BCL2 like 1
$BCLX_L$	B-cell lymphoma-extra large
BCR	B- cell receptor
BFL1	BCL2 related gene expressed in foetal liver
BH	BCL2 homology
BID	BH3 interacting domain death agonist
BSA	Bovine serum albumin

BTK	Bruton's tyrosine kinase
C*. elegans*	Caenorhabditis elegans
CAD	Caspase-activated DNase
Cas9	CRISPR associated protein 9
CD	Cluster of differentiation
CDK	Cyclin dependent kinase
cDNA	Complimentary DNA
CHOP	Cyclophosphamide, doxorubicin, vincristine, prednisolone
CI	Combination index
CICD	Caspase independent cell death
CLL	Chronic lymphocytic leaukemia
CLPB	Caseinolytic peptidase B protein homolog
COO	Cell of origin
CR	Complete response
CRISPR	Clustered regularly interspaced short palindromic repeats
Ct	Cycle threshold
CTG	Cell titer glo
DHL	Double hit lymphomas
DISC	Death inducing signalling complex
DKO	Double knock out
DLBCL	Diffuse large B-cell lymphoma

DMSO	Dimethyl sulfoxide
DRP-1	Dynamin-related protein
DTT	Dithiothreitol
EBV	Epstein–Barr virus
EC_{50}	Half maximal effective concentration
EDTA	Ethylenediaminetetraacetic acid
EGTA	Ethylene glycol-bis(β-aminoethyl ether)-N,N,N′,N′-tetraacetic acid
EMA	European Medicines Agency
ER	Endoplasmic reticulum
ETC	Electron transport chain
F	Female
FACS	Fluorescence activated cell sorting
FBS	Foetal bovine serum
FCCP	Carbonyl cyanide-p-trifluoromethoxyphenylhydrazone
FDA	Food and drug administration
FISH	Fluorescence in situ hybridisation
FITC	Fluorescin isothiocyanate
FL	Follicular lymphoma
FSC	Forward scatter
GAPDH	Glyceraldehyde 3-phosphate dehydrogenase

GC	Germinal centre
GCB	Germinal centre like B-cell
G-CHOP	Obinutuzumab, clophosphamide, doxorubicin, vincristine, prednisolone
GEP	Gene expression profiling
HEPES	4-(2-hydroxyethyl)-1-piperazineethanesulfonic acid)
HGBL	High-grade B-cell lymphoma
HHT	Homoharrintone
IAP	Inhibitors of apoptosis
IBR	Ibrutinib
IC_{50}	The half maximal inhibitory concentration
Ig	Iimmunoglobulin
IgH	Immunoglobulin heavy chain
IgL	Immunoglobulin light chain
IHC	Immunohistochemistry
IL	Interleukin
IMM	Inner mitochondrial membrane
IMS	Inter membrane space
JAK	Janus kinase
Ki	Inhibitory constant
M	Male

MCL	Mantle cell lymphoma
MCL1	Myeloid cell leukaemia (sequence) 1
MEB	Mannitol experimental buffer
MEF	Mouse embryonic fibroblast
MiMOMP	Minority mitochondrial outer membrane permeabilisation
miR	Micro RNA
miRNA	Micro RNA
MM	Multiple myeloma
MOMP	Mitochondrial outer membrane permeabilisation
MZL	Marginal zone lymphoma
NCT	National clinical trial
NFκB	Nuclear factor kappaB
NMR	Nuclear magnetic resonance
ORR	Overall response rate
OS	Overall survival
P	Probablility
P/S	Penicillin and streptomycin
P1-4	Pocket 1-4
PB	Peripheral blood
PBMC	Peripheral blood mononuclear cell
PBS	Phosphate buffered saline

PBS-T	phosphate buffered saline with 0.05% Tween-20
PFS	Progression free survival
PI	Propidium iodide
PI3K	Phosphatidylinositol-3 kinase
PTM	Post-translational modification
R/R	Relapsed/ refractory
R-CHOP	Rituximab, clophosphamide, doxorubicin, vincristine, prednisolone
RIPK	Receptor interacting protein kinases
ROS	Reactive oxygen species
SD	Standard deviation
SDS-PAGE	Sodium dodecyl sulphate polyacrylamide gel electrophoresis
siRNA	Small interferring RNA
SPR	Surface plasma resonance
SSC	Side scatter
STAT	Signal transducer and activator of transcription
tBID	Truncated BH3 interacting domain death agonist
TEMED	Tetramethylethylenediamine
TG	Thioglycerol
THL	Triple hit lymphomas
TLS	Tumour lysis syndrome

TM	Transmembrane
TNF	Tumour necrosis factor related apoptosis inducing ligand
TPM	Transcripts per million
v/v	Volume per volume ratio
VDAC	voltage dependent anion channel
VDJ	Variable Diversity Joining
w/v	Weight per volume ratio
WHO	World Health Organisation
WM	Waldenstrom's Macroglobulinemia
WT	Wildtype
Δψm	Loss of mitochondrial membrane potential

1 Introduction

1.1 B-cell development

Bone marrow derived lymphocytes (B-cells) are a type of white blood cell which secrete and present antibodies on their cell surface as part of the adaptive immune response (LeBien and Tedder 2008, Pieper*, et al* 2013). Perturbation in B-cell development and function can lead to autoimmunity, malignancy, and immunodeficiency (LeBien and Tedder 2008, Pieper*, et al* 2013). B-cells have several differentiation stages characterised by the structure of the B-cell receptor (BCR) and expression of cluster of differentiation (CD) markers (Kuppers 2005, Pieper*, et al* 2013). Arising from a haematopoietic stem cell in the bone marrow which develop in secondary lymphoid tissues such as lymph nodes they become terminally differentiated plasma or memory cells (Figure 1-1).

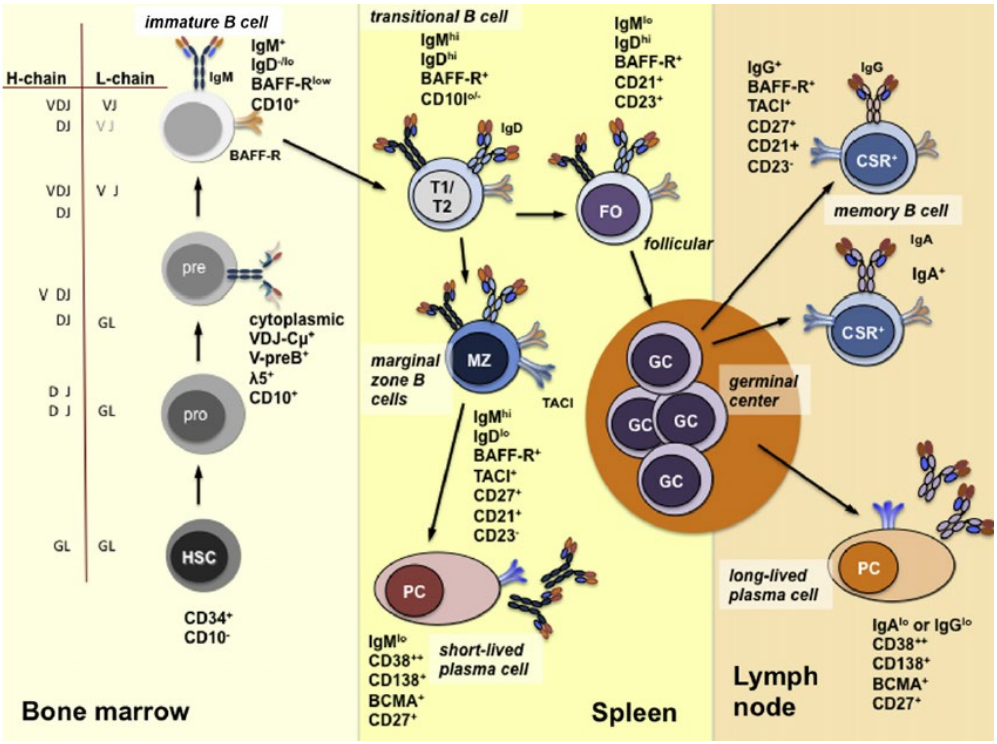

Figure 1-1 B-cell development.
Different developmental stages of a B-cell can be characterised by BCR expression and CD expression. B-cells originate in the bone marrow from haematopoietic stem cells and undergo rearrangements of the Ig gene. They mature within germinal centres of secondary lymphoid organs such as the spleen and lymph nodes where they undergo clonal expansion and hyper somatic mutations of the BCR. Activation of B cells induces AID and other components of the SHM/class-switch machinery, thus changing the affinity of the BCR and the isotype (IgM to IgG, IgA, or IgE). Finally, they differentiate into long-lived memory B-cells or plasma cells. (Taken from Pieper*, et al* 2013).

Early development is reliant on combinational rearrangements of the immunoglobulin (Ig) gene segments which encode the BCR. Within the variable region, the variable (V), diversity (D) and joining (J) segments of the heavy chain (IgH) and the V and J segments of the light chain (IgL) rearrange in two distinct stages, identifying three developmental stages of a B-cell (Pieper*, et al* 2013, Tonegawa 1987) (see Figure 1-2). These differential rearrangements (known as VDJ recombination) give rise to a large range of BCR which recognise a variety of antigens (LeBien and Tedder 2008). Cells which express a functional (and non-autoreactive) BCR migrate to secondary lymphoid tissues where they establish germinal centres (GC) and differentiate into naïve, follicular or marginal zone B-cells (Pieper*, et al* 2013). Antigen-activation of cells results in clonal expansion, class switching (replacement of IgH constant region with a one of another Ig) and somatic hypermutation of the rearranged Ig variable mediated by the protein activation-induced cytidine deaminase (AID) (Muramatsu*, et al* 2000). Cells with a BCR

that have an increased affinity for its antigen are selected for which differentiate into memory B-cells or plasma cells and leave the GC.

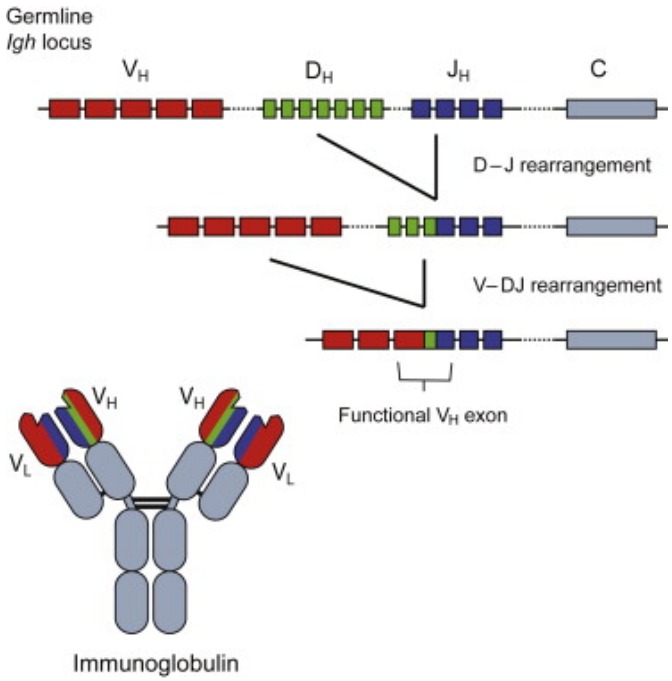

Figure 1-2 Remodelling of Ig during B-cell development
Variable Ig regions of rearrange in a process known as VDJ recombination. Within the IgH locus, one D gene sement is joined to one J gene segment, this DJ segment is then joined to a V gene segment resulting in VDJ recombined Ig variable exon. VJ recombination also occurs in IgL (not shown) (Taken from Little*, et al* 2015).

1.2 B-cell malignancies and lymphomagenesis

B-cell malignancies arise from genetic alterations which block B-cell development. Hence, each B-cell malignancy has a distinct phenotype which reflects the subclone from which it originates (Greaves 1986) (Figure 1-3). The malignant cell phenotype is known as the cell of origin (COO). Subtypes have been further characterised using gene-expression profiling (Alizadeh*, et al* 2000).

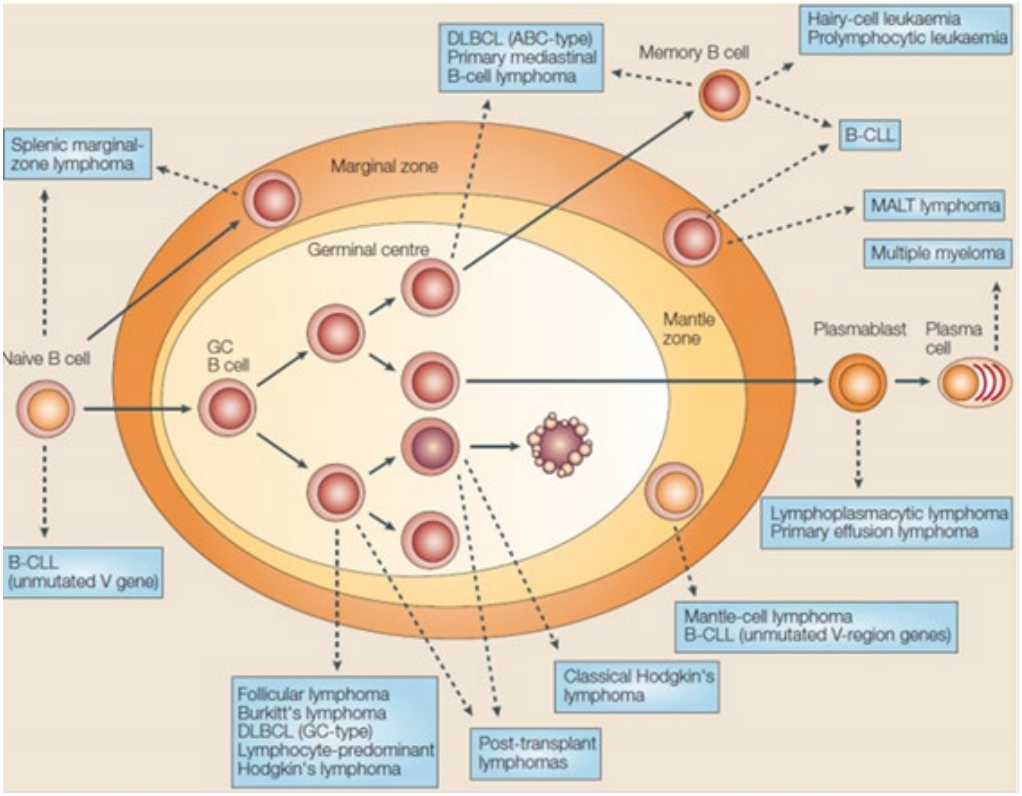

Figure 1-3 B-cell pathogenesis.
The cell of origin for each B-cell malignancy can be related to the phenotype of the cell at which the differentiation block occurs. Most malignancies derive from the GC or later subclones. Solid arrows denote B-cell differentiation steps and broken arrows assign the various lymphomas to their proposed normal counterpart. **(Taken from Kuppers 2005)**.

Chromosomal translocations involving one of the Ig gene and an oncogene are common in B-cell malignancies and understood to be a key transforming event (Kuppers 2005). It is therefore unsurprising that most B-cell malignancies derive from GC B-cells or later differentiation stages as this is the site of class switching and somatic hypermutations, two events which could result in chromosomal translocations. Somatic hypermutations have also been shown to promote tumorigenesis by mutating proto-oncogenes (Pasqualucci*, et al* 1998, Pasqualucci*, et al* 2001). The locus of BCL6 where most chromosomal-translocation breakpoints occur is the same region which is targeted by hypermutations (Pasqualucci*, et al* 2001). This indicates that as well as introducing mutations, the hypermutations could be favouring translocations.

As well as chromosomal translocations, signalling pathways are also deregulated to sustain growth. This includes loss of function mutations/deletions in tumour suppressor genes such as TP53 and gain of function mutations which activate oncogenic pathways such as the NFκB or phosphatidylinositol-3 kinase (PI3K) pathways. Viruses such as the

Epstein–Barr virus (EBV) have also been linked to the transformation of B-cells (Kuppers 2005).

1.3 Diffuse large B-cell Lymphoma

The most common form of non-Hodgkin lymphoma in adults is diffuse large B-cell lymphoma (DLBCL), with approximately 4,800 new diagnoses every year in the UK (Lymphoma Association 2017) and accounting for approximately 40% of cases globally (Horvat*, et al* 2018), with a median age of presentation at 60 years old (Beham-Schmid 2017, Horvat*, et al* 2018). This heterogeneous, mature B-cell neoplasm contains nuclei with an increased diameter more than two-fold compared to normal B-cells (Raut and Chakrabarti 2014).

1.3.1 Classification

DLBCL can be characterised by its COO. The 2008 World Health Organisation (WHO) classification recognised three groups: germinal centre like B-cell (GCB), activated B-cell (ABC), and unclassifiable, which could not be put into either category (Swerdlow*, et al* 2016). These molecular categories are based on gene expression profiles and they differ in chromosomal alterations, signalling pathways and clinical outcome (Beham-Schmid 2017, Swerdlow*, et al* 2016). These classifications are best identified by gene expression profiling (GEP) (Alizadeh*, et al* 2000, Lenz*, et al* 2008). As GEP is not widely used, a panel of antibodies are used in an immunohistochemistry assay based on the Han's algorithm to define GCB and non-GCB subgroups (Swerdlow*, et al* 2016). Nonetheless, this surrogate analysis is limited and cannot always reliably and reproducibly correlate to the molecular COO (Swerdlow*, et al* 2016). Due to the poorer outcomes associated with ABC DLBCL and the increased knowledge of the group's differential pathogenesis (Lenz*, et al* 2008), the revised WHO classification 2016 requires COO identification (Beham-Schmid 2017, Swerdlow*, et al* 2016). As the limitations of GEP still exist and is not a routine clinical test, classification via immunohistochemistry algorithms are accepted but their shortfalls are recognised (Beham-Schmid 2017, Swerdlow*, et al* 2016). Recently, several groups have used exome and transcriptome sequencing, DNA copy number analysis, structural variants and targeted amplicon resequencing to define new

genetic subgroups of the disease (Chapuy*, et al* 2018, Schmitz*, et al* 2018). These independent studies observed similar findings. Although these are yet to be used clinically, it is hoped that the identification of distinct mutational signatures could lead to improved classification and better treatment and outcomes.

1.3.2 COO gene expression

As mentioned, GEP can classify DLBCL into subgroups: GCB and ABC. An overview of the distinct molecular features of these subgroups are summarised in Figure 1-4. Patients with GCB DLBCL express genes which define the germinal centre B-cell signature such as cell surface markers CD10 and CD387 and DNA repair protein 8-oxoguanine DNA glycosylase (Alizadeh*, et al* 2000). Higher expression levels of transcription repressor BCL6 and MYC is also associated to the GCB subtype (Alizadeh*, et al* 2000, Lenz*, et al* 2008, Shaffer*, et al* 2012). Deletion of the tumour suppressor *PTEN* and amplifications of the micro RNA cluster miR17–92 microRNA is also detected more frequently in GCB DLBCL. This amplicon has been found to cooperate with MYC and reduce apoptosis (Lenz*, et al* 2008). The t(14;18)(q32;q21) translocation between anti-apoptotic protein, B-cell lymphoma 2 (BCL2) and Ig heavy chain is more prevalent within the GCB subgroup (Lenz*, et al* 2008).

Conversely, the ABC subgroup has elevated expression levels of genes which can also be found in post-germinal, peripheral blood B-cells which are activated *in vitro,* indicating an activated BCR phenotype (Alizadeh*, et al* 2000). These genes include FOXP1, IRF4, FLIP, CARD11 and BCL2 (Alizadeh*, et al* 2000, Lenz*, et al* 2008). ABCs can be further characterized by single or double loss of the *INK4A/ARF* locus (Lenz*, et al* 2008). Although their distinct molecular signatures can define each subgroup, gene expression heterogeneity still exists within the subgroups.

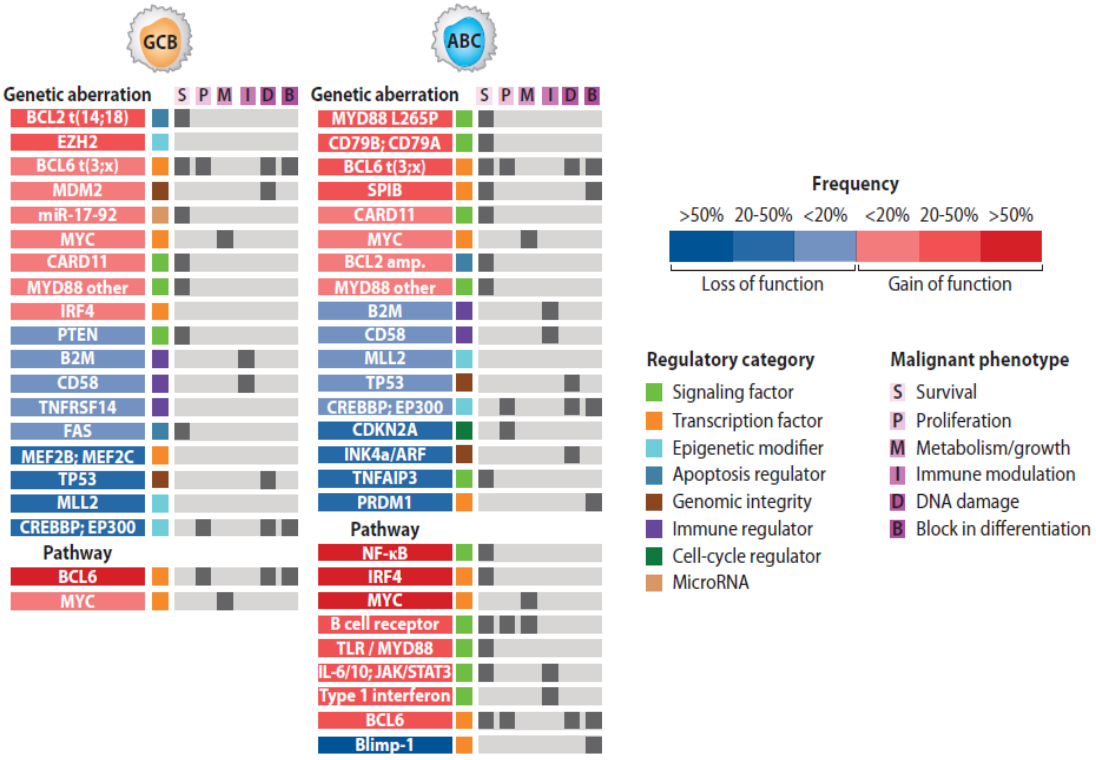

Figure 1-4 Molecular characteristics of GCB and ABC DLBCL.
Genetic aberrations and deregulated pathways/ genes critical for survival are coloured based on frequency and gain of function (red) or loss of function (blue) phenotypes. The role of each aberration is indicated. The regulatory category and malignant phenotype is also show. **(Adapted from Shaffer, *et al* 2012)**

Perhaps the most prominent difference between subgroups is the constitutive nuclear factor kappa B (NFκB) activity within the ABC group. GEP revealed increased expression rates of NFκB transcription factors for ABC which was consistent with a higher NFκB DNA binding activity (Davis, *et al* 2001). Furthermore, anti-apoptotic proteins BCL2, B-cell lymphoma-extra-large ($BCLX_L$) and BCL2 Related Protein A1 (BCL2A1) are downstream targets of the NFκB pathway which will also contribute toward cell survival. Multiple studies targeting the NFκB pathway using shRNA, small molecule inhibitors or retroviral transduction with dominant negative forms of IKKβ have identified the pathway as essential for the survival of ABC but not GCB-cells (Davis, *et al* 2001, Lam, *et al* 2005, Ngo, *et al* 2006). It has also been shown that the NFκB pathway induces the expression of interleukin (IL)-6 and IL-10 in ABC cells which leads to high levels of phosphorylated signal transducer and activator of transcription (STAT) 3 protein (Lam, *et al* 2008). A small molecule inhibitor of Janus kinase signaling was found to be toxic to ABC cells and synergized with inhibitors of the NFκB pathway (Lam, *et al* 2008).

These cellular subgroups also have different mechanisms of BCR signaling. BCR signaling is essential for mature B-cell survival (Kraus*, et al* 2004, Lam*, et al* 1997). This pathway is initiated by BCR aggregation, followed by phosphorylation cascade by Src-family kinases. This pathway results in the activation of other pathways: NFκB, Pi3K, MAP kinase and RAS. GCB-cells, like other mature, unstimulated B-cells, have been found to have "tonic" BCR signaling. This is independent of antigen activation but requires the PI3K pathway (Srinivasan*, et al* 2009). In contrast, ABC DLBCL signals via a chronically active BCR (Davis*, et al* 2010). This chronic activity explains the constitutively active NFκB pathway in this cell type as described above. This can be caused by activating mutations of proteins downstream of the BCR such as CD79a/b (Davis*, et al* 2010). An RNA interference screen identified a dependence on Bruton's tyrosine kinase (BTK) in ABC cells but not GCB-cells (Davis*, et al* 2010). BTK activates the NFκB pathway downstream of CD79a/b (Bajpai*, et al* 2000). Furthermore, BTK inhibitors have shown efficacy against ABC cell lines and ABC DLBCL patients (Davis*, et al* 2010, Wilson*, et al* 2015). GCB and ABC display distinct pathways to survive highlighting potential therapeutic targets.

1.3.3 Double hit and double expressor lymphomas

Double hit lymphomas (DHL) are fast progressing malignancies with poor prognosis, defined by two chromosomal translocations affecting MYC (8q24), BCL6 (3q27) and/or BCL2 (18q21) (Drexler*, et al* 2016). Triple hit lymphomas (THL) involving all three genes have also rarely been described (Drexler*, et al* 2016). These translocations typically juxtapose MYC or BCL2 with the promoter of IG heavy or light chain, however other partners have also been described (Drexler*, et al* 2016). At present, it is not known how to best treat patients with these translocations but the 2016 WHO classification recognises them as high-grade B-cell lymphoma (HGBL) (Beham-Schmid 2017, Swerdlow*, et al* 2016). Paradoxically, these double-hits are normally within the GCB COO which typically have better outcomes than ABC (Beham-Schmid 2017).

DHL and THL are detected by cytogenetic karyotyping and/ or fluorescence in situ hybridization (Drexler*, et al* 2016). It is not to be confused with double expressor lymphomas which is characterised immunohistochemically (Drexler*, et al* 2016). Double

expressor lymphomas overexpress MYC (present in over 40% blasts) and BCL2 (30-70%) independent of chromosomal translocations (Beham-Schmid 2017, Drexler*, et al* 2016, Swerdlow*, et al* 2016). Up to 25% of DLBCL cases are double expressors (Beham-Schmid 2017). The co-expression of MYC and BCL2 can be indicative of a poor prognosis however they are not as aggressive as HGBL (Swerdlow*, et al* 2016).

1.3.4 Current treatment of DLBCL

50-60% of patients are cured with R-CHOP immuno-chemotherapy (cyclophosphamide, vincristine, doxorubicin, prednisone and humanized monoclonal antibody directed at B-cell marker CD20, rituximab) (Raut and Chakrabarti 2014), although this is not without undesirable side effects, such as alopecia, fatigue, nausea and neutropenia. One study found an overall 10-year progression free survival (PFS) of 72% with a 10-year overall survival (OS) of 51% (Horvat*, et al* 2018). Worse outcomes are associated to the ABC subgroup of the disease, which could be caused by chemo-resistance due to constitutive NFκB signalling and consequential upregulation of anti-apoptotic proteins (Knittel*, et al* 2016).

New therapeutic strategies are required for patients who fail to remit with R-CHOP (10%) or who relapse within 2 years of initial therapy (30-40%) (Raut and Chakrabarti 2014). If those who relapse are chemo-sensitive, the patient undergoes high-dose chemotherapy followed by autologous stem cell transplantation (Raut and Chakrabarti 2014). If left untreated, patients with relapsed/refractory DLBCL have an average survival of 3-4 months (Pfreundschuh*, et al* 2006). This has led to a number of small molecule inhibitors being developed, targeting the deregulated pathways mentioned, for the improved treatment of DLBCL.

1.4 Cell death

Cell death is controlled by multiple highly regulated processes that are essential for multicellular organism survival. It is vital for tissue sculpting such as embryonic digit formation, the development of the immune system and the removal of cells which are damaged beyond repair. The best studied and evolutionarily conserved form of cell death is apoptosis. However, multiple other mechanism exist. Some viruses encode

apoptosis inhibitors (Smith*, et al* 2013), hence it has been suggested that other mechanisms have evolved to initiate cell death when apoptosis is not possible. Interplay exists between the different processes due to the existence of mutual mediators.

Too much or too little cell death has been linked to diseases such as auto-immunity, neurodegenerative diseases and cancer. The resistance of cell death is a key hallmark of cancer which is achieved via deletions of *TP53*, which is a sensor of DNA damage, and the deregulation of apoptotic proteins (Hanahan and Weinberg 2000, Hanahan and Weinberg 2011). The evasion of cell death and apoptosis is a likely a major contributor towards chemo-therapy resistance.

1.4.1 Necrosis and necroptosis

An un-programmed form of cell death which is likely the least regulated is necrosis. Caused by external stimulants such as infection, the cells swell and lose plasma membrane integrity, releasing the cellular contents into the extracellular space causing an inflammatory response (Proskuryakov*, et al* 2003). Necroptosis shares morphological likeness to necrosis however it is much more regulated. Extracellular cell death receptors such as tumour necrosis factor receptor (TNFR) and Fas initiate the pathway by indirectly activating receptor interacting protein kinases (RIPK) 1 and 3 (Tait*, et al* 2014). The mechanism by which these proteins initiate necroptosis remains elusive. During necroptosis, RIPK3 have been found to translocate to the mitochondria (Chen*, et al* 2013) before mitochondrial fission (Wang*, et al* 2012) and an increase in reactive oxygen species (ROS) (Zhang*, et al* 2009). However necroptosis still occurs in the presence of ROS scavenger or mitochondria depleted cells, indicating this is a mitochondria independent process (Tait*, et al* 2014, Tait*, et al* 2013). As with necrosis, necroptosis induces an inflammatory response which reportedly promotes tumour development and metastasis. Paradoxically, studies have also found that necroptotic cells in a tumour environment can enhance the immune response (Snyder*, et al* 2019). Ergo, inducing necroptosis during immunotherapy such as rituximab could improve outcomes.

1.4.2 Autophagic cell death

Autophagy is a process of recycling cellular macromolecules via a mediator protein (Beclin-1) allowing development under stress conditions such as starvation (Tait*, et al* 2014). As autophagy can be caused by cellular stress, before undergoing cell death some cells utilise this process to prolong survival. Despite this preceding event, autophagy is not the cause of cell death. This point notwithstanding, it has been reported that some forms of cell death are autophagy dependent (Lamy*, et al* 2013). Autophagy can lead to an increase in ROS due to the degradation of ROS scavengers (Yu*, et al* 2006). Autophagic cell death typically only occurs when there is a block in the apoptotic pathway such as BCL2 homologous antagonist/killer/ BCL2-associated X protein (BAK/BAX) deficiency (Shimizu*, et al* 2004) or inhibition of caspase 8 or 10 (Lamy*, et al* 2013, Yu*, et al* 2004).

1.4.3 Pyrotopsis

Pyrotopsis is an inflammatory caspase dependent form of cell death. However, unlike caspase dependent apoptosis, it is mitochondrial independent and does not result in the subsequent cascade of caspase cleavage (Bergsbaken*, et al* 2009). Caused by microbial infection, pyroptosis is characterised by ion influx, cell swelling and osmotic lysis which is dependent on caspase 1 and 11 (Bergsbaken*, et al* 2009, Miao*, et al* 2010). The complete mechanism of pyroptosis, such as caspase 1 substrates, remains unclear.

1.4.4 Ferroptosis

Ferroptosis is a recently described form of cell death characterised by reduced mitochondria volume, the loss of mitochondrial cristae and outer mitochondrial membrane rupture (Dixon*, et al* 2012). Ferroptosis induces iron dependent upregulation of ROS (Dixon*, et al* 2012) resulting in the loss of plasma membrane integrity due to membrane lipid peroxidation (Mou*, et al* 2019).

1.4.5 Parthanatos

Parthanatos is a mitochondrially dependent yet caspase independent form of cell death (Fatokun*, et al* 2014). Over-activation of PARP-1, accumulation of PAR polymer and

nuclear AIF translocation (the latter typically occurring in intrinsic apoptosis) causes large scale DNA fragmentation and cell death (Fatokun*, et al* 2014). This process is unaffected by caspase inhibitors (Yu*, et al* 2002) and does not form apoptotic bodies (Fatokun*, et al* 2014) identifying it as a distinct form of cell death.

1.4.6 Caspase independent cell death

Intracellular stress signals can induce mitochondrial outer membrane permeabilisation (MOMP) resulting in the release of cytochrome C and a caspase cleavage cascade (see 1.4.7.2 Intrinsic apoptosis). Inhibition of caspases post MOMP frequently result in cell death hence MOMP is understood to be the 'point of no return' in terms of cell death. Nonetheless sub-lethal apoptotic stress can engage caspases without cell death in a process termed minority MOMP (miMOMP) (Ichim*, et al* 2015). The limited caspase activity caused by miMOMP can lead to DNA damage, genomic instability and subsequent transformation (Ichim*, et al* 2015). An activation of the NFκB and STAT3 pathways due to ATM activation in response to DNA damage could also drive tumorigenesis (Liu*, et al* 2017). Moreover, several studies have found a potential oncogenic role of apoptosis as apoptotic cells can secret mitogens and promote surrounding cells to proliferate (Chaurio*, et al* 2013, Huh*, et al* 2004, Li*, et al* 2010, Ryoo*, et al* 2004).

These effects are caspase dependent, whereas caspase independent cell death (CICD) can occur post MOMP and has been suggested as an attractive anti-cancer treatment (Giampazolias*, et al* 2017, Roumane*, et al* 2018). Death receptor-induced CICD (usually resulting in extrinsic apoptosis via caspase 8 cleavage) has been found to occur via a necroptosis-like mechanism (Giampazolias*, et al* 2017). Notwithstanding, another mode of CICD which is dependent on MOMP (likened to intrinsic apoptosis) has been described, which is independent of necroptosis (Giampazolias*, et al* 2017). MOMP-dependent CICD produces several inflammatory cytokines leading to immune infiltration (unlike apoptosis which is immunologically silent) (Giampazolias*, et al* 2017, Roumane*, et al* 2018). It has been suggested that under apoptotic conditions, caspases inactivate NFκB signalling, preventing the trigger of the immune response (Giampazolias*, et al* 2017). Alternatively, apoptosis is a much more rapid form of cell

death which may not allow the time for cytokine production. One study tested the anti-tumorigenic benefit of apoptosis vs CICD in mice models (Giampazolias*, et al* 2017). Tumours which were targeted by CICD saw an increase in pro-inflammatory cytokines, an increase in T-cell infiltration and subsequent greater reduction in tumour regression (Giampazolias*, et al* 2017).

1.4.7 Apoptosis

As mentioned, apoptosis is the most evolutionary conserved form of cell death, initially characterised by its morphological features, such as membrane blebbing, nuclear condensation, DNA fragmentation, phosphatidylserine exposure and the formation of apoptotic bodies, which are then degraded (Kerr*, et al* 1972, Wyllie*, et al* 1980). Apoptosis can be initiated via extracellular ligands (extrinsic apoptosis) or internal signals (intrinsic apoptosis). Both converge upon the cleavage of caspase 3 (see figure 1-4). Genetic analysis of the nematode, Caenorhabditis elegans (C. *elegans)* identified *ced-3* and *ced-9* as positive and negative regulators of apoptosis respectively (Ellis and Horvitz 1986, Hengartner*, et al* 1992). Homologues of these have been identified in higher eukaryotes, which interact in much more complex pathways due to divergent evolution leading to multiple proteins with similar functions (Hengartner and Horvitz 1994, Strasser and Vaux 2018, Yuan*, et al* 1993). The mammalian homologue of ced-9 is anti-apoptotic protein BCL2, which is discussed below in further detail (1.5 The BCL2 family).

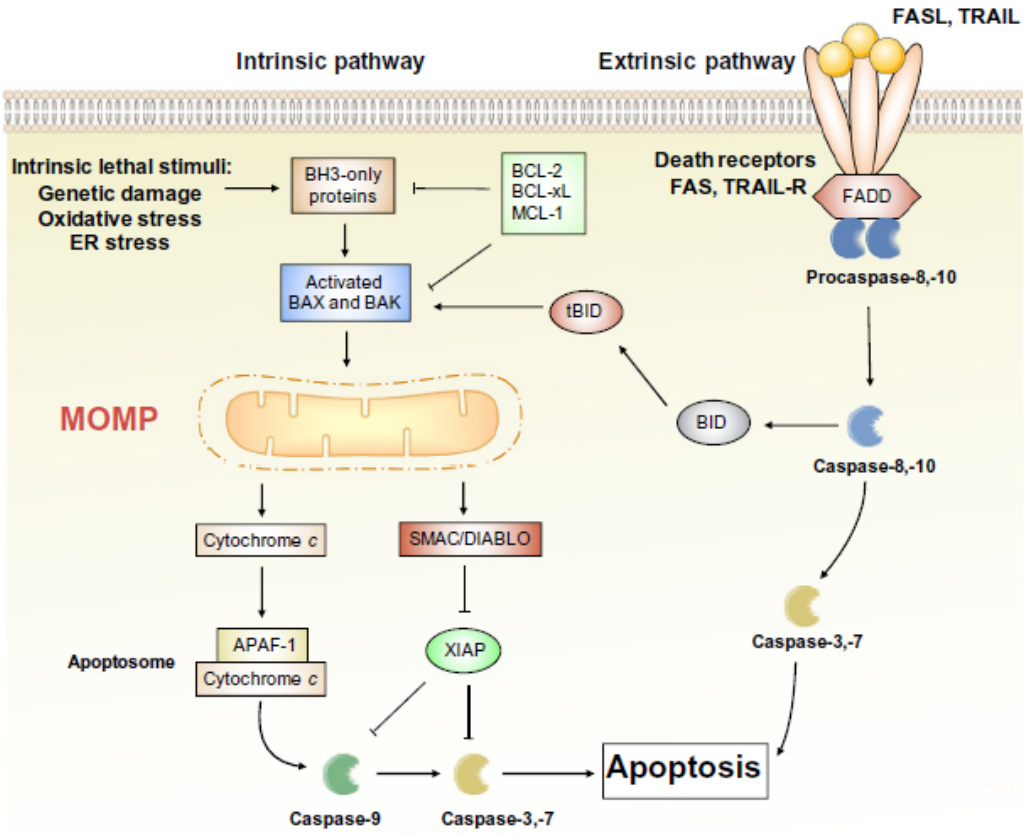

Figure 1-5 Mechanisms of apoptosis
Apoptosis is a form of cell death which can be activated either by external factors in the extrinsic pathway or internal signals through the intrinsic pathway. Both pathways involve different mechanisms of initiation and initiator caspases but converge upon cleavage of executioner caspases 3 and 7. This leads to widespread substrate cleavage and subsequent cell death. Cross-talk exists between the pathways as activated caspase 8 (extrinsic) can cleave and activate BID which can indirectly result in MOMP (intrinsic). (Taken from Cao and Tait 2018).

The C. *elegans ced-3* gene mammalian homologue is capsase-9 (previously interleukin -1β processing enzyme) (Yuan*, et al* 1993). This protein is part of a family of cysteine proteases which all contain a conserved QACXG pentapeptide and are essential effectors of apoptosis (Stennicke and Salvesen 1999). Caspases are synthesised as inactive proenzymes which require proteolytic cleavage at specific aspartate residues in order to be activated (Yamin*, et al* 1996). Caspases can be subdivided based on their functions (initiators and effectors of apoptosis) or on their substrate specificity however clustering based on either distinction is very similar indicating a high structure-function correlation (Degterev*, et al* 2003). Caspases transmit and amplify death signals via auto-proteolysis and the activation of downstream caspases. Caspases can cleave multiple targets outside of the caspase family which can explain many of the morphological features of apoptosis. The degradation of cytoskeletal proteins results in the loss of

cellular structure and shape and DNA fragmentation is caused by the cleavage of inhibitor of caspase-activated DNase (CAD) (Degterev*, et al* 2003, Nagata 2000, Rudel and Bokoch 1997).

1.4.7.1 Extrinsic Apoptosis

The extrinsic apoptotic pathway is stimulated by external ligands binding to plasma transmembrane death receptor proteins such as TNF receptor 1, TNF related apoptosis inducing ligand (TRAIL) receptor 1 and 2 and FAS. Upon binding, the death inducing signalling complex (DISC) forms and recruits caspase 8 via adaptor proteins (Scaffidi*, et al* 1998). Caspase 8 is activated via dimerisation (Scaffidi*, et al* 1998). The autocatalytic activation of caspase 8 leads to a cascade of caspase cleavages via caspase 3 and 7 (Hirata*, et al* 1998, Juo*, et al* 1998). Caspase 8 is also able cleave the pro-apoptotic BCL2 member, BID (Luo*, et al* 1998). This introduces cross-talk between extrinsic and intrinsic apoptosis as processed BID can translocate to the mitochondria, cause MOMP, release of cytochrome C and initiate the caspase cleavage cascade typical of intrinsic apoptosis (Korsmeyer*, et al* 2000, Luo*, et al* 1998). It has been suggested that this cross-talk between mechanisms may provide mitochondrial amplification of signal when there is not enough activated caspase 8 (Scaffidi*, et al* 1998).

1.4.7.2 Intrinsic apoptosis

The intrinsic pathway is triggered by internal signals such as DNA damage or oncogene activation, which results in MOMP (Green and Llambi 2015). Regulation is achieved by a balance between a large number of anti and pro apoptotic proteins within the BCL2 family (see 1.5 The BCL2 family). MOMP releases several noxious mitochondrial proteins into the cytosol (Saelens*, et al* 2004).

One such protein is cytochrome C, which is an intermembrane, essential protein within the electron transport chain (ETC), required for aerobic ATP generation (Liu*, et al* 1996, Saelens*, et al* 2004). After MOMP, there is a loss of mitochondrial membrane potential ($\Delta\psi_m$) and the generation of ROS due to the dysregulation of the ETC (Ricci*, et al* 2003). Studies have shown that the release of cytochrome C into the cytosol without caspase activation is sufficient to cause this loss of $\Delta\psi_m$ (Deshmukh*, et al* 2000). Yet, it is

thought that downstream caspase activity can propagate this loss by causing further damage to the ETC and mitochondrial function, suggesting a positive feedback mechanism for rapid $\Delta\psi_m$ loss (Ricci*, et al* 2003). Once translocated to the cytosol, cytochrome C binds to apoptotic protease activating factor-1 (APAF-1) in a heptameric complex with pro-caspase 9 to from the apoptosome (Zou*, et al* 2003). The formation of this complex homo-oligomerises and activates caspase 9 which in turn cleaves executioner caspase 3.

Endonuclease G, an inner mitochondrial membrane (IMM) protein that is released upon MOMP, cooperates with CAD to induce DNA fragmentation (Widlak*, et al* 2001). Endonuclease G KO mice are viable and derived KO mouse embryonic fibroblasts (MEFS) are as sensitive to apoptosis as wildtype (WT) MEFs with no obvious difference in DNA degradation (David*, et al* 2006, Irvine*, et al* 2005). In contrast, CAD KO thymocytes could not undergo DNA degradation but when phagocytosed, the DNA was digested by DNase II present in macrophage lysosomes (Kawane*, et al* 2003). Taken together, this data indicates there are several mechanisms of DNA fragmentation working in parallel and although endonuclease G can propagate DNA degradation, it cannot compensate for the function of CAD.

Apoptosis inducing factor (AIF) is an IMM protein that is cleaved and becomes untethered, allowing its release into the cytosol during apoptosis. Under normal conditions, AIF is a free radical scavenger, protecting cells from oxidative stress (Miramar*, et al* 2001). Yet in apoptotic cells, once released into the cytosol, the protein translocates to the nucleus, where it associates with DNA and leads to chromatin condensation and degradation (Ye*, et al* 2002). AIF contains no endonuclease domain, so it is unclear how it performs its DNA degradation role. It has been suggested that it may recruit other proteins, such as endonuclease G (Wang and Youle 2009). Due to its essential role in maintaining mitochondrial respiration as a free radical scavenger, its necessity in apoptosis has been difficult to ascertain.

Caspases can be directly inhibited by members of the inhibitors of apoptosis (IAP) family, providing another level of regulation for apoptosis (Liston*, et al* 1996). Family members XIAP, c-IAP1 and c-IAP2 were previously thought to directly inhibit active

caspases 3 and 7 by binding to their active sites (Roy*, et al* 1997). It is now known that only XIAP can directly bind to caspases and that other family members may sequester IAP antagonists therefore acting indirectly (Eckelman and Salvesen 2006, Eckelman*, et al* 2006). A distinct domain of XIAP is also able to bind to caspase 9 (Deveraux*, et al* 1999), preventing its homo-dimerisation (Shiozaki*, et al* 2003). Homo-dimerisation of caspase 9 is essential for its activation, thus XIAP sequesters caspase 9 in its monomeric catalytically inactive state (Shiozaki*, et al* 2003). IAPs can be sequestered by pro-apoptotic proteins, which are released from the inter membrane space (IMS) during MOMP: Smac/ DIABLO and OMI/ Htra2 (Du*, et al* 2000, Hegde*, et al* 2002, Suzuki*, et al* 2001, Verhagen*, et al* 2000). The latter of which not only binds to IAPs but also directly cleaves them rendering them irreversibly inactivated (Yang*, et al* 2003b). Ultimately, the role of IAP antagonists is limited to the contribution of IAPs in the apoptotic response which has not yet been fully characterised, partly due to the redundant roles of IAP proteins and their antagonists (Wang and Youle 2009). Studies have found a basal level of active caspase 3 in some cancer cell lines without apoptosis due to an increased expression of IAPs (Yang*, et al* 2003a). This could make IAPs ideal molecular targets for cancer treatment either alone or in combination with chemotherapy.

1.5 The BCL2 family

The BCL2 family is comprised of both pro- and anti-apoptotic proteins that tightly regulate the induction of MOMP. All proteins within the family contain at least one of the four BCL2 homology (BH) domains and interact with each other via hydrophobic interactions (Kale*, et al* 2018). The BCL2 family proteins can be divided into three groups, based on function and number of domains: multi-domain pro-apoptotic proteins/ the effectors (BAK and BAX), BH3-only pro-apoptotic proteins (BID, BIM, BAD, BIK, NOXA, PUMA, BMF and HRK) and multi-domain anti-apoptotic proteins (BCL2, $BCLX_L$, BCLW, MCL1, BCL2A1) (Kale*, et al* 2018). Thus, this family can be regarded as a tripartite apoptotic switch. In brief, when there is cellular stress, the pro-apoptotic BH3-only proteins are upregulated to inhibit the anti-apoptotic proteins and activate the effectors BAK and BAX (Leber*, et al* 2007). Although not fully understood, it has been hypothesised that these effector proteins oligomerise and form ring-like structures, creating pores within the OMM, allowing cytochrome C release and the initiation of

apoptosis (Shamas-Din*, et al* 2013). The fate of the cell is determined by the ratio and interactions between pro- and anti-apoptotic proteins within a cell.

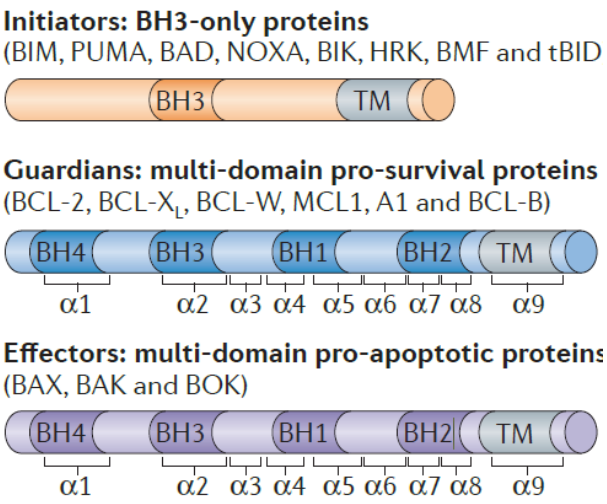

Figure 1-6 BCL2 family homology
The multi-domain members (anti-apoptotic and effector pro-apoptotic) share all four BH domains. BH3-only proteins only contain the BH3 amphipathic helix which mediates their interactions and specificity. Most proteins also contain a transmembrane (TM) domain to allow anchoring to the mitochondria (Taken from Czabotar*, et al* 2014)

1.5.1 The discovery of BCL2

The founding and eponymous protein, BCL2, was first discovered as one of the genes involved in the t(14;18) translocation present in follicular lymphoma (FL) (which is juxtaposed to the Ig heavy chain locus) (Tsujimoto, et al 1984). Mature B-cells containing this translocation have significantly more BCL2 mRNA (Graninger, et al 1987). Further investigations revealed that the breakpoint on chromosome 14 (IGH) is close to the 5' end of the J heavy chain segment indicating that this translocation arises due to errors in the process of VDJ joining in pre-B-cell differentiation (Tsujimoto, et al 1985). As BCL2 expression is normally high during B-cell development and is then downregulated during maturation, the translocation only becomes pathologically relevant later in B-cell development (Graninger, et al 1987). Despite the identification of the protein and its correlation of expression in B-cell malignancies, little was known about its function as ectopic expression of the protein did promote tumorigenesis but did not display a phenotype classic of other known oncogenes such as RAS (Reed, et al 1988). Functional studies in haematopoietic cells with overexpression of BCL2 alone or in combination with c-myc overexpression revealed that BCL2 co-operated with c-myc for oncogenesis (Vaux, et al 1988). A key experiment in ascertaining the role of BCL2

was introducing the expression of the protein in growth factor IL-3 dependent cells in the absence of IL-3 (Vaux, et al 1988). These cells, although arrested, did not undergo cell death (Vaux, et al 1988). Other studies found that overexpression of BCL2 could protect cells from other cellular stresses (Sentman, et al 1991, Tsujimoto 1989). Taken together, this data identified BCL2 as a key regulator of cell survival involved in the evasion of cell death rather than cell growth or proliferation. Since the discovery of BCL2 the family has expanded to over 30 proteins containing a BH3 domain, involved in the regulation of MOMP and subsequent apoptosis.

1.5.2 Role of the BCL2 in apoptosis

The regulation of apoptosis via the BCL2 family members has remained controversial, as different experimental approaches have led to different suggested models (see Figure 1-7).

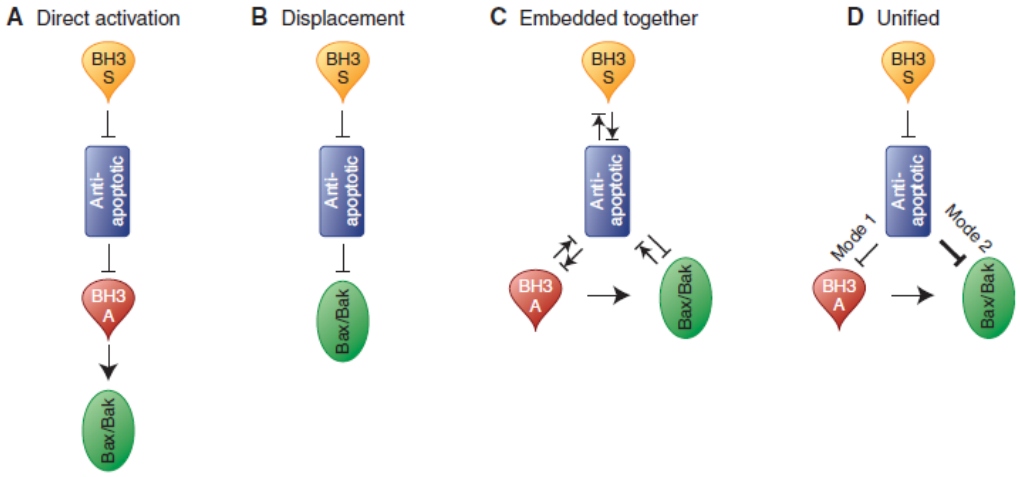

Figure 1-7 Schematic diagram of proposed mechanisms of MOMP
Several models have been suggested to explain the involvement of the BCL2 proteins in the initiation of MOMP. A. The direct activation model requires the activation of BAK/BAX by BH3-only proteins, however these can be sequestered by anti-apoptotic proteins. B. The displacement model describes constitutively active BAK/BAX which needs to be repressed by the anti-apoptotic proteins. BH3-only proteins are able to sequester the anti-apoptotic proteins. C. The embedded model describes a dual role of the anti-apoptotic proteins as they can sequester partially active BAK/BAX and the BH3-only proteins preventing their interaction BAK/BAX. BH3-only sensitiser proteins are able to competitively bind to the anti-apoptotic proteins. D. The unified model extends this further by separating the roles of the anti-apoptotic proteins into two different modes. It has been proposed that mode one is less efficient. (Activation is denoted by '→', inhibition is denoted by 'T' and mutual sequestration is denoted by '→|'. (Taken from Shamas-Din, *et al* 2013).

1.5.2.1 Direct activation

In this model, the effectors (BAK and BAX), require direct activation by the BH3-only proteins (Kim, *et al* 2006, Letai, *et al* 2002). The BH3-only proteins can be categorised as activator or sensitiser proteins (see 1.5.4 - Pro-apoptotic BH3-only proteins) (Letai, *et al* 2002). Under stress conditions, the activator proteins directly bind to BAK/ BAX activating them causing their oligomerisation and MOMP (Kim, *et al* 2006). However the anti-apoptotic proteins can sequester the BH3-only proteins preventing BAK/BAX activation (Kim, *et al* 2006, Letai, *et al* 2002). BH3-only sensitizer proteins cannot directly activate BAK/BAX but they can interact with the anti-apoptotic proteins therefore liberating the activators allowing their association with BAK/BAX (Kim, *et al* 2006). In this model the anti-apoptotic proteins cannot dimerise with BAK/BAX hence their anti-apoptotic ability is reliant on their ability to sequester the BH3-only proteins.

1.5.2.2 Displacement

The displacement model is the opposite of direct activation as BAK/BAX are constitutively active and are inhibited by interactions with anti-apoptotic proteins (Willis*, et al* 2005). The BH3-only proteins do not interact with BAK/BAX but are able to competitively bind to the anti-apoptotic proteins, releasing BAK/BAX and inducing MOMP.

1.5.2.3 Embedded together

As the name would suggest, the embedded together model incorporates both the direct activation and displacement model to suggest a novel mechanism of MOMP activation. Studies have shown that BAK/BAX activation is a multi-step procedure (Leber*, et al* 2007, Shamas-Din*, et al* 2013). Plus BCL2 family interactions can cause reversible structural conformation changes resulting in differential affinities for their binding partners (Garcia-Saez*, et al* 2009). For example, when BCL2 or BAX is mitochondrially associated (through its TM domain) there is an increased binding affinity for BH3 domains in comparison to their cytoplasmic counterparts (Edlich*, et al* 2011). Much of the data that has been implicated in the direct activation or displacement mechanisms has been generated using truncated proteins and peptides which is often overexpressed above physiologically relevant levels (Leber*, et al* 2007). Taken together, this data indicated that previous data may have been interpreted incorrectly due to differential conformations of the proteins. In the embedded together model, the BAK/BAX proteins require activation via BH3-only proteins but the anti-apoptotic proteins are able to compete and directly inhibit BAK/BAX or sequester the activator BH3-only proteins (Billen*, et al* 2008). Therefore, when sensitiser BH3-only proteins interact with the anti-apoptotic proteins they can displace BAK/BAX (similar to displacement) and liberate activator BH3-only proteins (similar to direct activation). In this model, the cellular fate and interactions is determined by the abundance of pro- and anti-apoptotic family members and their post-translational modifications which determine binding affinity (Leber*, et al* 2007).

1.5.2.4 Unified

This model is very similar to the embedded together model but it differentiates the mechanisms of apoptosis prevention via anti-apoptotic proteins sequestering BH3-only proteins (mode 1) or sequestering BAK/BAX (mode 2) (Llambi*, et al* 2011). In this model, mode 1 is a less efficient mechanism and easier to target therapeutically (Llambi*, et al* 2011). In this model, protein interactions and the mode employed are dependent on the intensity of cellular stress as opposed to protein abundance (Llambi*, et al* 2011).

1.5.3 Anti-apoptotic multi-domain proteins

Anti-apoptotic BCL2 family members (BCL2, $BCLX_L$, myeloid leukaemia sequence 1 (MCL1), BC2A1 and BCLW) contain all four BH domains (see Figure 1-6). Structure-function analysis of BCL2 shows that the BH1 and BH2 domains are functionally important as deletion of any of the domains results in the suppression of its anti-apoptotic ability and prevents association to other BCL2 family proteins such BAX and its homologs (Reed*, et al* 1996). The BH4 domain was found to also be important for its anti-apoptotic function but was not required for heterodimerisation with other BCL2 family members (Reed*, et al* 1996). Three dimensional structures have been solved for all of the anti-apoptotic proteins. Typically there is an eight helix bundle (encoded within the BH1, 2 and 3 domains) which form the binding groove for BH3 domains of other BCL2 family members to bind via hydrophobic interactions and a C-terminal TM domain (Lessene*, et al* 2008). Interactions are modulated by four hydrophobic pockets (p1-4) within the binding groove which are occupied by conserved hydrophobic residues of BH3 domain (Bharatham*, et al* 2011, Sattler*, et al* 1997). Isoforms of these proteins exist which may not contain all of these domains (Lessene*, et al* 2008).

1.5.3.1 BCL2

BCL2 contains two central hydrophobic helices surrounded by five amphipathic helices forming the binding pocket and a C-terminal TM domain (Petros*, et al* 2001). Via this binding pocket, BCL2 (and other anti-apoptotic proteins) has also been found to bind to the BH3 domain of Beclin-1 (Liang*, et al* 1998, Pattingre*, et al* 2005). Under normal conditions, these proteins form a complex at the endoplasmic reticulum (ER) (Pattingre*,*

et al 2005). Under stress, BCL2 dissociates and Beclin-1 activates autophagy (Pattingre*, et al* 2005). Studies have revealed that short term nutrient deprivation caused the dissociation of BCL2 from Beclin-1 but it did not dissociate from BAX until a longer time of nutrient deprivation was achieved (Wei*, et al* 2008). Caused by a weaker binding between BCL2 and Beclin1 (Decuypere*, et al* 2012), the differential dissociations can result in a cell survival process or death thus equating the response to the level and duration of stress. Nuclear BCL2 has been found to negatively affect trafficking of transcriptional factors therefore inhibiting several transcriptional factors such as p53, NKκB, AP1 and CRE (Beham*, et al* 1997, Massaad*, et al* 2004). This function of BCL2 is dependent on its TM (Massaad*, et al* 2004).

Although this is not completely characterised, BCL2 has also been found to interact with other proteins (which do not contain a BH3 domain) through its BH4 domain. BCL2 can sequester proteins involved in DNA mismatch repair machinery and DNA double strand break repair therefore increasing DNA damage and mutagenesis (Hou*, et al* 2007, Wang*, et al* 2008). BCL2 expression inhibits the progression from G1 to S during the cell cycle (Mazel*, et al* 1996) and its phosphorylation has been linked to a block at G2/M phase (Furukawa*, et al* 2000). Although not involved in forming the BH3 binding groove, this implicates the BH4 domain of the BCL2 as functionally important in other processes besides apoptosis.

Controversial studies have also identified a splice variant isoform of BCL2 which lacks the TM domain known as BCL2β. The role and function of this isoform is not clear with conflicting data published thus far as to the necessity of the TM domain for BCL2's anti-apoptotic function (Borner*, et al* 1994, Kawatani*, et al* 2003, Tanaka*, et al* 1993). Due to its cytosolic location, BCL2β may be able to interact BID preventing its cleavage and activation (Schinkothe*, et al* 2006).

1.5.3.2 BCLX

$BCLX_L$ is encoded by the *BCL2-like 1 (BCL2L1)* gene which has 44% homology to BCL2 (Warren*, et al* 2019). The binding pocket is composed of two central hydrophobic helices which are surrounded by five amphipathic helices (Muchmore*, et al* 1996). The

gene has two splice variants giving rise to aforementioned $BCLX_L$ and pro-apoptotic $BCLX_S$ (Boise*, et al* 1993). The BH3 domain of $BCLX_S$ is vital for its pro-apoptotic function and it has been shown that this domain allows heterodimerisation with $BCLX_L$ therefore directly inhibiting its function (Chang*, et al* 1999). It has also been suggested that the opposing functions could be caused by different selectivity for binding partners (Plotz*, et al* 2012). Rather than sequestering effector proteins, $BCLX_S$ has been shown to interrupt BAX-voltage dependent anion channel (VDAC) interaction, consequently exposing the BAX binding groove allowing activation (Plotz*, et al* 2012). $BCLX_S$ mRNA is highly expressed in cells undergoing a high rate of turnover such as developing lymphocytes whereas $BCLX_L$ is typical of long lived cells such as those in the brain (Boise*, et al* 1993). The favour of splice variant has been shown to change after exposure to cellular stress such as DNA damage (Shkreta*, et al* 2011).

$BCLX_L$ has also been shown to have a role in mitochondrial Ca^{2+} uptake (Huang*, et al* 2013), and has been shown to regulate Ca^{2+} signalling when localised to the ER (Eno*, et al* 2012). Although not fully understood, $BCLX_L$ may have a large role within neuronal signalling. $BCLX_L$ expression can increase the rate of fusion and fission of mitochondria and consequently mitochondrial biomass in neurons (Berman*, et al* 2009) and regulates synaptic vesicle endocytosis (Li*, et al* 2013). As with BCL2, interactions with Beclin-1 via its BH3 domain at the ER have been shown to inhibit autophagy (Oberstein*, et al* 2007). In order for the development and differentiation of cellular sub-types it can be important to inhibit apoptosis. $BCLX_L$ KO is embryonic lethal due to extensive cell death in the central nervous system, liver and haematopoietic stem cells (Motoyama*, et al* 1995). Post development, the differentiation of megakaryocytes to platelets is dependent on the anti-apoptotic role of $BCLX_L$ (Josefsson*, et al* 2011).

1.5.3.3 MCL1

The MCL1 binding groove differs to BCL2 and $BCLX_L$ with only one central hydrophobic helix surrounded by six helices which are less densely packed giving rise to a wider binding pocket (Day*, et al* 2005). MCL1 also exists as multiple isoforms due to splice variants: $MCL1_L$, $MCL1_S$ and $MCL1_{ES.}$ The latter two are pro-apoptotic and the former is anti-apoptotic (Bae*, et al* 2000, Kim*, et al* 2009b). $MCL1_L$ residues 170-300 share

structural and sequential homology to BCL2 and $BCLX_L$ which allows the sequestration of pro-apoptotic proteins (Thomas*, et al* 2010). Notwithstanding its structural similarity, it is unique to the other BCL2 anti-apoptotic family members as the extended N-terminus of the protein contains a PEST domain (Kozopas*, et al* 1993) (see Figure 1-8). This domain contains multiple sites for post-translational modifications (PTMs) such as phosphorylation, ubiquitination and caspase cleavage which affect binding affinity and vastly increase the turnover rate of the protein (Thomas*, et al* 2010). In addition to the protein, MCL1 mRNA has a short half-life and can be inhibited by mir-29, which is often down regulated in cancerous cells (Mott*, et al* 2007). The stabilisation and degradation of this protein is another layer of regulation of MOMP execution and can influence cell fate.

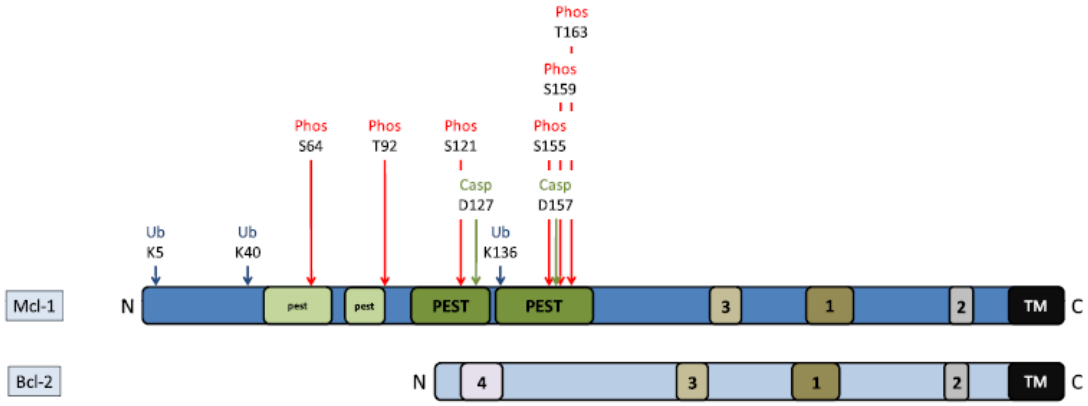

Figure 1-8 MCL1L domains
Schematic representation of the domains within the long form MCL1 compared to homolog BCL2. Relative sites of PTMs on MCL1 are also indicated. (Adapted from Thomas*, et al* 2010)

The pro-apoptotic, shorter form, $MCL1_S$ does not contain exon 2 of the gene. This results in the loss of the BH1, BH2 and TM domains (Bae*, et al* 2000). Hence it functions in a similar manner as BH3 proteins and antagonising the long form of MCL1 (Bae*, et al* 2000). Fewer investigations have been undertaken on the $MCL1_{ES}$ isoform which lacks exon 1, partially removing the PEST domain (Kim*, et al* 2009b). Hereinafter, MCL1L will be referred to as MCL1.

As with the other anti-apoptotic protein, MCL1 has other functions outside of the apoptotic pathway. Cell cycle progression is partly regulated via MCL1 interactions with cyclin dependent kinase 1 and checkpoint 1 protein (Jamil*, et al* 2008, Jamil*, et al* 2005)

and MCL1 depletion reduces efficiency of DNA double strand repairs (Mattoo*, et al* 2017). MCL1 knock outs are embryonic lethal due to an uncharacterised function in preimplantation development and implantation (Rinkenberger*, et al* 2000). Conditional knockouts have also shown that the protein is essential for the development and survival of subsets of cells, such as haematopoietic stem cells, B and T lymphocytes, granulocytes, macrophages and neurons (Arbour*, et al* 2008, Opferman*, et al* 2005, Opferman*, et al* 2003, Steimer*, et al* 2009, Vikstrom*, et al* 2016). Moreover its expression is required throughout B-cell development, opposed to $BCLX_L$, which promotes immature B-cell survival, and BCL2, which is highly expressed in mature B-cells (Vikstrom*, et al* 2016). Cardiac-specific MCL1 KO lead to fatal cardiac failure and mitochondrial dysfunction (Wang*, et al* 2013). Blocking apoptosis via BAK/BAX KO reduced lethality yet cells still exhibited signs of mitochondrial abnormalities indicating MCL1 has a role in mitochondrial respiration (Wang*, et al* 2013).

1.5.3.4 BCL2A1

BCL2A1 (also known as BCL2 related gene expressed in fetal liver, BFL1) is a poorly investigated anti-apoptotic protein that has not been fully characterised. The overall sequence homology to the other anti-apoptotic proteins is relatively low. Nonetheless, the three-dimensional structures are very similar, with the BH1, 2 and 3 domains giving rise to a helical bundle forming the BH3 binding cleft (Herman*, et al* 2008). BCL2A1 is associated to the mitochondrial outer membrane via its C-terminus, despite its lack of a well-defined TM domain unlike the other anti-apoptotic proteins (Brien*, et al* 2009). *BCL2A1* is mainly a haematopoietic tissue-specific gene (Lin*, et al* 1993), the expression of which increases upon maturation and BCR/TCR engagement (Trescol-Biemont*, et al* 2004, Verschelde*, et al* 2003). Lymphocyte specific transgenic Eμ-BCL2A1 mice displayed perturbations in B-cell development with an expansion of Pro-B-cells (Chuang*, et al* 2002). This indicates a key role of the protein in the pro- to pre-B-cell differentiation stage (Chuang*, et al* 2002). The limited characterisation of the protein is due in part to difficulties in gene targeting with conventional methods, as the locus has undergone gene quadruplication in mice but not in humans (Hatakeyama*, et al* 1998). Deletion of one of the loci in mice has implicated a role of the protein in neutrophil survival (Hamasaki*, et al* 1998). Conditional knockdown of BCL2A1 using shRNA could

not recapitulate this result, potentially due to incomplete knock down. Despite this, they did identify the protein as a potential mediator of tonic and chronic BCR signalling and B-cell development (Sochalska*, et al* 2016). As mentioned, BCL2A1 is a target gene of the NFκB pathway, therefore it has been suggested that upon antigen engagement and NFκB activation, BCL2A1 expression is essential for B-cell development and mature B-cell survival (Sochalska*, et al* 2016). In contrast, recent advances have led to the generation of mice with the complete loss of BCL2A1, which resulted in minor defects, suggesting the protein is redundant (Schenk*, et al* 2017).

Little is known about the BCL2A1 splice variant, $BFL1_S$ which has a premature stop codon in exon 3 (Ko*, et al* 2003). It has been proposed that it localises to the nucleus through its C-terminal rather than mitochondria (Ko*, et al* 2003). Co-expression with BAX revealed that the proteins could still interact indicating the short form retains its anti-apoptotic function (Ko*, et al* 2003).

1.5.3.5 BCLW

BCLW is comprised of a central helix surrounded by amphipathic helices with similar topology to BCL2 and $BCLX_L$ (Hinds*, et al* 2003). It has been shown that the C-terminus of the protein folds over and restricts access to the hydrophobic groove (Denisov*, et al* 2003, Hinds*, et al* 2003). Once displaced by binding BH3 domains, the C-terminus is able to insert into membranes (Denisov*, et al* 2003, Hinds*, et al* 2003). C-terminal truncations of the protein increase affinity for BH3 domains, ergo the C-terminus may regulate binding (Denisov*, et al* 2003).

Eμ-myc, BCLW KO mice display decreased p53 pathway inactivation compared to Eμ-myc, BCLW WT mice suggesting there may be a cross talk between p53 and BCLW through an uncharacterised mechanism (Adams*, et al* 2017). Eμ-myc, BCLW KO mice also exhibited great latency in lymphoma development (Adams*, et al* 2017). BCLW expression has been shown to be partly regulated indirectly by MYC (Adams*, et al* 2017). As miR15 has been shown to inhibit BCLW expression (Adams*, et al* 2017, Yang*, et al* 2015) and MYC can regulate the expression of many microRNAs (miRNAs) including

miR15 (Bui and Mendell 2010), it has been hypothesised that MYC could regulate the expression of BCLW via the miR15 family (Adams*, et al* 2017).

1.5.4 Pro-apoptotic BH3-only proteins

BH3-only proteins are upregulated either transcriptionally or through PTMs under cellular stress (Happo*, et al* 2012). They are relatively disordered proteins that contain a ~26 residue amphipathic helix within the BH3 domain (Hinds*, et al* 2007, Sattler*, et al* 1997). This helix is vital for interactions with other BCL2 family members, as it mediates the insertion of four hydrophobic residues into the hydrophobic pockets (p1-4) on its partner and the formation of a salt bridge between a conserved Asp residue in the BH3 domain and a conserved Arg residue in the BH1 domain of its partner (Hinds*, et al* 2007, Liu*, et al* 2003, Sattler*, et al* 1997) (see Figure 1-9). Despite these specific interactions, hydrophobic and electrostatic interactions across the interface contribute to differential binding affinitities (Sattler*, et al* 1997). It is now accepted that they function via the direct activation of the effectors plus the neutralisation of anti-apoptotic proteins; hence the group has been divided into activator and sensitiser proteins (Kuwana*, et al* 2005).

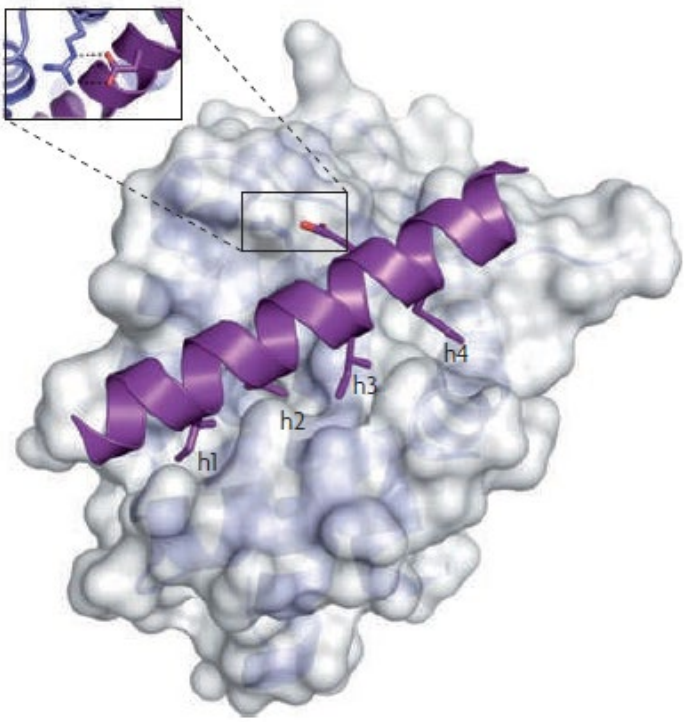

Figure 1-9 Crystal structure of the interaction of MCL1 and BIM-BH3 peptide
Four conserved hydrophobic residues on the BH3 domain (purple) insert into four hydrophobic pockets within the binding groove (grey). A salt bridge between conserved aspartic acid on the BH3 and conserved arginine on the anti-apoptotic protein also forms (red) (Taken from Lessene*, et al* 2008).

1.5.4.1 BH3-only activator proteins

The activator BH3-only proteins, BIM, tBID and PUMA can directly bind to BAK and BAX, promoting their oligomerisation and pore formation. They can also sequester and be sequestered by all of the anti-apoptotic proteins. Upregulation of the proteins results in spontaneous apoptosis, whereas KO mice develop major abnormalities such as fatal autoimmune kidney diseases (Happo*, et al* 2012). They can be upregulated by several transcriptional factors (FOXO3a, CHOP, MYC) in response to stress and can be modulated via PTMs such as phosphorylation (Happo*, et al* 2012).

The BH3 interacting domain death agonist (BID) differs to the other BH3-only proteins as its homology is actually more similar to the multi-domain BCL2 proteins, with the BH3 domain being buried within the protein, thus making it inactive (McDonnell*, et al* 1999). It is only upon cleavage by caspase 8 (during extrinsic apoptosis) (tBID) that the BH3 domain is exposed and can function as an activator BH3-only protein (McDonnell*, et al* 1999).

1.5.4.2 BH3-only sensitiser proteins

The sensitiser BH3-only proteins such as BAD and NOXA have more specific binding and primarily function by sequestering the anti-apoptotic proteins. Their specificity for the anti-apoptotic proteins varies due to differences in their amphipathic helix. The classification of activators and sensitizers is somewhat blurred by reports that, under some circumstances, the sensitiser proteins can also directly activate the effectors (Du*, et al* 2011). Nonetheless, the binding affinities for BAK/BAX are up to 1000 times weaker than the activators and typically occur in the absence of BIM, BID and PUMA (Du*, et al* 2011). The knock-out of sensitiser proteins has a considerably less detrimental effect than activator proteins.

PUMA and NOXA are direct transcriptional targets of p53 and consequently play a role in DNA damage responses (Villunger*, et al* 2003). PUMA KO cells are resistant to γ-irradiation and DNA damaging chemotherapy whereas NOXA KO cells are resistant to UV radiation (Naik*, et al* 2007, Shao*, et al* 2010, Villunger*, et al* 2003).

1.5.5 Pro-apoptotic multi-domain effector proteins

BCL2 associated X protein (BAX) was first identified in 1993 in complex with BCL2 via co-immunoprecipitation (Oltvai*, et al* 1993). Despite sharing sequence homology with BCL2, the overexpression of BAX promoted cell death (Oltvai*, et al* 1993). Another pro-apoptotic protein, BCL2 antagonist/ killer (BAK) was discovered shortly after in 1995 (Chittenden*, et al* 1995). Cells with either protein knocked could still undergo apoptosis, however double knockouts were resistant to most death stimuli (Wei*, et al* 2001). As discussed previously, it is now known that during intrinsic apoptosis, the effector BCL2 family members (BAK and BAX) perform the essential function of oligomerising and permeabilising the mitochondrial outer membrane releasing several noxious proteins (see 1.4.7.2 -Intrinsic apoptosis). The mechanism of BAK/BAX activation and pore formation is an area of intense research and it is still not fully characterised.

BAK and BAX share topology with the anti-apoptotic proteins homologs. There is a nine helix bundle forming a hydrophobic pocket and C-terminal TM domain (Moldoveanu*, et al* 2006, Suzuki*, et al* 2000). Through this TM domain, even in non-stressed conditions,

BAK is always associated to the mitochondrial outer membrane (Griffiths*, et al* 1999). Conversely, in non-stressed cells BAX is typically cytosolic, as it employs a structure similar to BCLW (Suzuki*, et al* 2000, Wolter*, et al* 1997). Helix 9 of the protein (which is involved in membrane insertion), bends back on itself and binds to its binding groove via hydrophobic interactions (Suzuki*, et al* 2000). Upon binding to a BH3 domain, the helix is displaced, allowing mitochondrial membrane tethering (Wolter*, et al* 1997). Studies have shown that in healthy cells, BAX is constantly retro-translocating between the mitochondria and cytosol, the latter movement potentially regulated via interactions with anti-apoptotic proteins (Edlich*, et al* 2011, Schellenberg*, et al* 2013). The positioning of helix 9 and thus protein localisation is therefore a level of regulation in BAX activation.

Binding of activator BH3-only proteins to the hydrophobic BAK/BAX binding cleft result in large conformational changes resulting in the exposure of the BH3 domain allowing homo-dimerization (Moldoveanu*, et al* 2013) (Dewson*, et al* 2008, Dewson*, et al* 2012). Furthermore, BH3-only proteins interact via a 'hit and run' mechanism in which they quickly dissociate, allowing BAK/BAX homo-dimerization at the same site (Moldoveanu*, et al* 2013). These symmetric dimers can then oligomerise to higher ordered structures via disulphide bonds (Dewson*, et al* 2009). Several studies have found that activator BH3-only proteins are required to be tethered to the mitochondrial membrane before interacting with the effectors (Lovell*, et al* 2008, Walensky*, et al* 2006, Wilfling*, et al* 2012). It is indicated that the recently exposed BH3 domain of activated, monomer BAK/BAX can be sequestered by anti-apoptotic proteins, preventing their homo-dimerization (Adams and Cory 2018, Kale*, et al* 2018).

A controversial, alternative binding site on BAX has been identified via NMR on the opposite side to the hydrophobic cleft known as the rear binding site (Gavathiotis*, et al* 2010, Gavathiotis*, et al* 2008). Mutagenesis at this site disrupted BH3 peptide binding and prevented cytochrome C release (Gavathiotis*, et al* 2008). It has been proposed that activator BH3-only peptides can bind to the rear binding site, accelerating the exposure of the TM domain and ergo it's tethering to the mitochondria (Gavathiotis*, et al* 2010). It is possible that post rear activation, the BH3 protein dissociates allowing symmetrical BAX homodimer formation (Moldoveanu*, et al* 2013). However, it has been suggested

that when activated via the rear site, BH3 proteins can remain associated to BAX during homo-oligomerisation which occurs via its canonical front binding site (Kim*, et al* 2009a). Based on this, an asymmetrical model of oligomerisation has been hypothesised, where the newly exposed BH3 domain of the activated BAX binds to the rear pocket of another BAX, thus auto-activating it and leading to a chain of subsequent activated BAX proteins (Gavathiotis*, et al* 2010). It is worth considering that experiments identifying this binding site were performed with truncated peptides and/or membrane free solutions, so it is unclear if this is a true active site. Furthermore, independent groups have had contrasting results when trying to recapitulate the mutagenesis studies on the rear site (Dengler*, et al* 2019, Peng*, et al* 2013). In contrast, mutations at the canonical front binding pocket abolished interactions with tBID and BAX (Peng*, et al* 2013, Zhang*, et al* 2010).

BAK and BAX have been shown to become activated in the absence of BH3-only proteins via other stimulants such as small molecules, heat, pH, detergents and metabolites (Kale*, et al* 2018). This spontaneous apoptosis indicates that BH3-only protein engagement may be catalytic rather than mandatory. Studies have found that once anti-apoptotic proteins are neutralised, BH3-only proteins are dispensable for apoptosis (Greaves*, et al* 2019, Zhang*, et al* 2016).

Conflicting studies have suggested different models for BAK/BAX pore formation. One such model suggests that their insertion into the membrane would increase membrane tension promoting bilayer disruption (Westphal*, et al* 2014). It has been suggested that the recruitment of BAK/BAX homo- dimers can enlarge pores, which is consistent with Cyro-EM images of arcs and rings formed by BAX (Salvador-Gallego*, et al* 2016).

Mice with either BAK or BAX KO have webbed feet and imperforate vaginas due to blocks in developmental apoptosis (Lindsten*, et al* 2000). Double KO mice are typically embryonic lethal, with those who are born dying of an autoimmune disease, highlighting the importance of apoptosis in development and survival (Lindsten*, et al* 2000).

The effectors have also been linked to mitochondrial fusion/fission dynamics. During apoptosis mitochondrial structural dysfunction occurs due to the involvement of fission regulatory protein, dynamin-related protein (DRP-1) (Frank*, et al* 2001). Similar to BAX, DRP-1 cycles between the cytosol and mitochondrial membrane but is recruited to the mitochondria during apoptosis via an unclear mechanism (Frank*, et al* 2001). It has been proposed that BAX and DRP-1 are binding partners and translocate together (Wang*, et al* 2015). There are conflicting studies about the requirement of DRP-1 or mitochondrial fission for apoptosis (Martinou and Youle 2011).

1.5.6 The binding code

Cell fate is determined by the balance between anti- and pro-apoptotic proteins, nevertheless there is another layer of regulation by the BCL2 family, as the binding grooves exhibit different selectivity for the BH3 peptides (Chen*, et al* 2005). From this understanding, a binding map was generated (see Table 1-1). The activator peptides (BID, BIM and PUMA) are able to antagonise all of the anti-apoptotic proteins whereas the sensitiser proteins exhibit binding preferences (Chen*, et al* 2005). The evolution of different BH containing proteins with different selectivity may allow regulation of cell death via different stresses, different pathways and different tissue types (Shamas-Din*, et al* 2013).

	BID	BIM	BAD	BIK	NOXA	PUMA	BMF	HRK
BCL2	++	++	++	+	-	++	++	-
$BCLX_L$	++	++	++	++	-	++	++	++
BCLW	++	++	++	++	-	++	++	-
MCL1	++	++	-	+	++	++	++	-
BCL2A1	++	++	-	-	-	++	-	-

Table 1-1 The binding code.
Summary of the differential binding between BH3 peptides and anti-apoptotic proteins. Strong binding is denoted by ++, moderate binding is indicated by +, and no binding is shown as -. (Adapted from Del Gaizo Moore and Letai 2013).

1.6 BCL2 family proteins in cancer

BCL2 family members are often mutated or dysregulated in malignant cells resulting the evasion of apoptosis, which is recognised as a hallmark of cancer (Hanahan and Weinberg 2000, Hanahan and Weinberg 2011). It is indicated that the dysregulation of BCL2 family members has a key roles in tumour development and maintenance, often allowing cells to stay alive and acquire other driver mutations. For instance, overexpression of any of the anti-apoptotic proteins have been shown to accelerate MYC driven leukaemia (Beverly and Varmus 2009). The overexpression of anti-apoptotic proteins is also considered to be a poor prognostic marker and a key resistance mechanism to chemotherapy (Correia*, et al* 2015).

1.6.1 BCL2 family dysregulation

As discussed previously, BCL2 was the first member identified, due to its role in FL. The t(14;18) translocation has also been identified in DLBCL (Schuetz, et al 2012). Overexpression of BCL2 has also been found in Chronic lymphocytic leukaemia (CLL), but the incidence of the t(14;18) translocation is low and when it does occur the breakpoints are distinct to that which typically occur in FL or DLBCL (Dyer, et al 1994). Instead, overexpression is understood to be caused by 13q deletions (occurring in 61% of CLL cases) (Edelmann, et al 2012). This causes the deletion of microRNA cluster miR-15/16, a suppressor of multiple proteins including BCL2, thus identifying another

mechanism, besides translocation, of BCL2 deregulation (Calin, et al 2002, Cimmino, et al 2005).

High BCLW expression has been associated with Burkitt's lymphoma and has been suggested as a marker for aggressive DLBCL (Adams*, et al* 2017). One study found a negative correlation between BCL2 and BCLW expression within DLBCL, indicating distinct protein dependence within subset of the disease (Adams*, et al* 2017). BCL2A1 overexpression has been found in multiple malignancies and several studies have suggested it can facilitate cell transformation and tumour progression (Vogler 2012). Nevertheless, the effect of BCL2A1 in leukemic mice was less significant than the other anti-apoptotic BCL2 family members (Beverly and Varmus 2009). MCL1 and $BCLX_L$ are overexpressed due to copy number variations in many liquid and solid cancers (Beroukhim*, et al* 2010). One study found gene amplifications or chromosomal gains of MCL1 in 23% of ABC DLBCL (Wenzel*, et al* 2013). The upregulation of BCL2, $BCLX_L$ and BCL2A1 could be caused by dysregulated NFκB signalling (Knittel*, et al* 2016).

mRNA expression comparisons using data from COSMIC (Tate*, et al* 2019) between different cancer types shows upregulation of the anti-apoptotic proteins across different cell types with potentially different expression in cell types (Figure 1-9, see also (Vogler*, et al* 2017)).

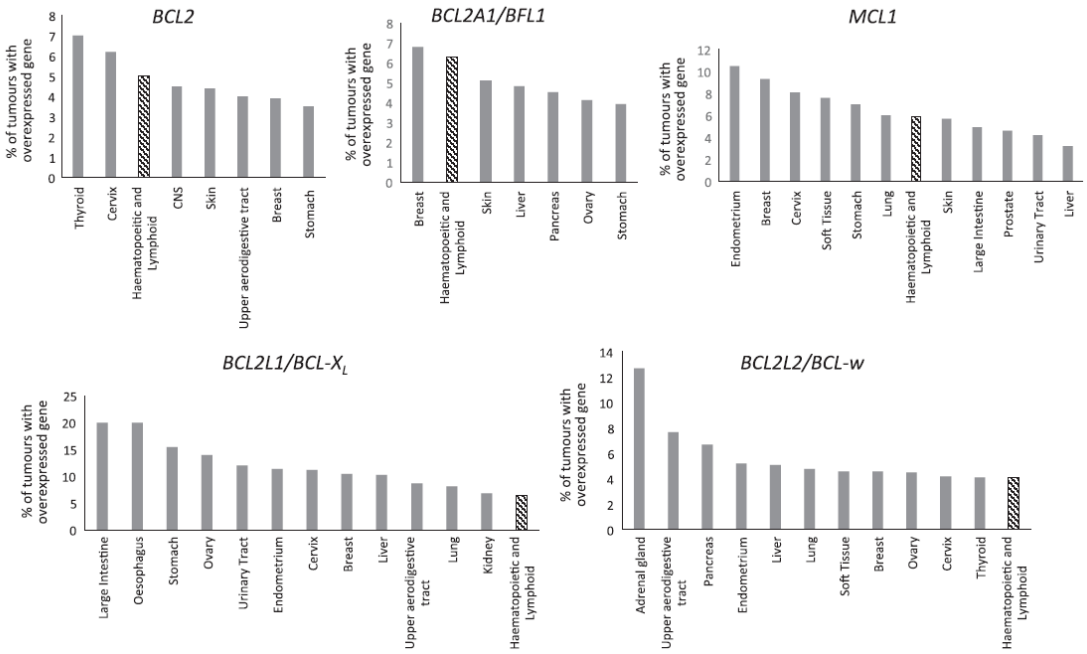

Figure 1-10 Expression of anti-apoptotic BCL2 genes in cancer
Data from COSMIC (Tate*, et al* 2019) (December 2016) was analysed to display the variation of anti-apoptotic BCL2 protein overexpression in cancers deriving from different tissues. (Taken from Vogler*, et al* 2017).

Downregulation of pro-apoptotic proteins also leads to an apoptotic resistance in malignancies. Deletion of both BIM alleles is present in 17% of mantle cell lymphomas (MCL) (Tagawa*, et al* 2005) and BIM and PUMA is often downregulated in Burkitt's lymphoma due to promoter hypermethylation (Garrison*, et al* 2008, Richter-Larrea*, et al* 2010). p53 is mutated in over 50% of cancer, which affects many cellular functions, such as cell cycle, DNA damage and metabolism (Perri*, et al* 2016). Inactivation of p53 would prevent transcriptional upregulation of NOXA and PUMA in response to DNA damage.

Taken together, this data indicates that there are multiple mechanisms that can deregulate the BCL2 family members in malignant cells. A recent study analysed gene expression of the family in malignant B-cells compared to naïve B-cells (see Figure 1-11) (Tessoulin*, et al* 2018). This data supports similar findings that anti-apoptotic proteins are often upregulated and pro-apoptotic proteins were downregulated.

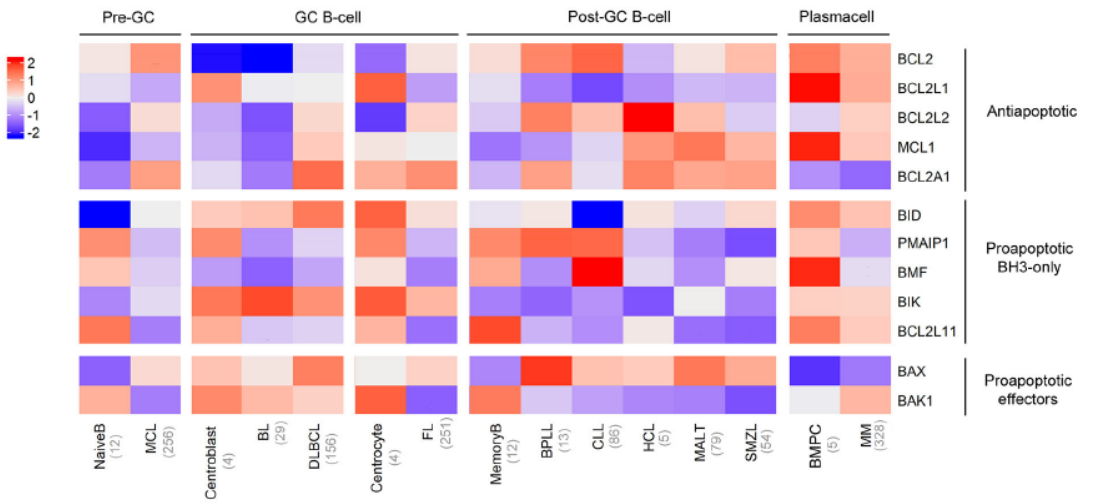

Figure 1-11 Dysregulation of BCL2 family members in B-cell malignancies
Heat map of BCL2 gene expression profiles. Higher expression is represented in red and lower transcript abundance is blue. (Taken from Tessoulin*, et al* 2018).

1.6.2 BCL2 family mutations

BCL2 is the most commonly mutated protein in DLBCL, with 95 out of 469 cases reported as mutated on COSMIC (Tate*, et al* 2019).

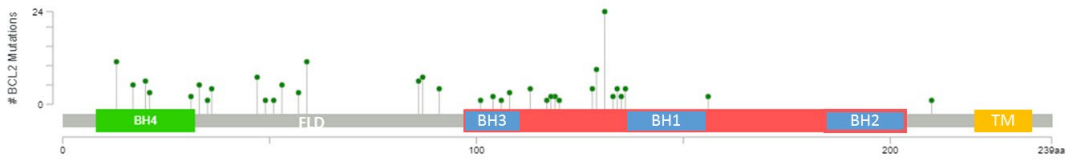

Figure 1-12 Spectrum of BCL2 mutation in lymphomas
Schematic diagram of the location and frequency of mutations found in *BCL2* in lymphomas. Data obtained from COSMIC (Tate*, et al* 2019) and figures adapted from cBioPortal.org (Cerami*, et al* 2012, Gao*, et al* 2013).

These mutations are not selected for by inhibitors and tend to cluster in the BH4 domain and BH3 domain. The consequences of these mutations remain largely unknown but have been implicated in the regulation of BCL2 transcription, binding of non-BCL2 family members and non-canonical functions, cell proliferation and apoptosis dysregulation (Singh and Briggs 2016). In contrast, $BCLX_L$ (0/391) and MCL1 (7/394) mutations are hardly reported in DLBCL (Tate*, et al* 2019).

1.6.3 BCL2 family dependence and priming for death

As mentioned, despite BH3-only protein upregulation due to cellular stress, many malignancies overexpress anti-apoptotic proteins to counteract this. These cells often become 'addicted' or dependent on this one/few anti-apoptotic proteins (Kale*, et al* 2018). Despite this and the hallmark of evading apoptosis, there is mounting evidence that malignant cells are 'primed for death' (Certo*, et al* 2006). Cells which are primed will have an abundance of activated effectors or activator BH3-only proteins, though they are sequestered by an anti-apoptotic protein (which they are addicted to) (Certo*, et al* 2006). Therefore, primed cells should die readily upon neutralisation of the anti-apoptotic proteins.

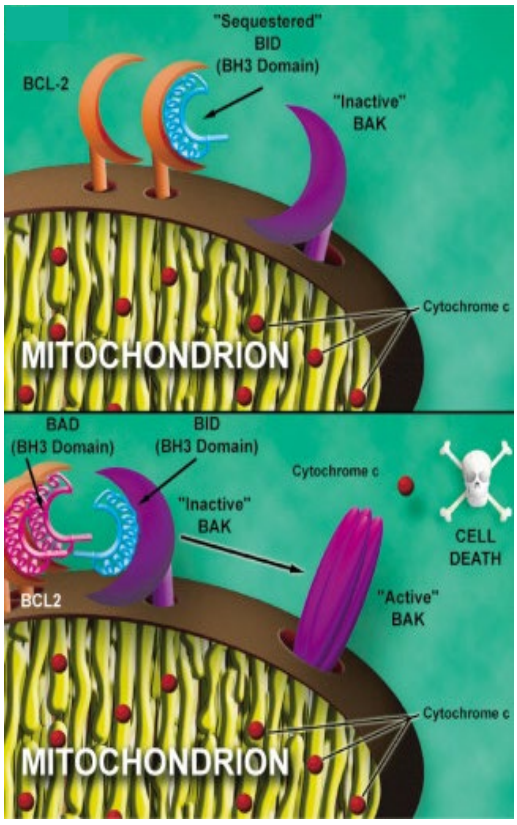

Figure 1-13 Primed for death
When activators such as BID are sequestered by anti-apoptotic proteins such as BCL2 the cell is primed for death. The addition of sensitiser proteins such as BAD are able to neutralise the anti-apoptotic protein, displacing BID, causing oligomerization of BAK and cytochrome C release. (Taken from Letai*, et al* 2002).

1.6.4 BH3 profiling

A functional assay known as BH3 profiling has be suggested to be able to ascertain the level of mitochondrial priming and anti-apoptotic protein dependence (Certo*, et al*

2006). By exposing the cells to known concentrations of synthetic BH3 peptides that specifically inhibit anti-apoptotic proteins, the protein which the cell is addicted to can be determined by measuring $\Delta\psi_m$ or cytochrome C release (see Figure 1-14) (Certo*, et al* 2006) (Del Gaizo Moore and Letai 2013, Ryan and Letai 2013).

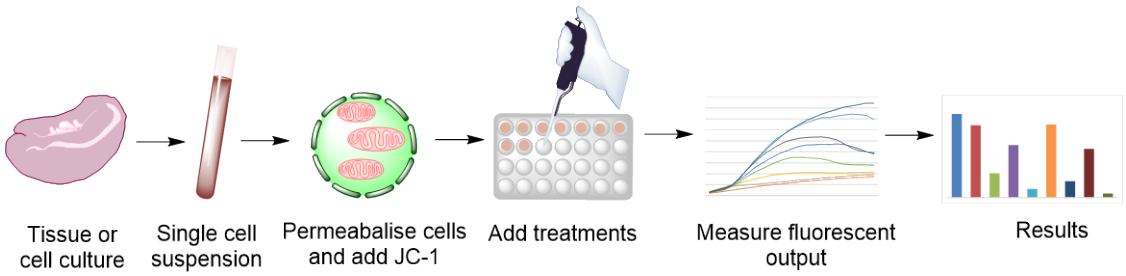

Figure 1-14 BH3 profiling technique
Single cell suspensions are gently permeabilise and stained with mitochondrial membrane potential probe, JC-1. Cells are treated with synthetic peptides specific for anti-apoptotic proteins and the $\Delta\psi_m$ is measured over time via fluorescence signal. A profile is generated for the sample.

Understanding of the binding code (see 1.5.6) is important to be able to correctly interpret data from this technique (Chen*, et al* 2005). High concentrations of the BH3 peptide mimic of BIM would induce $\Delta\psi_m$ in any apoptotic competent cell (wild type BAK and BAX) (Certo*, et al* 2006). Cells which are primed would display greater $\Delta\psi_m$ and require lower concentrations of the BIM peptide (Deng*, et al* 2007). Conversely, a cell that underwent apoptosis after exposure to a NOXA mimetic is likely to be dependent on MCL1, due to its selective binding. Binding affinities of synthetic peptides and anti-apoptotic proteins is shown in Table 1-2. As it is possible for cells to be dependent on more than one protein, this creates a profile.

	BIM	BAD	MS1	XXa1_Y4eK	FS2
BCL2	0.19	<0.1	2900	124	2400
$BCLX_L$	<1	5	2400	<0.1	>5000
BCLW	0.98	7	1500	382	>5000
MCL1	<1	>1000	7.9	>1000	3200
BCL2A1	<1	>1000	>10000	>1000	21

Table 1-2 Binding pattern of synthetic peptide and anti-apoptotic proteins
The binding pattern between the synthetic peptides used for BH3 profiling and the anti-apoptotic proteins with relevant Ki values (nM). High affinity is denoted with a green box and no binding is shown by a red box (Dutta*, et al* 2015, Foight*, et al* 2014, Jenson*, et al* 2017).

BH3 profiling could prove to be a useful laboratory tool that could be used to determine the anti-apoptotic dependence of cell lines and primary samples (Del Gaizo Moore and Letai 2013). BH3 profiling has been proposed to be able to correctly predict responses to chemotherapy, as sensitive cells will be more mitochondrially primed (Deng*, et al* 2007). This technique has been used to confirm that some B-cell malignancies, such as CLL, are dependent on the BCL2 protein (Del Gaizo Moore and Letai 2013). As inhibitors of the anti-apoptotic proteins are developed, the assay could be used clinically. It is a quick and relatively cheap technique, making it an ideal method to stratify patients. That being so, viable malignant cells are not always readily available if the disease is compartmentalised. In the case of DLBCL, the disease may be restricted to lymph nodes and malignant peripheral cells are vulnerable to spontaneous apoptosis once biopsied.

1.7 BH3 Mimetics

Due to the dysregulation of apoptosis and the BCL2 family members, the anti-apoptotic proteins became an attractive therapeutic target. A BH3 mimetic is a small helical peptide containing molecule which can specifically bind in the hydrophobic groove of an anti-apoptotic protein, neutralising it. As it mimics a sensitiser BH3-only protein, it will not be able to directly activate the effectors thus can only induce apoptosis in cells which are 'primed for death'. Consequently, BH3 mimetics could not only prove an effective treatment for R/R disease but also be more beneficial, with fewer side effects than traditional chemotherapy. Nevertheless, the development of specific BH3

mimetics has been challenging due to the similarities in topology of the hydrophobic grooves and the difficulty of targeting protein-protein interactions.

When development of mimetics began, it was unclear whether all anti-apoptotic proteins would require neutralising or if there would be a dependency. The discovery of the binding code (Chen*, et al* 2005) and the solved structures of BH3 proteins in complex with anti-apoptotic proteins provided great insight for the development of BH3 mimetics. Stapled peptides and peptidomimetics inhibiting anti-apoptotic proteins were used as laboratory tools and allowed interrogation of interactions in cell models (Lessene*, et al* 2008). Nonetheless, their poor pharmacological properties meant it was difficult for them to progress to clinical trials (Lessene*, et al* 2008). Natural molecule and fragment based screening identified several candidate BH3 mimetics. Their interactions with anti-apoptotic proteins *in vitro* notwithstanding, cell death occurred independent of BAK/BAX indicating the initiation of other cell death pathways (van Delft*, et al* 2006).

Consequently, Lessene and colleagues (2008) proposed four essential criteria in order to define a bone fide BH3 mimetic. These are listed below:

- Apoptosis must occur in a BAK/BAX dependent manner.
- The binding affinity between the drug and at least one anti-apoptotic protein must be at least in the low nano-molar range.
- Cytotoxic activity should be correlated with cellular BCL2 protein family levels and the binding profile of the drug to the BCL2 family members.
- Treatment with the molecules *in vivo* should produces relevant biomarkers (for example drugs targeting BCL2 should kill CLL cells and there should be a reduction in platelet level when targeting $BCLX_L$).

After the establishment of these criteria, many putative BH3 mimetics were disregarded (summarised in Table 1-3). For example, GX15-070 (obatoclax) binds to BCL2, $BCLX_L$, BCLW and MCL1 (at low affinity in the micromolar range) (Billard 2013). Studies have found that the drug is potent in BAK-/- BAX-/- mouse models indicating that non-apoptotic cell death is occurring (Billard 2013). Also, there is no correlation between the

efficacy of the drug and the concentration of the anti-apoptotic proteins within the cell (Lessene*, et al* 2008). According to the above criteria it is not a true BH3 mimetic and its mechanism of action is probably due to BCL2 independent pathways. Nevertheless, this molecule has been used in clinical trials both as a single agent and in combinational therapies, although clinical development has now ceased (Soderquist and Eastman 2016). Other molecules, such as gossypol and S1, have been found to increase NOXA levels through the unfolded protein response (by increasing intercellular calcium or reactive oxygen species) (Albershardt*, et al* 2011, Soderquist and Eastman 2016, Vogler*, et al* 2009b). The addition of small interfering RNA (siRNA) against NOXA stopped apoptosis, showing that these drugs do not directly bind to anti-apoptotic proteins but sequester them indirectly (Soderquist*, et al* 2014a, Soderquist*, et al* 2014b). This does not mean that they could not prove therapeutically valuable for MCL1 inhibition but they should not be considered as true BH3 mimetics and are consequently likely to have other toxicities.

The first confirmed true BH3 mimetic was a BCL2, $BCLX_L$ and BCLW inhibitor called ABT-737 (Oltersdorf*, et al* 2005), (Lessene*, et al* 2008). Since then, several other *bone fide* BH3 mimetics have been developed (summarised in Table 1-4). Note that there are not currently any specific inhibitors of BCLW or BCL2A1. Henceforth there will be a focus on ABT-737, ABT-199, A1331852, A1210477 and S63845, as these were used to generate the data in this thesis.

Putative mimetic	Proposed target	Apoptosis BAK/BAX dependent?	Binding affinity in Nanomolar range?	Appropriate biomarkers?
Gossypol[1]	Pan-BCL2	No[12, 13, 15, 18]	No- µMolar[2]	Does not kill CLL cells[13,19] or platelets[19] Induces NOXA expression[13,19]
Agossypol[2]	Pan-BCL2	No[12, 13]	No- µMolar[2]	Does not kill CLL cells[13] Induces NOXA expression[13]
S1[3]	Pan-BCL2		No- µMolar [3]	Does not kill CLL cells[13, 20] or platelets[20] Induces NOXA expression[13,20]
HA14-1[4]	BCL2	No[12, 13, 18]	No- µMolar [4]	Does not kill CLL cells at low concentrations[13] Induces NOXA expression[13]
2 Methyloxy Antimycin A3[5]	BCL2, $BCLX_L$	No[13, 18]	No- µMolar[5]	Does not kill CLL cells at low concentrations[13] Induces NOXA expression[13]
Obatoclax (GX15-070)[6]	Pan-BCL2	No[12, 13,15]	No- µMolar[6]	Does not kill CLL cells at low concentrations[13] Induces NOXA expression[13]
BXI-61[7]	$BCLX_L$	N.D	Yes[7]	Does not kill platelets[21] Induces NOXA expression[21]

BXI-72[7]	$BCLX_L$	N.D	Yes[7]	Does not kill platelets[21] Induces NOXA expression[21]
TW37[8]	BCL2, $BCLX_L$, MCL1	N.D	BCL2, MCL1- nM[8] $BCLX_L$ -μM[8]	Does not kill CLL cells[14] Induces NOXA expression[14]
MIM1[9]	MCL1	N.D	No- μMolar[9]	Does not kill MCL1 dependent cells[14] Induces NOXA expression[21]
UMI-77[10]	MCL1	Yes[17]	Yes[10]	Induces NOXA expression[21]
Maritoclax[11]	MCL1	Yes[16]	No- μMolar[11]	Induce death in cells lacking MCL1[16]

Table 1-3 Molecules previously thought to be BH3 mimetic

Putative BH3 mimetic, their target proteins and criticisms are indicated. N.D-not determined. 1(Kitada, *et al* 2003), 2 (Becattini, *et al* 2004), 3 (Zhang, *et al* 2007), 4 (Wang, *et al* 2000), 5 (Tzung, *et al* 2001), 6 (Nguyen, *et al* 2007), 7 (Park, *et al* 2013), 8 (Verhaegen, *et al* 2006), 9 (Cohen, *et al* 2012), 10 (Abulwerdi, *et al* 2014), 11 (Doi, *et al* 2012), 12 (Vogler, *et al* 2009b), 13(Albershardt, *et al* 2011), 14 (Varadarajan, *et al* 2013), 15 (Tse, *et al* 2008), 16 (Varadarajan, *et al* 2015), 17 (Wei, *et al* 2015), 18 (van Delft, *et al* 2006), 19 (Soderquist, *et al* 2014b), 20 (Soderquist, *et al* 2014a), 21 (Soderquist and Eastman 2016)

BH3 mimetic	Year published	Target Protein and binding affinities	Development stage
ABT-737 [1]	2005	$BCLX_L$ (Ki <0.5nM, IC_{50} 1nM) BCL2 (Ki <1nM, IC_{50} 103nM) BCLW (Ki <0.9nM)	Lab use only (low oral bioavailability)
ABT-263 [2]	2008	$BCLX_L$ (Ki <0.5nM) BCL2 (Ki< 1nM) BCLW (Ki<1nM)	Phase I/II clinical trials (NCT00788684, NCT0048109, NCT03181126)
BM-1197 [3]	2014	$BCLX_L$ (Ki< 1nM, IC_{50} 5.2nM) BCL2 (Ki 0.7nM, IC_{50} 3.5nM)	Derivative BM-1252 (APG-1252) in phase I clinical trials (NCT03387332, NCT04001777, NCT03080311)
S44563 [4]	2014	$BCLX_L$ (IC_{50} 140nM) BCL2 (IC_{50} 131nM)	
BCL2-32 [5]	2014	$BCLX_L$ (Ki 8.5nM) BCL2 (Ki 3.3nM)	
Compound 32 (BM1074) [6]	2013	$BCLX_L$ (Ki <1nM, IC_{50} 6.9nM) BCL2 (Ki <1nM, IC_{50} 1.8nM)	
ABT-199 [7]	2013	BCL2 (Ki <0.01nM)	FDA approved

S55746 [8]	2018	BCL2 (Ki 1.3nM)	Phase I clinical trials (NCT02920697)
WEHI-539 [9]	2013	$BCLX_L$ (Ki< 1nm, IC_{50} 1.1nM)	Superseded by A1155463
A1155463 [10]	2014	$BCLX_L$ (Ki <0.01nM)	Superseded by A1331852
A13331852 [11]	2015	$BCLX_L$ (Ki <0.01nM)	Pre-clinical
Compound 9 [12]	2013	MCL1 (IC_{50} 310nM)	
A1210477 [13]	2015	MCL1 (Ki 0.454nM, IC_{50} 26.2nM)	
Compound 34 [14]	2015	MCL1 (Ki 3nM)	
S63845 [15]	2016	MCL1 (Ki<1.2nM)	Derivative S64315/ MIK665 in phase I clinical trials (NCT02992483, NCT02979366, NCT03672695)
AMG176 [16]	2018	MCL1 (Ki 0.05nM)	Phase I clinical trials (NCT03797261- Suspended to evaluate safety)
AZD5991 [17]	2018	MCL1 (Ki 0.002nM, IC50 0.72nM)	Phase I clinical trials (NCT03218683)

Table 1-4 Characterisation of bone fide BH3 mimetics

Confirmed BH3 mimetics, their target proteins and binding affinity and their stage in development, FDA Food drug administration. References for each drug are annotated by numbers correlating to the following: 1- (Oltersdorf*, et al* 2005), 2(Tse*, et al* 2008), 3(Bai*, et al* 2014), 4(Nemati*, et al* 2014), 5 (Adam*, et al* 2014), 6(Aguilar*, et al* 2013), 7(Souers*, et al* 2013), 8 (Casara*, et al* 2018), 9 (Lessene*, et al* 2013), 10 (Tao*, et al* 2014), 11 (Leverson*, et al* 2015a), 12 (Richard*, et al* 2013), 13 (Leverson*, et al* 2015b), 14 (Burke*, et al* 2015), 15 (Kotschy*, et al* 2016), 16 (Caenepeel*, et al* 2018), 17 (Tron*, et al* 2018).

1.7.1 ABT-737 and ABT-263

BCL2, $BCLX_L$ and BCLW inhibitor, ABT-737 was first discovered in 2005 using nuclear magnetic resonance (NMR)-based screening and structure based design (Oltersdorf*, et al* 2005). Based on solved structures and mutagenesis studies, hydrophobic pockets 2 and 4 (P2 and P4) were identified on BCL2 and $BCLX_L$ as essential binding hotspots (Sattler*, et al* 1997). Chemical linking of fragments that bound in these pockets created a molecule which had nano-molar binding affinity to $BCLX_L$, BCL2 and BCLW, known as ABT-737 (Oltersdorf*, et al* 2005). This molecule induced apoptosis in cells in a BAK/BAX dependent manner and synergised with MCL1 downregulation (van Delft*, et al* 2006, Vogler*, et al* 2009b).

ABT-737 is a hugely useful laboratory tool but it is not successful as a drug due to its poor oral availability (Lessene*, et al* 2008, Tse*, et al* 2008). Modifications led to the development of ABT-263 (also known as Navitoclax), (Tse*, et al* 2008). ABT-263 maintained binding specificity affinity for the anti-apoptotic proteins (Ki <1nM for BCL2, $BCLX_L$ and BCLW) (Tse*, et al* 2008). In a side by side study comparing the two compounds, ABT-737 killed CLL cell more efficiently, which could be accounted for by ABT-263's increased albumin binding (Vogler*, et al* 2010).

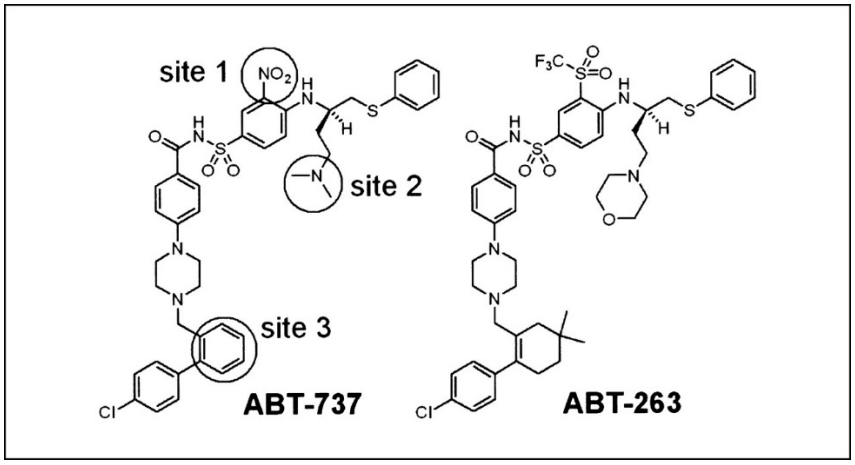

Figure 1-15 Displayed chemical structures of ABT-737 and ABT-263
Displayed structures of ABT-737 and ABT-263. Sites of modification are indicated on ABT-737. Taken from (Tse*, et al* 2008)

ABT-263 has been found to be an effective single agent treatment for some B-cell malignancies and non-small cell lung cancer with dependence on either BCL2 or $BCLX_L$

and low MCL1 expression in both cell and xenograft models (Tse*, et al* 2008, Vogler 2014). The addition of ABT-263 to chemotherapeutic agents resulted in a significantly greater response *in vitro* and *in vivo* (Ackler*, et al* 2010, Chen*, et al* 2011). Single agent and in combination with immuno/chemotherapy phase 1 and 2 trials in R/R CLL showed promising activity (Kipps*, et al* 2011, Roberts*, et al* 2015, Roberts*, et al* 2012, Wilson*, et al* 2010). In one study, 35% of patients achieved a partial response and 27% maintained stable disease for more than six months (Roberts*, et al* 2012). A phase 2 trial of previously untreated CLL using CD20 antibody rituximab with and without ABT-263 found significantly better responses when used in combination (Kipps*, et al* 2015). Both studies observed similar response rates between patients with and without 17p deletions, indicating that the drug could be effective for patients with p53 deletions/mutations (Kipps*, et al* 2015, Roberts*, et al* 2015). The major dose-limiting toxicity was thrombocytopenia due to on target effects of $BCLX_L$ inhibition and their role in platelet survival (Kipps*, et al* 2015, Roberts*, et al* 2015, Roberts*, et al* 2012). It has also been indicated that ABT-737 could induce autophagy by disrupting the BCL2/xL:Beclin1 interaction (Maiuri*, et al* 2007). This is yet to be evaluated *in vivo*. Due to the development of BCL2 specific ABT-199 (see 1.7.2), which displayed fewer cytotoxicities, most lymphoid malignancy trials with ABT-263 have been completed/ withdrawn without progression, with the exception of a trial combining the two molecules (NCT03181126). There are still several active trials assessing the safety and efficacy of ABT-263 as a single agent and in combinations in solid cancers (NCT02143401, NCT02520778, NCT02079740, NCT03366103, NCT01989585).

1.7.2 ABT-199

It was hypothesised that the inhibition of BCL2 could be an effective therapy for lymphoid malignancies whilst sparing platelets and preventing thrombocytopenia. The BCL2 inhibitor, ABT-199 (venetoclax), was developed as a derivative of ABT-263 (Souers*, et al* 2013). Due to the limited effect on platelets, higher concentrations of the compound are accepted *in vivo* without cytotoxicities (Souers*, et al* 2013). Initial studies demonstrated that the compound had an effective response in various lymphoid cell models, xenografts and patient derived CLL cells (Souers*, et al* 2013). Exceptional responses were noted in CLL, a disease with high dependence on BCL2 (Del Gaizo

Moore*, et al* 2007, Souers*, et al* 2013). As the molecule is only selective for BCL2 it would not be potent in cancers which are dependent on other anti-apoptotic proteins but has been shown to enhance the efficacy of immune-chemotherapy (Souers*, et al* 2013). Interestingly, cells resistant to ABT-199 induced death have been shown to dissociate Beclin1 from BCL2, leading to autophagy (Bodo*, et al* 2016). The potential consequences of this have not been investigated *in vivo.*

A Phase I study of venetoclax monotherapy in R/R CLL documented an overall response rate (ORR) of 79% and complete response (CR) in 20% of those enrolled (Roberts*, et al* 2016). It was also reported that responses after a single dose were more efficacious and occurred more quickly than those seen after single dose of ABT-263 (Roberts*, et al* 2016). A phase 2 study in R/R CLL with 17p deletion documented similar results with an ORR of 74.9% (Stilgenbauer*, et al* 2016). Based on these results, in January 2015, the drug received Food and Drug Administration (FDA) Breakthrough therapy designation for patients with relapsed/ refractory (R/R) CLL with del(17p). A second Breakthrough designation was granted for ABT-199 in combination with CD20 antibody, Rituximab for patients with R/R CLL after the success of a Phase 1b study (ORR 86%) (Seymour*, et al* 2017). Conversely, a retrospective comparison of ABT-199 monotherapy or in combination with CD20 therapy in heavily pre-treated R/R CLL reported comparative outcomes between the groups (ABT-199 mono 81% ORR vs vombination 84% ORR) (Mato*, et al* 2019). In December 2016, the approval of treatment of R/R CLL with either del(17p) or patients who have previously failed BTK inhibitor treatment was granted by the European Medicines Agency (EMA) due to a successful phase 2 study of R/R CLL patients who have failed treatment with ibrutinib or idelalisib (Jones*, et al* 2016). Early trials indicated a high risk of tumour lysis syndrome (TLS), consequently ramp up dosage regimens and prophylaxis for high risk patients were implemented which has greatly reduced the incidence and severity of TLS (Cheson*, et al* 2017). A phase III trial investigating the effect of ABT-199 in combination with CD20 antibody, obinutuzumab, in previously untreated CLL patients reported 88.2% progression free survival at month 24 with a similar safety profile to that of immuno-chemotherapy (Fischer*, et al* 2019). This led to FDA approval of venetoclax in combination with CD20 antibody, obinutuzumab, as a chemotherapy free regimen for untreated CLL in May 2019 (Abbvie

2019a). ABT-199 has also received accelerated FDA approval for patients with acute myeloid leukeamia (AML) who are over the age of 75 or have comorbidities making them ineligible for chemotherapy (Abbvie 2018) which was based on the success of two ongoing trials (NCT02203773, NCT02287233).

Despite remarkable responses in CLL, response rates to ABT-199 in other non-hodgkin lymphomas vary. Initial trials in multiple myeloma (MM) documented promising results with an ORR of 21%, which increased to 40% for patients who harboured the t(14;18) translocation (Kumar*, et al* 2017). However trials were temporarily suspended after the treatment group had substantially higher mortality rates (Abbvie 2019c). The CANOVA trial was resumed in June 2019 after new mitigation measures and an updated protocol were put in place (Abbvie 2019b). The overexpression of BCL2 due to the t(14;18) translocation notwithstanding, the ORR in R/R FL is 38% (Davids*, et al* 2017). It has been hypothesised that sensitivity could be correlated to expression of BIM (Bodo*, et al* 2016). Of interest to the data in this report, it was reported that the mono-treatment of DLBCL with ABT-199 ORR was 18% (Davids*, et al* 2017). Results from the CAVALLI trial report that the addition of immune-chemotherapy (R or G-CHOP) increased the ORR to 88.9% (Zelenetz*, et al* 2019). Nonetheless, durable complete remissions can be achieved with mono-treatment of ABT-199 in DLBCL without significant toxicities (Walter*, et al* 2019).

Figure 1-16 Treatment of primary cutaneous DLBCL leg type with single agent ABT-199
Chemotherapy relapsed leg type DLBCL was treated successfully with single agent 400/800mg ABT-199. ^{18}F-labeled fluorodeoxyglucose–positron emission computed tomography images to show disease before **(A)**, and two months after treatment **(B)**. Photographs of disease before **(C)**, 7 days after **(D)** and 3 months after treatment with ABT-199 **(E)**. (Walter*, et al* 2019).

1.7.3 A1331852

Although ABT-263 caused platelet toxicity due to the inhibition of $BCLX_L$, the search for specific $BCLX_L$ inhibitors has continued. $BCLX_L$ has been indicated as a key anti-apoptotic protein in solid cancer and some haematological malignancies (Amundson*, et al* 2000). The first true inhibitor was WEHI-539, which was identified through High-Throughput Screening and structure guided medicinal chemistry (Lessene*, et al* 2013). However, its use was limited to a laboratory tool. A1155463 and an orally bioavailable version, A1331852, were developed through NMR screening (Tao*, et al* 2014). This compound selectively inhibits $BCLX_L$, as supported by the reversible thrombocytopenia in treated mice and the reduction of growth of $BCLX_L$ dependent tumours such as those in small cell lung cancer xenografts (Tao*, et al* 2014). The clinical efficacy of this drug is yet to be tested.

1.7.4 A1210477

The large, rigid binding pocket of MCL1 caused challenges in the development of specific MCL1 inhibitors. A1210477 is a MCL1 inhibitor derived by NMR-based fragment screen and structure-guided drug discovery (Leverson*, et al* 2015b). It has been shown to induce apoptosis in MM and NSCLC cell lines that are dependent on the protein (determined by siRNA and BH3 profiling) and synergize with the effects of ABT-263 and ABT-199 in a panel of cancer cell lines dependent on MCL1 (Leverson*, et al* 2015b). Studies have shown that cell death is BAK/BAX dependent without causing an upregulation of NOXA and despite its inhibition, MCL1 protein levels increase due to

increased protein stability and reduced degradation (Leverson*, et al* 2015b), confirming A1210477 is the first BH3 mimetic which selectively targets MCL1. Conversely, it has also been reported that A1210477 can induce cell death *via* cytochrome C release in a BAK/BAX independent manner without MOMP (Mallick*, et al* 2019). A1210477 exhibits sub-nanomolar binding affinity to MCL1 (Ki=0.45nM), yet micromolar concentrations are required to induce apoptosis, which limited its use (Leverson*, et al* 2015b).

1.7.5 S63845

A collaboration between Servier and Vernalis has led to the development of MCL1 specific S63845 (Ki <1.2nmol/l) by NMR-based fragment screening (Kotschy*, et al* 2016). It effectively induces BAK/BAX dependent apoptosis in MCL1 dependent cancer cells whilst sparing normal cells (Kotschy*, et al* 2016). S63845 is approximately 1000 times more potent than A1210477, due to reduced albumin binding and increased MCL1 affinity (Kotschy*, et al* 2016). The molecule has exhibited anti-tumour activity in MCL1 dependent haematological cell lines and could synergise with other small molecule inhibitors in solid cancer cell lines (Kotschy*, et al* 2016). As discussed previously, MCL1 is known to have other essential non-apoptotic functions and gene targeting of this protein has led to detrimental and fatal effects (Rinkenberger*, et al* 2000, Wang*, et al* 2013). Nonetheless, inhibition of MCL1 *in vitro* using S63845 was well tolerated at therapeutically efficacious doses in mouse cancer models (Kotschy*, et al* 2016). This indicates that other functions of MCL1 are not effected by drug inhibition or conditional inactivation of the protein is not as toxic as complete knock-out. S63845 has not progressed into clinic but a derivative, S64315/MIK665 (for which a structure has not been published) is in trials as a monotherapy for MM, DLBCL and AML (NCT02979366, NCT02992483) and in combination with ABT-199 for AML (NCT03672695). No data from these have been published yet.

1.7.6 Suggested mechanisms of sensitivity to BH3 mimetics

There is a clear need to identify biomarkers to distinguish patients which would be sensitive to ABT-199 to allow the rational use of this drug. This is particularly relevant for heterogeneous diseases such as DLBCL. BH3 profiling could prove to be an effective

method of determining protein dependence and therefore mimetic sensitivity. Some studies have found that the relative expression of apoptotic proteins could predict sensitivity to the BH3 mimetics (Pham*, et al* 2018). It is thought that non-targeted anti-apoptotic proteins may act as 'sink' to sequester BH3-only proteins in a process known as 'partner swapping'. One study reported that in MM cell lines co-expression of $BCLX_L$ and MCL1 corroborated resistance to ABT-199 (Punnoose*, et al* 2016). S63845 sensitivity has been inversely correlated to $BCLX_L$ mRNA expression level (Kotschy*, et al* 2016). Sensitivity to ABT-199 in FL has been associated to expression of BIM and the ratio of BCL2:BIM (Bodo*, et al* 2016). Conversely, studies have also suggested that BH3-only proteins are not required for MCL1 or $BCLX_L$ mediated apoptosis (Greaves*, et al* 2019). The dispensability of BH3-only proteins could be supported by a hypothesis that sensitivity to ABT-263 or A1210477 is determined by the abundance of $BCLX_L$-BAK and MCL1-BAK respectively (Dai*, et al* 2015a). PTMs of the anti-apoptotic proteins have also been implicated in sensitivity. Studies have indicated that the phosphorylation of BCL2 mediates resistance to ABT-199 (Deng*, et al* 2000, Konopleva*, et al* 2006, Song*, et al* 2016).

To this end, there have been several studies documenting that the con-current inhibition of multiple anti-apoptotic proteins is more effective than single treatment. Klanova and colleagues identified two subgroups within DLBCL which were susceptible to either BCL2 inhibition by ABT-199 or inhibition of MCL1 translation by homoharringtone (HHT) (the latter could be identified as expressing little/ no BCL2) (Klanova*, et al* 2016). The combination of both compounds was synthetically lethal in cell lines and xenograft models (Klanova*, et al* 2016). It is worth considering that HHT not only targets MCL1 but other short lived proteins, so the results like those in other studies which target MCL1 through cyclin dependent kinase inhibitors, cytostatics or NOXA amplification (Li*, et al* 2015, Liu*, et al* 2018, Phillips*, et al* 2015) may not be a MCL1 specific response. Nonetheless, inhibition of BCL2 and MCL1 using specific BH3 mimetics has shown promising results. The combination has been shown to be synergistic in multiple models, such as AML and mantle cell xenografts and T-cell acute lymphoblastic leukaemia cell lines and a zebrafish model (Li*, et al* 2019, Moujalled*, et al* 2019, Prukova*, et al* 2019).

1.7.7 Combinations of BH3 mimetics with other molecules

As with most cancers, relapse and resistance are inevitable. Combination therapies are thought to improve response rates, hence co-targeting anti-apoptotic proteins and other pathways to treat leukaemias/lymphomas have been an area of intense research. Due to its further stage in development, most of these studies have focused on ABT-199.

Although inhibiting BCL2 has an exquisite effect on circulating CLL cells, it has been suggested that cells in the lymph nodes could develop micro-environmental mediated resistance (Vogler*, et al* 2009a). CD40L and cytokine stimulation result in NFκB signalling and subsequent $BCLX_L$ and BCL2A1 upregulation (Vogler*, et al* 2009a). BCR stimulation has also been shown to upregulate MCL1 (Bojarczuk*, et al* 2016). Both mechanisms are thought to be able to shift dependency of anti-apoptotic proteins, conferring resistance to BCL2 specific ABT-199. This is supported by the immediate clearance of circulating malignant cells in CLL patients treated with ABT-199 whereas the clearance of disease in lymph nodes and bone marrow is much slower (Leverson and Cojocari 2018, Roberts*, et al* 2017). Conversely, the observation of TLS in early trials of ABT-199 in R/R CLL was the result of the clearance of bulky disease (Roberts*, et al* 2016). Assessment of disease clearance from lymph nodes has not been fully characterised and it is unclear whether cells in these niches are killed at these sites or if they killed during migration (Leverson and Cojocari 2018). Nonetheless, the evacuation of malignant cells from nodes to the periphery blood has been proposed to increase the efficacy of BCL2 inhibitors.

BTK inhibitors such as ibrutinib, reduce activity of the NFκB pathway and mobilise malignant cells due to disrupted BCR signalling and have consequently been identified as a potential combination treatment with ABT-199 (Byrd*, et al* 2013). Ibrutinib has received FDA approval for the treatment of R/R CLL, MCL, and Waldenstom's macroglobulinemia (Kuo*, et al* 2017). One study has reported complete/ partial responses in 37% in ABC DLBCL patients (Wilson*, et al* 2015). Despite these notable responses, ibrutinib monotherapy is limited due to partial remissions and the emergence of resistance mutations (Cervantes-Gomez*, et al* 2015).

Multiple studies have indicated that the combination of ABT-199 and BTK inhibitors would be therapeutically advantageous than either molecule alone (Cervantes-Gomez*, et al* 2015, Deng*, et al* 2017, Hillmen*, et al* 2019, Kuo*, et al* 2017, Mathews Griner*, et al* 2014). Serial samples from CLL patients after ibrutinib treatment exhibited decreased MCL1 expression and increased sensitivity to ABT-199 (Cervantes-Gomez*, et al* 2015). Furthermore, BH3 profiling has been used to show a shift in dependence to the BCL2 protein after ibrutinib treatment, providing rationale for combining the molecules (Deng*, et al* 2017). This data led to a phase II study in R/R CLL combining ibrutinib and venetoclax (CLARITY) which reported 89% of patients responded and 51% achieved complete remission (Hillmen*, et al* 2019). It has been reported that inhibitors of NFκB can further propagate the cytotoxicity of the ABT-199/ibrutinib combination *ex vivo* in CLL and MCL (Jayappa*, et al* 2017).

Studies within DLBCL have also suggested that the combination is successful. A high throughput screen of ABC DLBCL cell lines identified a synergistic relationship ibrutinib and ABT-199 (Mathews Griner*, et al* 2014). This has been supported by the generation of an ibrutinib resistant ABC DLBCL cell line which expressed elevated BCL2 levels and increased sensitivity to ABT-199 (Kuo*, et al* 2017). The synergistic combination of these compounds was observed in this generated cell line and other DLBCL cell lines (Kuo*, et al* 2017). There is an ongoing clinical trial testing the efficacy of combining ABT-199, ibrutinib and CD20 antibody, rituximab in R/R DLBCL (NCT03136497). Other studies have suggested that the downregulation of MCL and subsequent sensitising of cells to ABT-199 is more effective with inhibitors of other kinases within the BCR pathway such as SYK (Bojarczuk*, et al* 2016).

JAK/STAT signalling through IL-4 stimulation has been found to regulate IgM expression and thus BCR signalling (Aguilar-Hernandez*, et al* 2016). Consequently, the JAK/STAT pathway has been suggested to mediate resistance to ABT-199 (Karjalainen*, et al* 2017). Combinations of JAK 1/2 inhibitors and ABT-199 have displayed synergism in AML and CLL patient samples and AML xenografts (Karjalainen*, et al* 2017) (Blunt*, et al* 2017).

MCL1 downregulation can also be achieved with PI3K inhibitors. Dual inhibitor of PI3K-δ and PI3K-γ, duvelisib, is currently in late stage clinical assessment of haematological

malignancies but complete remissions are rare (Patel*, et al* 2017). GEP of CLL patients who have undergone treatment with duvelisib revealed increased expression of BCL2 (Patel*, et al* 2017). Consequently, samples post-treatment displayed higher sensitivity to ABT-199 compared to pre-treatment samples (Patel*, et al* 2017). Synergistic activity of ABT-199/ PI3K inhibitors has been observed in a range of DLBCL, FL, AML and MCL cell lines and xenograft models (Choudhary*, et al* 2015a, Faia*, et al* 2018, Lee*, et al* 2015, Rahmani*, et al* 2018). This has been supported by a study which found that short and long term exposure to ABT-199 resulted in downregulation of PTEN and subsequent upregulation of the PI3K pathway (Pham*, et al* 2018). PI3K and AKT small molecule inhibitors have been shown to perpetuate the effect of ABT-199 in ABT-199 sensitive DLBCL and MCL cell lines (Pham*, et al* 2018). It has been suggested that both intrinsically resistant and acquired resistant DLBCL cell lines utilise the AKT pathway for survival, hence providing rationale for combining PI3K inhibitors and ABT-199 (Pham*, et al* 2018).

Cyclin E/ cyclin dependent kinase (CDK) 2 activity has been reported to phosphorylate MCL1 in its PEST domain, resulting in increased protein stability (Choudhary*, et al* 2015b). CDK9 is a transcriptional regulator of MCL1 (Chen*, et al* 2014). Due to the degradation of MCL1, several studies have found that CDK inhibitors can synergistically kill lymphoma/ leukaemia cells when used in combination with ABT-199 (Bogenberger*, et al* 2017, Chen*, et al* 2014, Chen*, et al* 2016, Choudhary*, et al* 2015b, Dey*, et al* 2017, Zhou*, et al* 2018). CHK1 inhibition has also been proposed to downregulate MCL1 expression via a CDK dependent mechanism enhancing the effect of ABT-199 in AML (a typically MCL1 dependent disease) (Zhao*, et al* 2016).

TP53 mutations are commonly observed in malignant cells, however their frequency is much lower in haematological cancers compared to solid tumours (Pan*, et al* 2017). Genetically modified colon cancer cells which have constitutive high p53 expression have an increased mitochondrial priming which is susceptible to $BCLX_L$ inhibition (Le Pen*, et al* 2016). This has also been confirmed via BH3 profiling (Le Pen*, et al* 2016). As previously mentioned, p53 activity upregulates pro-apoptotic NOXA (which inhibits MCL1) and PUMA (which can directly activate the effectors). However, the cell death induced upon $BCLX_L$ inhibition was unaffected by transcriptional inhibition (Le Pen*, et al* 2016).

Moreover, p53 activator, idasanutlin (RG7388) does not have a significant effect on MCL1 mRNA level (Pan*, et al* 2017) suggesting the mechanism of p53 priming is independent of its transcriptional targets. Instead it has been hypothesised that p53 activation regulates MCL1 phosphorylation (via the MAPK pathway) thus resulting in the degradation of MCL1 and increased dependence on BCL2 and $BCLX_L$ (Pan*, et al* 2017). Studies have found that the combination of p53 activators or MAPK inhibitors and ABT-199 is synergistic in p53 wildtype AML models, a disease which is typically MCL1 dependent (Han*, et al* 2019, Lehmann*, et al* 2016, Pan*, et al* 2017). Furthermore, the addition of ABT-199 to p53 activator treated cells promoted cell death as opposed to G1 arrest (Lehmann*, et al* 2016, Pan*, et al* 2017).

In addition to high expression of $BCLX_L$ and MCL1, the expression of BCL2A1 has also been proposed as a mechanism of resistance to ABT-199 (Esteve-Arenys*, et al* 2018). In a panel of DH cell lines, patient samples and mouse xenografts, low ABT-199 sensitivity correlated to high BCL2A1 expression which could be overcome by BET bromodomain inhibitor CPI203 (Esteve-Arenys*, et al* 2018).

As mentioned previously, the mitochondria structure is dysregulated during apoptosis (Frank*, et al* 2001). Treatment with BH3 mimetics, ABT-199, A1331852 and S63845 have been reported to induce mitochondrial swelling, loss of matrix density, mitochondrial fragmentation and ruptured outer mitochondrial membranes independent of/ upstream of caspase activity in sensitive cells (Henz*, et al* 2019). A genome wide clustered regularly interspaced short palindromic repeats (CRISPR) /CRISPR associated protein 9 (Cas9) screen in AML identified proteins involved in mitochondria structure, such as caseinolytic peptidase B protein homolog (CLPB) that are upregulated in the disease and mediate resistance to ABT-199 (Chen*, et al* 2019a). It has been suggested that targeting CLPB results in cristae remodelling and mitochondria stress therefore making the cells more susceptible to ABT-199 and cell death (Chen*, et al* 2019a). ABT-199 resistant generated AML cell lines displayed a higher number of more dense cristae accompanied by higher levels of CLPB (Chen*, et al* 2019a). Down-regulation of CLPB using either sgRNA or shRNA re-sensitised cells to ABT-199 (Chen*, et al* 2019a).

Taken together, there have been several pathways which have been proposed to mediate resistance to ABT-199, the targeting of which is synergistic in combination with ABT-199. The mechanisms of such pathways typically result in the downregulation of other anti-apoptotic proteins $BCLX_L$ or MCL1, hence increasing dependence on BCL2 and susceptibility to ABT-199.

1.7.8 Acquired resistance to ABT-199

Patients who have undergone treatment with ABT-199 often acquire resistance. Multiple studies have attempted to define the underlying mechanism using either resistant cell lines derived from chronic exposure to the mimetic or patient sample analysis. AML cell line models have suggested that resistance is caused by an upregulation of expression and switch in dependence of anti-apoptotic proteins, MCL1 or $BCLX_L$ (Konopleva*, et al* 2006, Lin*, et al* 2016). Co-targeting these proteins during ABT-199 treatment delayed the emergence of resistance (Konopleva*, et al* 2006, Lin*, et al* 2016). However, a different study found conflicting results, as upregulation of MCL1 did not cause resistance to ABT-737 (Vogler*, et al* 2009a). Instead, it was suggested that NFκB activation upregulated $BCLX_L$ and BCL2A1, which lead to resistance. Generated FL resistant cell lines had a reduced expression of BCL2 and almost no expression of BIM (Bodo*, et al* 2016). A more comprehensive study of genetic and protein expression level in seven NHL ABT-199 resistant derived cell lines identified that there several mechanisms of resistance (Tahir*, et al* 2017). Similar to previous studies, derived cell lines exhibited an upregulation of either $BCLX_L$ or MCL1, which became sensitive to their respective inhibitors (Tahir*, et al* 2017). Some cell lines also had a reduced expression of BIM or BAX (Tahir*, et al* 2017). Moreover, one derived cell line was BAX deficient, which could be traced back to a BAX deficient sub-clone in the parental cell line (Tahir*, et al* 2017). Changes in the BCL2 family expression were sometimes associated to gene copy number gains/losses but they also occurred without such changes (Tahir*, et al* 2017). This indicates protein expression changes could also be regulated by altered signalling pathway. Elevated MCL1 protein was not always associated to an increased mRNA level, suggesting there is an increase in protein stabilisation (Tahir*, et al* 2017). Taken together this suggest there are multiple mechanisms of protein expression changes.

Conversely, resistant cells generated from murine human-like MCL models only exhibited a temporary change in anti-apoptotic protein expression, which reversed upon drug withdrawal (Fresquet*, et al* 2014). However missense mutations F101C and F101L in murine BCL2 and G179E in murine BAX were detected in the resistant cells but not the parental (Fresquet*, et al* 2014). The BCL2 mutations were shown to impede interactions with ABT-199 (Fresquet*, et al* 2014) and the BAX mutation located in the C-terminal prevented mitochondrial localisation and subsequent activation (Fresquet*, et al* 2014). The murine F101 residue in BCL2 corresponds to human F104. Subsequent surface plasma resonance (SPR) studies with human BCL2 $^{F104L/C}$ confirmed the reduced binding affinity to ABT-199 and solved structures of BCL2^{F104L}: ABT-199 identified a reduced P2 area as the likely cause (Birkinshaw*, et al* 2019). These mutations have not been reported in patients who have undergone ABT-199 treatment. However, the BCL2^{F104I} mutation has been observed in ABT-199 relapsed FL (Blombery*, et al* 2019b). SPR analysis confirmed that this mutation resulted in ~300 fold decrease in binding affinity to ABT-199 (Blombery*, et al* 2019b).

Alternatively, a novel G101V mutation has been identified as a mediator of resistance to ABT-199 in CLL. In one study, 7 out of 15 relapsed patients harboured this mutation at progression but it could not be detected at study entry (Blombery*, et al* 2019a). This mutation, impedes the interaction between BCL2 and ABT-199 by reducing the binding affinity ~180 fold (Blombery*, et al* 2019a). Further analysis of this mutation has revealed that the reduced binding is due to the large valine side chain causing a knock on effect on adjacent residue E152, resulting in a slight change to the P2 pocket (Birkinshaw*, et al* 2019). The proportion of cells containing this mutation at time of progression varied between 26-60%, indicating sub-clonality or other causes of resistance (Blombery*, et al* 2019a). Separation of subclones within one patient's disease allowed the identification of another mechanism of resistance (Blombery*, et al* 2019a). One clone contained the G101V mutation but it was absent from the major subclone, which displayed increased $BCLX_L$ expression (Blombery*, et al* 2019a). An independent study has also found the BCL2^{G101V} mutation in 3 out of 4 relapsed CLL patients (Tausch*, et al* 2019). This study also reported novel mutation D103Y, which occurred on another subclone within a disease also containing the G101V mutation (Tausch*, et al* 2019).

It is most likely that there are several mechanisms of resistance and it may be malignancy or patient specific. As there is further development of other BH3 mimetics, resistance will ensue with likely distinct mechanisms. These are yet to be characterised. From current data is it not clear whether these mechanisms of resistance arise from selection of resistant subclones or involve adaptive responses and 'rewiring' of cells. Resistany mutations identified could not be detected at earlier time points but it is possible that the mutation was present but at a frequency too low for detection.

1.8 Aims of the study

Currently, patients with DLBCL have several therapeutic options, but there is no screening/ selection process to determine the best treatment option for each individual patient. The primary aim of this study is to identify biomarkers which can define subgroups of the disease based on the cells' dependence to each of the anti-apoptotic BCL2 family members. There is a hope that this can be translated clinically by matching patients to the rational use of BH3 mimetics. A comparative study of a panel of DLBCL cell lines using immuno-blot analysis to assess BCL2 protein expression will be performed. These data will be compared to the cell lines' responses to BH3 mimetics (ABT-737, ABT-199, A1331852 and S63845) assessed by Cell Titer Glo and Annexin/PI staining. This information may indicate a correlation between protein abundance and sensitivity to the drugs. In conjunction with this, a functional assay, BH3 profiling, which has been suggested to accurately predict the cells' dependence on anti-apoptotic proteins, will be used to compare with this data and assess its efficacy. It is possible that some cell lines will have joint dependence on multiple anti-apoptotic proteins. For this reason, the effect of combining BH3 mimetics in a panel of cell lines will also be investigated.

Although primary resistance is a major barrier to widespread use of BH3 mimetics in aggressive B-cell malignancies, it is likely that, as in CLL, acquired resistance to BH3 mimetics will become a significant problem. The second aim of this project is to investigate the molecular basis of this using resistance generated cell lines derived from sensitive parental cell lines. BH3 mimetic resistant cell lines will be developed from extremely sensitive DLBCL cell lines. Two RIVA cell lines resistant to ABT-737 and ABT-199 will be generated and compared to their parental counterpart via drug sensitivity, protein expression, BH3 profiling and sensitivity to other specific inhibitors. This data may allow a hypothesis to be made about acquired resistance to BCL2 inhibition. RCK8 cell lines resistant to ABT-737 and A1331852 will also be generated and characterised in a similar way.

2 Materials and Methods

2.1 Cell culture

2.1.1 Cell lines

DLBCL cell lines were provided by Professor M. Dyer. RCK8, RIVA, SUDHL-2, SU-HDL-6, SUDHL-8, SUDHL-10, TMD8, TMD8 RO, TMD8 RI, CTB-1, U2932, U2946, HBL-1, MedB1, RAD, AME and Pfeiffer were maintained in RPMI-1640 with L-glutamine (Gibco 11875093) supplemented with 10% fetal bovine serum (FBS) (Sigma F9665) and 1% penicillin and streptomycin (P/S) (Gibco 10378016). OCI-LY1, OCI-LY3 and OCI-LY10 were maintained in IMDM with L-glutamine (Gibco 12440053) supplemented with 20% FBS, 1% P/S and 0.0004% β-mercatoethanol (Sigma-Aldrich M6250). Wildtype and BAX/BAK double knock out (DKO) MEFs were provided by Doctor M. Vogler and cultured in DMEM high glucose medium (Thermo Fisher 41965039) supplemented with 10% FBS and 1% P/S. All cultures were incubated at 37°C in a humidified atmosphere with 5% CO_2. Cells were passaged every 3-4 days once the flasks became approximately 80% confluent. Cells were routinely STR profiled and tested for mycoplasma contamination.

2.1.2 Cell counting

Cells were counted using the BioRad TC20 automated cell counter following manufacturer's instructions. Cell suspensions were mixed at a 1:1 ratio with trypan blue stain (Sigma-Aldrich T8154) to assess cell viability and loaded into cell counting slides (BioRad 1450011). The slide was inserted into the instrument and cell number and percentage of live cells were recorded.

2.1.3 Resistant generated cell lines

Resistant cell lines, RIVA-737R, RIVA-199R, RCK8-737R and RCK8-A133R were generated from parental RIVA or RCK8 cells by continual, increasing treatments with ABT-737, ABT-199 or A1331852, respectively. T25 flasks were seeded with $5x10^6$ cells in 10ml of RPMI-1640 plus 10% FBS and 1% p/s and maintained at 37°C with 5% CO_2. Initial treatment started at 0.3nM of compound. Every 3-4 days, $5x10^6$ cells were seeded into new flasks

and apoptosis was measured via AnnexinV/PI stain analysis with flow cytometry (2.3-Flow cytometry). If the fraction of cells alive were more than 70%, the drug concentration was increased. If number of cells alive were between 30 and 70%, the drug treatment was kept at the same concentration. If less than 30% of the cells were alive, the cells were allowed to recover without the addition of drug. After 30 passages, at least 1000x resistant cell lines were established, they were sub-cultured in the presence of 0.3uM of their corresponding drugs. Control flasks with an equal volume of dimethyl sulfoxide (DMSO) (Sigma-Aldrich 41640) treatment were also maintained under the same conditions to ensure results were not due to long term culture.

Cell lines TMD8 ONO-4059 resistant (TMD8 RO) and TMD8 ibrutinib resistant (TMD8 RI) were generated and provided by the Dyer lab using the method described above.

2.1.4 Isolation and culture of PBMCs

Peripheral blood (PB) was obtained from consenting patients with DLBCL and stored in the Dyer Lab biobank with appropriate ethics. Peripheral blood mononuclear cells (PBMCs) were isolated from whole blood using density gradient separation. Typically, 20-30ml of PB was taken from patients into heparinised test tubes. Heparinised blood was diluted 1:1 v/v with sterile phosphate buffered saline (PBS) (Sigma-Aldrich D8537). 25-30ml of diluted blood was layered onto 15ml Histopaque density medium (Sigma-Aldrich 10771) in 50ml falcon tubes. The samples were centrifuged at 400g for 30 minutes at room temperature without brakes. As the components of blood vary in density, after centrifugation the blood is separated into a top layer of plasma, a thin white layer of PBMCs, a layer of Histopaque medium and a sediment of red blood cells. The PBMC layer in-between serum and Histopaque was carefully collected using a Pasteur pippette. The cells were re-suspended in 30ml of warm RPMI-1640 media, centrifuged at 250g for 10 minutes at room temperature and the supernatant was discarded. Cells were re-suspended in 10ml RPMI-1640 with L-glutamine supplemented with 10% FBS and 1% p/s, and counted (see 2.1.2- Cell counting). The proportion of B-cells within each sample were quantified via flow cytometry (see 2.3.2). Cells were either used immediately or resuspended in FBS supplemented with 10% v/v DMSO and stored at -80°C or liquid nitrogen.

When required, stored PBMCs were thawed, resuspended in 10ml of RPMI-1640 with L-glutamine supplemented with 10% FBS and 1% p/s and centrifuged to remove DMSO. Cells were resuspended in an appropriate volume of RPMI-1640 with L-glutamine supplemented with 10% FBS and 1% p/s and rested overnight at 37°C in a humidified atmosphere with 5% CO_2 to remove apoptotic cells before further their use in further assays.

2.2 CellTiter-Glo Viability Assay

Cell lines were seeded at $4x10^4$ cells per 100µl/ well in a 96-well plate and were incubated for 24-72 hours with specific compounds either as a single agent or in combination at concentrations varying between 0-10µM (see Table 2-1). PBMCs from patient samples were seeded at a higher concentration of $1x10^5$ cells per 100 µl/ well and were incubated for 24 hours due to their reduced rate of cellular division and increased rate of spontaneous apoptosis.

Compound	Target	Supplier
ABT-737	BCL2, $BCLX_L$, BCLW	Selleck Chemicals (S1002)
ABT-199 (venetoclax)	BCL2	Selleck Chemicals (S8048)
A1331852	$BCLX_L$	Selleck Chemicals (S7801)
S63845	MCL1	AppexBio (A8737)
Selumetinib	MEK1/2	Selleck Chemicals (S1008)
CAL-101 (Idelaslib)	PI3K	Selleck Chemicals (S2226)
Palbociclib	CDK4/6	AppexBio (B7798)
IMD-0354	IKKβ	Selleck Chemicals (S2864)
Ibrutinib	BTK	Selleck Chemicals (S2680)
CUDC-907	PI3K and HDAC	Selleck Chemicals (S2759)
Fedratinib	JAK2	Selleck Chemicals (S2736)
MG-132	Proteasome	Selleck Chemicals (S2619)

Table 2-1 List of compounds used.

Cell viability was measured using CellTiter-Glo (Promega G7572). 5% v/v of the reagent was added to each well and incubated for 5 minutes in the dark at room temperature before the luminescent signal was measured using a HidexSense plate reader. The

luminescent output is relative to the amount of adenosine triphosphate (ATP) present, which is proportional to the number of cells present and their rate of metabolism (based on the equation in Figure 2-1). Data were normalised to control samples (treated with an equal volume of DMSO). Cell line experiments were performed in technical duplicates with a minimum of three biological replicates. Primary sample experiments were performed in technical triplicates but, due to the nature of the samples, biological replicates were not always possible.

Figure 2-1 The luciferase reaction.
Mono-oxygenation of luciferin is catalyzed by luciferase in the presence of Mg^{2+}, ATP and molecular oxygen (Taken from Promega 2015).

2.3 Flow cytometry

2.3.1 Cell death analysis

Fluorescein isothiocyanate (FITC) conjugated AnnexinV was used to measure externalisation of phosphatidylserine and propidium iodide (PI) staining was used to determine membrane integrity, to measure the percentage of cells which were undergoing apoptosis/necrosis. Cells were treated with compounds as in 2.2 for 8-72 hours before resuspension in 150µl annexin buffer (10mM 4-(2-hydroxyethyl)-1-piperazineethanesulfonic acid (HEPES), 150mM NaCl, 5mM KCl, 1mM $MgCl_2$, 1.8mM $CaCl_2$ [pH7.4]) and stained with 0.3 µg/ml AnnexinV-FITC and 0.25µg/ml of PI (Sigma Aldrich P4170). Samples were analysed via flow cytometry using either a BD FACSCanto II or a Beckman Coulter Cytoflex. Cells were gated by forward and side scatter to exclude debris (Figure 2-1). 10^4 events within this gate were detected by the 530/30 nm and 585/42 nm wavelength filters and quantified (Figure 2-1). Compensation was performed using single stained samples. Data analysis was performed using FlowJo.

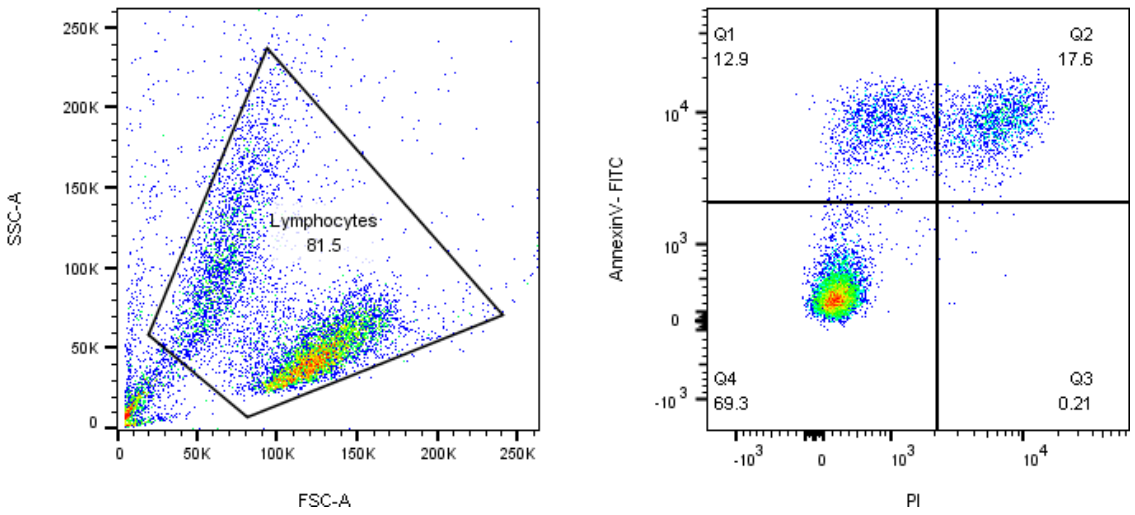

Figure 2-2 A representative gating for AnnexinV PI staining *via* flow cytometry
Cells were gated by forward and side scatter to exclude debris. Cells (lymphocytes) were detected by the 530/30nm (FITC) and 585/42nm (PE) filters to quantify cells positive for annexinV and or PI respectively.

2.3.2 Quantification of B-cells within PBMCs

The percentage of B-cells were assessed within PBMC samples using a fluorescent conjugated CD19 antibody. $2x10^5$ cells were washed in 500µl of sterile PBS before resuspension in 100µl fluorescence activated cell sorting (FACS) buffer (2% FBS (BSA) v/v in PBS). Samples were stained with 1% v/v CD19-PE (Biolegend 302207) (concentration determined based on previous titration experiments) for 20 minutes in the dark at 4°C. Samples were washed with 500µl of FACS buffer and resuspended in 300µl of FACS buffer for immediate analysis via flow cytometry. If samples were not analysed immediately they were fixed using FACS buffer with 2% v/v PFA for 20 minutes in the dark at 4°C. Samples were washed and resuspended in with 300µl of FACS buffer and stored in the dark at 4°C until analysis. Samples were analysed via flow cytometry using a BD FACSCanto II. Cells were gated by forward and side scatter to exclude debris (Figure 2-3). 10^4 events within this gate were detected by the 530/30nm wavelength filter and quantified (Figure 2-3). Data analysis was performed using FlowJo.

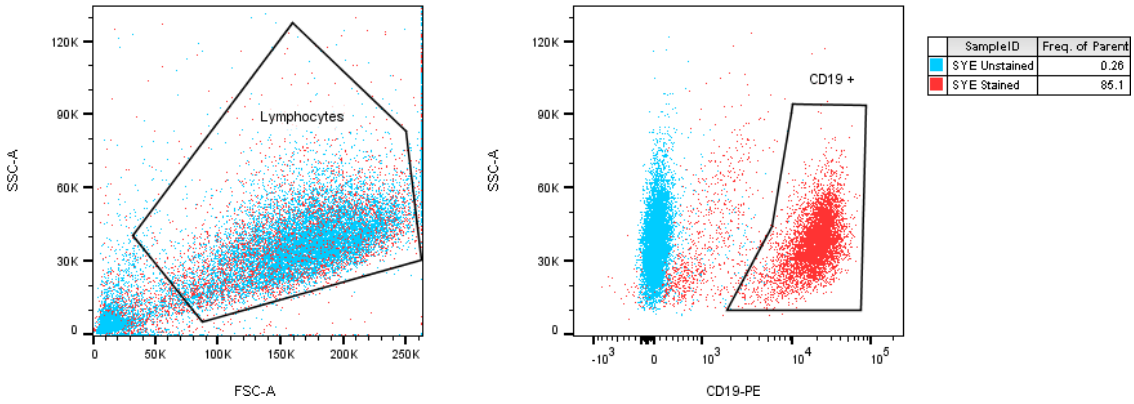

Figure 2-3 A representative gating for CD19 quantification *via* flow cytometry
Cells were gated by forward and side scatter to exclude debris. Cells (lymphocytes) were detected by the 530/30nm (FITC) filter to quantify cells positive for CD19. Representative plot shown is for sample SYE. Unstained cells are in blue, those incubated with CD19-PE are in red. Percentage of cells positive for CD19 are indicated.

2.4 Immunoblot

2.4.1 Cell lysate preparation

All steps were carried out at 4˚C or on ice. Cell pellets were collected from cell lines or patient PBMCs by spinning $5x10^6$ cells at 250g for three minutes. Cells were washed once with ice cold PBS. The pellets were re-suspended in 50-100µl whole cell lysis buffer (150mM NaCl, 20mM TrisHCl, 0.5% TritonX [pH 8], 1x protease inhibitor cocktail [Sigma-Aldrich P8340] and 1x phosphatase inhibitor cocktail 2 [Sigma-Aldrich P5726]). The suspension was left for 15 minutes on ice with intermittent vortexing. Samples were centrifuged at 16,000g for 15 minutes at 4°C. The supernatant was removed, and this was used as the cell lysate. Samples were either analysed immediately or stored at -80°C until required.

2.4.2 Bradford assay

A Bradford assay was used to quantify the protein concentration of the samples harvested. A Tecan Infinite F50 plate reader was used to measure the absorbance of 1ul of the sample in 200µl of Pierce Coomassie plus assay reagent (Thermo Fisher 23236) at A595nm. The protein concentration could be determined using a standard curve, which was generated using known concentrations of bovine serum albumin (BSA) (Thermo Fisher 23209) diluted in the assay reagent.

2.4.3 SDS-Page gel electrophoresis and transfer

50-75µg of total protein was mixed with sample buffer (60mM Tris-HCl [pH6.8], 5% glycerol, 2% SDS, 2.5% β-mercaptoethanol,0.05% bromophenol blue) in the ratio of 1:1 and was denatured by heating to 95°C for three minutes. Proteins were separated by sodium dodecyl sulphate polyacrylamide gel electrophoresis (SDS-PAGE) using 10-15% resolving gel with 4% stacking gel (Table 2-2) Gels were submerged into an electrode tank filled with SDS electrode running buffer (25 mM Tris, 192 mM glycine, 0.1% SDS). ThermoFisher Scientific page ruler plus prestained protein ladder (26620) was run simultaneously in lane 1 as a reference marker. An electric current of 110v was applied to the tank to separate proteins by molecular weight.

	Resolving Gel (10%)	Stacking Gel (4%)
Tris pH8.8	0.375M	0.125M
SDS	0.1%	0.1%
Acrylamide	10%	4%
Ammonium Persulfate (APS)	0.1%	0.1%
Tetramethylethylenediamine (TEMED)	0.1%	0.1%
dH_20	-	-

Table 2-2 Recipe for SDS-PAGE gels used for immunoblot

Once the loading dye had run to the bottom of the gel, the gel was removed and placed flat on to a nitrocellulose membrane. This was sandwiched between transfer buffer-soaked filter paper and sponges and placed into the electrode tank with transfer buffer (25 mM Tris, 192 mM glycine, 10% methanol) and an ice block. A current of 350mAmps was applied for 90 minutes.

The membrane was blocked against non-specific binding for a minimum of 30 minutes using 5% BSA w/v in PBS supplemented with 0.05% Tween-20 (Thermo Scientific TA-125-TW) (PBS-T). The membrane was incubated in the target primary antibody diluted in PBS-T overnight at 4°C (Table 2-3). The membrane was washed thrice in PBS-T for ten minutes and incubated in the corresponding secondary antibody for one hour at room

temperature (Table 2-4). Membranes were washed two more times with PBS-T for 10 minutes and once with PBS for 10 minutes. Membranes were scanned using the LiCOR Odyssey imaging system. Proteins were quantified by measuring the densitometry of bands using the LiCOR associated Image Studio software. Values were normalised against the loading control (α-tubulin).

Target Protein	Source	Clonality	Dilution	Supplier
BCL2	Mouse	Monoclonal (4D7)	1:1000	Oncogene (OP91)
BCL2	Mouse	Monoclonal (124)	1:1000	Dako (M0887)
$BCLX_L$	Rabbit	Polyclonal	1:1000	Abcam (ab32310)
MCL1	Rabbit	Polyclonal	1:1000	Santa Cruz (SC-819)
BCL2A1	Rabbit	Polyclonal	1:1000	Abcam (ab75887)
BCLW	Rabbit	Monoclonal (31H4)	1:1000	Cell signalling (2724)
BAK	Rabbit	Monoclonal (D4E4)	1:1000	Cell signalling (12105)
BAX	Rabbit	Polyclonal	1:1000	Abcam (ab7977)
BIM	Rabbit	Polyclonal	1:1000	Sigma (B7929)
NOXA	Mouse	Monoclonal (114C307)	1:1000	Abcam (ab13654)
PUMA	Rabbit	Polyclonal	1:1000	Abcam (ab9643)
Cytochrome C	Mouse	Monoclonal (7H8.2C12)	1:1000	Invitrogen (MA511674)
Caspase 3	Rabbit	Polyclonal	1:1000	Cell signalling (9962)
Caspase 8	Mouse	Monoclonal (1C12)	1:1000	Cell signalling (9746)
Caspase 9	Rabbit	Polyclonal	1:1000	Cell signalling (9502)
VDAC	Rabbit	Polyclonal	1:1000	Abcam (ab15895)
Tubulin	Mouse	Monoclonal (B-5-1-2)	1:5000	Sigma (T5168)

Table 2-3 Primary antibodies used for immunoblots.

Reactivity	Host	Dye conjugate	Dilution	Supplier
Rabbit	Goat	IRDye 680RD	1:5000	LiCOR (926-32210)
Mouse	Goat	IRDye 800CW	1:5000	LiCOR (926-68071)

Table 2-4 Secondary antibodies used for immunoblots.

2.4.4 Co-immunoprecipitation

Immunoprecipitation was performed using the following antibodies: hamster anti-BCL2 (BD Bioscience, 551051, Heidelberg, Germany), rabbit anti-$BCLX_L$ (Abcam, ab32370), rabbit anti-MCL1 (Enzo, ADI-AAP-240F), mouse anti-BAX (BD Bioscience, 610983) rabbit anti-BAK (Abcam, ab32371). Antibodies were crosslinked to Protein G dynabeads (Invitrogen, Karlsruhe, Germany). Cells were washed with ice cold PBS and suspended in 5PCV of CHAPS lysis buffer (Thermo Scientific 28300) for 30 minutes. Lysates were incubated overnight at 4°C with the antibody-Protein G complexes before washing of precipitates in lysis buffer and analysis by immuno- blotting (see 2.4.3).

2.5 RNA Analysis

2.5.1 RNA extraction

RNA was extracted from pellets of $1x10^6$ DLBCL cell lines using the ReliaPrep RNA cell miniprep system (Promega Z6011) according to protocol. Pellets were washed in ice cold sterile 1X PBS and centrifuged at 300g for 5 minutes. Pellets were resuspended in 250µl chilled BL+ TG buffer and passed through a 20-gauge needle 4-5 times before the addition of 85µl isopropanol. The lysate was transferred to a minicolumn in a collection tube and centrifuged at 14,000g for 30 seconds at room temperature. The minicolumn was washed in 500µl of RNA wash solution and centrifuged at 14,000g. Columns were incubated with 30µl of DNase I incubation mix, containing yellow core buffer, $MnCl_2$ and DNase I, for 15 minutes at room temperature. Columns were then washed with 200µl of column wash solution followed by 500µl of RNA wash solution, both centrifuged at 14,000g for 30 seconds. A final wash of 300µl of RNA wash solution was added to the column and centrifuged at 14,000g for two minutes before elution via the addition of 30µl of nuclease free water and centrifugation at 14,000g for one minute. The concentration of RNA and A_{260}/A_{280} ratio was assessed using the Nanodrop spectrophotometer (ThermoScientific).

2.5.2 Reverse transcription

cDNA was synthesised in duplicate using Superscript II reverse transcriptase (Invitrogen 18064). 1µl of 10mM dNTP mix (Thermo Scientific RO191) and 0.2µg of random primers (Thermo Scientific SO142) were added to RNA and the volume was made up to 12µl using RNase-free water in microcentrifuge tubes. Using a Techne Prime thermal cycler (5PRIME/02) samples were heated to 65°C for 5 minutes and then cooled to 10°C for one minute to allow for primer annealing. Samples were removed and 1x first-strand buffer, 0.01M dithiothreitol (DTT), 40 units of RNaseOUT (Invitrogen 1077-019) and 200 units of SuperScript II were added to each sample and gently mixed. Samples were briefly centrifuged and were returned to the thermocycler to be heated to 25° for 5 minutes, before being heated to 50°C for one hour. Finally, samples were heated to 70°C for 15 minutes and then held at 4°C. Control samples were also set up containing either no RNA or no reverse transcriptase. Samples were either used immediately or stored at -20˚C.

2.5.3 Quantitative polymerase chain reaction

cDNA was kept on ice and diluted 1:7 in RNase free water. Each reaction contained 5µl of cDNA, 10µl of SensiMix SYBR NO-ROX (QT650-05) and 100nM of each primer pair (see Table 2-5). Glyceraldehyde 3-phosphate dehydrogenase (GAPDH) was used as an endogenous control gene. Reactions were performed in triplicate in a 96-well plate format. The plate was sealed using Thermal Seal RTTM Sealing Film (Alpha Laboratories) and centrifuged briefly for 1 minute. The reactions were performed using a Lightcycler 480 Real Time PCR machine (Roche). Thermocycler conditions were 95˚C for 10 minutes followed by 40 cycles of denaturation at 95˚C for 15 seconds and annealing and elongation at 60˚C for one minute. Finally there was a dissociation cycle for melting curve analysis which was used to prove the specificity of the primers. Baseline threshold values for the amplification plots were adjusted to exclude background data.

Primer	Sequence
GAPDH	Forward: TCT CTG CTC CTC CTG TTC
	Reverse: GCC CAA TAC GAC CAA ATC C
BCL2	Forward: GGT GGG GTC ATG TGT GTG G
	Reverse: CGG TTC AGG TAC TCA GTC ATC C
BCL2L1 (BCLX)	Forward: GAG CTG GTG GTT GAC TTT CTC
	Reverse: TCC ATC TCC GAT TCA GTC CCT
BCL2L2 (BCLW)	Forward: GCG GAG TTC ACA GCT CTA TAC
	Reverse: AAA AGG CCC CTA CAG TTA CCA
MCL1	Forward: GTG CCT TTG TGG CTA AAC ACT
	Reverse: AGT CCC GTT TTG TCC TTA CGA
BAK1 (BAK)	Forward: ATG GTC ACC TTA CCT CTG CAA
	Reverse: TCA TAG CGT CGG TTG ATG TCG
BAX	Forward: CCC GAG AGG TCT TTT TCC GAG
	Reverse: CCA GCC CAT GAT GGTTCT GAT
BCL2L11 (BIM)	Forward: TTA GTT CTG AGT GTG ACC TAG G
	Reverse: GCT CTG TCT GTA GGG AGG TAG G
BAD	Forward: CCC AGA GTT TGA GCC GAG TG
	Reverse: CCC ATC CCT TCG TCG TCC T
BBC3 (PUMA)	Forward: GAC CTC AAC GCA CAG TAC GAC
	Reverse: AGG AGT CCC ATG ATG AGA TTQ T

Table 2-5 Primers used for Q-PCR

The relative expression of target genes was calculated using the double delta Ct equation as described below.

$$\Delta \mathbf{Ct}_{\mathbf{target}} = \mathbf{Ct}_{\mathbf{target}} - \mathbf{Ct}_{\mathbf{control\ gene}}$$

$$\Delta\Delta \mathrm{Ct}_{\mathrm{target}} = \Delta \mathrm{Ct}_{\mathrm{target}} - \Delta \mathrm{Ct}_{\ \mathrm{reference\ sample}}$$

$$\text{Expression Fc} = 2^{-\Delta\Delta \mathrm{Ct}}$$

2.6 BH3 Profiling

This method was adapted from Ryan and Letai, 2013 (Ryan and Letai 2013). All steps were performed at room temperature. DLBCL cell lines were counted, washed with PBS and resuspended in mannitol experimental buffer (MEB) (150mM mannitol, 50mM KCl, 20µM ethylenediaminetetraacetic acid (EDTA), 20µM ethylene glycol-bis(β-aminoethyl ether)-N,N,N',N'-tetraacetic acid (EGTA), 0.1% BSA, 5mM succinate 10mM HepesKOH [pH 7.5]). Cell suspensions were seeded at $5x10^5$ cells per 100µl/ well in a 96-well, black plate or $5x10^4$ cells per 10µl/ well in a 384-well, black plate. Cell concentration was optimised for DLBCL cell lines and was determined during titration experiments to allow for a maximal fold change between control values (DMSO and carbonyl cyanide-p-trifluoromethoxyphenylhydrazone (FCCP) treatments) whilst preventing large hyperpolarisations which result in overloading of the cells.

Wells were treated as required, either with 0.1-10µM of a peptide (see Table 2-6), 10µM FCCP (Sigma C2920) or an equal volume of DMSO. Immediately before anaylsis, e0ither 100µl (96-well plate) or 10µl (384-well plate) of freshly made 2x staining solution (25µM oligomycin (Sigma O4876), 0.005% w/v digitonin (Sigma D5628), 4µM JC-1 (VWR 89166-014) and 10µM β-mercaptoethanol in MEB) was added to each well. Digitonin concentration was optimised for DLBCL cell lines and was determined during titration experiments to allow for a maximal fold change between control values which are stable for several hours throughout the assay.

Fluorescence intensity (ex. 545nm +/- 10nm, em. 590nm +/- 10nm) was measured at 5 minute intervals for 120 minutes with intermittent shaking at 30°C using a HidexSense plate reader. This fluorescent signal is specific to the aggregate form of the probe which is proportional to mitochondrial membrane integrity.

Peptide	Binding partners	Sequence
BIM[1]	All	Ac-MRPEIWIAQELRRIGDEFNA- NH_2
BAD[1]	BCL2/W/X_L	Ac-LWAAQRYGRELRRMSDEFEGSFKGL-NH_2
MS1[2]	MCL1	Ac-RPEIWMTQGLRRLGDEINA-NH_2
XXa1_Y4Ek[3]	$BCLX_L$	Ac-RPEIWYAQGLKRFGDEFNAYKAR-NH_2
w-HRK[1]	$BCLX_L$	Ac-SSAAQLTAARLKALGDELHQY-NH_2
FS2[4]	BCL2A1	Ac-QWVREIAAGLRRAADDVNAQVER-NH_2

Table 2-6 Peptides for BH3 profiling
Synthetic peptides designed and published for their use for BH3 profiling. (1- Deng, *et al* 2007, Dutta, *et al* 2015, Foight, *et al* 2014, Jenson, *et al* 2017)

The area under each response curve (AUC) was calculated and normalised to the controls (DMSO and FCCP) based on the following formula:

$$\text{Depolarisation} = 1 - \frac{\text{AUC}_{\text{Sample}} - \text{AUC}_{\text{FCCP}}}{\text{AUC}_{\text{DMSO}} - \text{AUC}_{\text{FCCP}}}$$

2.7 Statistical analysis

The half-maximal response (EC_{50}) to drugs were calculated in GraphPad Prism using a sigmoidal dose response curve (unequal variance) based on CTG data with upper and lower constraints set to 100 and 0%.

To assess whether the EC_{50} drug responses, quantified protein expression and BH3 profile responses followed Gaussian distribution, D'Agostino & Pearson normality tests were performed in GraphPad Prism. As both the EC_{50} drug responses and BH3 profile responses followed Gaussian distribution, correlation analysis of these parameters were performed in GraphPad Prism using linear regression analysis and Pearson's coefficient. Conversely, the quantified protein expression did not follow Gaussian distribution and therefore correlation between EC_{50} drug responses and protein expression was assessed using linear regression analysis and Spearman's rank in GraphPad prism. Probability (P) values less than 0.05 were considered statistically significant.

Multiple unpaired t-tests were performed using Graphpad Prism to assess differences between BH3 profile responses, protein expression or mRNA level of the resistant

generated cell lines compared to their parental counterpart. All t-tests were performed on raw data (ΔΨm, protein densitometry relative to loading or ΔCT), not fold change values. P values were corrected for using the Holm-Sidak method and those less than 0.05 were considered statistically significant.

When two drugs are used in combination, their effects can be described as additive, antagonistic or synergistic (Chou, 2010). Combination indexes were calculated using Calcusyn via the Chou-Talalay method (Chou 2010, Chou and Talalay 1984). The significance of these values is presented in Table 2-7. In short, values below 0.9 are considered synergistic, values between 0.9-1.1 are additive and values above this are antagonistic.

Combination Index (CI)	Result
<0.1	Very strong synergism
0.1-0.3	Strong synergism
0.3-0.7	Synergism
0.7-0.85	Moderate synergism
0.85-0.9	Slight synergism
0.9-1.1	Nearly additive
1.1-1.2	Slight antagonism
1.2-1.45	Moderate antagonism
1.45-3.3	Antagonism
3.3-10	Strong antagonism
>10	Very strong antagonism

Table 2-7 Classification of combination index (CI) values
Classification of synergism in drug combination studies analysed by the Chou-Talalay method and represented as combination indices (CI). Adapted from (Chou 2008).

3 Results Chapter 1

3.1 Validation of BH3 Mimetics

A BH3 mimetic is a small molecule which can bind in the hydrophobic groove of an anti-apoptotic protein, displacing other bound proteins such as BH3-only proteins or BAK/BAX, and thus mimicking a sensitizer protein (Soderquist and Eastman 2016). There have been concerns about the selectivity of some these compounds (Soderquist and Eastman 2016, Vogler*, et al* 2009b). For this reason, it has been proposed that any potential BH3 mimetic should be validated to bind and induce intrinsic apoptosis in a BAK/BAX dependent manner with relevant biological markers (Lessene*, et al* 2008).

Several studies have shown that the mechanism of action of ABT-737, ABT-199, A1331852 and A1210477 is dependent on BAK and BAX and can induce typical biomarkers (Leverson*, et al* 2015a, Leverson*, et al* 2015b, Soderquist and Eastman 2016, Souers*, et al* 2013, Tao*, et al* 2014, Vogler*, et al* 2009b). During the course of this work, a novel MCL1 inhibitor, S63845 was developed (Kotschy*, et al* 2016). Although, it had been less characterised than the other mimetics, it was also used in this study.

To confirm the drugs used in this study were 'true' BH3 mimetics, murine embryonic fibroblasts (MEFs) were used, both wild type (WT) and those with BAK/BAK double knock out (DKO). After 72 hours incubation with varying concentrations of the mimetics, cell viability was assessed using Cell Titer Glo (CTG) (Figure 3-1 A). Cell death was also analysed by measuring PS externalisation by AnnexinV-FITC and cell membrane integrity by PI exclusion staining (Figure 3-1 B). As shown in Figure 3-1 B, there was more spontaneous cell death in the WT cells compared to the DKO without compound, most likely due to DKO cells lacking the ability to undergo intrinsic apoptosis. The WT MEFs were more resilient and require >0.3μM of each mimetic to induce apoptosis. The WT cells died at high concentrations of the mimetics, whereas there was little change in the DKO cells. This was recapitulated by the viability assay, as there was a greater reduction of viability in the WT cells compared to the DKO cells. The only concentration to affect the DKO cell's viability was at 10μM. Nonetheless, this viability measurement by CTG quantifies ATP generation and metabolism, so although it is indicative of cell growth

and life it does not directly measure cell death. In fact, annexinV/ PI staining confirms that this concentration does not cause cell death (Figure 3-1). This indicates that the off-target cytotoxicities caused by high concentration of the mimetics is impacting cell growth but the mechanism of cell death is BAK/BAX dependent.

Taken together, these data confirm previous findings that the mechanism of cell death by these drugs is BAK/BAX-dependent intrinsic apoptosis and therefore they are *bone fide* BH3 mimetics.

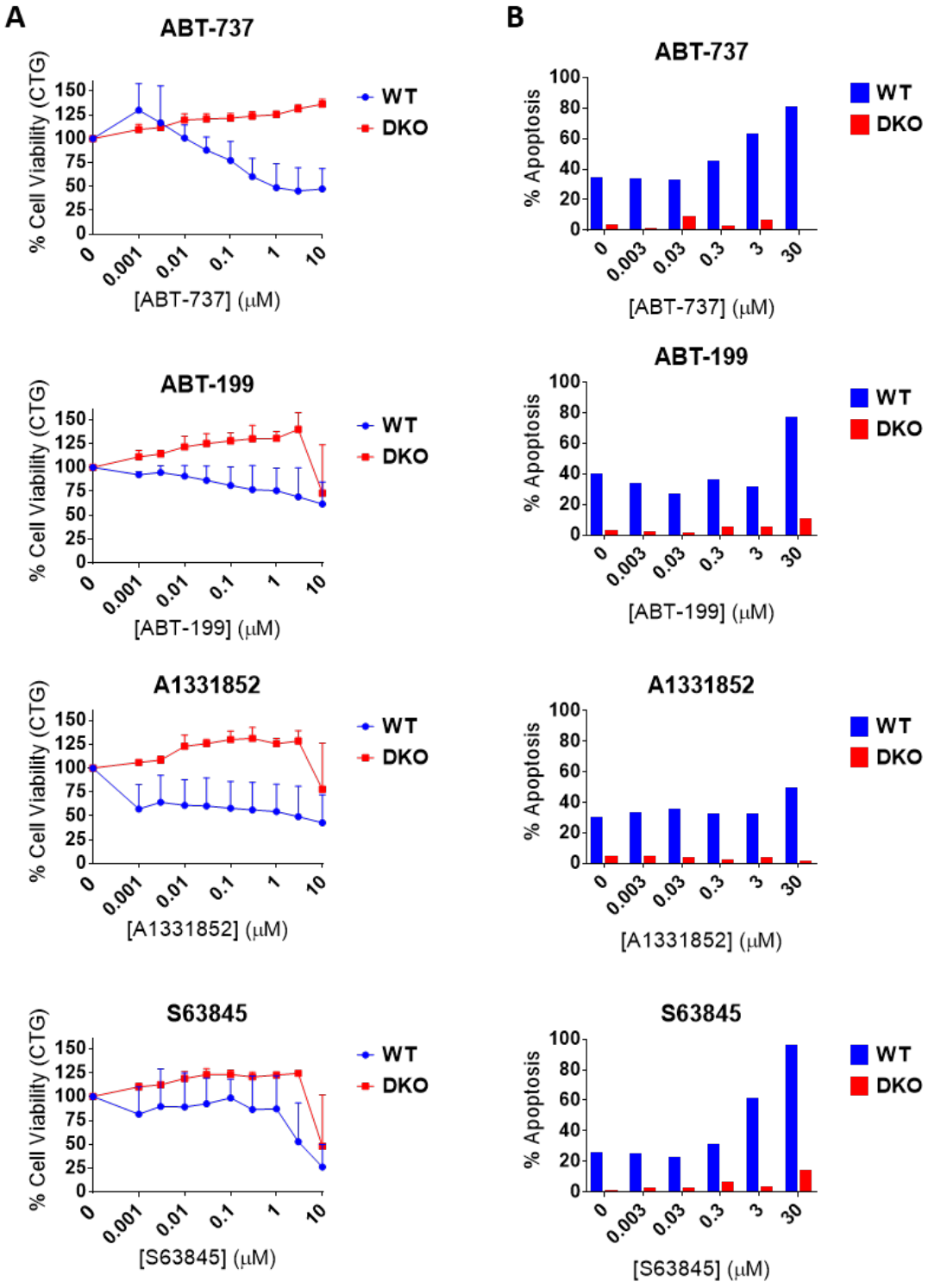

Figure 3-1 Validation of BH3 mimetics

A. Viability curves of WT and DKO MEFs. Cells were exposed to ABT-737, ABT-199, A1331852 and S63845 at 0-10 μM for 72 hours. Cell viability was analysed by CellTiterGlo viability assay. Data were normalised to DMSO treated control. Data are expressed as mean and standard deviation (SD) (n=3). **B. Cell death analysis.** Cells were exposed to 0-30 μM ABT-737, ABT-199, A1331852 and S63845 for 72 hours before cell death analysis by AnnexinV-FITC and PI staining measured via flow cytometry (n=1).

3.2 S63845 is a more potent MCL1 inhibitor than A1210477

As both A1210477 and S63845 were confirmed as 'true' BH3 mimetics that selectively target MCL1 (Kotschy, *et al* 2016, Leverson, *et al* 2015b), their effects were compared in a panel of DLBCL cell lines. Cells were incubated with the drug for 72 hours before analysis by CTG (Figure 3-2 A-B). Similar to previous findings, A1210477 had very limited effects in cell (Kotschy, *et al* 2016, Leverson, *et al* 2015b). In contrast, S63845 significantly reduced the viability of some of the cell lines that were unaffected by A1210477. As confirmed by the calculated EC_{50} values (Figure 3-2 C), S63845 was up to 4000x more potent in cell lines such as SUDHL10 and TMD8.

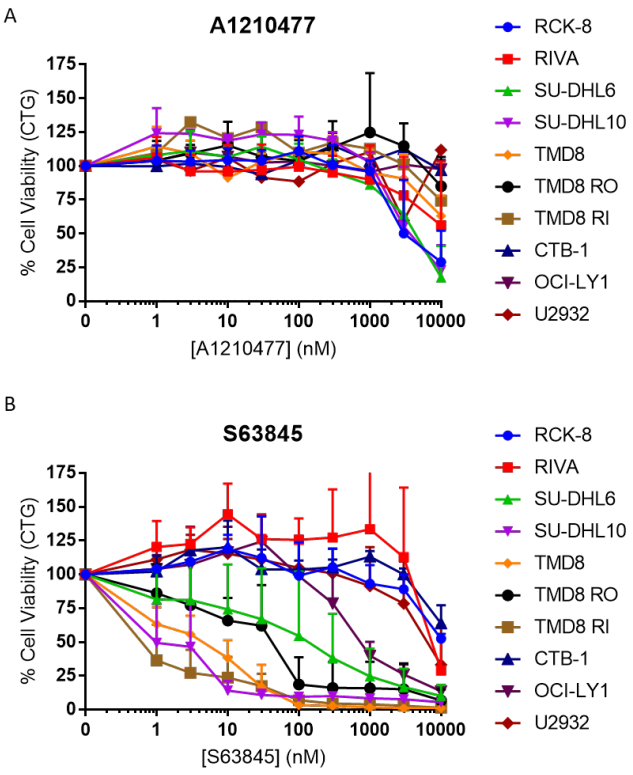

C

	EC_{50} (nM)	
	A1210477	S63845
RCK-8	3,987	10,682
RIVA	13,664	>10,000
SU-DHL6	4,036	**29.84**
SU-DHL10	3,998	**1.058**
TMD8	14,341	**3.362**
TMD8 RO	>10,000	**29.25**
TMD8 RI	>10,000	**0.2505**
CTB-1	>10,000	~ 10,683
OCI-LY1	>10,000	932.7
U2932	>10,000	6,485

Figure 3-2 Comparison of A1210477 and S63845 in DLBCL cell lines
DLBCL cell lines were plated and exposed to 0-10000nM of A1210477 (**A**) and S63845 (**B**) for 72 hours. Cell viability was analysed by CellTiterGlo viability assay. Data were normalised to DMSO treated control. Data are expressed as mean + SD (n>2). Corresponding EC_{50} values were calculated (**C**). Values in red represent sensitive responses (EC_{50} <100nM).

3.3 Heterogeneous response to BH3 mimetics in DLBCL patient samples

To test the sensitivity of primary DLBCL to BH3 mimetics, primary DLBCL cells were isolated from 8 patients (Table 3-1) and were exposed to different concentrations of

the specific mimetics, ABT-199, A1331852 and S63845 before cell death and viability analysis by AnnexinV/PI staining at 8 hours (Figure 3-3) and CTG at 24 hours (Figure 3-4). The use of specific mimetics denotes dependence on specific anti-apoptotic proteins.

Patient Sample	Age	M/F	COO	Other markers at diagnosis	Treatment status	Percentage of B-cells
AME	56	F	GCB	**FISH:** t(14;18)		87.8%
CAT						73.1%
CW						93.1%
ELV	29	F	ABC		Refractory to R-CODOXM-IVAC	89.5%
GRG	72	M	Non-GCB	**IHC**: BCL2+, p21-, p53- Ki-67 fraction low	Relapse to R-CHOP	75.9%
LSE	43	M	Non-GCB	**IHC:** BCL2+, p53-	Relapsed following R-CHOP and Ibrutinib	84.7%
RAD	56	M	Non-GCB	**IHC:** BCL2+ Ki-67 fraction ~50% **FISH:** MYC rearrangement	Refractory to R-CHOP	92.8%
SYE	77	M	Non-GCB	**IHC**: BCL2+ Ki-67 fraction high **Fish:** No MYC, BCL6 or BCL2 rearrangements	Relapsed following R-CHOP, treatment with ONO-4059 and CAL-101	85.1%

Table 3-1 Summary of patient samples
Information of patients whose samples have been used for this study. Where available, patient age, sex (male (M), female (F), cell of origin (COO) (germinal centre B-cell (GCB), activated B-cell (ABC), other markers at diagnosis determined by fluorescent in situ hybrisation (FISH) or immunohistochemistry (IHC) and treatment status at time the sample was taken is indicated. The percentage of B-cells within PBMC sample used is also indicated as determined via flow cytometry.

Despite only being in culture for a short period of time, the annexinV-FITC/PI staining revealed a high rate of spontaneous apoptosis within the samples. At time of analysis, the LSE sample was less than 10% alive and was therefore excluded from this analysis. The average cell death across all samples for the controls was 56.95%. This is likely due to the withdrawal of the cells from the essential interactions that occur within the tumour microenvironment. In particular, it has been suggested that CD40 (CD40L/ CD154) is essential for primary DLBCL long term culture (Ito*, et al* 2012). However such

culturing models have not been fully investigated and it is likely that the supra-maximal NFκB signalling induced by CD40L stimulation creates *in vitro* artefacts. As this study is investigating the effect of inhibiting anti-apoptotic proteins (of which several are downstream targets of NFκB), CD40L was not used in culture.

Nonetheless, cell death analysis after drug treatment can provide some insights into anti-apoptotic protein dependence within the samples. For example, AME and RAD were most sensitive to ABT-199 and therefore showed the greatest addiction to BCL2. In comparison, CAT and GRG showed a similar response to all mimetics and therefore equal dependence on these proteins. It is worth considering that there is not yet a specific inhibitor of BCL2A1 or BCLW that could be used to test for a greater dependence of these proteins. SYE also had a similar response to all mimetics but had greatest dependency on MCL1, as shown by the response to S63845. In contrast, ELV displayed a greater sensitivity to S63845 and therefore dependence on MCL1. Due to the low viability of the sample, it was difficult to distinguish between spontaneous and drug dependent death in CW; however, S63845 showed some response.

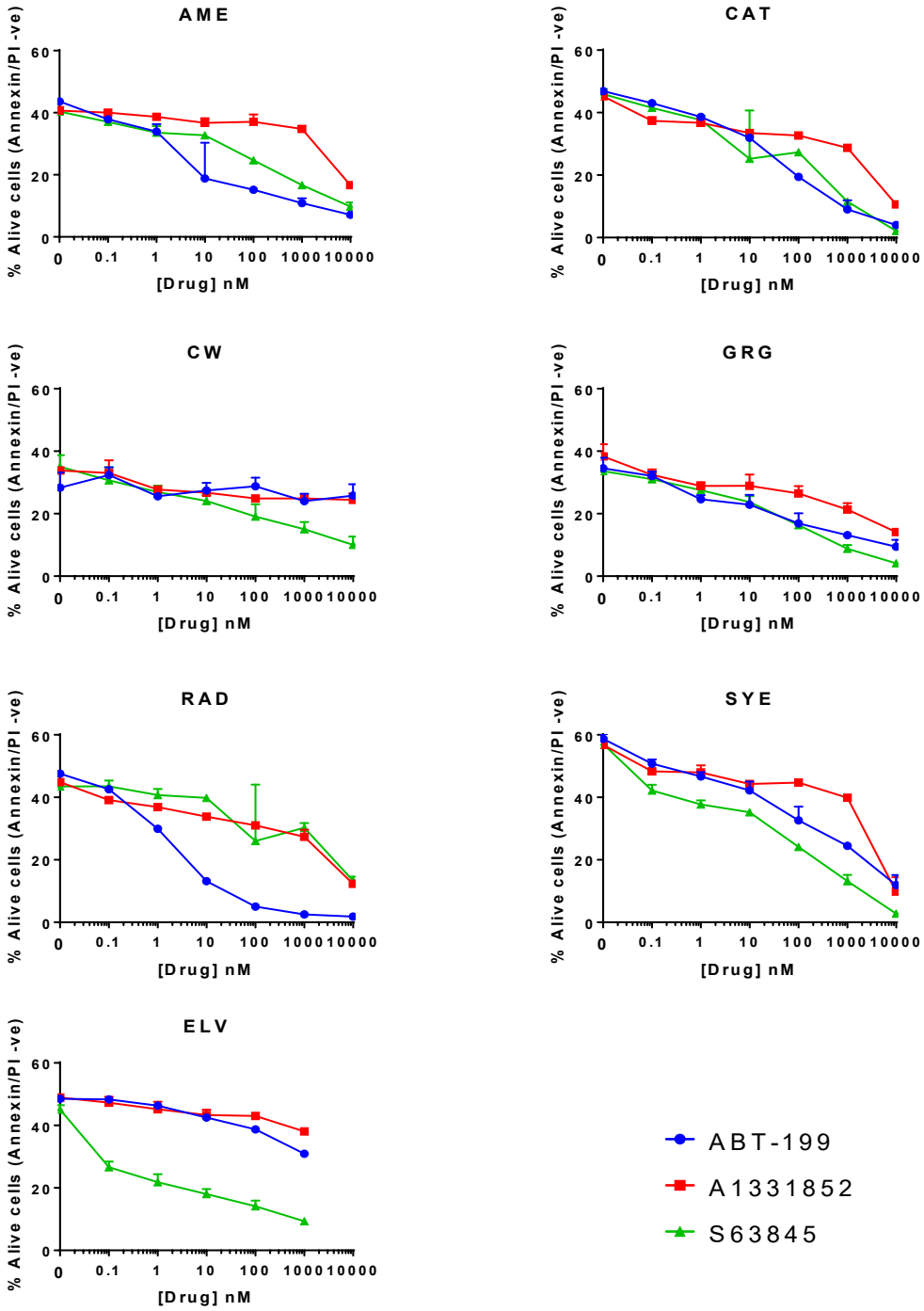

Figure 3-3 Cell death after treatment with BH3 mimetics in DLBCL patient samples
PBMCs isolated from DLBCL patients were incubated with 0-10,000nM concentrations of ABT-199, A1331852 and S63845 for 24 hours. Cell death was analysed by AnnexinV-FITC/PI staining measured by flow cytometry. DMSO was used as a time matched control. Experiments were performed in technical triplicate and data are represented as mean + SD.

Cell viability assays (normalised to control values) recapitulated many of the results seen with the death assay plus allowed greater interrogation into results that were previously only small changes (Figure 3-4). These data also confirmed that RAD was

dependent on BCL2. However, as the data have been normalised to their respective controls, it can be seen that RAD is more sensitive to ABT-199 than AME, a distinction which was hard to make previously. AME also appeared to have a joint dependence on MCL1 too. This was hard to distinguish based on the drug assay alone due to the variability and error bars of the previous data. CAT and GRG still exhibit similar responses to all mimetics but S63845 was more potent at lower concentrations in GRG. ELV displayed a clear dependence on MCL1 as it was only sensitive to S63845.

Taken together, all three proteins seem to be important to DLBCL cell survival, with samples exhibiting dependencies on one or more proteins. However, sample heterogeneity was high. Although there were no samples with a clear sole dependence on $BCLX_L$, there were samples, such as CW, that responded in a dose-dependent manner to A1331852.

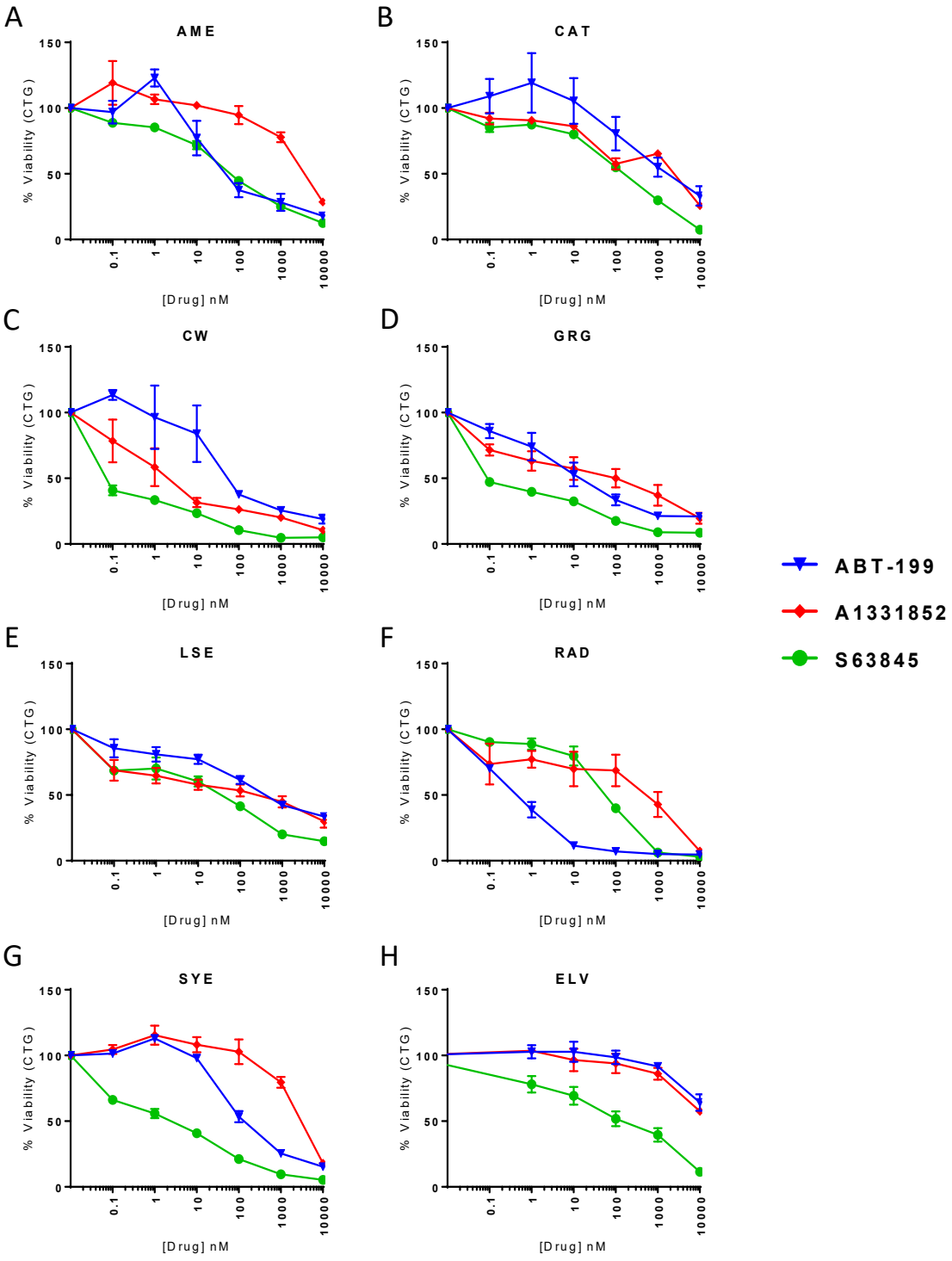

Figure 3-4 Cell viability after treatment with BH3 mimetics in DLBCL patient samples displayed by patient
PBMCs isolated from DLBCL patients were incubated with 0-10000nM of ABT-199, A1331852 and S63845 for 24 hours. Cell viability was analysed by CellTiterGlo viability assay. Data were normalised to DMSO treated control. Experiments were performed in technical triplicate and data are represented as mean +/- SD.

When the same CTG data are displayed separated by mimetic rather than by patient sample, the heterogeneity between samples is even more apparent (Figure 3-5). All

three drugs can induce a dose dependent response in some samples but the potency varied between patients.

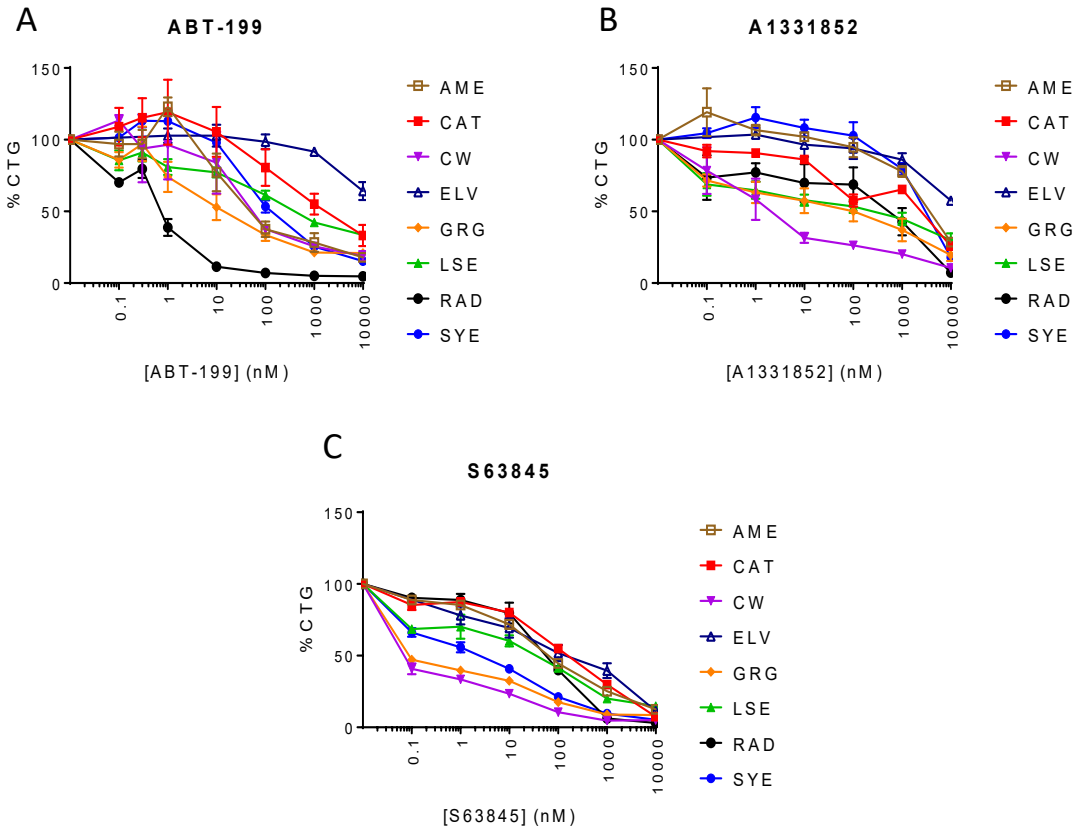

Figure 3-5 Cell viability after treatment with BH3 mimetics in DLBCL patient samples displayed by drug
Data from Figure 3-4 presented in a different format. PBMCs isolated from DLBCL patients were incubated with 0-10,000nM of ABT-199 **(A)**, A1331852 **(B)** and S63845 **(C)** for 24 hours. Cell viability was analysed by CellTiterGlo viability assay. Data were normalised to DMSO treated control. Experiments were performed in triplicate and data are represented as mean +/- SD.

3.4 Expression of anti-apoptotic proteins in DLBCL patient

Six out of eight patient samples were subjected to immuno-blotting to determine expression of the targeted anti-apoptotic proteins (Figure 3-6). α-tubulin was used as loading control and VDAC as a measure mitochondrial mass. As the proteins investigated in this study are often mitochondrially associated, it may be relevant to compare protein expression to relative mitochondrial mass. Unfortunately, due to the limited amount of sample, this could only be performed once and it is therefore inappropriate to quantify bands. Taken together with the reduced loading of RAD and AME (potentially due to quality of sample), it is difficult to make correlations between

protein expression and sensitivity to the specific inhibitors. Be that as it may, GRG, SYE and CW were mostly MCL1 dependent and appeared to express more MCL1 than the other samples. However, they expressed other anti-apoptotic proteins including BCL2 and $BCLX_L$. CW was sensitive to A1331852 yet its $BCLX_L$ expression was quite similar to other samples. Further correlations between expression and protein dependence may be possible when considering ratios between the anti-apoptotic proteins. For example RAD was solely dependent on BCL2 as only sensitive to ABT-199 and protein expression indicates a relatively high expression of BCL2 and low expression of $BCLX_L$ and MCL1.

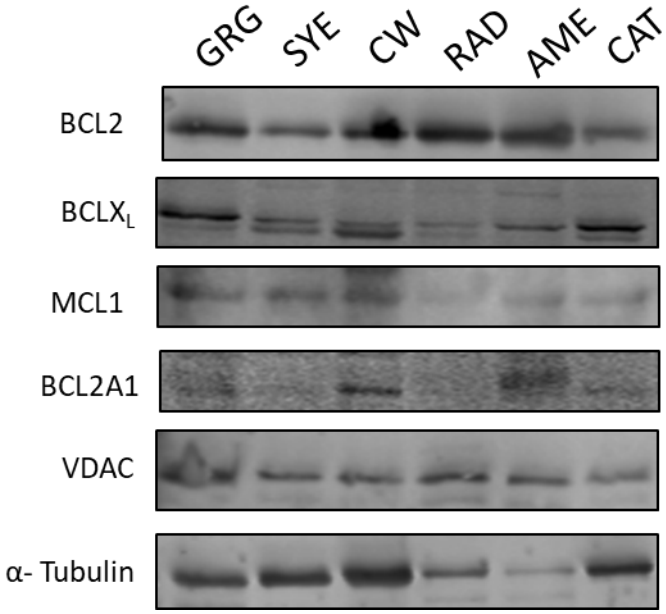

Figure 3-6 Expression of anti-apoptotic proteins in DLBCL patient samples
Whole cell lysates were prepared from the patient PBMC samples. 75µg of protein lysate was loaded in each lane. Expression of anti-apoptotic proteins were determined by immuno-blotting. α-tubulin was used as a loading control and VDAC was used an indicator or mitochondrial mass. (n=1).

3.5 Relapse after ibrutinib treatment does not affect response to BH3 mimetics

After the sample above was taken, patient ELV was treated with the BTK inhibitor, ibrutinib. The patient displayed a brief but dramatic response (including tumour lysis) before rapidly progressing. Analysis of a sample taken at time of progression indicates there was no great change in sensitivity to BH3 mimetics (Figure 3-7). There was a slight increase in sensitivity to BCL2 and $BCLX_L$ inhibition (both NFκB targets). However, response was still limited until higher concentrations were used and there remained a greater dependence on MCL1. Although worthwhile information, this change in ABT-

199 and A1331852 sensitivity must not be over-inferred or generalised, as this data is based on one patient for which there are no biological replicates.

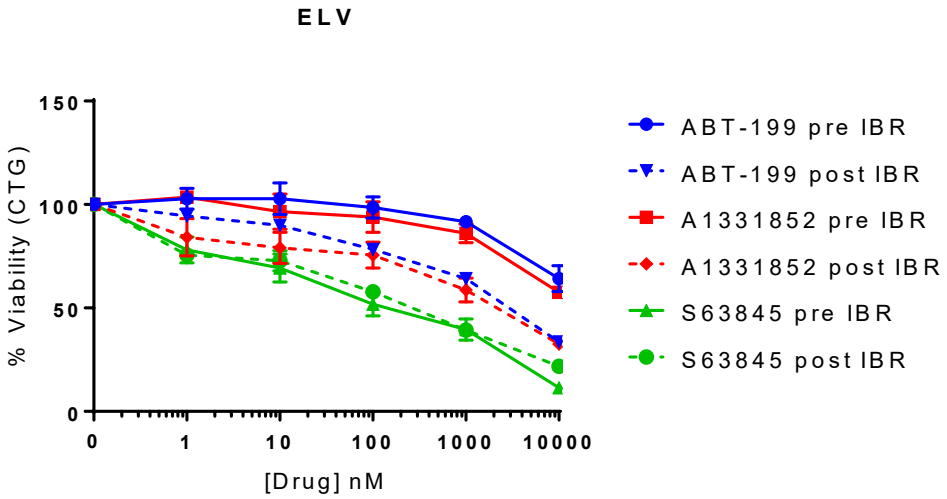

Figure 3-7 Response to BH3 mimetics after ibrutinib relapse
Serial samples from patient ELV (before and after relapse ibrutinib) were exposed to 0-10,000nM of ABT-199, A1331852 and S63845 for 24 hours. Cell viability was analysed by CellTiterGlo viability assay. Data were normalised to DMSO treated control. Experiments were performed in technical triplicate and data are represented as mean +/- SD.

Previous studies have also found that ibrutinib-resistant DLBCL cells had an increased sensitivity to ABT-199 (Kuo*, et al* 2017). The same study reported a synergistic effect of combining ABT-199 and ibrutinib in DLBCL cell lines and ibrutinib resistant cells (Kuo*, et al* 2017). This synergy was not displayed in ELV, as the addition of ibrutinib to ABT-199 treated cells had no additional effect (Figure 3-8).

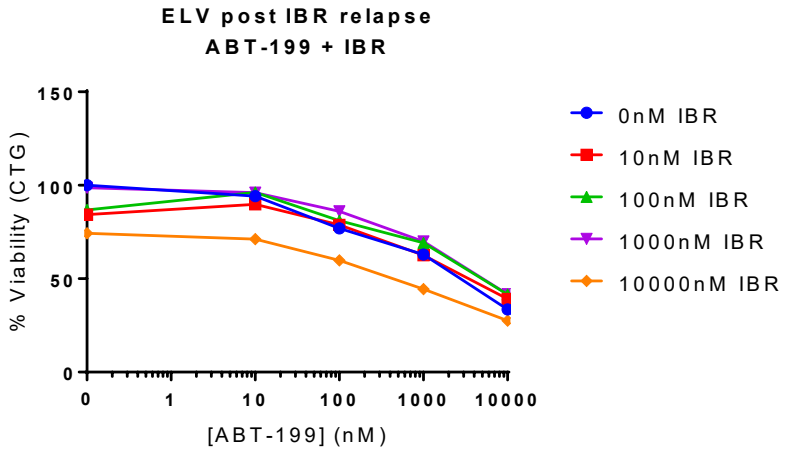

Figure 3-8 Combination of ABT-199 and ibrutinib in DLBCL patient sample after relapse to ibrutinib therapy
PBMCs isolated from ELV patient after relapse to ibrutinib (IBR) were exposed to 0-10000nM of ABT-199 in combination with 0-10,000nM ibrutinib for 24 hours. Cell viability was analysed by CellTiterGlo viability assay. Data were normalised to DMSO treated control. Experiments were performed in triplicate and data are represented as mean.

3.6 Side-by-side analysis of patient samples and cell lines

Two cell lines derived from patient samples RAD and AME, named UOL-RAD and UOL-AME respectively were generated by Dr. Sandrine Jayne in the Dyer lab. Analysis of these cell lines in comparison to the original patient samples allowed an investigation into the use of cell lines and how well they recapitulate primary samples. The derived cell lines were exposed to varying concentration of the BH3 mimetics and analysed by CTG (Figure 3-9).

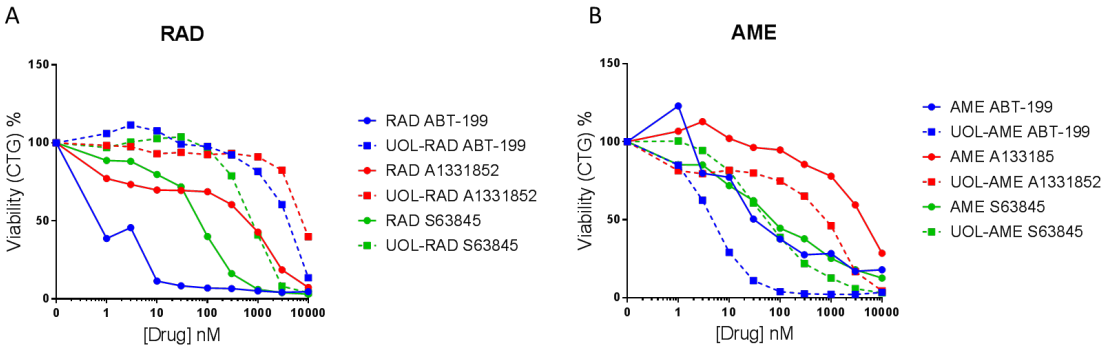

C

	EC_{50} (nM)			
	RAD	UOL-RAD	AME	UOL-AME
ABT-199	1.223	3472	69.48	4.663
A1331852	237	7768	3997	433
S63845	60.82	754.7	87.22	59.57

Figure 3-9 Comparison of response to BH3 mimetics in patient samples and derived cell lines
RAD (**A**) and AME (**B**) derived cell lines (UOL-RAD and UOL-AME respectively) were exposed to 0-10,000nM of ABT-199, A1331852 and S63845 for 72 hours. Cell viability was analysed by CellTiterGlo viability assay. Data were normalised to DMSO treated control. Data are represented as mean (n=4). These are shown on the same graphs as response of the primary samples from which the cell lines derive (data presented previously in Figure 3-4). **C.** EC_{50} values were calculated using Graphpad Prism. Values in red are <100nM, therefore represent sensitive responses.

Interestingly, the derived RAD cell lines became more resistant to all inhibitors compared to the patient sample (Figure 3-9). According to their calculated EC_{50} values (Figure 3-9 C), the cell line was 2800 more times resistant to ABT-199, 32 times more resistant to A133182 and 12 times more resistant to S63845. This is of particular importance for ABT-199 and S63845, as the patient sample was sensitive to the drugs (<100nM) and the cell line was not. Whether the changes that cause this resistance are acquired during growth in response to adaptation or whether they pre-exist in a sub-clone of the patient sample is not yet known.

During the generation of a cell line, there any many selective pressures due to the removal of cells from their microenvironment and inducing immortality. Moreover, the generation of the UOL-RAD cell line was achieved following passage in immuno-deficient mice (Dr Sandrine Jayne, unpublished observations). Therefore, it could be that the cell line is a result of an expansion of cells that are most adapted to grow in this environment. It may be of interest to perform immuno-phenotyping, deep sequencing and single cell studies of both samples to trace a sub-clone within the patient sample from which the cell line derived.

In contrast, the AME derived cell line, UOL-AME, became more sensitive to all of the mimetics. Despite this, the overall trend of sensitivity and dependence stayed the same with primary sensitivity to ABT-199 followed by S63845. Although the cell line is more sensitive to A1331852 compared to the patient sample, it remains resistant (>100nM). This cell line may mimic the patient sample response better than the RAD cell line as AME was generated through a more direct method: the malignant cells were directly seeded into culture media and grew spontaneously, perhaps reducing selective pressures during establishment.

Consequently, the use of cell lines may need to be taken with caution, as they do not always mimic original patient samples. However, it is worth considering that the responses seen in patient samples are based on the overall response of multiple clones and the cell line may represent only one or a few sub-clones within this, therefore becoming clinically relevant.

Due to the nature of the patient samples, response to mimetics could only be evaluated once (in technical triplicates), whereas the data presented for the cell lines is an average of 4 repeats. This may account for some variability between the samples such as with AME where the trend of sensitivity remained. Nonetheless, this highlights a key point: cell line models can provide unlimited samples, whereas primary cells are limited to amounts acquired at biopsies. Therefore, not only are the number of experiments/repeats restricted but, due to their susceptibility to spontaneous apoptosis, the types of experiments are also limited. For this reason, cell line models are an invaluable tool for interrogation of diseases such as DLBCL, but some restraint may be required when interpreting data without primary sample references.

3.7 Response to BH3 mimetics in DLBCL cell lines

As patient-derived DLBCL cells are limited and freshly isolated PBMCs are susceptible to spontaneous apoptosis, investigations were continued using DLBCL cell lines. Displayed in Figure 3-10 are the DLBCL cell lines used in this study along alongside the patient age and sex, COO, identified driver mutations and BCL2 family associated mutations and aberrations. UOL-AME and UOL-RAD are cell lines derived from patient sample as

described in Figure 3-9). TMD8 RO and TMD8 RI cell lines (provided by the Dyer lab), are derived from TMD8 with generated resistance to BTK inhibitors ONO-4059 (>1000x) and ibrutinib (>3000x) respectively.

The sensitivity of the DLBCL panel to ABT-737, ABT-199, A1331852 and S63845 mimetics were established by CTG (Figure 3-10). Due to the number of cell lines on each graph, error bars were excluded from this figure. The corresponding EC_{50} values for these drugs were calculated using GraphPad Prism and can be seen in Table 3-2.

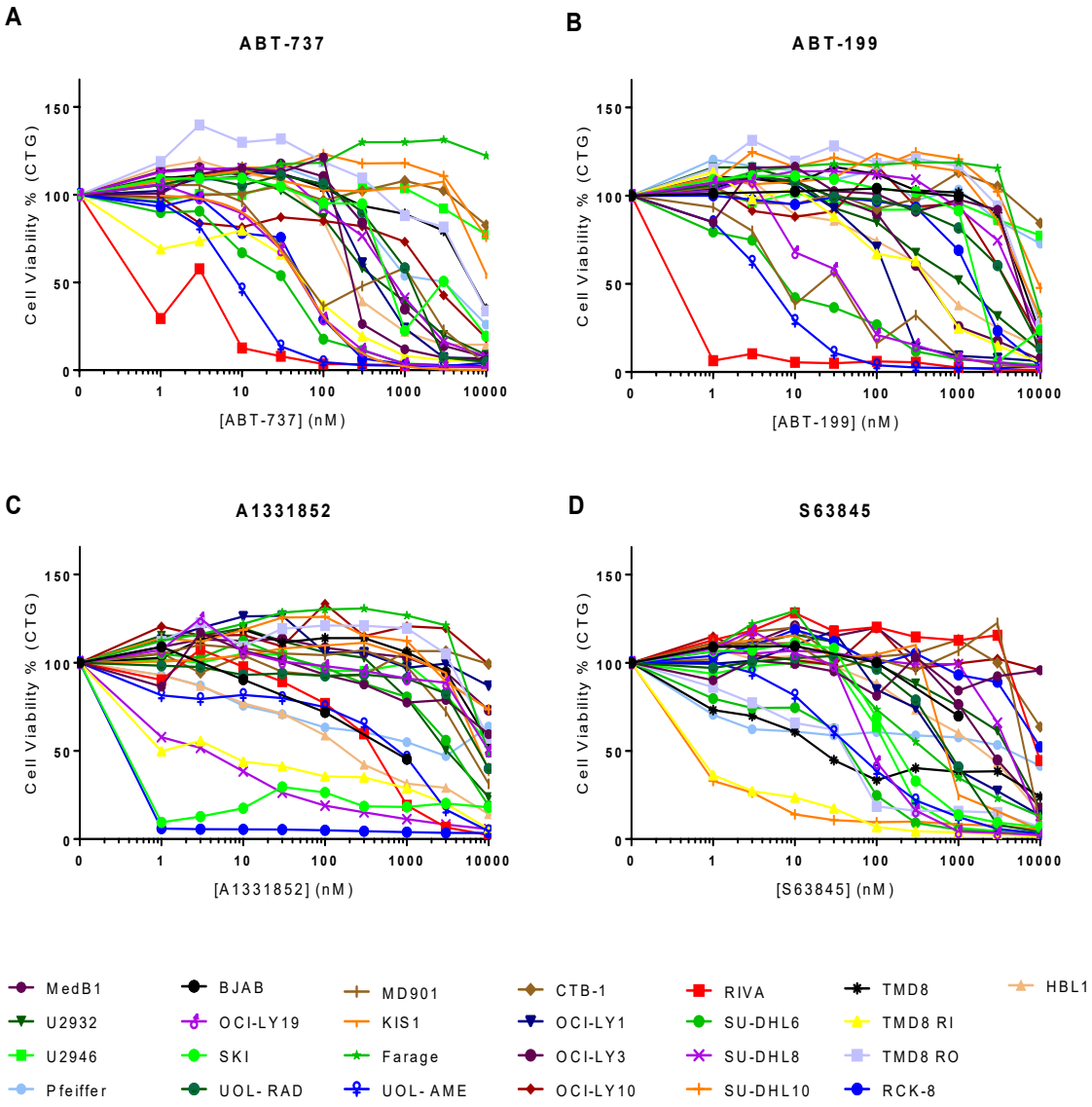

Figure 3-10 Viability of DLBCL cell lines after exposure to BH3 mimetics
25 DLBCL cell lines were plated and treated with 0-10,000nM of ABT-737 **(A)**, ABT-199 **(B)**, A1331852 **(C)** and S63845 **(D)** for 72 hours. Cell viability was analysed by CellTiterGlo viability assay. Data were normalised to DMSO treated control. Data are shown as mean (n=2-6).

	EC_{50} (nM)			
	ABT737	ABT199	A1331852	S63845
RCK8	53.15	1545	**<1**	10682
RIVA	**0.6084**	**<1**	341.3	~ 9858
SUDHL6	26.7	11.02	3322	29.84
SUDHL8	789	5066	2.646	3893
SUDHL10	N.C	~ 9937	>10,000	**<1**
TMD8	6735	6439	10866	49.33
TMD8 RO	6770	7330	~ 10267	29.25
TMD8 RI	41.06	366.2	3.884	**0.2505**
CTB-1	~ 11758	~ 11839	N.C	~ 10683
OCI-LY1	463.8	144.6	>10,000	851.7
OCI-LY3	763.9	476.8	>10,000	2701
OCI-LY10	2113	3983	N.C	N.C
U2932	593	1005	3333	3419
HBL1	293	549.4	202.9	1595
U2946	>10,000	>10,000	11557	140.7
Pfeiffer	2364	>10,000	7873	4343
UOL-AME	8.801	4.657	432.1	59.56
Farage	N.C	~ 9406	~ 9997	506.3
KIS1	~ 10165	7064	8461	~ 915.6
MD901	273.6	19.27	5931	~ 8443
MedB1	~ 288.8	5505	>10,000	9.81[21]
UOL-RAD	1126	3472	7768	754.7
SKI	1296	1659	**<1**	197.4
OCI-LY19	53.95	36.12	10291	96.73
BJAB	N.C	N.C	643.9	1215

Table 3-2 EC_{50} values of BH3 mimetics in DLBCL cell lines
The EC_{50} values for ABT-199, A1331852 and S63845 in DLBCL cell lines (presented in Figure 3-10) were calculated using Graphpad Prism. Values in red indicate the EC_{50} is less than 100nM and is therefore sensitive. Values in bold are less than 1nM indicating ultra-sensitivity. Values which could not be calculated due to the lack of convergence of the response with the x-axis are denoted as N.C, not converged.

There was a heterogeneous response to each of the mimetics across the panel of cell lines, with at least one 'ultra-sensitive' cell line for each specific mimetic (EC_{50}< 1nM represented in bold); the EC_{50} values for these cell lines are approximate as

concentrations below 1nM were not investigated. Nonetheless, the values were within the pico-molar range, indicating extreme sensitivity. Out of the 24 cell lines analysed, 6 cell lines were sensitive to BCL2, $BCLX_L$ and BCLW inhibition by ABT-737 (EC_{50} <100 nM), 6 were sensitive to BCL2 inhibition by ABT-199, 4 were sensitive to $BCLX_L$ inhibition by A1331852 and 7 were sensitive to MCL1 inhibition by S63845. Interestingly, 3 cell lines did not respond to any mimetic at sub-micromolar concentrations.

Consistent with the multi-targeting by ABT-737, cell lines sensitive to ABT-737 were also sensitive to either of the specific mimetics ABT-199 or A1331852. These cell lines are also often more sensitive to the specific inhibitors, most likely due to these drugs' increased binding affinity to their respective proteins (Table 1-4). For example, ABT-737 sensitive RCK8, is extremely sensitive to $BCLX_L$ specific A1331852 but not BCL2 specific ABT-199, which indicates that this cell line response to ABT-737 is due to a strong $BCLX_L$ dependence. On the other hand, the ABT-737 sensitive RIVA was sensitive to ABT-199 but not A1331852 implying that these cells had a dependence on BCL2. The exception for this were MEDB1 and U2932, which exhibited greater sensitivity to ABT-737 than either of the specific inhibitors potentially, indicating a joint protein dependence requiring concomitant sequestration.

RIVA, OCI-LY1 and MD901 respond primarily to ABT-199, indicating a BCL2 dependence. RCK8, SUDHL-8 and SKI primarily responded to A1331852 hence demonstrating $BCLX_L$ dependency for survival. In contrast, SUDHL-10, TMD8 (and derived resistant cell lines), were primarily dependent on MCL1 for survival. These cell lines were all primarily sensitive to one specific BH3 mimetic, indicating that the cells were dependent on only one anti-apoptotic protein for survival. Conversely, SUDHL-6, OCI-LY19, TMD8-RI and UOL-AME exhibited dual dependence on two anti-apoptotic proteins. There are some cell lines which have not been defined as sensitive (EC_{50}<100nM). However, cell lines such as U2932, U2946**,** Farage and UOL-RAD exhibited greater sensitivity to one of the specific inhibitors compared to the others. This would indicate that the protein targeted is functionally more dominant than the other proteins, but there may be interactions with other BCL2 family members, such as partner swapping, which limit the protein's potency. CTB-1, OCI-LY10 and Pfeiffer did not respond to any mimetic at sub-micromolar concentrations. Cell lines with either limited responses or resistance to

mimetics may be susceptible to joint inhibition of anti-apoptotic proteins. It is worth remembering that as of yet, no specific inhibitors of BCLW or BCL2A1 have been developed. These proteins may be functionally important in cell lines that do not respond well to the mimetics already developed.

Interestingly, the derived ibrutinib resistant TMD8 cell line, TMD8-RI, became more sensitive to $BCLX_L$ inhibition by A1331852. This could suggest that resistance to BTK inhibitors results in a greater dependence on the anti-apoptotic proteins for survival. As mentioned, ibrutinib resistant DLBCL cells have been reported to become more sensitive to ABT-199 (Kuo*, et al* 2017). Although the ibrutinib resistant TMD8-RI became approximately 17x more sensitive to ABT-199, the EC_{50} was 366nM, rendering it insensitive to ABT-199, with a greater dependence on $BCLX_L$ and MCL1. Interestingly, in comparison, the TMD-RO with acquired resistance to the more selective BTK inhibitor ONO-4059/tirabrutinib (Kozaki*, et al* 2018) had no significant change in sensitivity to ABT-199 or A1331852.

In order to investigate whether the COO of DLBCL could determine anti-apoptotic protein dependence and thus mimetic sensitivity, an un-paired t-test was performed to compare the EC_{50} values between each group. As EC_{50} values more than 10,000nM were determined by graph extrapolation (as concentrations higher than this were untested), these values are unreliable and were therefore excluded from this analysis. The response to the BH3 mimetics was independent of the cell line's COO classification (Figure 3-11). Consequently, cell lines originating from different COO did not differentially depend on anti-apoptotic proteins.

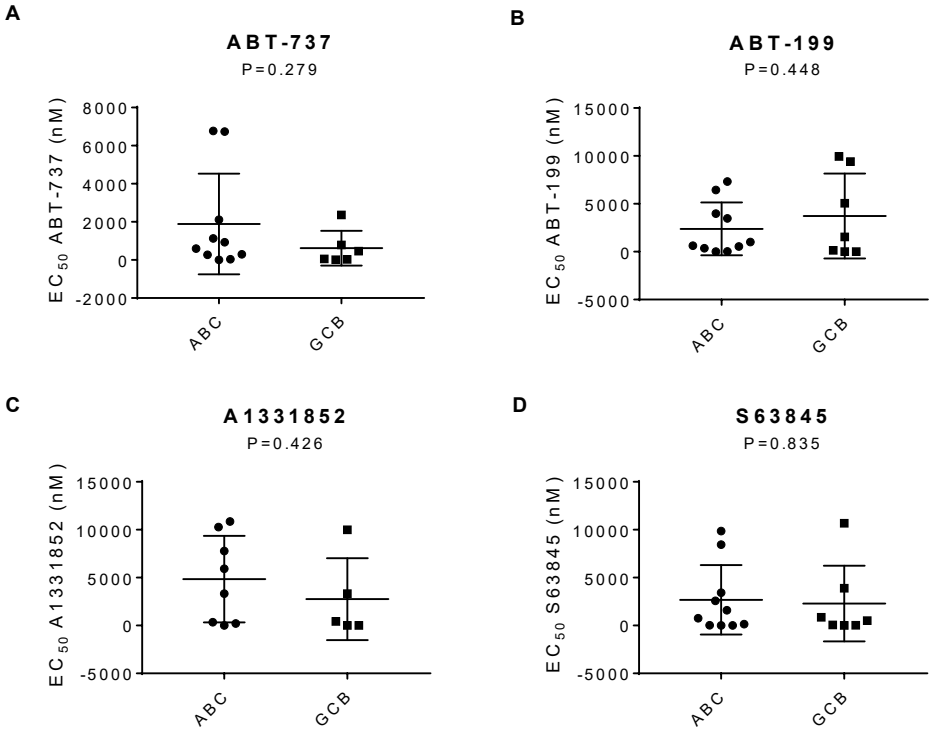

Figure 3-11 Comparison of BH3 mimetic response in ABC and GCB DLBCL
Comparison of the EC_{50} values for ABT-737 **(A)**, ABT-199 **(B)**, A1331852 **(C)** and S63845 **(D)** between ABC (n=10) and GCB (n=8) subtypes. See Appendix 1 for the subtype of each cell line. Cell lines with an EC_{50} values >10,000nM were excluded. Data presented as mean and S.D. with each cell line represented as a dot (ABC) or square (GCB). Unpaired t-test was performed on the two groups and probability (P) values are indicated, $p<0.05$ indicates statistical significance.

As ABT-199 selectively targets BCL2, cell lines containing either the t(14;18)(q32;q21) translocation involving *IGH-BCL2* and DH cell lines were also correlated to ABT-199 sensitivity (Figure 3-12). No statistical significance was found within these groups.

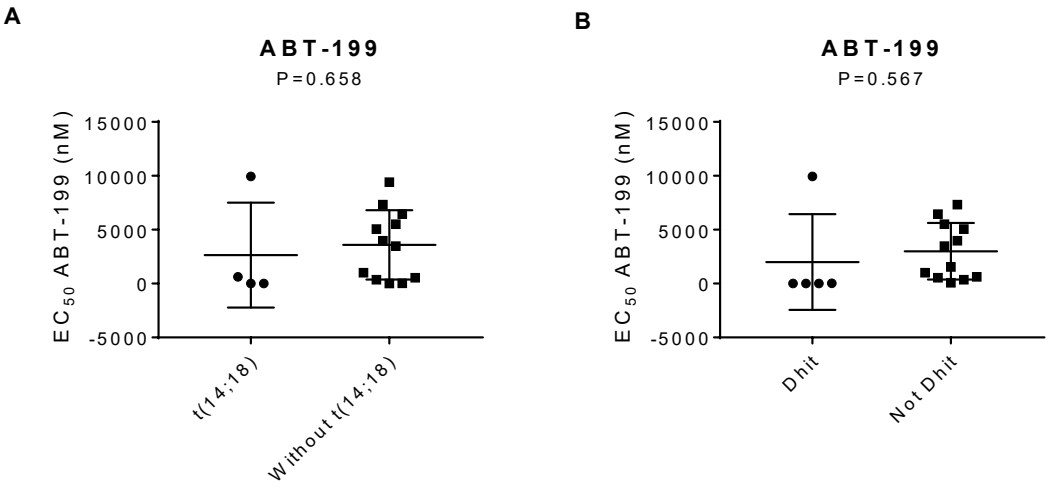

Figure 3-12 Comparison of ABT-199 response in t(14;18) and Dhit cell lines
Comparison of the EC_{50} values for ABT-199 between cell lines either with (n=6) or without the t(14;18) IGH-BCL2 (n=12) **(A)** and Dhit cell lines (Dhit n=7, not Dhit n =12). See Appendix 1 for the characterisation of each cell line. Cell lines with EC_{50} values >10,000nM were excluded. Data presented as mean and S.D. with each cell line represented as a dot (ABC) or square (GCB). Unpaired t-test was performed on the two groups and probability (P) values are indicated, $p<0.05$ indicates statistical significance.

The CTG assay measures ATP and is therefore a measurement of cell number and metabolism. To confirm that BH3 mimetics were inducing cellular death and not growth arrest, a selection of cell lines were also analysed *via* AnnexinV/PI staining (Figure 3-13). ABT-199 was able to induce cell death in RIVA, OCI-LY1 and to a lesser extent OCI-LY3 and U2932. A1331852 induced remarkable cell death in the RCK8 cell line at low concentrations. The cell line, SUDHL6 could be killed by either ABT-199 or S63845. Conversely, CTB-1 was resistant to all mimetics and no cell death occured even after the addition of 10,000nM of any of the mimetics. These data recapitulate the response curves generated using the CTG assay confirming that the mimetics induce a cytotoxic opposed to cytostatic effect.

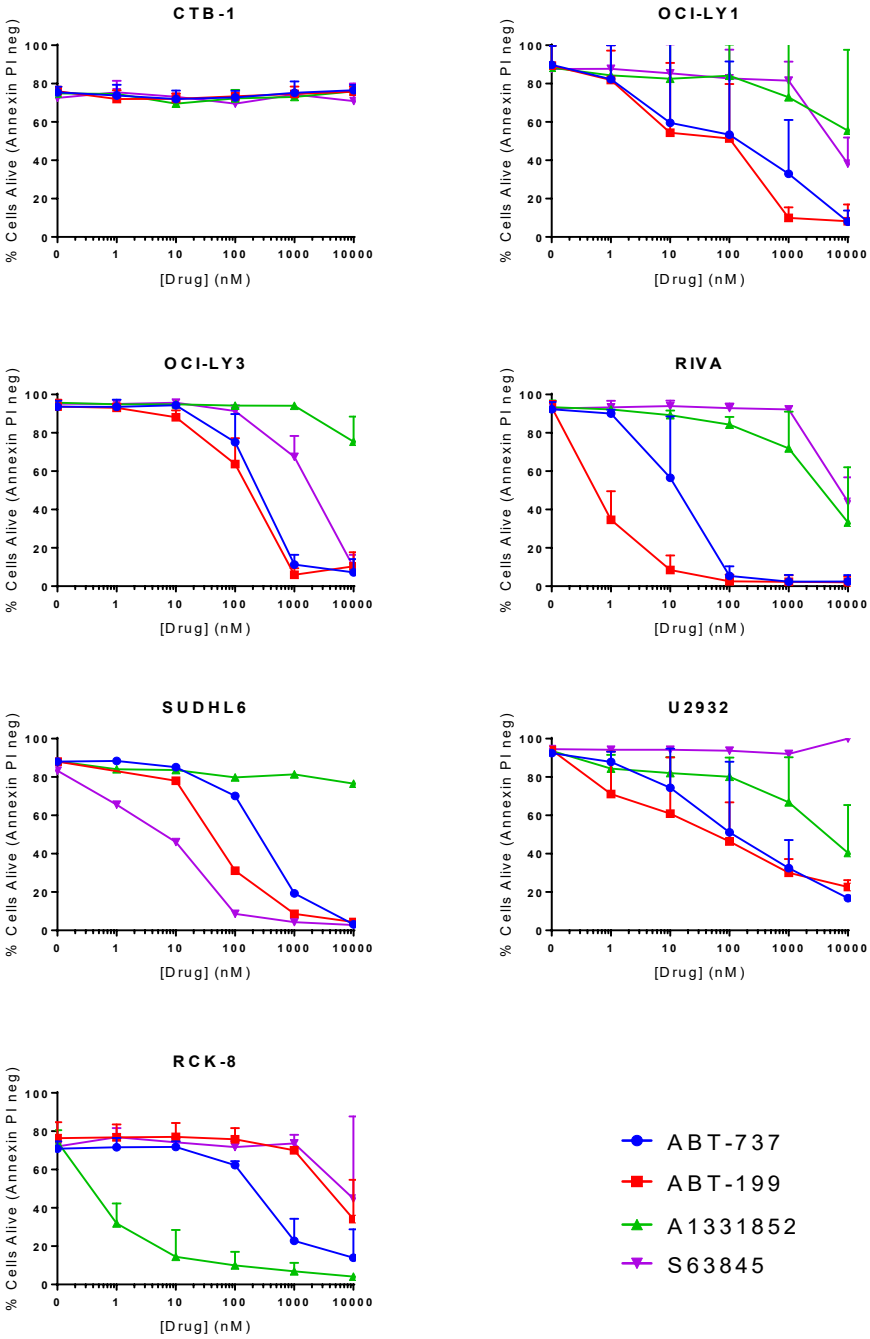

Figure 3-13 Cell death of DLBCL cell lines after treatment with BH3 mimetics
DLBCL cell lines were incubated with 0-10,000nM concentrations of ABT-199, A1331852 and S63845 for 72 hours. Cell death was analysed by AnnexinV-FITC/PI staining measured by flow cytometry. DMSO was used as a time matched control. Data are shown as mean + SD (n=1-4).

The mechanism of cell death was further interrogated by assessing the cleavage of caspases after treatment with ABT-199 (Figure 3-14). There was cleavage of caspase 9 and 3, further confirming the involvement of intrinsic apoptosis.

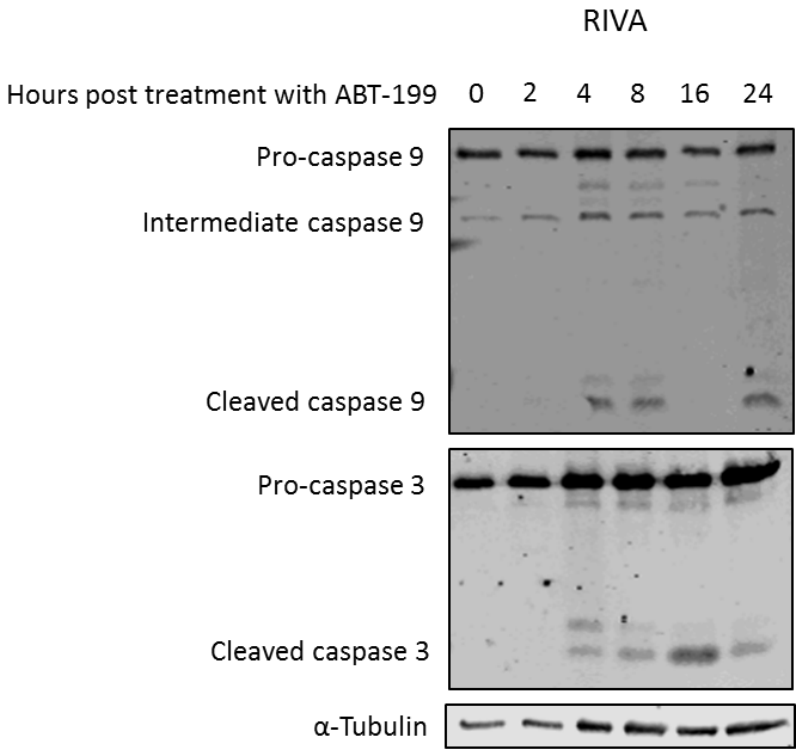

Figure 3-14 Caspase cleavage by ABT-199 in RIVA
Cells were treated with 10nM of ABT-199 for 0, 2, 4, 8, 16 and 24 hours before lysis. 50µg of protein lysate was loaded in each lane. Cleavage of caspases were determined by immuno-blotting. α-tubulin was used as a loading control (n=1).

3.8 Expression of BCL2 family members in DLBCL cell lines

From the initial large panel of DLBCL cell lines, a selection of cell lines were chosen for immuno-blot analysis to determine the expression of BCL2 family members (Figure 3-15). Protein expression was quantified relative to the expression of α-tubulin and displayed as a heat map in Figure 3-15. The expression of VDAC was also assessed as a measure of mitochondrial mass. This did not vary significantly between the cell lines. Expression of BCL2 family members were highly variable across the samples.

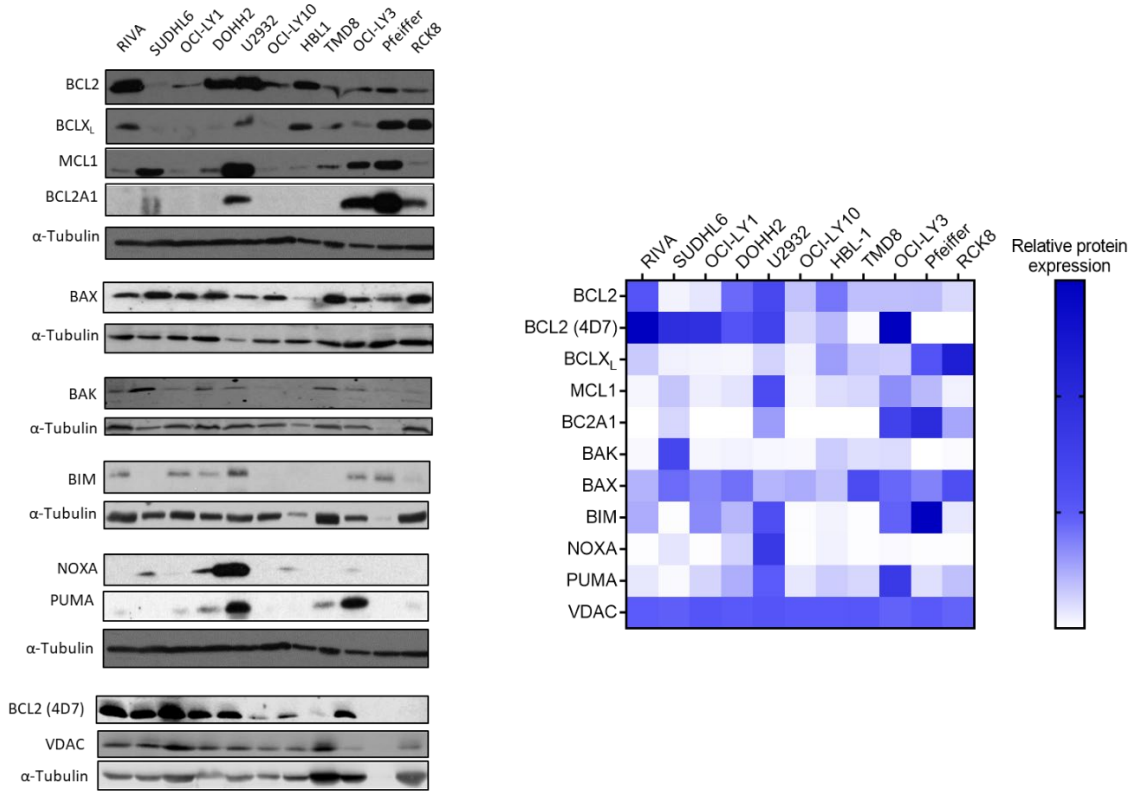

Figure 3-15 BCL2 family protein expression in DLBCL cell lines
Whole cell lysates were prepared from DLBCL cell lines. 75µg of protein lysate was loaded in each lane. Expression of BCL2 family proteins were determined by immuno-blotting and a representative blot is shown. α-tubulin was used as a loading control and VDAC was used an indicator or mitochondrial mass. Bands were quantified using Image Studio Lite and normalised to α-tubulin expression. (n=1-3).

RIVA was very sensitive to ABT-199 (Ec_{50} <0.1nM), so it was unsurprising that it expressed a high amount of the drug's target, BCL2. SUDHL6 is also sensitive to ABT-199 (EC_{50}= 11nM). However, the corresponding band for BCL2 is almost negligible. This is unexpected, as this cell line has a chromosomal translocation resulting in BCL2 overexpression (t(14;18)(q32;q21) → *IGH-BCL2*). It has previously been reported that SUDHL6 contains a $BCL2^{I48F}$ mutation, which is within the epitope recognised by standard BCL2 antibodies (clone 124, aa 41-54) (Masir*, et al* 2010). Therefore, it is likely that this result is 'pseudo-negative'. For this reason, BCL2 expression was also assessed with an alternative antibody (clone 4D7), which recognises a distinct epitope on the protein (aa 61-76). This antibody was able to detect high expression of BCL2 in SUDHL6.

To test whether BH3 mimetic sensitivity correlated with target protein expression, linear regression and Spearman's rank correlation analysis was performed. There was a statistically significant correlation between the EC_{50} values for ABT-199 and expression

of BCL2 (p=0.002, r=-0.86) (Figure 3-16). Further analysis in different panel of cell lines also indicated a statistically significant correlation between BCL2 protein expression and ABT-199 sensitivity (Smith*, et al* 2019) (Appendix 3).

High $BCLX_L$ expression was detected in A1331852 sensitive cell line RCK8, whereas resistant cell line OCI-LY1 expressed very little. However, this correlation was not statistically significant, likely due to cell lines such as Pfeiffer which expressed a high level of $BCLX_L$ yet were resistant to inhibition by A1331852 (Figure 3-16). There was no correlation between MCL1 protein expression and sensitivity to S63845 (Figure 3-16).

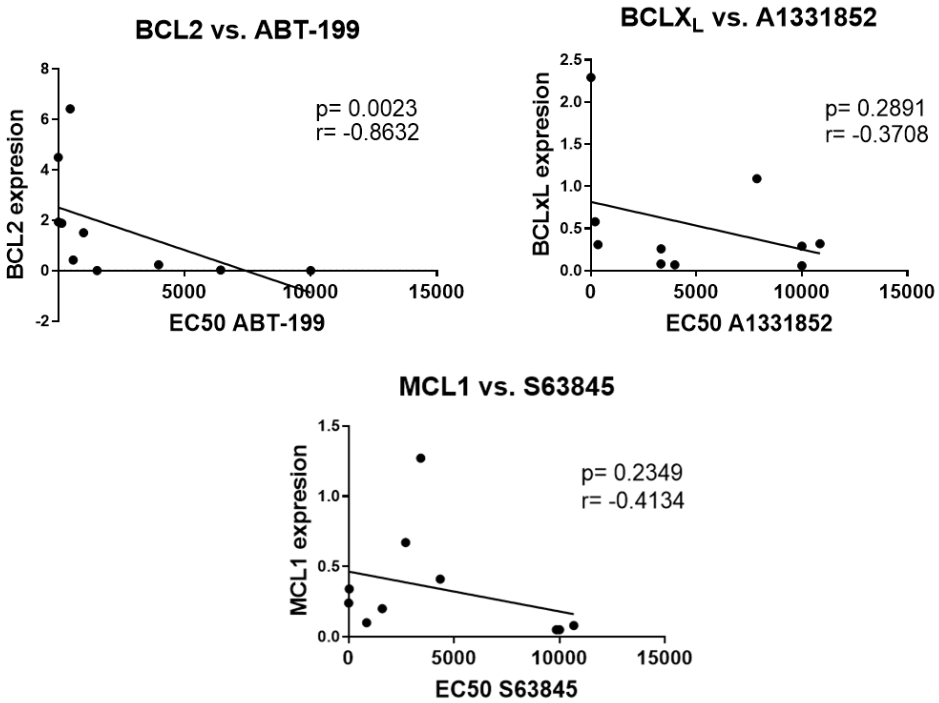

Figure 3-16 Correlations of anti-apoptotic proteins and mimetic sensitivity
The EC_{50} of ABT-199, A1331852 and S63845 were correlated with the quantified expression of the corresponding target protein (BCL2, $BCLX_L$ and MCL1). Each dot is representative of one cell line and the solid line is representative of the linear regression line. Spearman's rank correlation co-efficient (r) and the statistical significance values (P) are indicated on each graph. P values less than 0.05 are statistically significant.

As all of these proteins are anti-apoptotic and may to an extent, be able to compensate for each other, some literature suggests that the expression of MCL1 and/or $BCLX_L$ can be used as a marker of resistance to ABT-199 (Lin *et al.*, 2016). For this reason, the expression of the anti-apoptotic proteins compared to the other proteins has been correlated to the sensitivity to mimetics (Figure 3-17). The correlation between ABT-199 sensitivity and the ratio BCL2 expression versus the combined expression of $BCLX_L$

and MCL1 remained statistically significant (p=0.004). Conversely, there was no correlation for A1331852 or S63845 sensitivity and the ration of its respective target protein expression versus other anti-apoptotic protein expression.

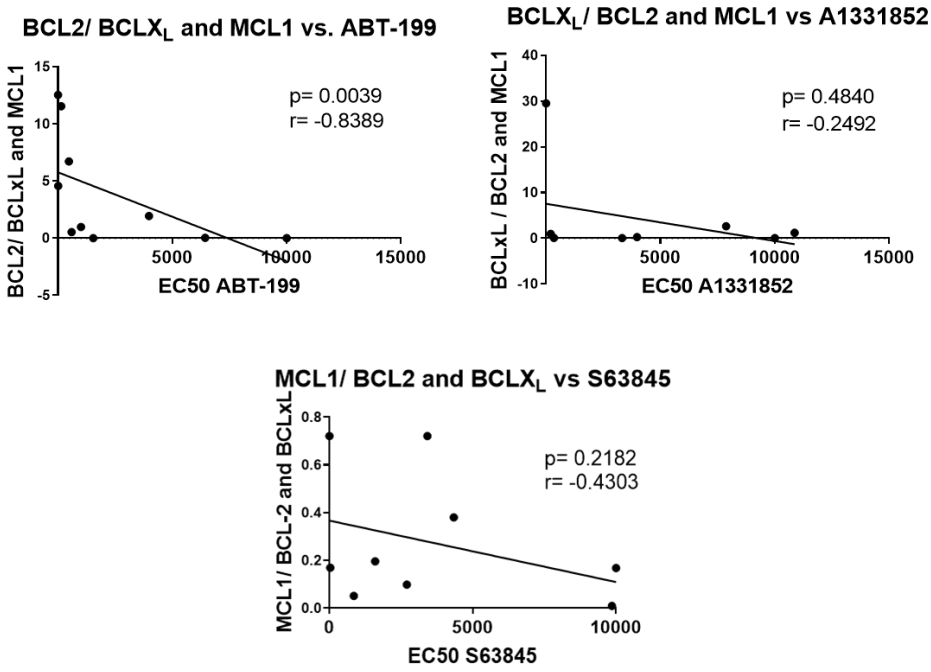

Figure 3-17 Correlation of anti-apoptotic protein ratio and mimetic sensitivity
The EC_{50} of ABT-199, A1331852 and S63845 were correlated with the ratio of the corresponding target protein vs the other anti-apoptotic proteins. Each dot is representative one cell line and the solid line is representative of the linear regression line. Spearman's rank correlation co-efficient (r) and the statistical significance values (P) are indicated on each graph. P values less than 0.05 are statistically significant

Inverse correlations between mimetic sensitivity and protein expression of those which were not targeted were also calculated (Figure 3-18). There was a weak relationship between $BCLX_L$ protein expression and S63845 sensitivity but this is not statistically significant. However, this inverse correlation was statistically significant when assessed in a different panel (Smith*, et al* 2019) (Appendix 3). There was a weak relationship between expression of MCL1 and ABT-199 sensitivity (r=0.52), which has been previously reported (Klanova*, et al* 2016). This could suggest that high levels of MCL1 expression might be a negative marker for sensitivity to BCL2 inhibition. However, this did not reach statistical significance within this data set.

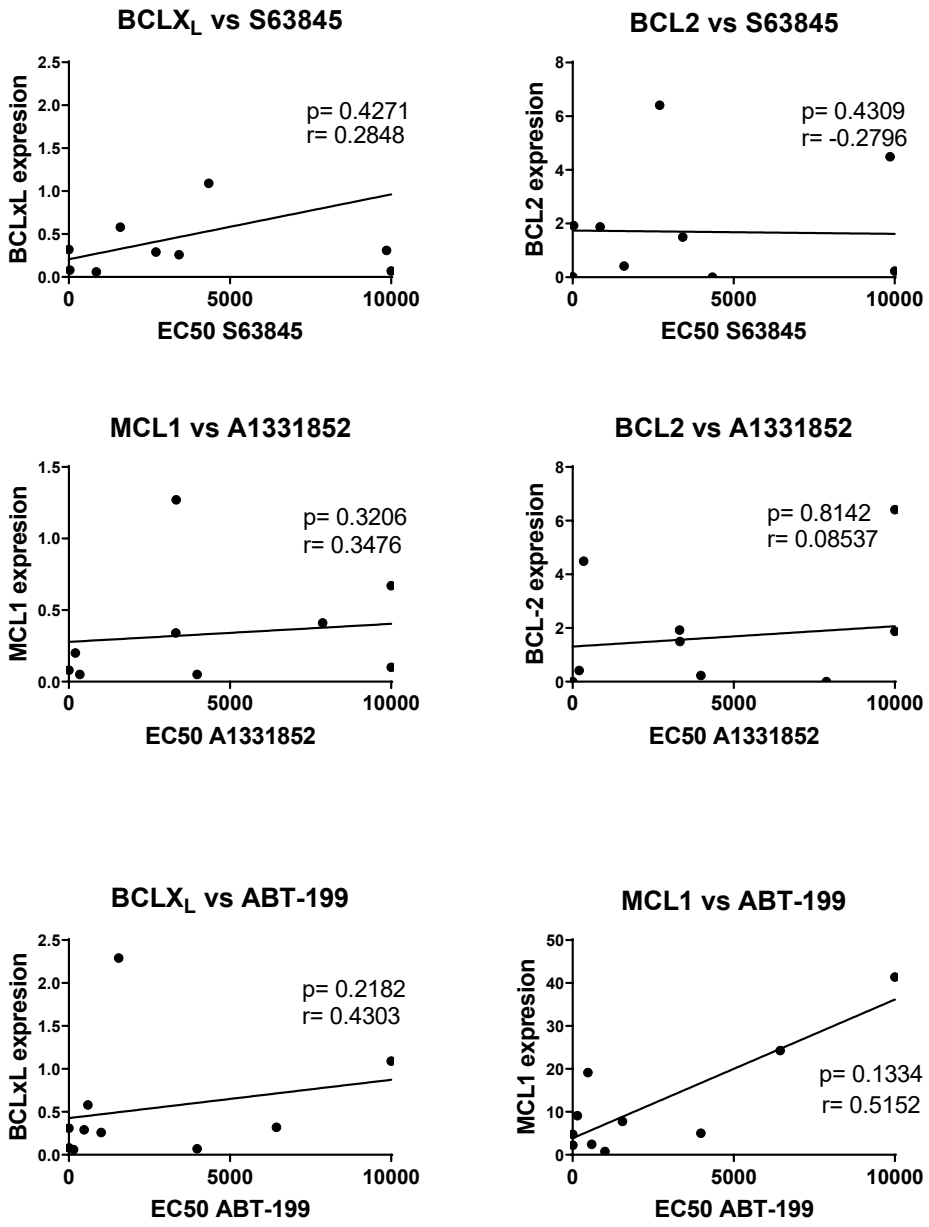

Figure 3-18 Correlations of mimetic sensitivity and expression of proteins which are not targeted
The EC_{50} of ABT-199, A1331852 and S63845 were correlated with the quantified expression of anti-apoptotic proteins which are not targeted by that mimetic. Each dot is representative of one cell line and the solid line is representative of the linear regression line. Spearman's rank correlation co-efficient (r) and the statistical significance values (P) are indicated on each graph. P values less than 0.05 are statistically significant.

As NOXA can selectively bind to and sequester MCL1, it was hypothesised that high expression of NOXA could inhibit MCL1 rendering MCL1 inhibitors ineffective. This could provide rationale for the U2932 cell line which was not sensitive to S63845 despite a high expression of MCL1 as there was also a high expression of NOXA. Therefore high MCL1 to NOXA ratio could be a predictor of sensitivity to S63845. However when analysed, this correlation was not apparent in other cell lines (Figure 3-19). It has been hypothesised that sensitivity can be determined via BCL2: BIM protein expression ratio

in FL (Bodo *et al.,* 2016). This correlation was also observed in this data set (Figure 3-19). However this correlation (r=-0.644) was weaker than the correlation of total BCL2 expression versus ABT-199 sensitivity (r=-0.83).

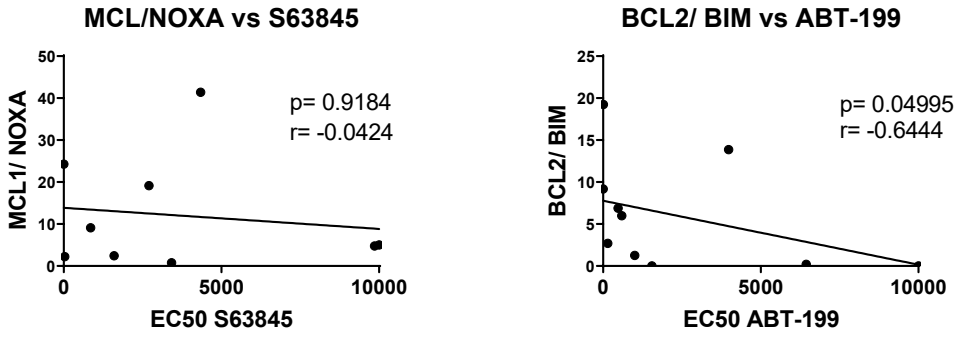

Figure 3-19 Correlations of anti-apoptotic proteins and binding partners
The EC_{50} of S63845 and ABT-199 were correlated with the ratio of the corresponding target protein vs its binding partner. Each dot is representative of one cell line and the solid line is representative of the linear regression line. Spearman's rank correlation co-efficient (r) and the statistical significance values (P) are indicated on each graph. P values less than 0.05 are statistically significant.

Taken together, high expression of BCL2 may be an indicator of ABT-199 sensitivity and low expression correlates with ABT-199 sensitivity. However this correlation is partly driven by low and high expressers and may be difficult to interpret for intermediate expressors. Despite the high expression of $BCLX_L$ and MCL1 proteins in cell lines which were sensitive to their respective inhibitors, the correlations were weak and not statistically significant. Therefore BCL2 family member expression cannot be used to accurately predict sensitivity to A1331852 or S63845.

3.9 BH3 Profiling

As discussed previously, BH3 profiling is a functional assay proposed to be able to determine anti-apoptotic protein dependence and predict sensitivity to selective BH3 mimetics (Certo*, et al* 2006). BH3 profiling was performed in a series of DLBCL cell lines and the results were compared to cell's viability response curves to BH3 mimetics, to determine whether this method can correctly predict protein dependence. An overview of the cell line responses can be seen in Figure 3-20. All cell lines had a loss of mitochondrial membrane potential after treatment with 10µM BIM (which can bind to all anti-apoptotic proteins), indicating that the cells have functional BAK and BAX. As

expected, the response to lower concentrations of BIM was dose dependent. The levels of response to lower concentrations of BIM are indicative of how primed the cells are. For example, TMD8 and U2946 were highly primed compared to OCI-LY10, potentially suggesting a mechanism of resistance in this cell line.

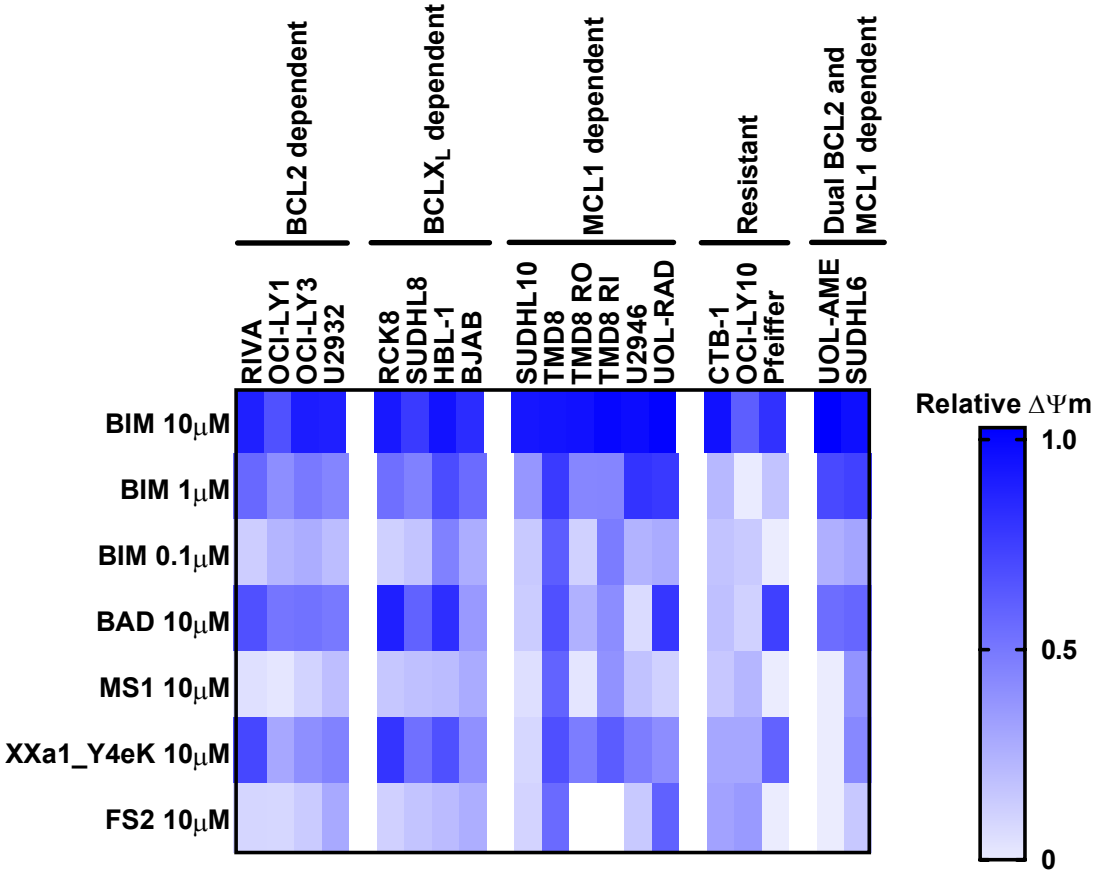

Figure 3-20 Overview of BH3 profiling in DLBCL cell lines
Heat map displaying the relative loss of mitochondrial membrane potential (ΔΨm) during BH3 profiling assay. Cells were gently permeabalised, treated with synthetic peptides and stained with mitochondrial membrane potential probe, JC-1, immediately before analysis. Fluorescence intensity (ex. 545nm, em. 590nm) was measured at 5 minute intervals for 120 minutes with intermittent shaking at 30°C using a HidexSense plate reader. The area under the curve for each treatment was calculated and normalised to DMSO and FCCP treated control cells. Cell lines are organised due to anti-apoptotic dependencies based on previous CellTiterGlo viability assays (see Figure 3-10). Data displayed as mean (n=2-15). Data not collected for FS2 response in TMD8-RO and TMD8-RI.

The cell lines' BH3 profiles have been displayed based on their dependence of anti-apoptotic proteins determined *via* the CTG data. The BH3 profiles of BCL2 dependent cell lines (RIVA, OCI-LY1 and OCI-LY3) are displayed in Figure 3-21. The ABT-199 EC_{50} for OCI-LY3 and U2932 is over 100nM, however the response was much greater than that of any other mimetic and has therefore been classified as mainly BCL2 dependent. In this assay there is no BCL2-specific peptide. However, all four cell lines respond to BCL2,

$BCLX_L$ and BCLW-specific peptide BAD. As expected, there was a minimal response to MCL1-specific MS1 or BCL2A1-specific FS2. However, all four cell lines also had significant mitochondrial depolarisation after the addition of $BCLX_L$-specific XXa1_Y4eK peptide. The XXa1_Y4eK depolarisation for OCI-LY1 and OCI-LY3 was lower than that of BAD. This may be a way to distinguish between BCL2 or $BCLX_L$ dependent profiles, but this becomes difficult to interpret. In contrast, the level of depolarisation for BAD and XXa1_Y4eK for RIVA were quite similar. RIVA has an EC_{50} of 341nM to $BCLX_L$ inhibitor A1331852, indicating some dependence on $BCLX_L$. This may explain the cell line profile, as it eludes to a dual dependence, however this does not distinguish between the exquisite sensitivity to BCL2 inhibition and only slight response to $BCLX_L$ inhibition. This highlights a key limitation of this technique, as without a BCL2 specific peptide it is difficult to distinguish whether large BAD and XXa1_Y4eK depolarisation is due to a singular $BCLX_L$ dependence or $BCLX_L$ and BCL2 joint dependence.

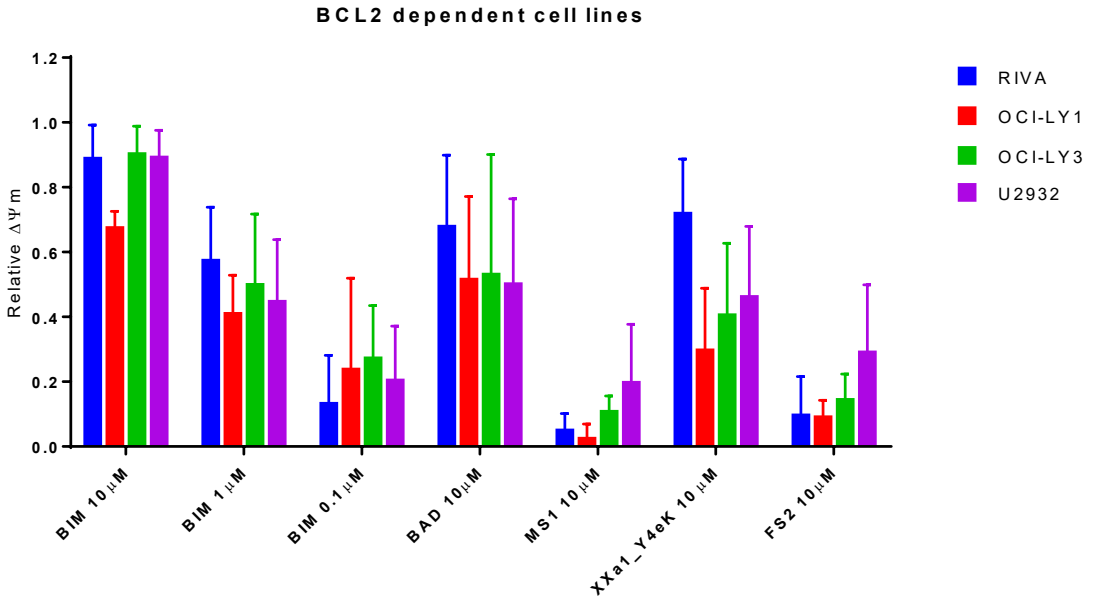

Figure 3-21 BH3 profile of BCL2 dependent cell lines
Cells were gently permeabalised, treated with synthetic peptides and stained with mitochondrial membrane potential probe, JC-1, immediately before analysis. Fluorescence intensity (ex. 545nm, em. 590nm) was measured at 5 minute intervals for 120 minutes with intermittent shaking at 30°C using a HidexSense plate reader. The relative loss of mitochondrial membrane potential ($\Delta\Psi m$) was calculated by normalising the area under the curve for each treatment to DMSO and FCCP treated control cells. Cell lines ordered by sensitivity to ABT-199. Data are expressed as mean + S.D. (n=7-15)

RCK8 and SUDHL8 were very sensitive to $BCLX_L$ inhibition by A1331852. HBL-1 and BJAB exhibited greater sensitivity to A1331852 than the other specific BH3 mimetics. BH3

profiling could correctly predict this as there is a large depolarisation caused by both BAD and XXa1_Y4eK at similar levels in these cell lines (Figure 3-22). However, as mentioned, a similar profile could be seen by BCL2 dependent RIVA.

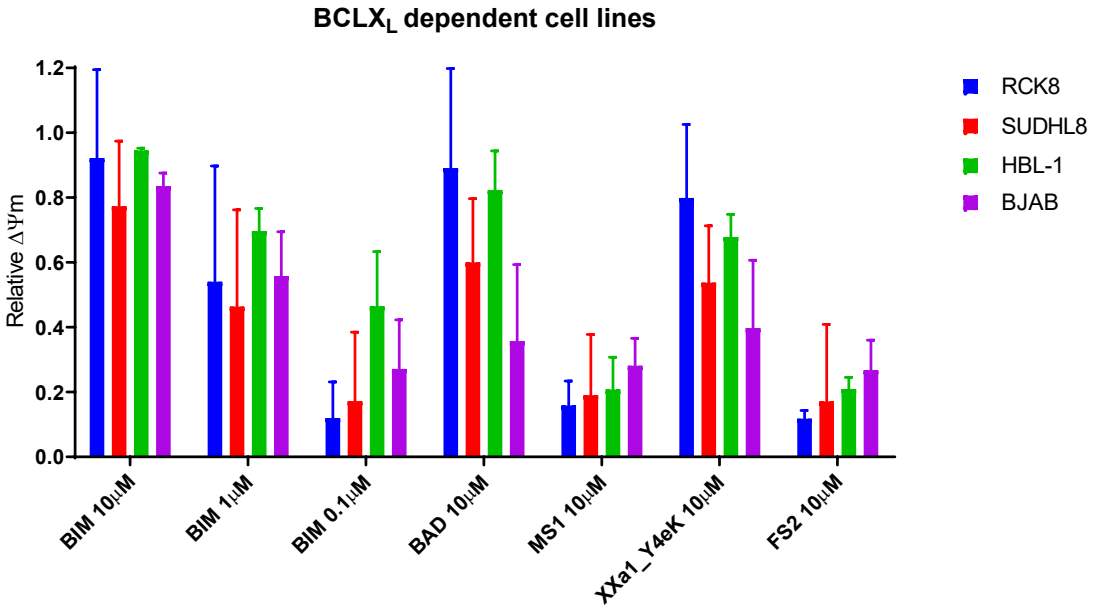

Figure 3-22 BH3 profile of BCLX$_L$ dependent cell lines
Cells were gently permeabalised, treated with synthetic peptides and stained with mitochondrial membrane potential probe, JC-1, immediately before analysis. Fluorescence intensity (ex. 545nm, em. 590nm) was measured at 5 minute intervals for 120 minutes with intermittent shaking at 30°C using a HidexSense plate reader. The relative loss of mitochondrial membrane potential (ΔΨm) was calculated by normalising the area under the curve for each treatment to DMSO and FCCP treated control cells. Cell lines ordered by sensitivity to A1331852. Data are expressed as mean + S.D. (n=3-12)

Although SUDHL10, TMD8 and TMD8 derived resistant cells were sensitive to MCL1 inhibition by S63845, there was only depolarisation by MS1 peptide for TMD8 and TMD8 RI (Figure 3-23). U2946 and UOL-RAD cell lines were also more sensitive to S63845 than any other specific BH3 mimetic yet did not respond to the MS1 peptide. TMD8 and TMD8 RI were highly primed, as can be determined by the large depolarisation from all the peptides, including low concentrations of BIM. Although these cell lines were the only ones to have more than 30% depolarisation after the addition of MS1, the response to other peptides was equally high, indicating this was an unspecific response from the primed state of the cells, increasing the ambiguity of this assay. Most MCL1-dependent cell lines also exhibited quite a high response to the BCLX$_L$ peptide XXa1_Y4ek. In the case of TMD8 RI, this may be due to dual MCL1 and BCLX$_L$ dependence, but it could be an unspecific response for the other cell lines.

UOL-RAD had a minimal response to MS1 but there was a mitochondrial depolarisation after the addition of either BAD, XXa1_Y4ek or FS2. UOL-RAD was resistant to either BCL2 or $BCLX_L$ inhibition but it was more sensitive to the unspecific ABT-737. Therefore, the cell line's BH3 profile and response to BAD might indicate a joint dependence on BCL2 and $BCLX_L$ that require simultaneous joint inhibition. The response to the FS2 peptide could also suggest a dependence on BCL2A1, which is currently unable to be confirmed due to the lack of BCL2A1 specific inhibitor.

In contrast, SUDHL10 (the most sensitive cell line to S63845) would be expected to have a large mitochondrial depolarisation after the addition of the MS1 peptide. However, the cell line had a minimal response to MS1 or any other peptide, suggesting that it was relatively un-primed and would not be sensitive to any BH3 mimetic. This cell line had previously been reported to have an apoptotic block assessed via BH3 profiling (Deng*, et al* 2007). This was further supported by an almost undetectable level of BAK and BAX protein expression via immunoblotting (Deng*, et al* 2007), providing a mechanism for its apoptotic block. Nevertheless, the data presented previously in this report showed that this cell line was uniquely sensitive to S63845 (EC_{50} <1nM). Hence, either the mechanism of the drug is independent of MCL1 and the intrinsic apoptotic pathway or the BH3 profiling assay cannot accurately determine MCL1 dependence. Based on the experiments performed in DKO MEFs, the former hypothesis is unlikely. Taken together, this data indicates that BH3 profiling is unable to correctly predict the sensitivity of cells to MCL1 inhibition.

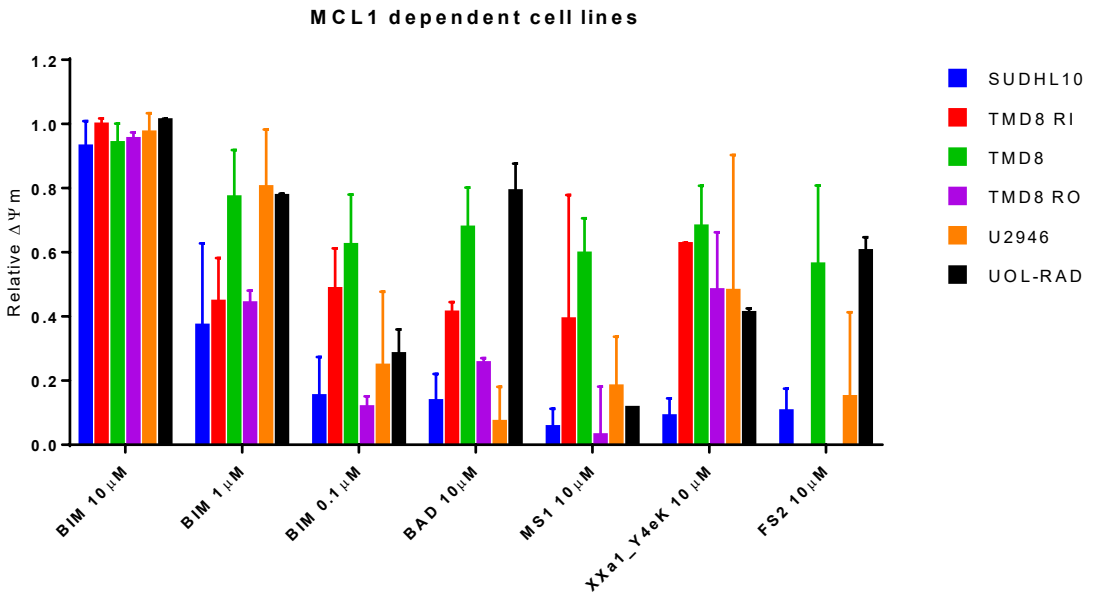

Figure 3-23 BH3 profile of MCL1 dependent cell lines
Cells were gently permeabalised, treated with synthetic peptides and stained with mitochondrial membrane potential probe, JC-1, immediately before analysis. Fluorescence intensity (ex. 545nm, em. 590nm) was measured at 5 minute intervals for 120 minutes with intermittent shaking at 30°C using a HidexSense plate reader. The relative loss of mitochondrial membrane potential (ΔΨm) was calculated by normalising the area under the curve for each treatment to DMSO and FCCP treated control cells. Data are expressed as mean + S.D. (n=2-5).

The resistant cell lines (EC_{50} to specific mimetics >10000nM), CTB-1, OCI-LY10 and Pfeiffer, had mitochondrial depolarisation after treatment with activator peptide, BIM, indicating they have functional BAK and BAX and are capable of intrinsic apoptosis (Figure 3-24). Their responses to the BIM peptide were also lower compared to the other cell lines, indicating a reduced level of priming. The response after the addition of the other peptides was minimal for CTB-1 and OCI-LY10, accurately representing the cells resistance to BH3 mimetics. Unexpectedly, the resistant cell lines did not have a greater response to the FS2 peptide compared to the other peptides. This suggests that the resistance to current BH3 mimetics was not due to a dependence on the BCL2A1 protein. Nevertheless, data presented here highlight some of the limitations of this technique and until a specific BCL2A1 inhibitor is developed, the reliability of using this technique to determine BCL2A1 dependence is unknown.

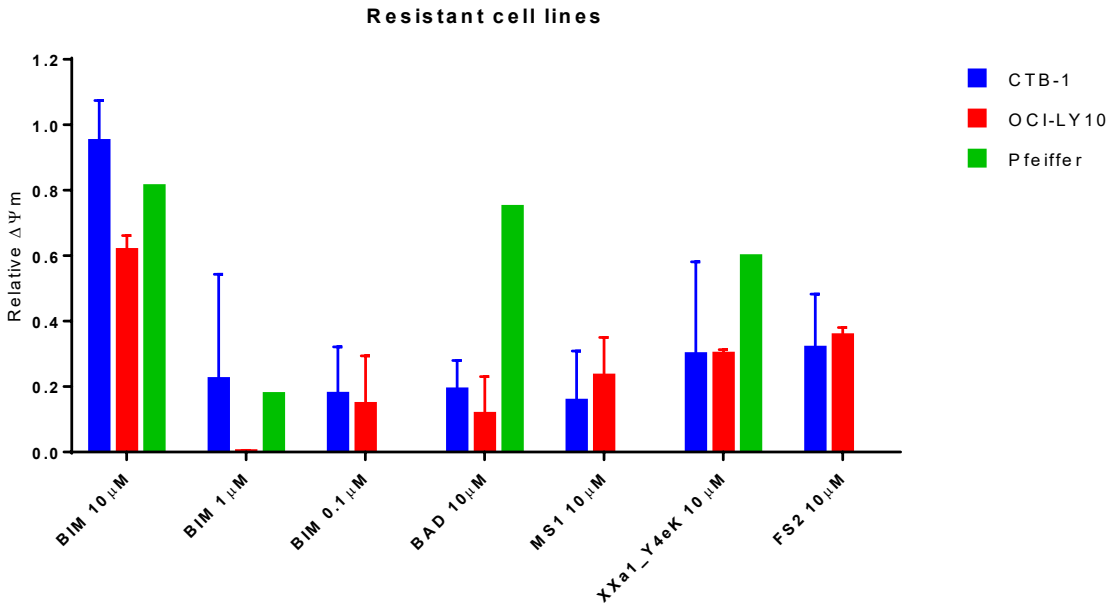

Figure 3-24 BH3 profile of BH3 mimetic resistant cell lines
Cells were gently permeabalised, treated with synthetic peptides and stained with mitochondrial membrane potential probe, JC-1, immediately before analysis. Fluorescence intensity (ex. 545nm, em. 590nm) was measured at 5 minute intervals for 120 minutes with intermittent shaking at 30°C using a HidexSense plate reader. The relative loss of mitochondrial membrane potential (ΔΨm) was calculated by normalising the area under the curve for each treatment to DMSO and FCCP treated control cells. Data are expressed as mean + S.D. (n=1-7)

Two cell lines, SUDHL6 and UOL-AME, exhibited great sensitivity to ABT-199 and S63845, indicating a joint dependence on both BCL2 and MCL1. The BH3 profile for SUDHL6 partially reflects this, as there was depolarisation after treatment with the BAD peptide or the MS1 peptide (Figure 3-25). However, there was also depolarisation after XXa1_Y4ek, suggesting that the responses to peptides could be unspecific, due to a high level of priming. Alternatively, the response to the XXa1_Y4ek peptide could be due to the un-specificity of this peptide. In contrast, the UOL-AME cell line had a profile of a BCL2 dependent cell line as there is depolarisation after BAD treatment but not the XXa1_Y4eK peptide. This cell line is more sensitive to ABT-199 than S63845 suggesting that the cells could be more dependent on BCL2. Nonetheless, there is still a dependence on MCL1 that cannot be predicted by the BH3 profile, further casting doubt on the specificity of the assay and the MS1 peptide.

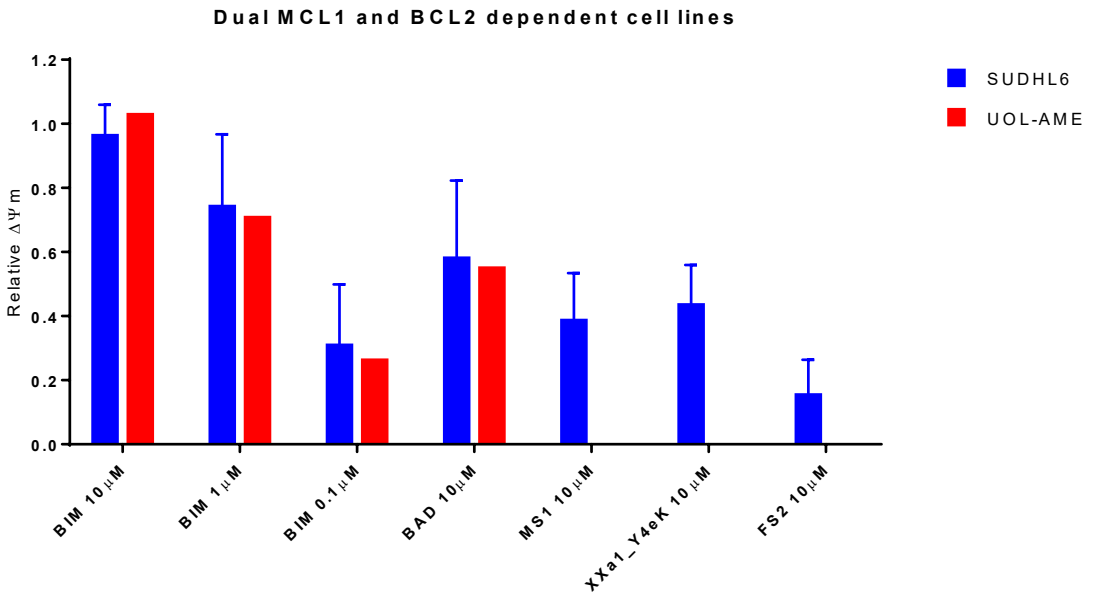

Figure 3-25 BH3 profile for BCL2 and MCL1 joint dependent cell lines
Cells were gently permeabalised, treated with synthetic peptides and stained with mitochondrial membrane potential probe, JC-1, immediately before analysis. Fluorescence intensity (ex. 545nm, em. 590nm) was measured at 5 minute intervals for 120 minutes with intermittent shaking at 30°C using a HidexSense plate reader. The relative loss of mitochondrial membrane potential (ΔΨm) was calculated by normalising the area under the curve for each treatment to DMSO and FCCP treated control cells. Data are expressed as mean + S.D. (n=1-6)

As discussed, the responses to the MCL1-specific peptide, MS1, were limited in all the cell lines, even for those that were sensitive to S63845 at sub-nanomolar concentrations. In contrast, the responses to the $BCLX_L$ specific peptide, XXa1_Y4eK was relatively high for all cell lines, even in those which did not respond to A1331852. These synthetic peptides have been manufactured to be more specific than endogenous BH3 proteins and they can have up to 1000x more selectivity for their target protein, compared to the other anti-apoptotic protein (Foight *et al*., 2014, Dutta *et al*., 2015, Jenson *et al*., 2017). That notwithstanding, the binding affinities for their respective proteins is different (MS1-MCL1 Ki=7.9nM, XXA1_Y4ek-$BCLX_L$ Ki< 0.1nM) (Dutta*, et al* 2015, Foight*, et al* 2014). The concentrations of peptides used for the assay in the data presented here were based on previously published data (Butterworth*, et al* 2016, Certo*, et al* 2006). The peptide concentration does not need to be pharmacologically relevant, as the cells are permeabalised to enable peptide entry. It is important to have target protein saturation without causing off-target cytotoxities. Nonetheless based on their differential binding affinities for their respective proteins perhaps the concentration of peptide used needed optimising.

It is possible that due to the lower binding affinity of the MS1 peptide for the MCL1 protein there was not complete target saturation. For this reason, increased concentrations of MS1 were investigated in a panel of cell lines with differential sensitivities to S63845 (Figure 3-26). By increasing the concentration of the peptide, it was anticipated that S63845 sensitive cell lines would respond but those resistant would not. In Figure 3-26 cell lines are organised by sensitivity to S63845. Despite the responses for all cell lines increasing in a dose dependent manner, there was no association between sensitivity and MS1 peptide concentration. Increased peptide concentration results in false positive for cell lines that are not MCL1 dependent. Moreover, the increased peptide concentration also increased variability in responses as is evident by the increased size of error bars for the higher concentrations.

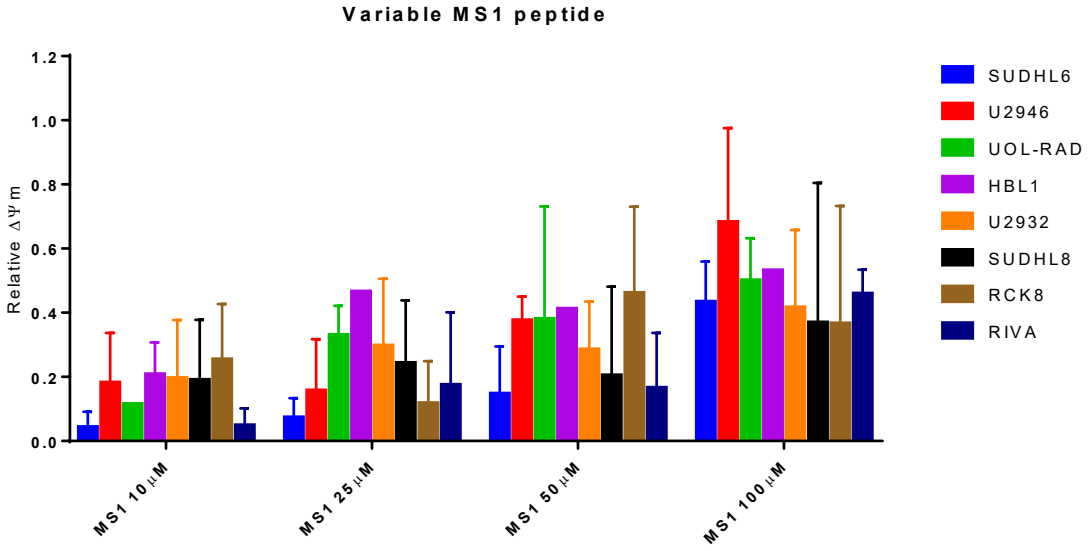

Figure 3-26 BH3 profiling using variable MS1 peptide concentrations
Cells were gently permeabalised, treated with 10, 25, 50 or 100μM of synthetic peptide, MS1 and stained with mitochondrial membrane potential probe, JC-1, immediately before analysis. Fluorescence intensity (ex. 545nm, em. 590nm) was measured at 5 minute intervals for 120 minutes with intermittent shaking at 30°C using a HidexSense plate reader. The relative loss of mitochondrial membrane potential (ΔΨm) was calculated by normalising the area under the curve for each treatment to DMSO and FCCP treated control cells. Cell lines are arranged in order of sensitivity to S63845. Data are expressed as mean + S.D. (n=2-5).

The response to the XXa1_Y4ek peptide was high for all cell lines, which may be reflective of its high binding affinity for $BCLX_L$. It was hypothesised that a lower concentration of the XXa1_Y4ek peptide would induce a more specific response, with only A1331852 sensitive cell lines responding. In Figure 3-27, cell lines are organised in order of sensitivity to A1331852. When the data are presented in this format, there is a

distinction in depolarisation with 10µM treatment between cell lines that respond to A1331852 with an EC_{50}<500nM (RCK8, SUDHL8, HBL1, and RIVA) and those that are resistant (depolarisation above and below 50%, respectively). As the concentration of XXa1_Y4ek is decreased, the response decreased in a dose dependent manner. However, the difference between A1331852 sensitive cell lines and resistant cells was more difficult to distinguish. Alternatively, using 5µM of the peptide created a distinction between cells that have an EC_{50} to A1331852 <10000nM and those that are completely resistant. Treatment with 1µM of the peptide removed any correlation of response and $BCLX_L$ dependence, plus induced more variability. Taken together, knowing the mitochondrial depolarisation after both 10µM and 5µM of XXa1_Y4ek may be more informative as to the extent of $BCLX_L$ dependence and A1331852. Nonetheless, due to the concentrations achievable for drug treatment, the distinction between EC_{50} above and below 500nM is more important, therefore rendering the treatment with 10µM the most informative.

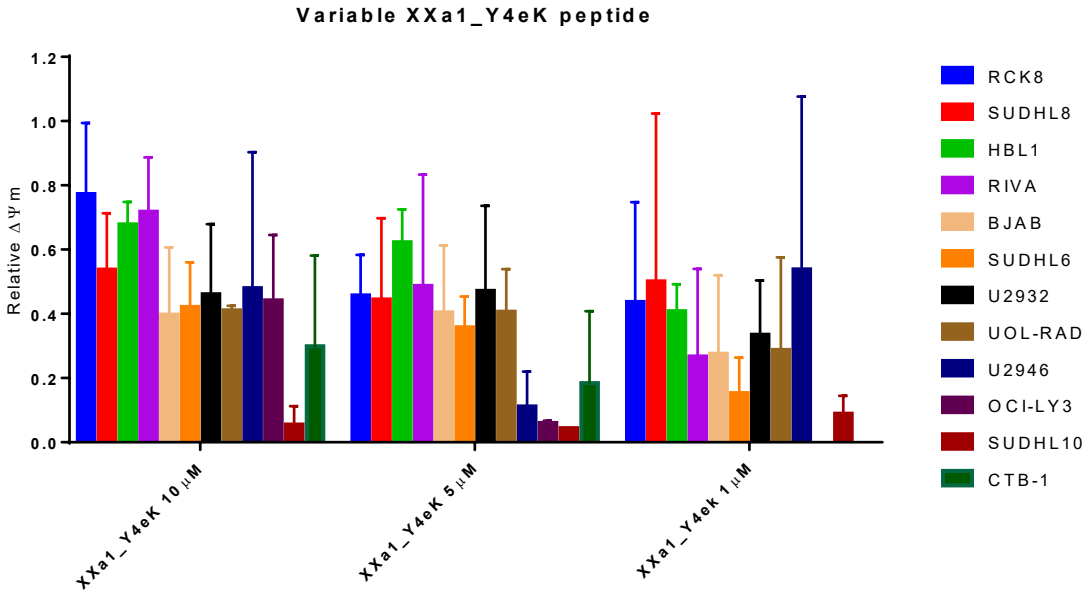

Figure 3-27 BH3 profiling using variable XXa1_Y4ek peptide concentrations
Cells were gently permeabalised, treated with 10, 5 or 1µM of synthetic peptide, XXa1_Y4eK and stained with mitochondrial membrane potential probe, JC-1, immediately before analysis. Fluorescence intensity (ex. 545nm, em. 590nm) was measured at 5 minute intervals for 120 minutes with intermittent shaking at 30°C using a HidexSense plate reader. The relative loss of mitochondrial membrane potential (ΔΨm) was calculated by normalising the area under the curve for each treatment to DMSO and FCCP treated control cells. Cell lines are arranged in order of sensitivity to A1331852. Data are expressed as mean + S.D. (n=4-7)

Despite the published data on the specificity and high binding affinity of XXa1_Y4ek for the protein $BCLX_L$ (Dutta*, et al* 2015), the recommended protocol for this assay uses a different peptide to indicate dependence for $BCLX_L$ (Ryan 2017). w-HRK is a synthetic peptide specific for $BCLX_L$. This peptide was also tested in several cell lines to investigate whether this could induce a more specific response for cell lines that are sensitive to A1331852. As can be seen in Figure 3-28, this peptide induced a much lower amount of mitochondrial depolarisation. Although it was not tested in as many cell lines as the XXa1_Y4ek, the data presented here indicates there is not as strong a correlation between $BCLX_L$ dependence and HRK-w peptide response.

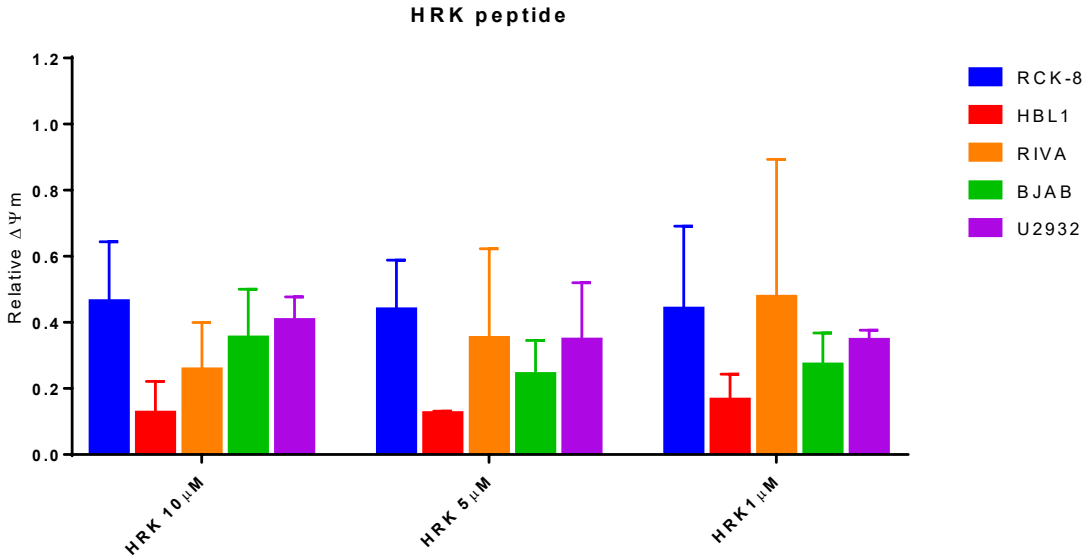

Figure 3-28 BH3 profiling using the HRK peptide
Cells were gently permeabalised, treated with 10, 5 or 1μM of synthetic peptide, HRK and stained with mitochondrial membrane potential probe, JC-1, immediately before analysis. Fluorescence intensity (ex. 545nm, em. 590nm) was measured at 5 minute intervals for 120 minutes with intermittent shaking at 30°C using a HidexSense plate reader. The relative loss of mitochondrial membrane potential (ΔΨm) was calculated by normalising the area under the curve for each treatment to DMSO and FCCP treated control cells. Cell lines are arranged in order of sensitivity to A1331852. Data are expressed as mean + S.D. (n=2-4).

BH3 profiling is a quick and relatively inexpensive assay, making it an ideal method to stratify patients in clinic. Although the profiles can provide mechanistic insight into the apoptotic pathways in each sample, the data can conflict with their mimetic responses. Presented in Figure 3-29 are correlations between BH3 profile responses and the EC_{50} values for the corresponding mimetic that targets the same protein/s. EC_{50} values that could not be calculated due to the response curves not converging with the x-axis were excluded from the calculations. As discussed previously, the accuracy of EC_{50} values over

10,000nM could be unreliable, as these concentrations were not actually tested. Nonetheless, exclusion of these data points puts more bias on responding cell lines and lower EC_{50} values. For this reason, these values were included in this analysis.

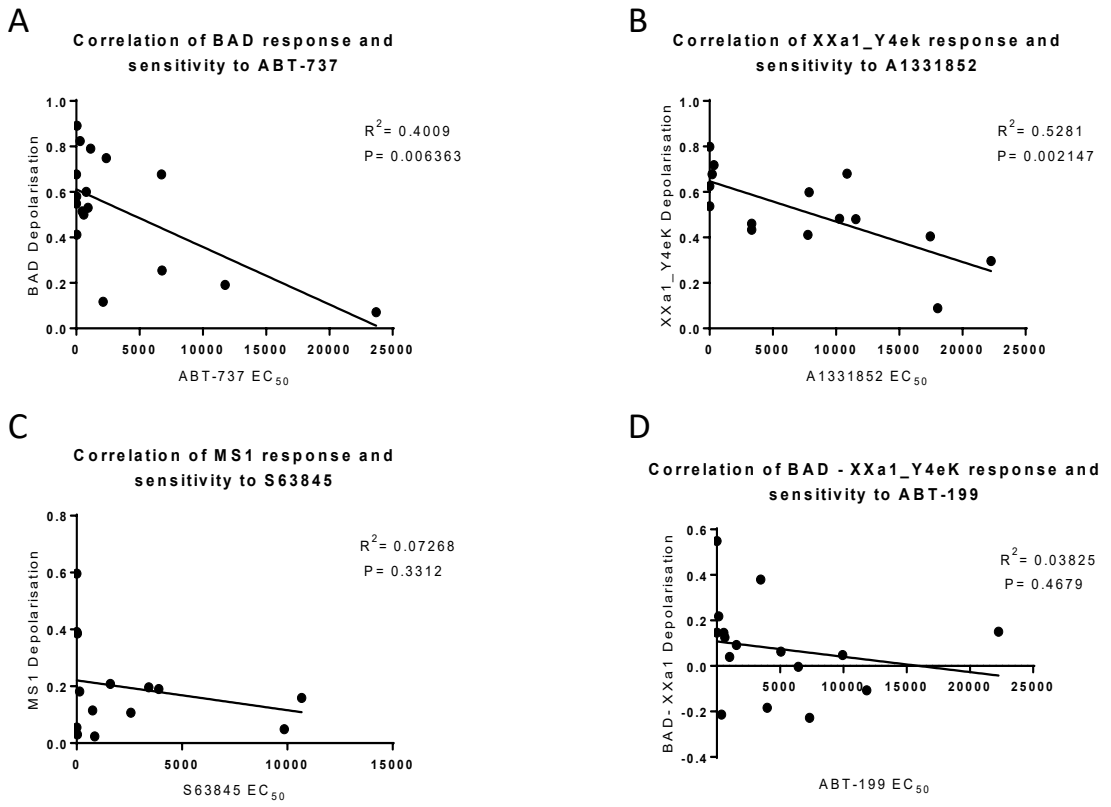

Figure 3-29 Correlation between BH3 profile responses and EC_{50} to correlating BH3 mimetics
Correlations between the EC_{50} of specific BH3 mimetics and the response to corresponding peptides (normalised loss of mitochondrial membrane potential) analysed via BH3 profiling. Each dot is representative of one cell line and the solid line is representative of the linear regression line. Pearson's co-efficient of determination (R^2) and the statistical significance values (P) are indicated on each graph. P values less than 0.05 are statistically significant. A. Correlation of BAD peptide response and the EC_{50} values for ABT-737. B. Correlation of XXa1_Y4ek peptide response and the EC_{50} values for A1331852. C. Correlation of MS1 peptide response and the EC_{50} values for S63845. D. Correlation of the BAD peptide response minus the response to XXa1__Y4ek and the EC_{50} values for ABT-199.

The BAD peptide, targeting BCL2, $BCLX_L$ and BCLW, had a statistically significant correlation with the EC_{50} values for ABT-737, which inhibits the same proteins (p= 0.006) (Figure 3-29 A). Due to the multiple proteins targeted, most of the cell lines had some response to this mimetic and had mitochondrial depolarisation after treatment with the BAD peptide. This has resulted in a cluster of high responders on the left hand side of the x-axis, which could be influencing the correlation data. Furthermore, the exclusion of the 2 cell lines with EC_{50} values over 10,000nM increases the P value to 0.31 and reduces the co-efficient of determination (R^2) value to 0.08 (graph not shown). Taken

together, it is likely that this correlation is driven by the extreme values of sensitive and resistant cell lines without a general trend throughout the range of values.

The correlation between the response to the $BCLX_L$ specific peptide, XXa1_Y4eK and the sensitivity to A1331852, which targets the same protein, was also statistically significant, with a p value of 0.002 and R^2 value of 0.53 (Figure 3-29 B). In contrast, it has a greater spread of responses and the correlation is less likely to be caused by extreme values. That notwithstanding, there are six A1331852-resistant cell lines with an EC_{50}> 10000nM and when these cell lines are excluded from the analysis, the p value increases to 0.094 (R^2 =0.34) (graph not shown). Although no longer statistically significant, there is still a trend between response to the XXa1_Y4ek peptide and sensitivity to A1331852.

The correlation between the response to the MCL1 specific peptide, MS1 and the sensitivity to S63845, which targets the same protein, was not statistically significant, with a p value of 0.33 and R^2 value of 0.07 (Figure 3-29 C). The low R^2 value for this data set is indicative of how unwell the data points fit the linear regression line. Removal of the two cell lines which have an EC_{50} >10,000nM (points overlap and appear as one dot on the figure) reduced the p value to 0.28 and increased the R^2 value to 0.11 (graph not shown). This is still statistically non-significant and is indicative of high variance compared to the linear regression line. These data confirm previous conclusions that responses to the MS1 peptide during BH3 profiling is a poor indicator of sensitivity to S63845.

As there is no specific peptide for BCL2, which was used in the panel for BH3 profiling, BCL2 dependence, and therefore ABT-199 sensitivity, should correlate to the response to the pan-specific BAD peptide minus the response to the $BCLX_L$ specific XXa1_Y4ek peptide. As shown in Figure 3-29 D, this correlation was very weak, with an R^2 value of 0.04 and is statistically non-significant, with a p value of 0.47. Exclusion of the two cell lines with an EC_{50} >10000nM increases this correlation slightly, as the R^2 value becomes 0.15 with a p value of 0.18 (graph not shown). However, this is still a very weak correlation and is not statistically significant. This may in part be due to quite large mitochondrial depolarisations after treatment with the XXa1_Y4ek peptide in cell lines

which had low sensitivity to A1331852. Therefore, the proportion of the BAD peptide response which is reliant on $BCLX_L$ is ambiguous. Hence, cell lines which are solely $BCLX_L$ dependent or dual dependent BCL2 and $BCLX_L$ are difficult to distinguish. Additionally, the BAD peptide will target BCL2, $BCLX_L$ and BCLW. Although the binding affinity for the latter is lower compared to the other proteins, it is worth considering that the response of BAD peptide minus XXa1_Y4eK may also be indicative of dependencies of BCLW. Without either a BCLW specific peptide for BH3 profiling or specific mimetic, the dependency on BCLW can only be further investigated using genetic modifications, such as transient knock downs and CRISPR/Cas9 technology.

3.10 Interactions of the BCL2 family members in DLBCL

In order to investigate the interactions between anti- and pro-apoptotic proteins, immunoprecipitations were performed by collaborator, Dr Meike Vogler. The BCL2-dependent cell lines (within the blue box: RIVA, U2932 and OCI-LY1), displayed a high proportion of BIM bound to BCL2, despite a high expression of $BCLX_L$ and MCL1. These cell lines also had a high proportion of BAX bound to BCL2. In the $BCLX_L$ dependent cell lines (within the red box: SUDHL8 and RCK8), the expression of BIM is relatively low compared to the other cell lines; moreover, interactions of this protein were hard to detect. Nonetheless, both BAK and BAX were sequestered by $BCLX_L$ in these cell lines. In contrast BIM was highly bound by MCL1 in the MCL1-dependent cell lines (those in the green box: SUDHL10, U2946 and TMD8). In these cell lines, BAK was sequestered by MCL1. These data are also consistent with previous reports, which indicate that BAK can be sequestered by MCL1 and $BCLX_L$ but not BCL2 (Willis*, et al* 2005).

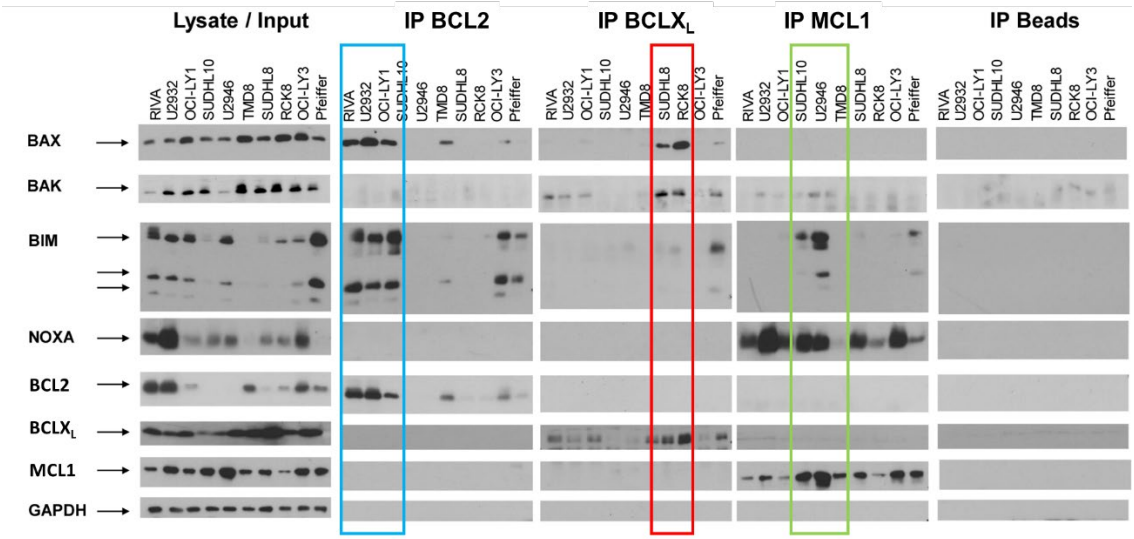

Figure 3-30 Interactions of BCL2 family members in DLBCL cell lines
Immunoprecipitation of BCL2, BCLX$_L$ and MCL1 were performed in untreated cell lysates from DLBCL cell lines, followed by analysis of binding of pro-apoptotics proteins (BIM, NOXA, BAX and BAK) via immuno-blot. Protein G beads without primary antibody were used to control for unspecific binding. Staining with BCL2, BCLX$_L$, MCL1 and GAPDH was performed to demonstrate efficient immunoprecipitation and equal protein loading, respectively. Mainly BCL2 dependent cell lines are in the blue box, mainly BCLX$_L$ dependent cell lines are in red and mainly MCL1 dependent cell lines are in the green box. Data shown are of one representative immuno-blot (n=2).

Further work performed in collaboration with Dr Meike Vogler, showed that the direct interaction between the anti-apoptotic proteins and BAK/BAX were disrupted upon treatment with BH3 mimetics (Smith*, et al* 2019) (Smith*, et al* 2019) (Appendix 3). Moreover, the knockdown of BIM or BAK only partly reduced cell death, whereas BAX was essential (Smith*, et al* 2019) (Appendix 3). This supports previous studies which found BAX to be essential for apoptosis (Greaves*, et al* 2019).

Taken together, these data suggests that DLBCL are highly primed and anti-apoptotic protein dependency of DLBCL cell lines is due to the proteins interactions with BIM, BAX and/or BAX. This is supportive of the unified model of apoptosis (Llambi*, et al* 2011). The basis for the differential preferential binding of these proteins to the anti-apoptotic proteins is unknown and cannot be explained by binding affinities as described in the binding code (Chen*, et al* 2005). This code was determined in membrane free systems and it has since been documented that BCLX$_L$ has different conformational changes and thus binding affinities in membrane free and membrane bound solutions (Yao*, et al* 2015). Other studies have indicated that PTMs of the BCL2 family members, such as BCL2 phosphorylation at Ser-70, may affect protein binding and complex stabilisation

(Deng, *et al* 2000). Therefore, it is possible that differential binding could be due to protein localisation or PTMs, which were not investigated in this study.

3.11 Combination of BH3 Mimetics

Some cell lines are indicated to have a joint dependence on more than one anti-apoptotic protein and could potentially benefit from the combination of BH3 mimetics. When two drugs are used in combination, their effects can be described as additive, antagonistic or synergistic (Chou, 2010). An additive effect is observed when the combination is equal to the product of the effects of each individual agent (this is the expected default result of combining two drugs). An antagonistic effect takes place when the drugs interact in a way to produce an undesirable effect, less than the expected outcome. In a synergistic effect, the effect of the combination of drugs is greater than the expected addition of both individual effects. Synergistic combinations are therapeutically promising because lower concentrations of the drugs are needed, reducing toxicities and potentially delaying resistance.

Combinations of BH3 mimetics have been tested in a panel of DLBCL cell lines. The efficacy of these combinations was assessed using Calcusyn software which uses the Chou-Talalay method to generate combination index (CI) values (Chou 2010, Chou and Talalay 1984). In short, values below 0.9 are considered synergistic, values between 0.9-1.1 are additive and values above this are antagonistic.

3.11.1 A1331852 and S63845

$BCLX_L$-specific A1331852 and MCL1-specific S63845 were tested in combination in a panel of cell lines (Figure 3-31, Figure 3-32). The combination in 8/11 cell lines was found to be additive or antagonistic. A synergistic effect was only observed in TMD8 and two cell lines that are derived from this. TMD8 was sensitive to single agent S63845 (EC_{50} = 49nM) but was resistant to single agent A1331852 (EC_{50} = 10866nM). Yet the combination of these two mimetics had a CI value of 0.12. This is highly synergistic, requiring only 10nM of S63845 and 1nM of A1331852 to result in 6.4% viability. The BH3 profile of this cell line indicated a high level of priming, which may partly explain

how low concentrations of the drugs can cause a large effect. More studies are required to understand the mechanism of this synergy.

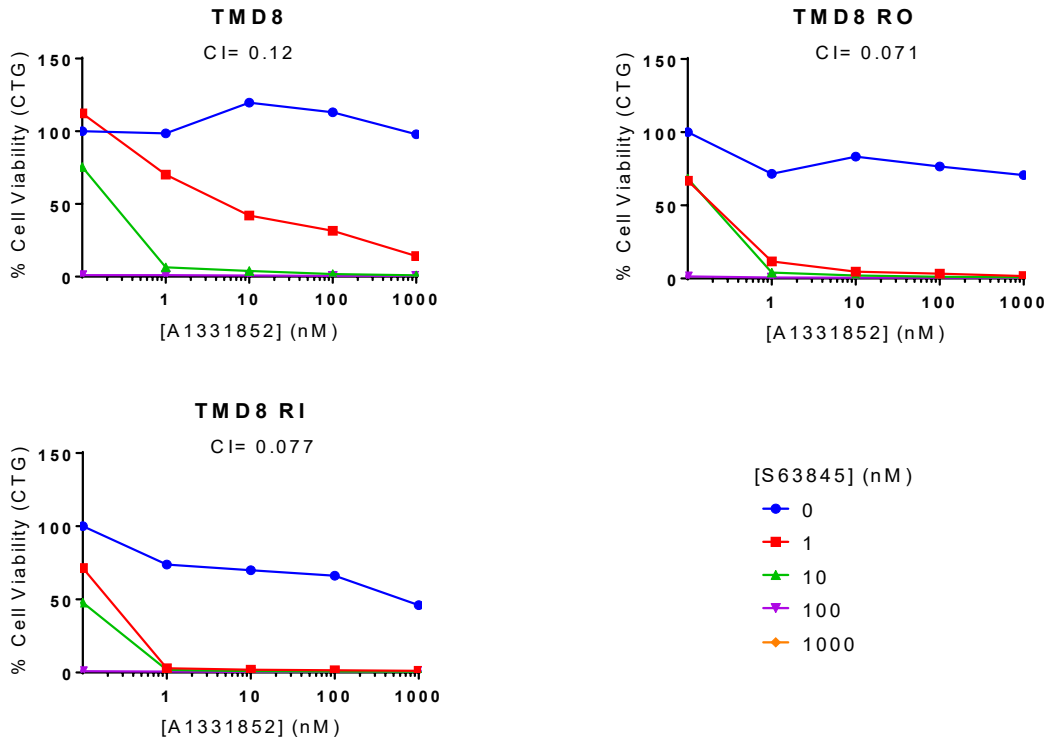

Figure 3-31 Synergistic combinations of A1331852 and S63845 in DLBCL cell lines
DLBCL cell lines were treated with 0-1000nM of A1331852 in combination with 0-1000nM S63845 for 72 hours. Cell viability was analysed by CellTiterGlo viability assay. Data were normalised to DMSO treated control. Data are expressed as mean (n=2-3) .Combination index (CI) values were calculated for each cell line using Calcusyn and are shown. CI values <1 are indicative of synergy.

This average CI value for the combination was additive/ antagonistic in other DLBCL cell lines tested (Figure 3-32). Although the overall combination in BJAB is not synergistic, there were certain concentration combinations which are. Both drugs had little effect on the cell line and as such when the data for 1nM of either drug are excluded from the calculation, the average CI value decreased to 0.9 which is slightly synergistic. This indicates there could be dual dependence on MCL1 and $BCLX_L$ within this cell line.

This combination was ineffective in BCL2 dependent RIVA indicating that the cell line is solely dependent on BCL2 and cannot be compensated by inhibiting the other proteins in combination. The combination on resistant cell line CTB-1 was also ineffective, therefore this cell lines resistance is not due to a dual dependence on $BCLX_L$ and MCL1 which require concomitant targeting.

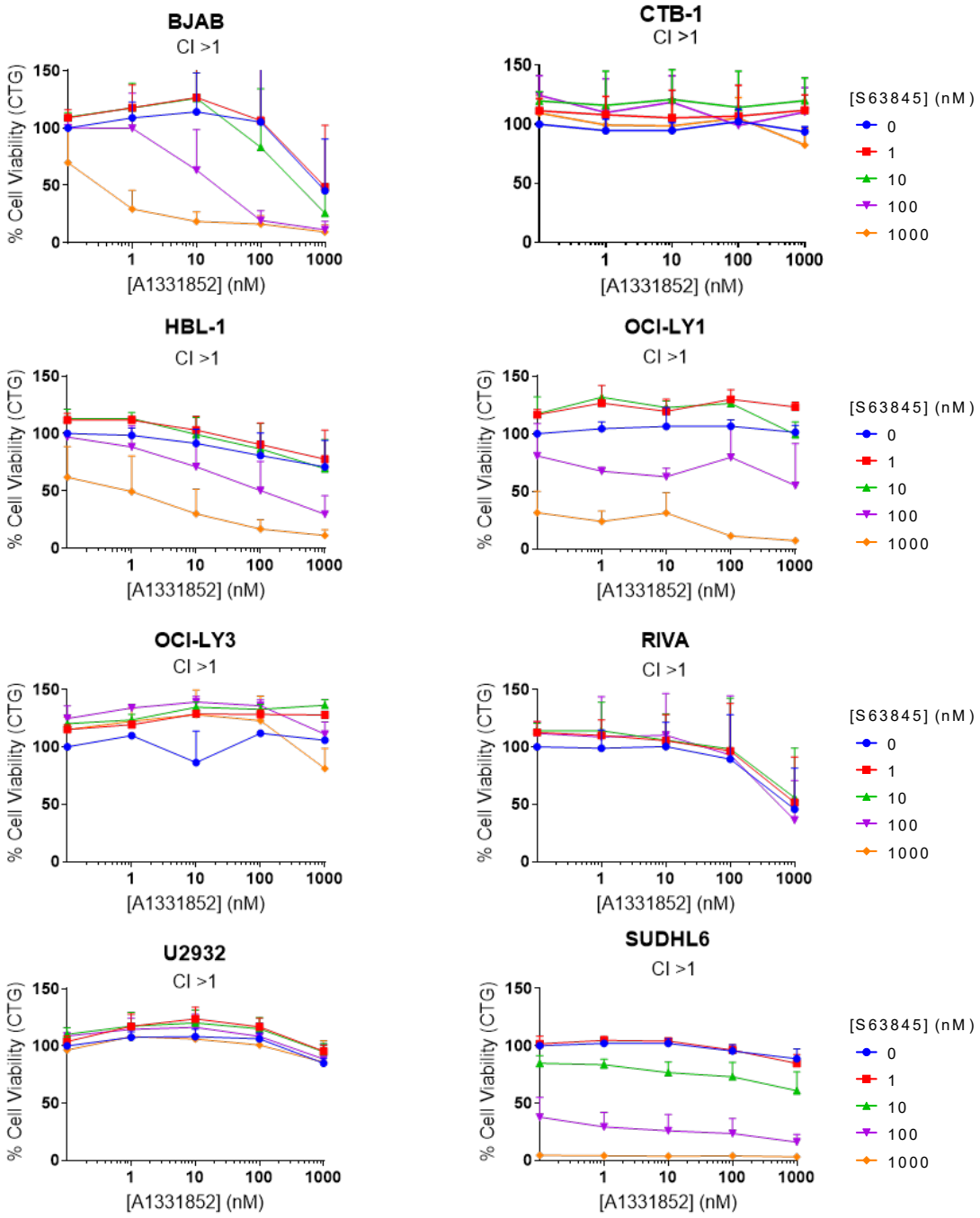

Figure 3-32 Additive and antagonistic combinations of A1331852 and S63845 in DLBCL cell lines
DLBCL cell lines were treated with 0-1000nM of A1331852 in combination with 0-1000nM S63845 for 72 hours. Cell viability was analysed by CellTiterGlo viability assay. Data were normalised to DMSO treated control. Data are expressed as mean +SD. (n=2-4) .Combination index (CI) values were calculated for each cell line using Calcusyn and are shown. CI values <1 are indicative of synergy.

3.11.2 ABT199 and S63845

Combinations of the BCL2-specific ABT-199 and MCL1-specific S63845 were found to be synergistic in 6/14 cell lines tested (Figure 3-33). SUDHL6 and OCI-LY19 displayed a synergistic loss of viability, with a CI value of 0.39 and 0.25, respectively (Figure 3-33). There was a joint dependence of BCL2 and MCL1 in these cell lines, as can be seen by their responses to single agent ABT-199 and S63845. This would provide a rational basis for the synergistic combination in these cell lines.

As mentioned, TMD8 was sensitive to single agent S63845 but responded quite poorly to single agent ABT-199 (EC_{50}= 6439nM). Yet, the combination of these two mimetics had a CI value of 0.1. This is highly synergistic, requiring only 10nM of each compound to result in 12% viability. The BTK inhibitor resistant derivatives also had this synergy. As shown previously, TMD8 also responded synergistically to MCL1 and $BCLX_L$ inhibition. The common denominator between the two combinations is the inhibition of MCL1, which could suggest that MCL1 is causing an apoptotic block in this cell line as inhibition of either of the other proteins alone had little to no effect on the cells but significantly perpetuates the effect of MCL1 inhibition. More studies such as co-immunoprecipitations and knock-downs are required to understand the mechanism of these synergies.

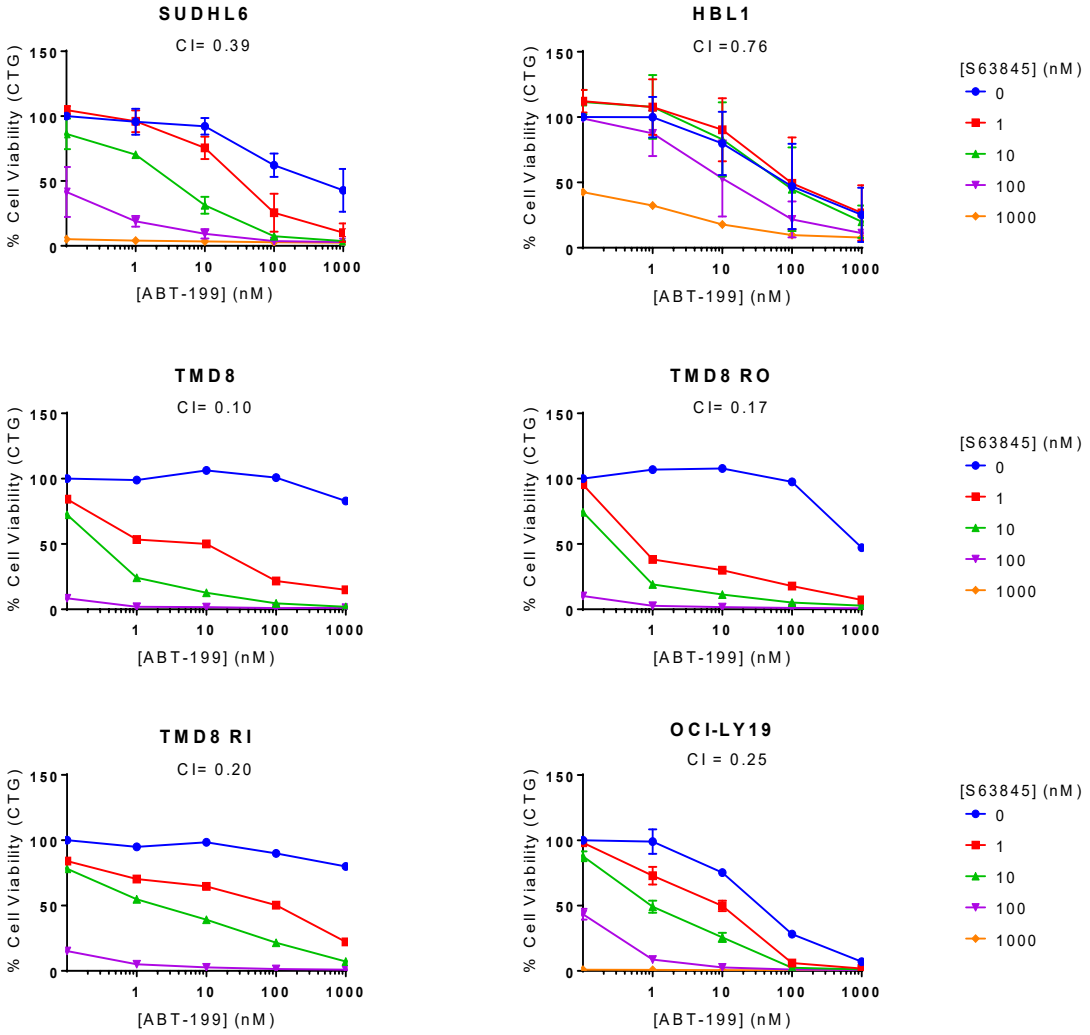

Figure 3-33 Synergistic combinations of ABT-199 and S63845 in DLBCL cell lines
DLBCL cell lines were treated with 0-1000nM of ABT-199 in combination with 0-1000nM S63845 for 72 hours. Cell viability was analysed by CellTiterGlo viability assay. Data were normalised to DMSO treated control. Data are expressed as mean +/- SD. (n=2-4) .Combination index (CI) values were calculated for each cell line using Calcusyn and are shown. CI values <1 are indicative of synergy.

The remainder 8/14 cell lines tested with this tested for this combination had an additive or antagonistic response (Figure 3-34). SUDHL8 and RCK8 (which are very BCL2 dependent) cannot be killed by targeting the other anti-apoptotic proteins in combination. As with the previous combination, CTB-1 is also resistant to the dual targeting of BCL2 and S63845. The inhibition of BCL2 and MCL1 has previously been reported to be synergistic in HBL1, OCI-LY19, OCI-LY1 and U2932 (Klanova*, et al* 2016). The synergy for the former two cell lines has been confirmed in this study, however the combination in OCI-LY1 and U2932 was found to be additive/ antagonistic. This difference could be due to the former study using an indirect inhibitor of MCL1

(homoharringtonine) which may also have non-specific effects not caused by S63845 (Klanova, *et al* 2016).

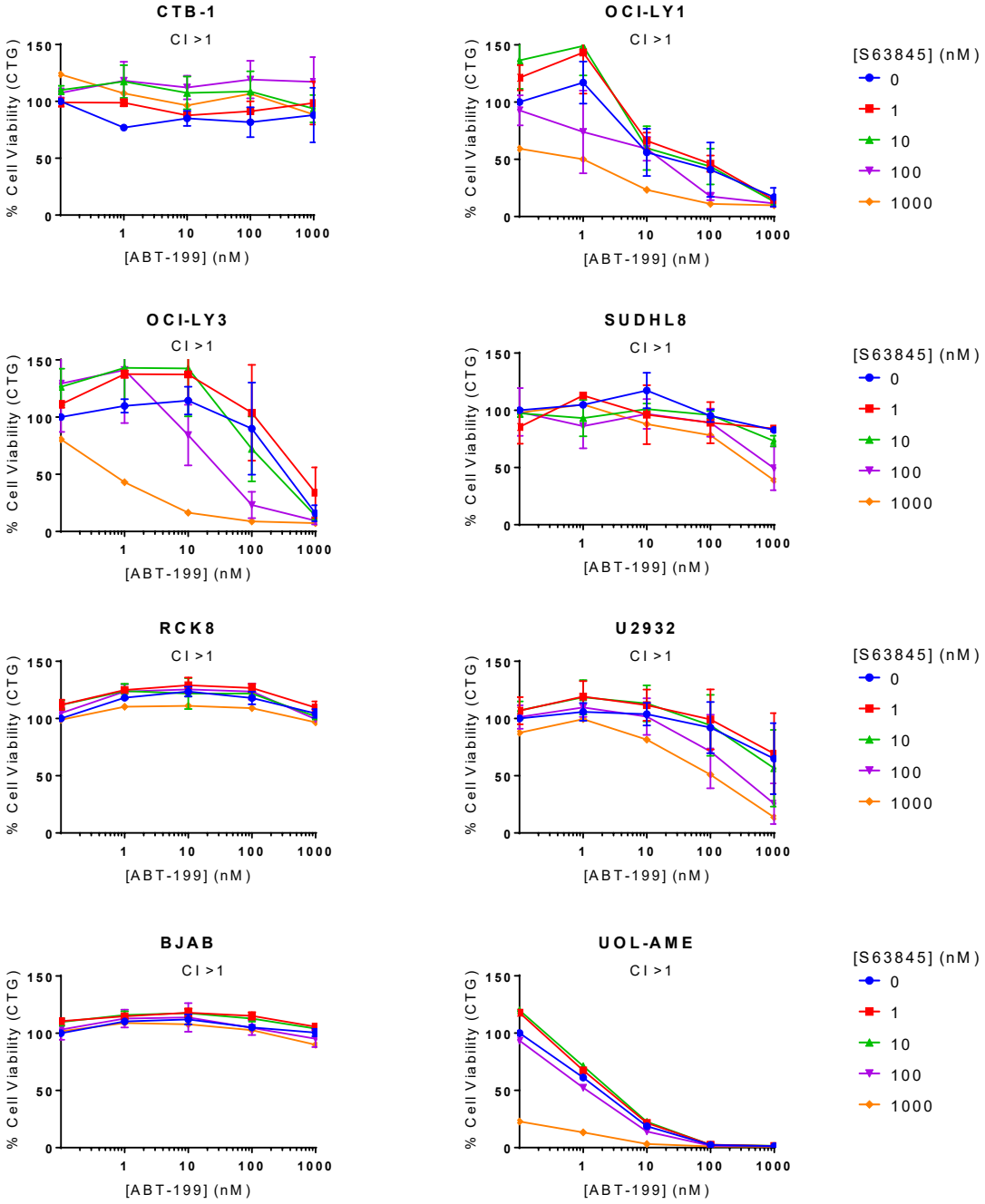

Figure 3-34 Additive and antagonistic combinations of ABT-199 and S63845 in DLBCL cell lines
DLBCL cell lines were treated with 0-1000nM of ABT-199 in combination with 0-1000nM S63845 for 72 hours. Cell viability was analysed by CellTiterGlo viability assay. Data were normalised to DMSO treated control. Data are expressed as mean +/ SD. (n=2-5) .Combination index (CI) values were calculated for each cell line using Calcusyn and are shown. CI values <1 are indicative of synergy.

3.11.3 ABT-199 and A1331852

The combination of BCL2 specific ABT-199 and $BCLX_L$ specific A1331852 has been tested in 8 cells lines. All cell lines tested had an additive or antagonistic effect. As no synergistic combinations have been found for this combination yet it is unclear whether this combination can be effective. Further cell lines will need to be tested.

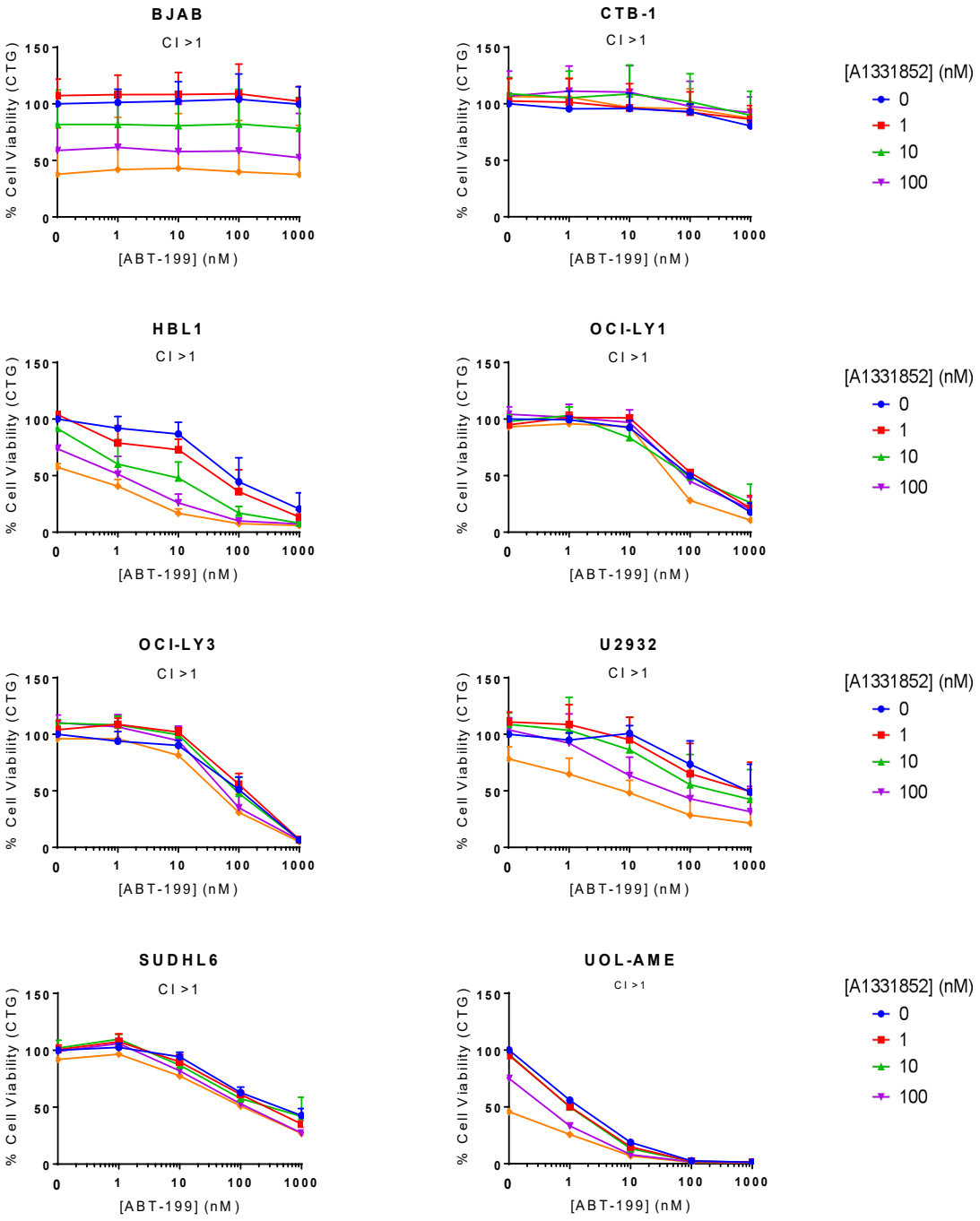

Figure 3-35 Additive and antagonistic combinations of ABT-199 and A1331852 in DLBCL cell lines
DLBCL cell lines were treated with 0-1000nM of ABT-199 in combination with 0-1000nM A1331852 for 72 hours. Cell viability was analysed by CellTiterGlo viability assay. Data were normalised to DMSO treated control. Data are expressed as mean +SD. (n=3-4) .Combination index (CI) values were calculated for each cell line using Calcusyn and are shown. CI values <1 are indicative of synergy.

3.12 Discussion

Firstly, the mimetics used in this study were confirmed as true *bona fide* BH3 mimetics as they could not induce cell death in BAK/BAX KO cells. A side-by-side comparison of

two MCL1 inhibitors, A1210477 and S63845 indicated that S634845 was much more efficacious than the former, likely due its increased binding affinity for the target protein (Kotschy*, et al* 2016, Leverson*, et al* 2015b).

The data presented using DLBCL patient samples have confirmed that within DLBCL there is a heterogeneous dependence on different anti-apoptotic proteins. As the amount of patient sample available is limited and they are often susceptible to spontaneous apoptosis, the remainder of the work was performed in DLBCL cell lines. The heterogeneous response to BH3 mimetics was recapitulated using these cell lines. Moreover, some cell lines exhibited remarkable sensitivity to one of the specific BH3 mimetics (EC_{50} < 1nM) indicating a sole dependency on one anti-apoptotic protein. The extreme sensitivity of these cell lines raises questions of stoichiometry, the transiency of drug interaction and the number of mitochondrial pores necessary to induce cell death. The biologically basis for this 'ultra-sensitivity' is not known and it is yet to be determined whether patient cells will be sensitive to BH3 mimetics to this extent. Additionally, there were cell lines which exhibited sensitivity to two BH3 mimetics. Conversely, three cell lines were identified which were resistant to any of the mimetics (EC_{50} >10000nM). As there are no specific mimetics for BCL2A1 or BCLW it is not clear whether these cell lines are functionally dependent on these proteins. Alternatively, they could harbour mutations, resulting in an apoptotic block, rendering the mimetics ineffective despite dependence.

Sensitivity to the mimetics did not correlate with disease COO, further highlighting the requirement to subgroup the disease based on anti-apoptotic protein member dependence and identify biomarkers for such groups. It could be hypothesised that cells which express a high level of BCL2 would depend upon that protein and therefore be susceptible to inhibition by ABT-199. Interestingly, DHL or cell lines with t(14;18)(q32;q21) *IGH-BCL2* did not signifigantly differ in response to the drug. It was unanticipated that a cell line such as SUDHL10 which contains this *IGH-BCL2* translocation is resistant to ABT-199 (EC_{50}~9937nM). In contrast, it is uniquely sensitive to S63845 (EC_{50}< 1nM). It is not known how these cells are able to undergo apoptosis upon MCL1 inhibition as there is a large expression anti-apoptotic BCL2. Within this cell line, BCL2 could be sequestered by one of the BH3 only proteins. Alternatively, the

protein could be performing other non-apoptotic functions and could therefore not be accessible at the mitochondria or apoptotic involvement. Conversely, there could be a mutation within BCL2.

Furthermore, sensitivity only partly correlated to target protein expression. There was a statistically significant correlation between BCL2 protein expression and sensitivity to BCL2 inhibitor ABT-199, however not all cell lines expressing high levels of BCL2 were sensitive to ABT-199. This correlation could not be recapitulated by the other anti-apoptotic proteins and their specific inhibitors. Sensitivity to A1331852 or S63845 also did not correlate to the ratio of target protein to the other anti-apoptotic proteins. Taken together, protein expression is a poor marker for anti-apoptotic protein dependence and BH3 mimetic sensitivity.

Based on protein expression analysis alone, it is unclear why cell lines such as RIVA and U2932 which also express high levels of $BCLX_L$ and MCL1 are functionally dependent on BCL2. Immunoprecipitations of these cell lines revealed that BAX and BIM were exclusively sequestered by BCL2, providing rationale for their drug sensitivity. However, the molecular basis for this preferential binding is not known. It is possible that the protein may not be accessible at the mitochondria or PTMs may affect binding. These were not investigated in this study. Immunoprecipitations in $BCLX_L$ dependent cell lines showed that BAK and BAX were exclusively bound to $BCLX_L$ and in MCL1 dependent cell lines there is a large proportion of BIM and BAK sequestered by MCL1. Hence, this suggests that mimetic sensitivity is mediated by protein interactions; in particular the sequestration of BIM, BAX and/or BAK by the anti-apoptotic proteins.

Cell lines identified from the responses to BH3 mimetics to be functionally dependent on more than one anti-apoptotic protein such as SUDHL6 and OCI-LY19 were also found to be synergistic to the combination of inhibitors. The mechanisms of these dual sensitivities are unknown and could perhaps be further investigated using co-immunoprecipitations. It could be hypothesised that more than one anti-apoptotic protein is sequestering BAK/BAX in these cell lines. Alternatively, there may be an excess of the anti-apoptotic proteins which can allow partner swapping when the other is inhibited. Unsurprisingly, TMD8 and derived resistant cell lines which were only

sensitive to S63845 exhibited a synergistic effect when treated with a combination of S63845 and ABT-199 or A1331852. This cell line is sensitive to BTK inhibition (data not shown) and unpublished work by the Dyer Lab has shown that the inhibition of BTK results in a suppression of the NFκB pathways, leading to a down-regulation of $BCLX_L$ and MCL1, eventually killing the cells. The expression of $BCLX_L$ and MCL1 does not change in the ibrutinib and ONO-4059 generated resistant cell lines (TMD8 RI and TMD8 RO) after treatment with their respective drugs (data not shown). Therefore resistance to BTK inhibitions in these cell lines could be due a dependence on MCL1 and $BCLX_L$, of which expression cannot be regulated by BTK inhibitors but is susceptible to direct inhibitors. This could provide an alternative treatment option for patients who have become resistant to BTK inhibitors. The combinations which are synergistic in TMD8 (S63845 & A1331852 and the S63845 & ABT-199) both involve the inhibition of MCL1. Moreover, the cell line is not sensitive to BCL2 or $BCLX_L$ inhibition without concomitant MCL1 inhibition. It is difficult to determine the interactions with MCL1 in the TMD8 cell line from the immunoprecipitation data presented here. However, it would be interesting to ascertain what is bound to MCL1 as the disruption of this complex is necessary for cell death which can be further enhanced by $BCLX_L$ and BCL2 inhibition. It is possible that MCL1 could be directly sequestering BAK, the alleviation of which can induce cell death. If BCL2 and/or $BCLX_L$ were bound to an activator BH3 protein then their release upon inhibition may perpetuate BAK activation and pore formation but not without the removal of MCL1 from BAK. Alternatively, BAK and BAX could be sequestered by more than one anti-apoptotic protein or upon MCL1 inhibition there may be a level of partner swapping occurring which suppresses apoptosis.

BH3 profiling has been proposed as a quick technique that can rapidly and accurately determine anti-apoptotic protein dependence and could be adapted for use in clinic (which would be faster than *in vitro* drug assays). In contrast, the data presented here indicates that BH3 profiling may be able to predict $BCLX_L$ protein dependence but is less accurate at assessing dependence on other proteins. It is also difficult to determine where the threshold for mitochondrial depolarisation to determine sensitivity should be. Profiles for cell lines which partially respond to A1331852 (such as RIVA) can be difficult to distinguish from those remarkably sensitive to the drugs (such as RCK8).

As there is no specific BCL2 inhibitor it is difficult to determine BCL2 dependence and the interpretation of results can be misleading between BCL2 or $BCLX_L$ or dual BCL2 and $BCLX_L$ dependence. The peptide used to determine MCL1 protein dependence was not indicative and did not improve upon increasing concentration. Even so, the BH3 profiles of OCI-LY10 and CTB-1 could predict the resistance to BH3 mimetics due to the low level of depolarisation after the addition of peptides. There have also been other reports of conflicting data between BH3 profiles and BH3 mimetic sensitivity (Butterworth*, et al* 2016).

An adaptation of this technique called 'dynamic profiling' has been described, where cells are pre-incubated with a drug before the exposure to the peptides (Montero*, et al* 2015). If the cells are sensitive to the drug, there should be a greater depolarisation caused by BIM, as the cells will be more primed. Short incubations with specific mimetics may also provide more information for cells that contain dual dependencies, as previously reported (Butterworth*, et al* 2016). As the number of specific BH3 mimetics are increasing, dynamic profiling could overcome some of the shortfalls caused by not having specific peptides. Dynamic profiling was not used within this study but it may provide a fast approach to determine cell sensitivities to not only BH3 mimetics but also other drugs.

The synthetic peptides used in this assay have been manufactured to be more specific than endogenous BH3 proteins and they can have up to 1000x more selectivity for their target protein compared to the other anti-apoptotic protein (Foight *et al*., 2014, Dutta *et al*., 2015, Jenson *et al*., 2017). However, it is important to consider that these synthetic peptides are not full-length proteins, so they may not be able to completely mimic a BH3 protein. The outcome of this assay is measuring loss of mitochondrial membrane potential and it is assumed that this will always result in cell death. However, as discussed in 1.4.6, it is now understood that sub-lethal stress can result in miMOMP. Therefore mitochondrial depolarisation may be an inappropriate surrogate of cell death. Furthermore, this assay requires the permeabilisation of cells to allow entry of the synthetic peptides. It is possible that this process may allow the evacuation of small, non-membrane bound BH3 proteins which could affect the dynamics of protein binding

and apoptosis induction. This could have been investigated by permeabalising the cells, collecting the supernatant and assessing protein content.

Additionally, there are other limitations that would require resolving before this assay could be used clinically. This technique is dependent on viable cells, which are not always available for patient samples, especially if the disease is restricted to the lymph nodes. Moreover, as data from Figure 3-3 suggests, DLBCL primary samples are susceptible to spontaneous apoptosis. During this assay, cells are permeabalised to allow peptide entry. In part due to the buffer used, this was well tolerated by stable cell lines used in this report. However, when performed on primary cells, the results were inconclusive due to a high basal rate of mitochondrial depolarisation (data not shown). This is most likely due to the cells being unable to withstand the stress of removal from their environment plus permeabilisation. It is possible that adjustments of the buffer composition may be able to compensate for this. Alternatively, if performed via flow cytometry, the live cells could be gated for. However, it is not clear whether this selection of cells would be representative of the whole cell population. The BH3 profiling technique used for DLBCL cell lines required several adjustments and optimisations, including number of cells used, digitonin concentration (data not shown) and peptide concentrations. It is quite likely that these would need further optimisation for primary samples and these could vary based on cell type/ type of lymphoma. Even after the optimisation of the protocol for DLBCL cell lines the data was still quite variable as is evident by the standard deviation. Extra precautions were taken, such as passaging cells at the same time point previous to BH3 profiling, but multiple repeats of the assay were required to ensure data was reliable. This highlights another potential pitfall of the application of this technique to clinic, as multiple samples from the same patient at the same time point are not often available. The assay's limitations mean that if $BCLX_L$ and MCL1 specific inhibitors are approved for the treatment of DLBCL, the data from BH3 profiling could not be used in isolation to determine a patient's therapy.

4 Results 2- Acquired resistance to BH3 mimetics

Patients who are initially sensitive to targeted therapies can develop acquired resistance. With references to BH3 mimetics, the majority of work investigating acquired resistance has focused on ABT-199 due to its advanced clinical development compared to the other specific mimetics. To investigate mechanisms of acquired resistance to BH3 mimetics in DLBCL, four resistant DLBCL cell lines were developed derived from two sensitive parental cell lines. Parental cell lines were treated with increasing low doses of BH3 mimetics until cells survived treatment and had therefore developed resistance. ABT-199 and ABT-737 resistant cell lines were generated from BCL2 dependent RIVA (RIVA-737R and RIVA-199R respectively). ABT-737 and A1331853 resistant cell lines were generated from $BCLX_L$ dependent RCK8 (RCK8-737R and RCK8-A133R respectively).

4.1 BCL2 inhibitor resistance in parental RIVA and derived cell lines

The RIVA cell line is extremely sensitive to BCL2 specific inhibitor, ABT-199, at pico-molar concentrations and is also sensitive to the lesser specific ABT-737 which also targets $BCLX_L$ and BCLW. Therefore, this cell line was an ideal candidate to investigate acquired resistance to BCL2 inhibitors.

4.1.1 Response to BH3 mimetics

The sensitivity to BH3 mimetics was assessed in RIVA and derived cell lines using the CTG assay (Figure 4-1). The corresponding EC_{50} values were also calculated as can be seen in Table 4-1. RIVA-737R and RIVA-199R displayed over 6000 times resistance to their respective drugs (ABT-737 and ABT-199) compared to the parental cells, as expected. As both mimetics target BCL2, the generated resistant cell lines showed marked resistance to the other mimetic. This indicates that the mechanism of acquired resistance was the same for both for both drugs. Both compounds bind BCL2 in the same binding pocket (Souers*, et al* 2013). Therefore if there is a mutation within the binding groove, such as the recently reported $BCL2^{G101V}$ (Blombery*, et al* 2019a), this would impair the binding and efficacy of both drugs. Alternatively, if there were an

upregulation of another anti-apoptotic protein and a switch in dependence, the inhibition of BCL2 by another drug would also be ineffective.

ABT-737 also inhibits $BCLX_L$ and BCLW (Oltersdorf*, et al* 2005). Hence, it was unsurprising that the ABT-737 resistant cell line was also 18 times more resistant to $BCLX_L$ inhibition by A1331852 compared to parental cells. Neither of the resistant cell lines' sensitivity to S63845 deviated significantly from the parental indicating that there was not a shift in dependence of anti-apoptotic protein towards MCL1. As specific inhibitors for BCL2A1 have yet to be developed, this data alone cannot determine whether protein dependence has been shifted towards BCL2A1.

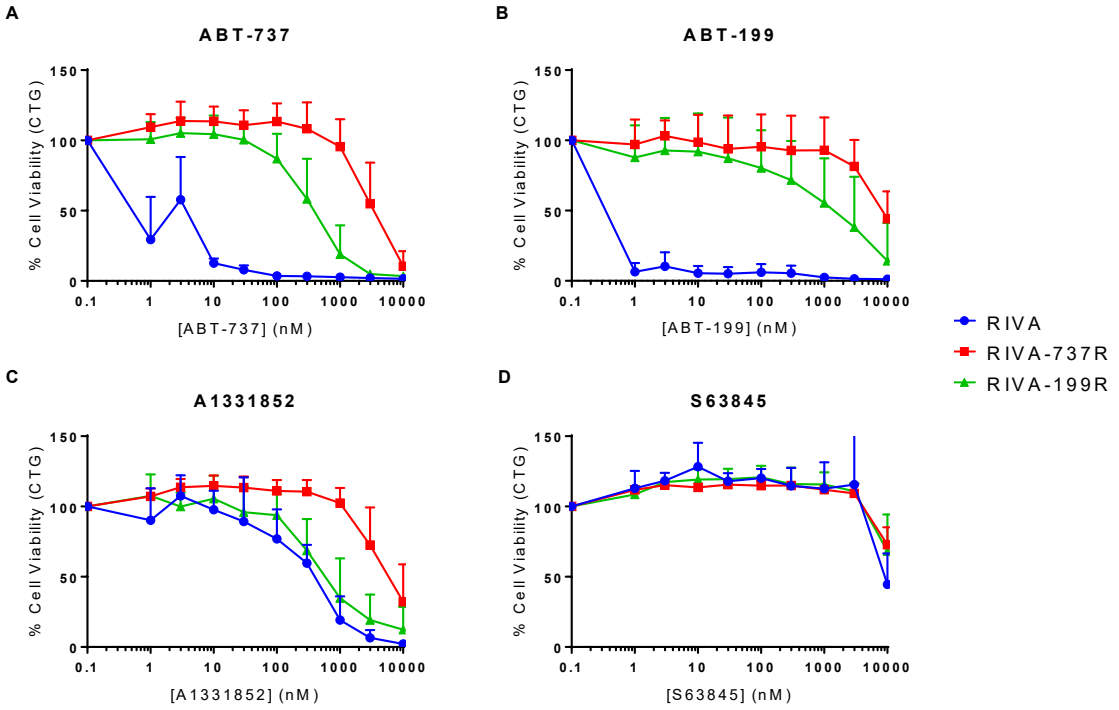

Figure 4-1 Sensitivity to BH3 mimetics in RIVA resistant cell lines
RIVA and derived resistant cell lines were plated and treated with 0-10,000nM of ABT-737 **(A)**, ABT-199 **(B)**, A1331852 **(C)** and S63845 **(D)** for 72 hours. Cell viability was analysed by CellTiterGlo viability assay. Data were normalised to DMSO treated control.Data are expressed as mean + SD (n=5-8).

	EC_{50} (nM)		
	RIVA	RIVA-737R	RIVA-199R
ABT-737	**0.6084**	3356	377.1
ABT-199	**<1**	8601	1142
A1331852	341.3	6102	662
S63845	9858	N.C	N.C

Table 4-1 EC_{50} values for BH3 mimetics in RIVA resistant cell lines
The EC_{50} values for ABT-737, ABT-199, A1331852 and S63845 in RIVA and resistant derived cell lines (presented in Figure 4-1) were calculated using Graphpad Prism. Values in red indicate the EC_{50} is less than 100nM and is therefore sensitive. Values in bold are less than 1nM indicating ultra-sensitivity. Values which could not be calculated due to the lack of convergence of the response with the x-axis are denoted as N.C, not converged.

The sensitivity to the BH3 mimetics in the resistant cell lines was confirmed via AnnexinV and PI staining (Figure 4-2). Similar to the CTG data, both resistant cell lines exhibit reduced cell death after treatment with either ABT-737 or ABT-199. However, the CTG data indicated that RIVA-737R displays a resistance to A1331852. This could not be confirmed *via* cell death analysis. Moreover, the cell line appears to be more sensitive to A1331852 than the parental cell line. However, the RIVA-737R cell line also has a reduced proportion of live cells in the control samples, and as these data are not normalised it is likely that the cell line is not an increased sensitivity in this cell line.

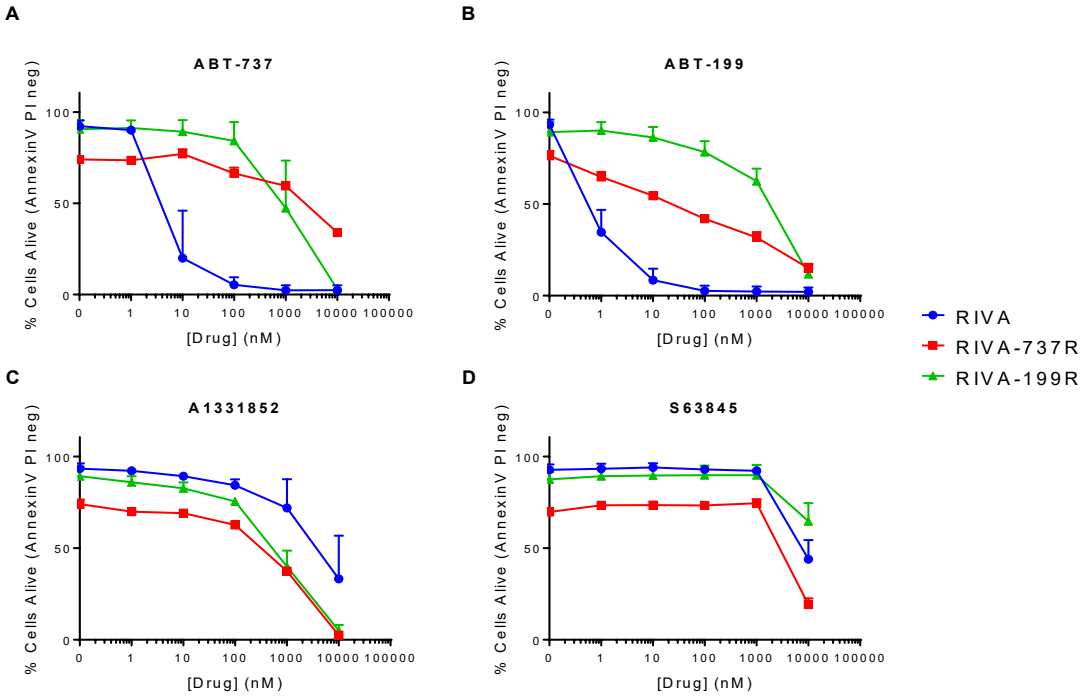

Figure 4-2 Cell death of RIVA resistant cell lines after treatment with BH3 mimetics
RIVA and derived resistant cell lines were incubated with 0-10,000nM concentrations of ABT-737, ABT-199, A1331852 and S63845 for 48 hours. Cell death was analysed by AnnexinV-FITC/PI staining measured by flow cytometry. DMSO was used as a time matched control. Data are shown as mean + SD (n=2-4).

4.1.2 BH3 profile

BH3 profiling was performed to assess whether there was a switch in dependence of anti-apoptotic proteins (Figure 4-3). As reported in Results Chapter 1, there are several limitations to BH3 profiling and the data generated can be ambiguous. That notwithstanding, the BH3 profiles for the resistant generated cell lines and parental RIVA cell line exhibited some significant differences.

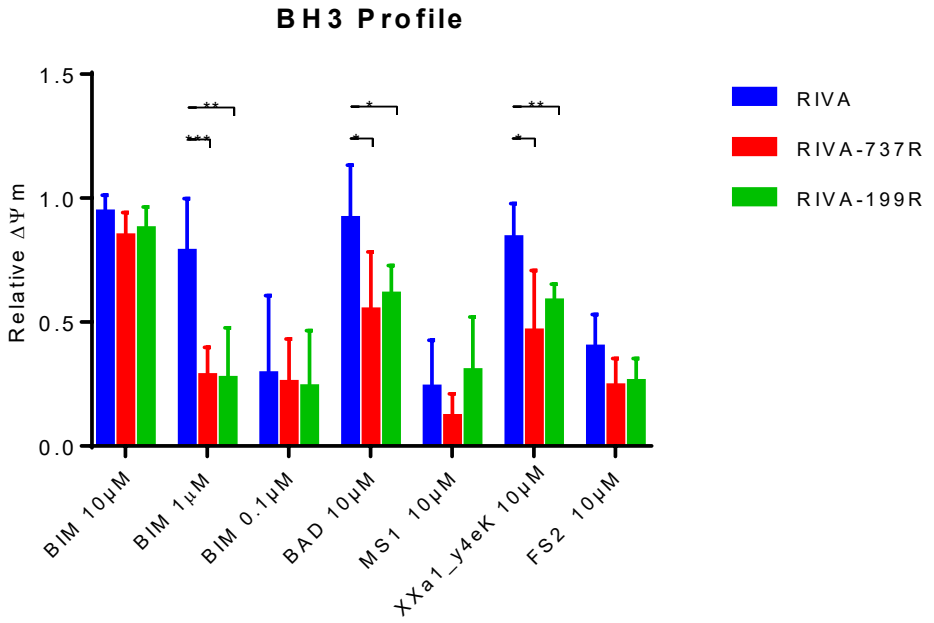

Figure 4-3 BH3 profiles of RIVA resistant cell lines
RIVA and derived resistant cell lines were gently permeabalised, treated with synthetic peptides and stained with mitochondrial membrane potential probe, JC-1, immediately before analysis. Fluorescence intensity (ex. 545nm, em. 590nm) was measured at 5 minute intervals for 120 minutes with intermittent shaking at 30°C using a HidexSense plate reader. The relative loss of mitochondrial membrane potential (ΔΨm) was calculated by normalising the area under the curve for each treatment to DMSO and FCCP treated control cells. Data expressed as mean + S.D (n=8). Multiple unpaired t-tests were performed, and p values were corrected for using the Holm-Sidak method; $p < 0.05$*, $p < 0.005$**, $p < 0.0005$***.

As shown in Figure 4-3, the resistant cell lines were less primed than their parental counterpart, as is evident by the statistically significant reduction of ΔΨm after the addition of 1µM of activator peptide, BIM. This indicates the resistant cells may have been able to withstand higher levels of cellular stress and may have acquired an apoptotic block such as reduced expression of effector proteins BAK and BAX.

There was also a statistically significant reduction of ΔΨm after treatment with 10µM of the peptide BAD (which targets BCL2, $BCLX_L$ and BCLW). This supports previous data that the cells developed resistance to BCL2 inhibitors. For RIVA-737R, this reduction may also have been mediated by the acquired resistance to $BCLX_L$ inhibition. It was therefore unsurprising that RIVA-737R also displayed a reduced response to treatment by $BCLX_L$ specific XXa1_Y4ek peptide. However, unexpectedly, a similar reduced response was also seen in the RIVA-199R cell line. Drug response analysis indicated that there was no difference between the parental and RIVA-199R cell line sensitivity to A1331852, hence the reduction in response to the XXa1_Y4ek peptide was not

anticipated. The peptide induced 58% mitochondrial depolarisation in RIVA-199R which is still indicative for the partial response to A1331852. However the reason for the reduction from the parental cell line (84%) is unclear. This further highlights the limitations of the BH3 profiling technique discussed previously. Nonetheless, when these cell line responses are plotted with the responses of the other cell lines (Figure 3-29), the strong correlation between A1331852 sensitivity and response to XXa1_Y4ek remained evident (p value of 0.001) (Figure 4-4).

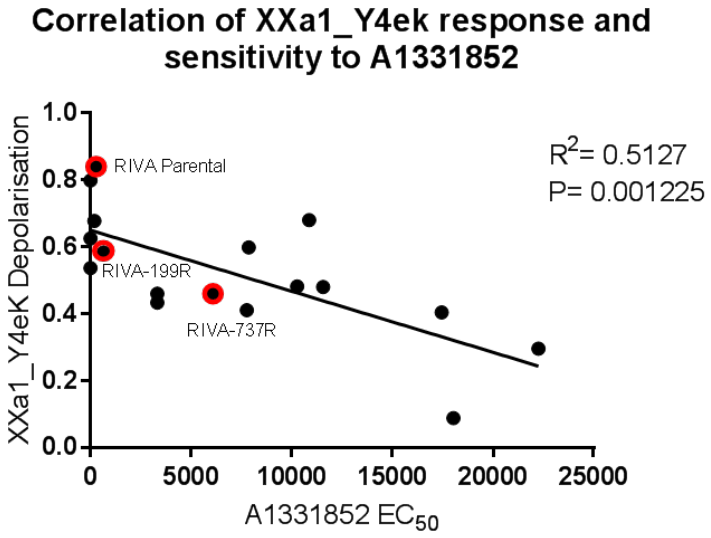

Figure 4-4 Correlation of XXa1_Y4ek response and sensitivity to A1331852 with RIVA resistant cell lines
Correlations between the EC_{50} of A1331852 and the response to XXa1_Y4eK (loss of mitochondrial membrane potential) analysed via BH3 profiling. Each dot is representative of one cell line and the solid line is representative of the linear regression line. RIVA resistant cell lines are circled in red and labelled. Pearson's co-efficient of determination (R^2) and the statistical significance values (P) are indicated on each graph. P values less than 0.05 are statistically significant.

In order to further investigate this correlation, other concentrations of XXa1_Y4eK were also tested in the RIVA resistant cell lines (Figure 4-5). Consistent with previous data, presented, decreasing the concentration of XXa1_Y4ek reduced the response. Furthermore, only the responses at 10µM were statistically significant. This confirms the optimal peptide concentration is 10 µM.

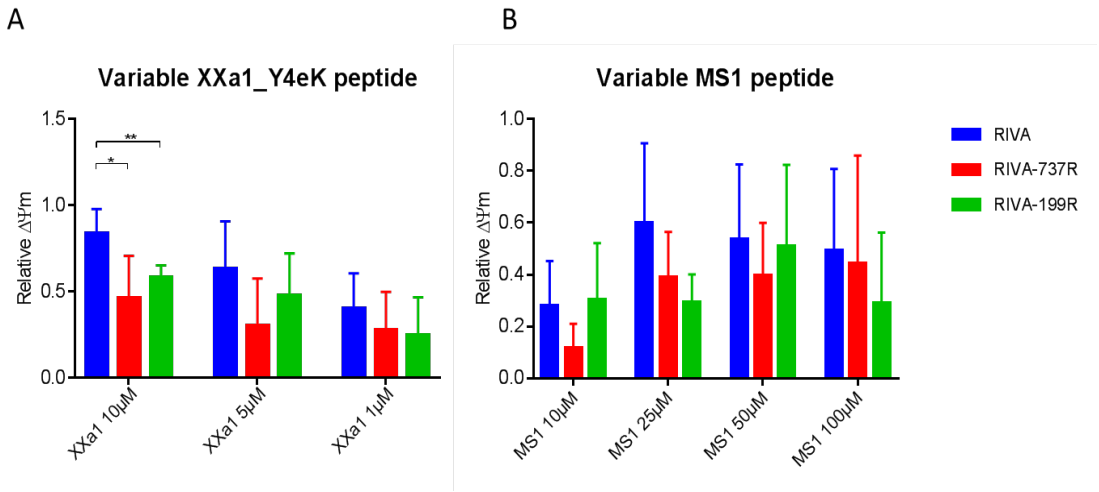

Figure 4-5 Variable XXa1_Y4eK and MS1 for RIVA resistant cell lines
The relative loss of mitochondrial membrane potential (ΔΨm) after the treatment with variable concentrations of the XXa1_Y4ek (A) or MS1 peptide (B). Cells were gently permeabalised, treated with 10, 5 or 1μM of synthetic peptide, XXa1_Y4eK or 10, 25, 50 or 100μM MS1. Cells were stained with mitochondrial membrane potential probe, JC-1, immediately before analysis. Fluorescence intensity (ex. 545nm, em. 590nm) was measured at 5 minute intervals for 120 minutes with intermittent shaking at 30°C using a HidexSense plate reader. The relative loss of mitochondrial membrane potential (ΔΨm) was calculated by normalising the area under the curve for each treatment to DMSO and FCCP treated control cells. Data are expressed as mean + S.D (n=6-8).

The mitochondrial depolarisation observed after the MS1 or FS2 peptide remained low and were not statistically different to the parental cell line. The response to the MS1 peptides supports the drug sensitivity data for S63845 and confirms there was not a switch in dependence to MCL1. Increasing the concentration of MS1 induced large variability and false positive data as previously discussed (Figure 4-5). As an increased response after FS2 treatment was not observed, it is likely there is also not a switch to BCL2A1. This would need confirming with siRNA or CRISPR/Cas9 studies.

4.1.3 BCL2 family protein expression

Although the data presented here suggests that the resistant cell lines did not shift anti-apoptotic dependence to another protein, previous reports have suggested that BCL2 inhibitor resistance is caused by a dysregulation of the BCL2 family member expression (Bodo*, et al* 2016, Konopleva*, et al* 2006, Lin*, et al* 2016, Tahir*, et al* 2017, Vogler*, et al* 2009a). Therefore, the protein levels of the BCL2 family proteins were assessed in the parental and resistant cell lines *via* immuno-blotting (Figure 4-6). α-tubulin was used as a loading control and VDAC was used a marker for mitochondria.

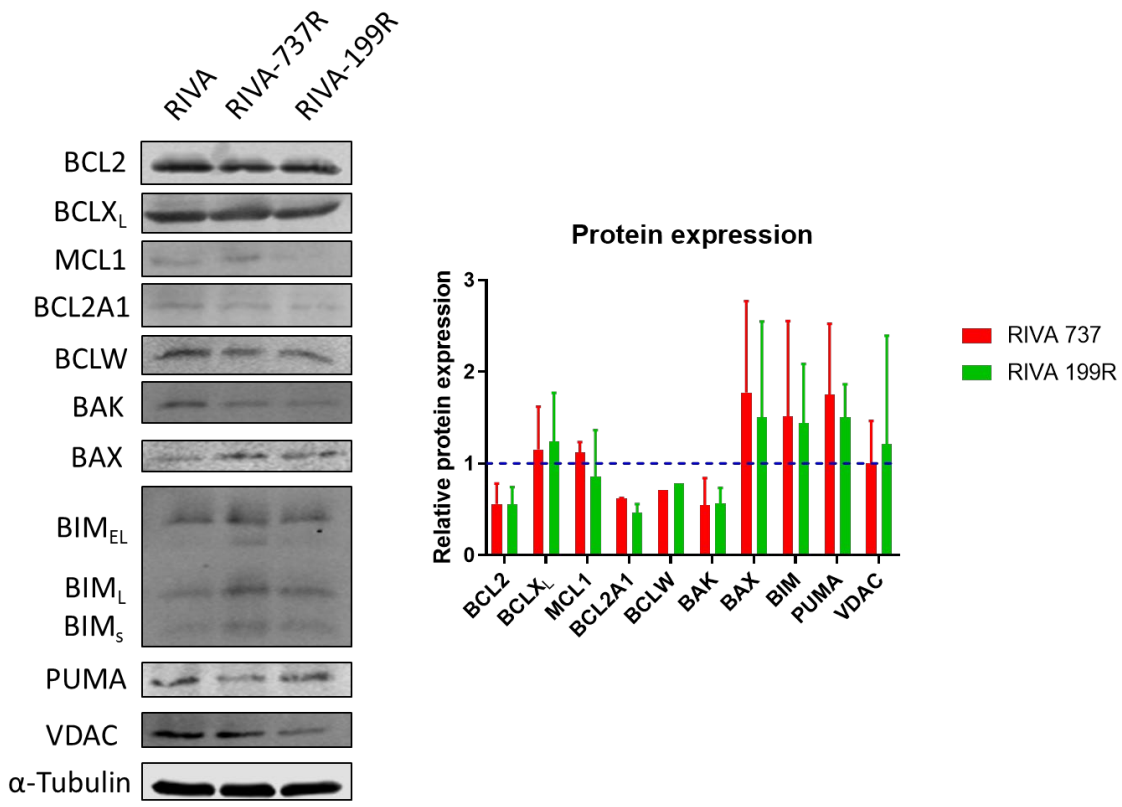

Figure 4-6 BCL2 family protein expression in RIVA resistant cell lines
Whole cell lysates were prepared from RIVA and derived resistant cell lines. 75µg of protein lysate was loaded in each lane. Expression of BCL2 family proteins were determined by immuno-blotting and a representative blot is shown. α-tubulin was used as a loading control and VDAC was used an indicator or mitochondrial mass. Bands were quantified using Image Studio Lite and normalised to α-tubulin expression. Data are shown as mean +SD (n=5). Multiple unpaired t-tests were performed on expression values relative to tubulin and p values were corrected for using the Holm-Sidak method; p <0.05*, p <0.005**, p <0.0005***.

Importantly, the levels of VDAC protein did not differ significantly between the parental and resistant cell lines, indicating there was no change in mitochondrial mass. However, the expression of BCL2 was reduced in the resistant cell lines. This reduction was not statistically significant but was likely to contribute to the resistance to BCL2 inhibition. There was not a significant upregulation of BCLX$_L$ or MCL1, further supporting the hypothesis that the resistance was not caused by a shift in protein dependence. The data in Figure 4-6 are presented as relative fold change to the parental RIVA cell line. For this reason, small changes of expression in proteins expressed at low-level such as BCL2A1 are exaggerated and may not be significant.

In terms of pro-apoptotic proteins, there was a decrease in the expression levels of BAK in the resistant cell lines which might indicate that the resistance was due to a direct apoptotic block for the cells undergoing mitochondrial outer membrane

permeabilisation. This supports the previous BH3 profiling data which showed that the resistant cells were less primed. In contrast, the level of BAX and BIM increased in the resistant cell lines. However, both were variable between biological samples, and overall the fold change was less than 2.

RNA expression of BCL2 family members was analysed *via* RT-qPCR (Figure 4-7). Overall, these data recapitulated the protein expression.

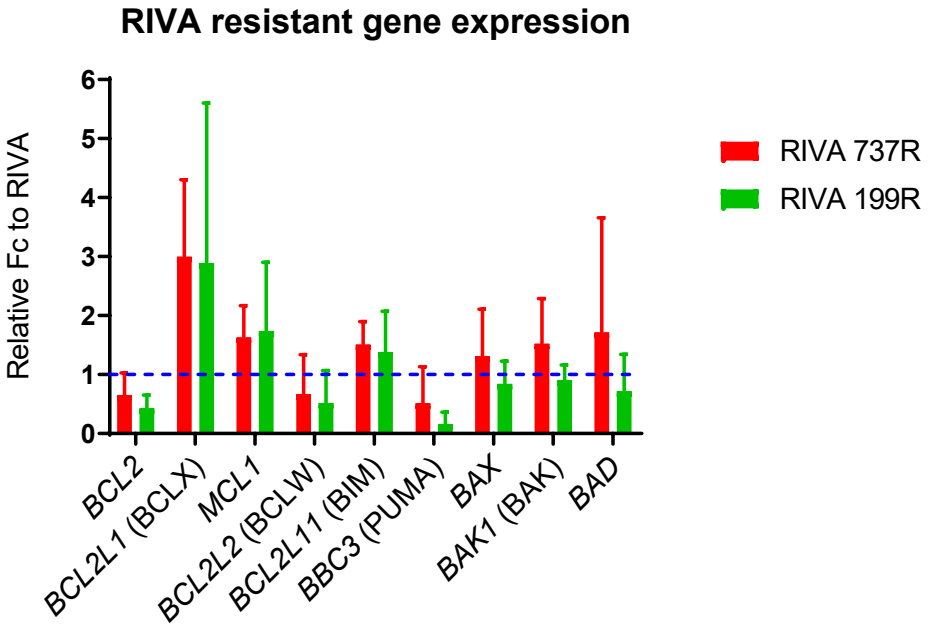

Figure 4-7 Gene expression of BCL2 family in RIVA resistant cell lines
cDNA was synthesised from RNA extracted from RIVA and derived resistant cell lines. qRT-PCR analysis was used to compare relative mRNA level of BCL2 family genes. GAPDH was used as to demonstrate equal cDNA loading. Resistant cell line data are shown as fold change relative to the parental cell line (blue dotted line). Data are expressed and mean +SD. (n=3). Multiple unpaired t-tests were performed on ΔCT values and p values were corrected for using the Holm-Sidak method; p <0.05*, p <0.005**, p <0.0005***.

The downregulation of BCL2 protein in the resistant cell lines was therefore at least partially due to a reduction in gene transcription. There was an approximately 3-fold increased level of *BCLX* mRNA in the resistant cell lines compared to the parental, which did not correlate to the immuno-blot data. However, the primer used for this gene was not splice specific and could therefore represent an increase in $BCLX_S$ protein. The upregulation observed at the mRNA level could be an error as there was quite large variability. Alternatively, the mRNA transcript and protein expression may not correlate due to other regulation mechanisms such as miRNA or protein degradation. The down-

regulation of BAK protein was not recapitulated at the RNA level. Again, this protein down-regulation could be caused protein degradation.

4.1.4 Drug screen

As the resistant cells cannot be targeted by other BH3 mimetics, other specific drugs were screened in the resistant and parental cell line (Figure 4-8). In Table 4-2, the compounds used in the screen are listed, detailing the drugs' targets and their current stage in development. The compounds used in this screen were chosen as they specifically target pathways that are often deregulated in DLBCL, as discussed in the introduction. It is possible that during the acquisition of resistance, the cells could upregulate one of these pathways and become more functionally reliant on it for survival and thus be sensitive to specific inhibitors. 5/8 of these compounds are already FDA approved making them ideal candidates for combinations with mimetics, as they could be re-purposed and used in clinic. Furthermore, 6/8 are in clinical trials for the treatment of lymphomas.

Drug	Target	Development stage
CUDC-907	PI3K and HDAC	Phase 1 and 2 trials including a phase 2 study in R/R DLBCL (NCT02674750)
Selumetinib	MEK1/2	FDA approved for neurofibromatosis Multiple other trails, mostly in combination with other drugs, including trials for treatment of lymphomas (NCT03155620, NCT03705507).
CAL-101 (idelalisib)	PI3Kδ	FDA approved for R/R CLL, SLL and FL Phase II trials including trial for R/R DLBCL (NCT03576443).
Palbociclib	CDK4/6	FDA approved for ER+, HER2- breast cancer Phase I/II trials including trials for lymphomas (NCT02310243, NCT03478514, NCT02159755)
IMD-0354	IKKβ	Pre-clinical
Ibrutinib	BTK	FDA approved for CLL, SLL, Waldenström's macroglobulinemia, MZL and MCL Multiple other trials, including use in combination with ABT-199 in R/R DLBCL (NCT03136497).
Fedratinib	JAK2	FDA approved for myelofibrosis
MG-132	Proteasome	Pre-clinical

Table 4-2 Compounds used in the drug screen
Compounds used in the drug screen are listed along with their targets and stage in development.
(1- www.fda.gov/ 2019)

The RIVA parental cell line and derived resistant cell lines were exposed to varying concentrations of the drugs and cell metabolism was assessed using CTG (Figure 4-8). Corresponding EC50 values were calculated and presented in Table 4-3.

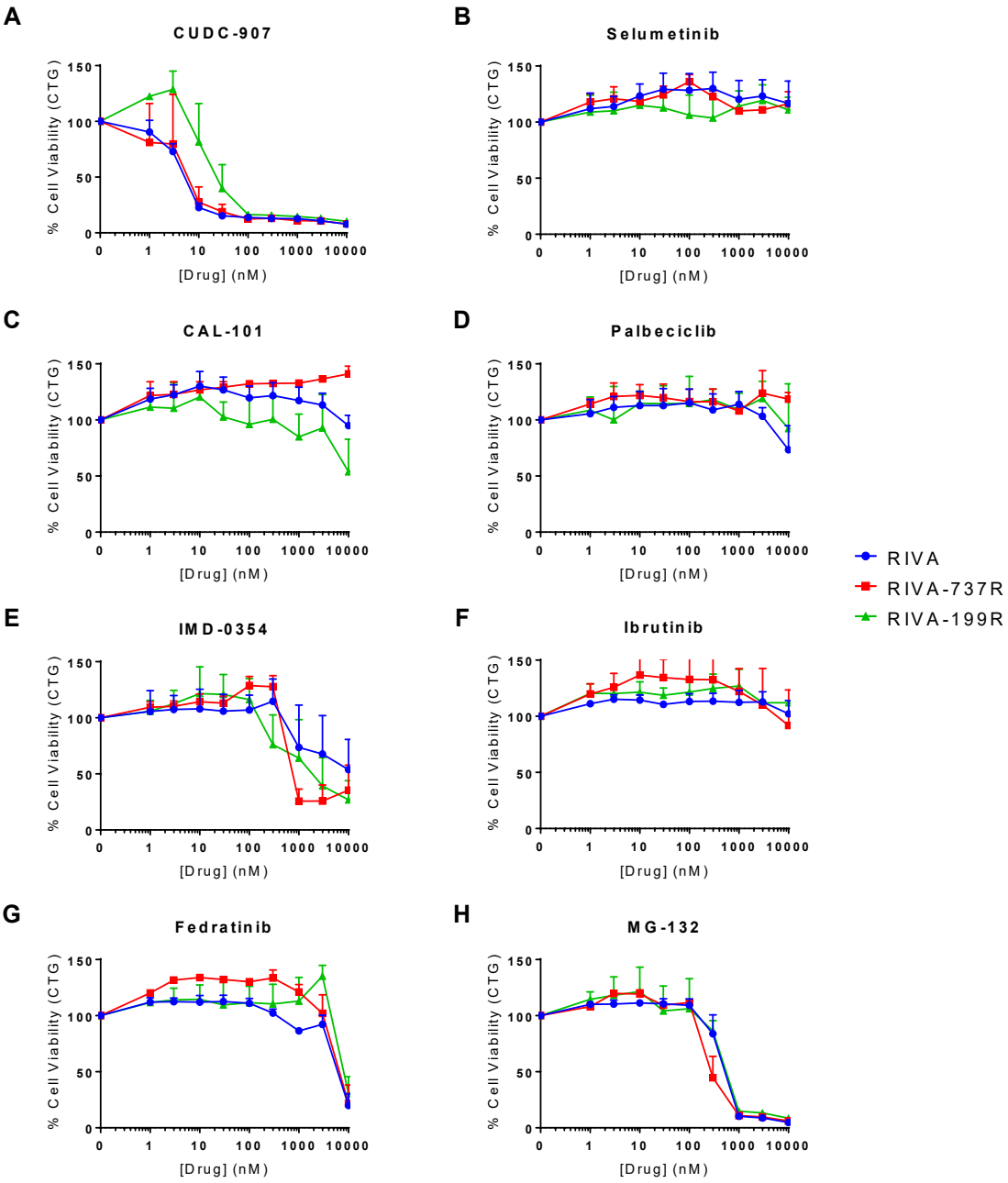

Figure 4-8 Drug screen in RIVA resistant cell lines
RIVA and derived resistant cell lines were plated and treated with 0-10,000nM of CUDC-907 **(A)**, selumetinib **(B)**, CAL-101 **(C)**, palbociclib **(D)**, IMD-0354 **(E)**, ibrutinib **(F)**, fedratinib **(G)** and MG-132 **(H)** for 72 hours. Cell viability was analysed by CellTiterGlo viability assay. Data were normalised to DMSO treated control. Data are expressed as mean + SD (n=3-6).

	EC_{50} (nM)		
	RIVA	RIVA-737R	RIVA-199R
CUDC-907	5.47	6.456	26.42
Selumetinib	N.C	N.C	N.C
CAL-101	N.C	N.C	>10,000
Palbeciclib	>10,000	N.C	N.C
IMD-0354	9388	925.9	2138
Ibrutinib	N.C	N.C	N.C
Fedratinib	N.C	6906	>10,000
MG-132	509.5	296.1	564.7

Table 4-3 EC_{50} vales for drug screen in RIVA resistant cells
The EC_{50} values for CUDC-907, selumetinib, CAL-101, Palbeciclib, IMD-0354, ibrutinib, fedratinib and MG-132 in RIVA and resistant derived cell lines (presented in Figure 4-8) were calculated using Graphpad Prism. Values in red indicate the EC_{50} is less than 100nM and is therefore sensitive. Values in bold are less than 1nM indicating ultra-sensitivity. Values which could not be calculated due to the lack of convergence of the response with the x-axis are denoted as N.C, not converged.

The RIVA parental cell line was only sensitive to the PI3K and HDAC inhibitor, CUDC-907 and had a partial response to the proteasome inhibitor MG-132. The RIVA parental displayed a resistance to CAL-101 (which specifically inhibits PI3Kδ). Therefore, the response to CUDC-907 could have been due to either the inhibition of other PI3K subunits or perhaps the inhibition of HDAC proteins. As a selective HDAC inhibitor was not tested this cannot be confirmed. This cell line was additionally resistant to all the other drugs screened, indicating there was not a functional dependence on any of these pathways tested for survival.

In general, the responses of the resistant cells to the various drugs did not differ greatly to the parental RIVA cell line. RIVA-199R became approximately 4x resistant to CUDC-907, but it is still displayed nanomolar sensitivity. However, these data variable between biological repeats.

Taken together, these data indicate that there was not an increase in activation or dependence on the pathways tested in the RIVA resistant cell lines. This could be further confirmed using immunoblotting to detect levels of activated proteins from these pathways or RNA analysis of target genes.

4.1.5 Targeted combinations to overcome resistance

The drugs identified from the above screen shown to induce the largest decrease in viability were assessed in combination with BH3 mimetics for synergistic interactions that could overcome resistance. As both resistant cell lines became resistant to ABT-199, this drug was tested in combination with CUDC-907, IMD-0354 and MG-132 (Figure 4-9). The RIVA parental cell line was extremely sensitive to ABT-199 mono-treatment, therefore the combination was not tested as the addition of another drug would likely induce a very minimal effect. The combinations were assessed using Calcusyn and the average CI values are indicated on each graph.

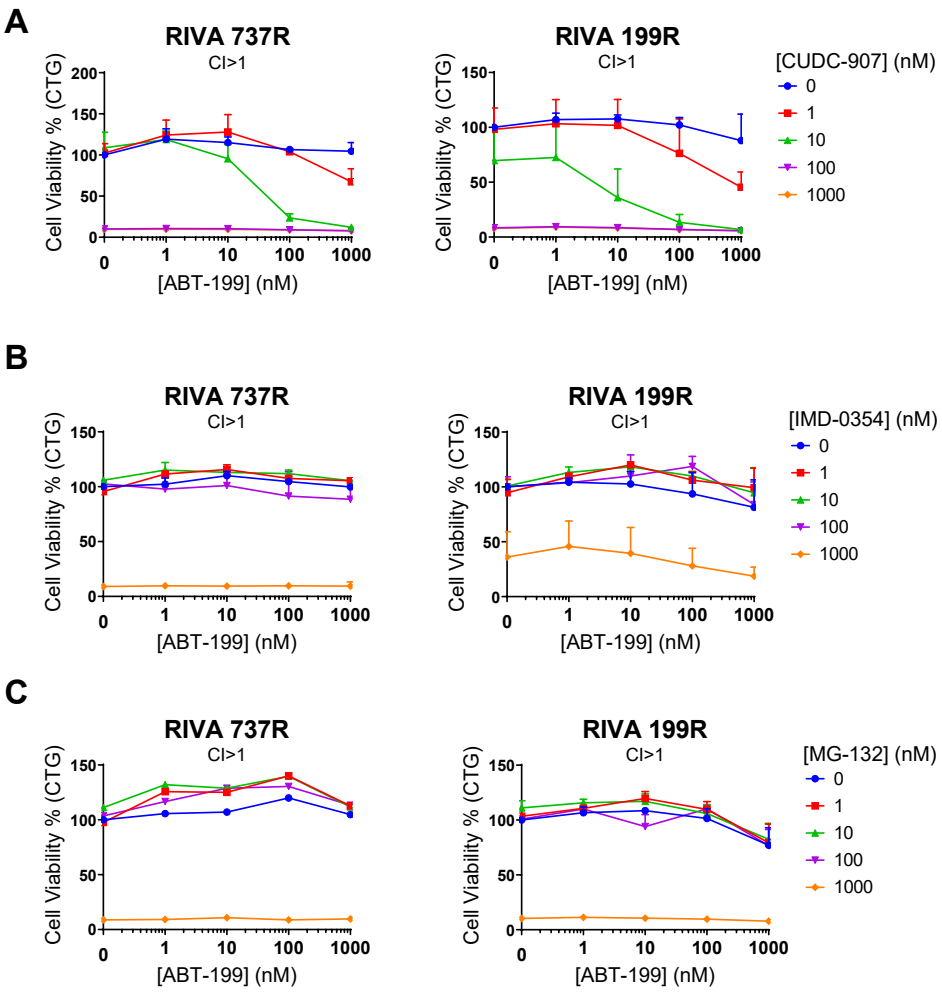

Figure 4-9 Drug combinations using ABT-199 in the RIVA resistant cells
RIVA derived resistant cell lines were treated with 0-1000nM of ABT-199 in combination with 0-1000nM of CUDC-907 **(A)**, IMD-0354 **(B)** or MG-132 **(C)** for 72 hours. Cell viability was analysed by CellTiterGlo viability assay. Data were normalised to DMSO treated control. Data are expressed as mean +SD (n=2-3) .Combination index (CI) values were calculated for each cell line using Calcusyn and are shown. CI values <1 are indicative of synergy.

Combinations of ABT-199 with either IMD-0354 or MG-132 were additive or antagonistic in both of the resistant cell lines Figure 4-9). The combination of ABT-199 with CUDC-907 displayed an overall additive interaction, however there were selective concentrations of each drug which had a synergistic effect. For example, the CI value for 100nM of ABT-199 and 10nM of CUDC-907 in RIVA-737R was 0.034 and in RIVA-199R this was 0.038. These values indicate that the combination at these concentrations are highly synergistic. The identification of synergistic interactions may provide information about the mechanism of resistance. CUDC-907 has been reported to supress the MAPK pathway, STAT3 signalling and reduce the expression of BCL2, $BCLX_L$ and MCL1 (Chen*, et al* 2019b). Moreover, the compound has been reported to have a synergistic effect when combined with ABT-199 in primary CLL cells (Chen*, et al* 2019b). Therefore, it could be possible that the downregulation of anti-apoptotic proteins by CUDC-907 is the cause of synergy when combined with ABT-199.

Both RIVA resistant cell lines displayed resistance to ABT-737, hence this drug was also tested in combination with CUDC-907, IMD-0354 and MG-132 (Figure 4-10). All combinations tested were additive/antagonistic.

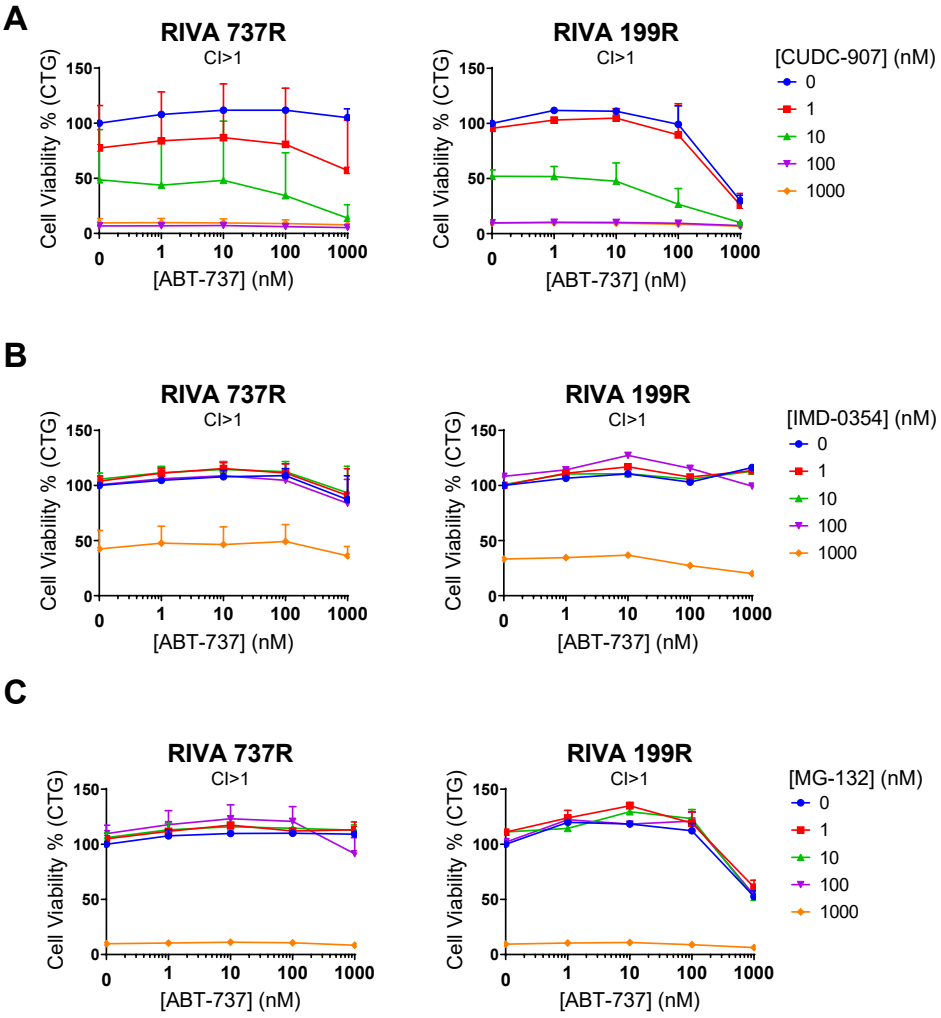

Figure 4-10 Drug combinations using ABT-737 in the RIVA resistant cells
RIVA and derived resistant cell lines were treated with 0-1000nM of ABT-737 in combination with 0-1000nM of CUDC-907 **(A)**, IMD-0354 **(B)** or MG-132 **(C)** for 72 hours. Cell viability was analysed by CellTiterGlo viability assay. Data were normalised to DMSO treated control. Data are expressed as mean +SD (n=2-3) .Combination index (CI) values were calculated for each cell line using Calcusyn and are shown. CI values <1 are indicative of synergy.

The parental RIVA cell lines partially responded slightly to $BCLX_L$ inhibition by A1331852. Therefore, combinations were also assessed in the parental and resistant cell lines using A1331852 (Figure 4-11). The average CI values for all concentrations tested indicate the combinations were additive/antagonistic.

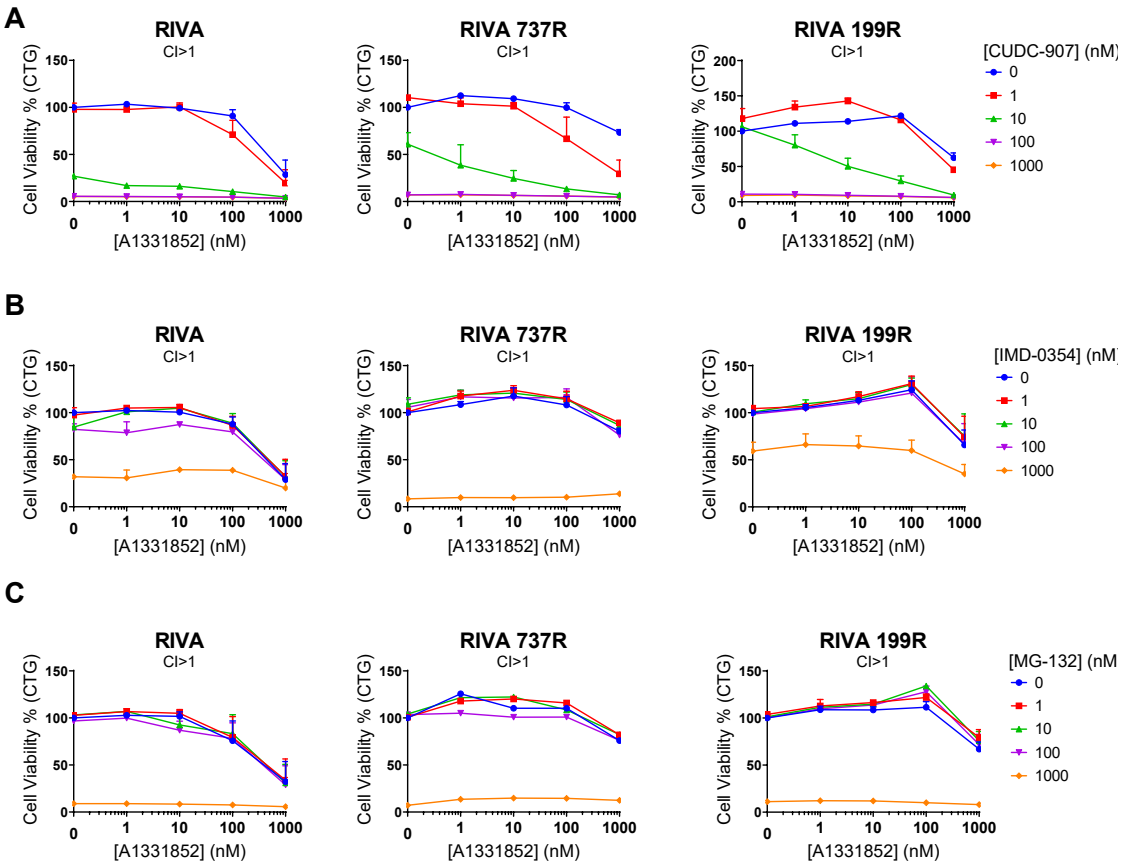

Figure 4-11 Drug combinations using A1331852 in the RIVA resistant cell lines
RIVA and derived resistant cell lines were treated with 0-1000nM of A1331852 in combination with 0-1000nM of CUDC-907 **(A)**, IMD-0354 **(B)** or MG-132 **(C)** for 72 hours. Cell viability was analysed by CellTiterGlo viability assay. Data were normalised to DMSO treated control. Data are expressed as mean +SD (n=2-3) .Combination index (CI) values were calculated for each cell line using Calcusyn and are shown. CI values <1 are indicative of synergy.

Although the average CI values were more than one, some individual combinations of A1331852 and CUDC-907 in the resistant cell lines were synergistic. In these cell lines, 1000nM of CUDC-907 had the same effect as 100nM. As this increase in concentration did not have an additional effect these values were excluded from the CI calculations. Hence, the CI for CUDC-907 and A1331852 in RIVA-737R was 0.907 and RIVA-199R was 0.4. As mentioned previously, this could be due to the down regulation of BCL2 or the multiple targeting of the anti-apoptotic proteins.

4.2 $BCLX_L$ inhibitor resistance in parental RCK8 and derivatives

As A1331852 and other specific $BCLX_L$ inhibitors are newer than the Abbott compounds (ABT-737/ -263 and ABT-199) and are yet to have been used clinically, there are not currently published data on acquired resistance to specific $BCLX_L$ inhibitors. Like RIVA in response to ABT-199, the RCK8 cell line was extremely sensitive to $BCLX_L$ specific inhibitor, A1331852, at pico-molar concentrations and was also sensitive to the lesser specific ABT-737 which also targets BCL2 and BCLW. Therefore, this cell line was an ideal candidate to investigate acquired resistance to $BCLX_L$ inhibitors.

4.2.1 Response to BH3 mimetics

The sensitivity to BH3 mimetics was assessed in RCK8 and derived cell lines using the metabolism assay, CTG (Figure 4-12). The corresponding EC_{50} values were also calculated, as can be seen in Table 4-4.

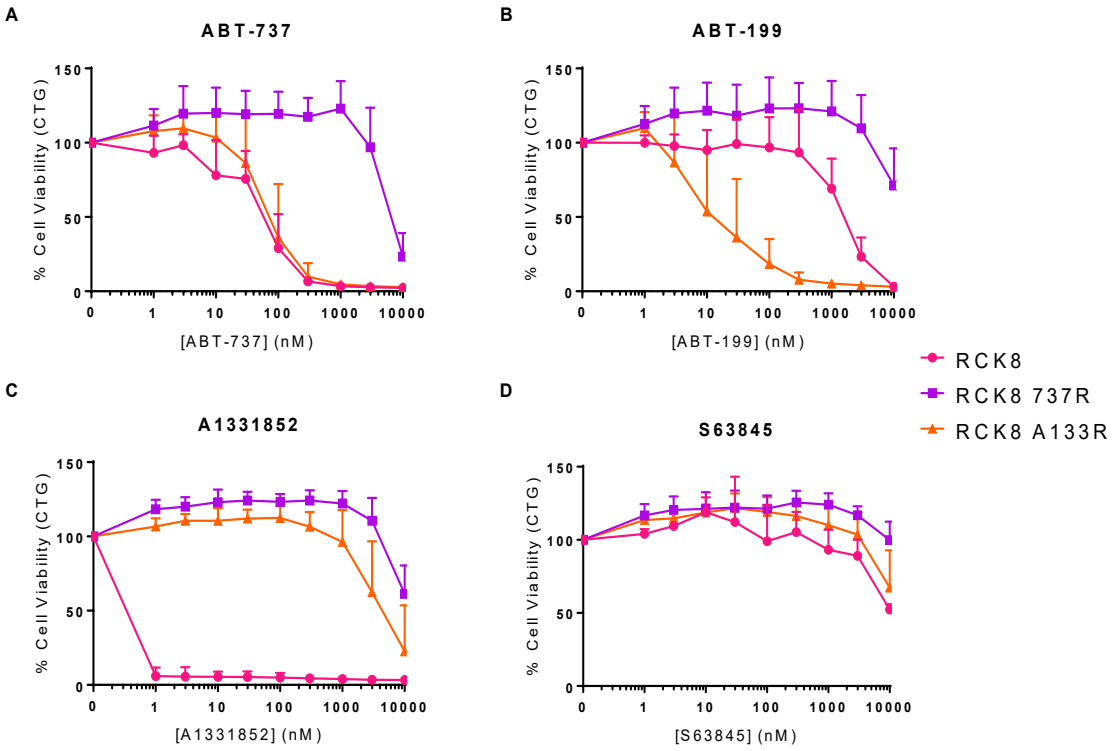

Figure 4-12 Sensitivity to BH3 mimetics in RCK8 resistant cell lines
RCK8 and derived resistant cell lines were plated and treated with 0-10,000nM of ABT-737 **(A)**, ABT-199 **(B)**, A1331852 **(C)** and S63845 **(D)** for 72 hours. Cell viability was analysed by CellTiterGlo viability assay. Data were normalised to DMSO treated control.Data are expressed as mean + SD (n=5-8).

	EC_{50} (nM)		
	RCK8	RCK8-737R	RCK8-A133R
ABT-737	53.15	7429	77.04
ABT-199	1545	N.C	16.45
A1331852	**<1**	N.C	4420
S63845	10682	N.C	10844

Table 4-4 EC_{50} values for BH3 mimetics in RCK8 resistant cell lines
The EC_{50} values for ABT-737, ABT-199, A1331852 and S63845 in RCK8 and resistant derived cell lines (presented in Figure 4-12) were calculated using Graphpad Prism. Values in red indicate the EC_{50} is less than 100nM and is therefore sensitive. Values in bold are less than 1nM indicating ultra-sensitivity. Values which could not be calculated due to the lack of convergence of the response with the x-axis are denoted as N.C, not converged.

RCK8-737R displayed approximately 140 times resistant to ABT-737. It was also resistant to the specific $BCLX_L$ inhibitor, A1331852 and BCL2 specific inhibitor, ABT-199 with EC_{50} values >10,000nM. It's response to MCL1 inhibition by S63845 was very similar to parental cells, indicating that there was not a shift in dependence to MCL1. RCK8-A133R was over 4000 times more resistant to A1331852 but the sensitivity to ABT-737 is retained. As the cell line was resistant to $BCLX_L$ inhibition, this sensitivity was likely due to the inhibition of BCL2 in the resistant cell line. This is supported by the approximately 90 times increased sensitivity to ABT-199 in RCK8-A133R. There was very little difference for the response to S63845. Taking these data together, it is likely that the mechanism of resistance to RCK8-A133R was due a switch in dependence from $BCLX_L$ to BCL2. The RCK8-737R mechanism of resistance to $BCLX_L$ resistance must be different. This is not surprising, as the inhibition of BCL2 by ABT-737 would prevent the shift in dependence to BCL2. The dependence on BCL2A1 could not be assessed as there is currently no specific inhibitor available.

To confirm that the BH3 mimetics' effect on cell metabolism correlated to cell death, the cells were also analysed via annexinV and PI staining (Figure 4-13). These data correlate with the CTG results and confirm that the RCK8-A133R cell line can be killed *via* BCL2 inhibition.

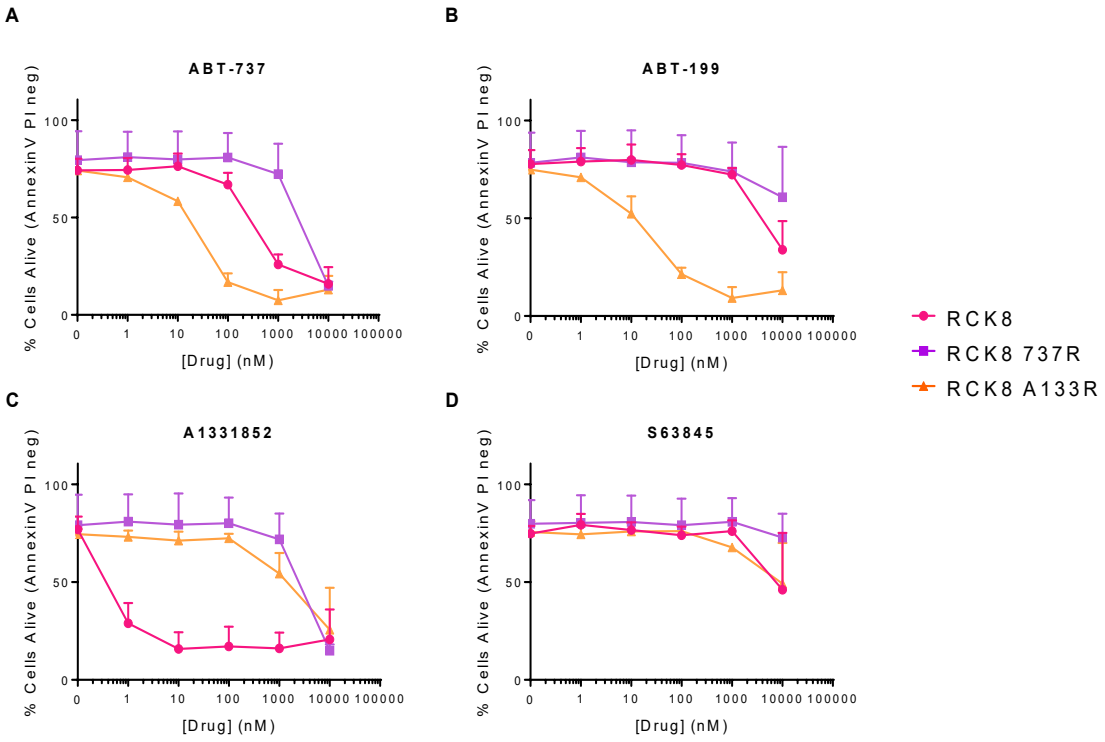

Figure 4-13 Cell death of RCK8 resistant cell lines after treatment with BH3 mimetics
RCK8 and derived resistant cell lines were incubated with 0-10,000nM concentrations of ABT-737, ABT-199, A1331852 and S63845 for 48 hours. Cell death was analysed by AnnexinV-FITC/PI staining measured by flow cytometry. DMSO was used as a time matched control. Data are shown as mean + SD (n=2-4).

4.2.2 BH3 profiling

To assess the anti-apoptotic protein dependencies in the RCK8 resistant cell lines, BH3 profiling was performed (Figure 4-14). As the sensitivity to ABT-737, ABT-199 and A1331852 was reduced in the RCK8-737R cell line it would be expected that there would be a reduction in ΔΨm for BAD and XXa1_Y4ek. However, the response to the BAD peptide remained comparable to the parental cell line. There was a reduction in response to the XXa1_Y4ek peptide but this was not statistically significant, likely due to the inherent variability of the assay and large standard deviation. However it should be noted that the data presented in Figure 4-14 are based on only two biological repeats.

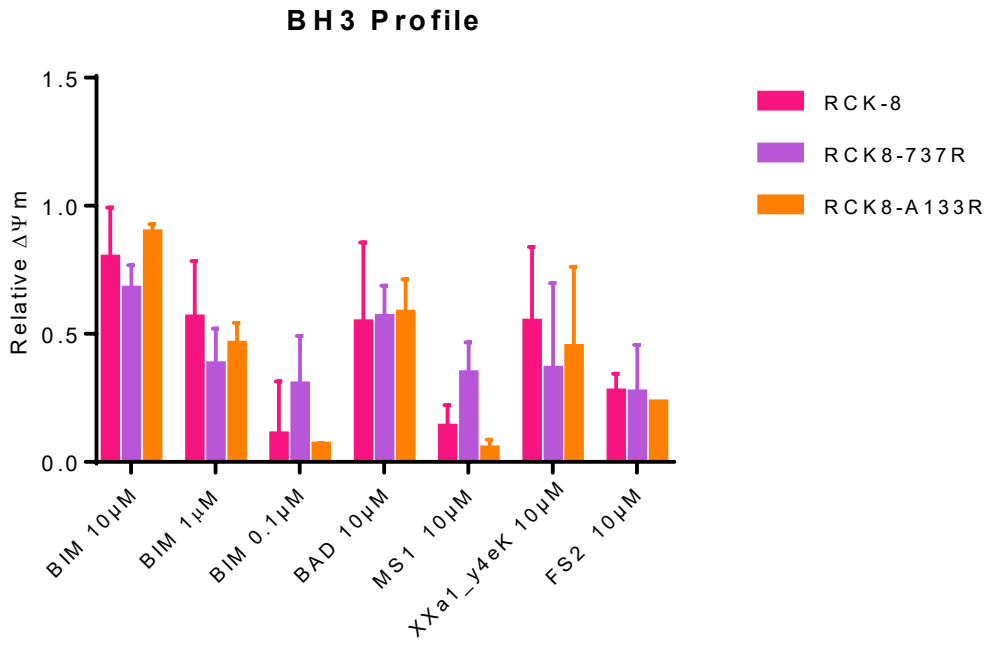

Figure 4-14 BH3 profile of RCK8 resistant cell lines
RCK8 and derived resistant cell lines were gently permeabalised, treated with synthetic peptides and stained with mitochondrial membrane potential probe, JC-1, immediately before analysis. Fluorescence intensity (ex. 545nm, em. 590nm) was measured at 5 minute intervals for 120 minutes with intermittent shaking at 30°C using a HidexSense plate reader. The relative loss of mitochondrial membrane potential (ΔΨm) was calculated by normalising the area under the curve for each treatment to DMSO and FCCP treated control cells. Data expressed as mean + S.D (n=2). Multiple unpaired t-tests were performed, and p values were corrected for using the Holm-Sidak method; p <0.05*, p <0.005**, p <0.0005***.

The RCK8-A133R cell line was resistant to $BCLX_L$ inhibition but displayed an increased sensitivity to BCL2 inhibition. For this reason, the expected BH3 profile for this cell line would be either an increased or similar ΔΨm after treatment with BAD compared to the parental cells but a reduction after the treatment with XXa1_Y4eK, indicating a shift in dependence to BCL2. The resistant cell line showed a similar response to the BAD peptide and a slight reduction to the XXa1_Y4eK peptide (49% depolarisation) but this was not statistically significant.

Taken together, both resistant cell lines exhibited a reduction in response to the XXa1_Y4ek. However the assay could not distinguish the cell lines differential response to ABT-199. RCK8-A133R and the parental cell line were plotted with the other cell lines A1331852 sensitivity and response to XXa1_Y4ek (Figure 4-15). RCK-737R could not be plotted as the EC_{50} for A1331852 for this cell line could not be calculated. Nonetheless, RCK8 and RCK8-A133R fit the correlation well with a p value of 0.004.

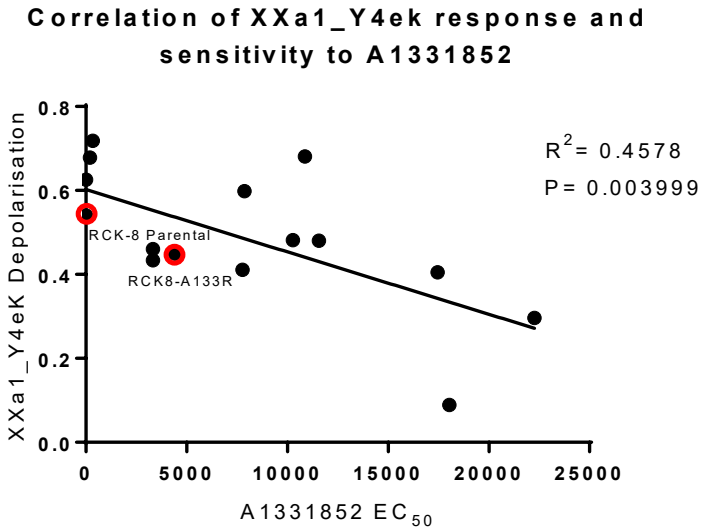

Figure 4-15 Correlation of XXa1_Y4ek response and sensitivity to A1331852 with RCK8 resistant cell lines
Correlations between the EC_{50} of A1331852 and the response to XXa1_Y4eK (loss of mitochondrial membrane potential) analysed via BH3 profiling. Each dot is representative of one cell line and the solid line is representative of the linear regression line. RIVA resistant cell lines are circled in red and labelled. Pearson's co-efficient of determination (R^2) and the statistical significance values (P) are indicated on each graph. P values less than 0.05 are statistically significant.

4.2.3 BCL2 family protein expression

The protein expression of BCL2 family members was investigated *via* immuno-blotting (Figure 4-16). The levels of VDAC expression did not differ significantly between the parental and resistant cell lines suggesting no significant change in mitochondrial mass.

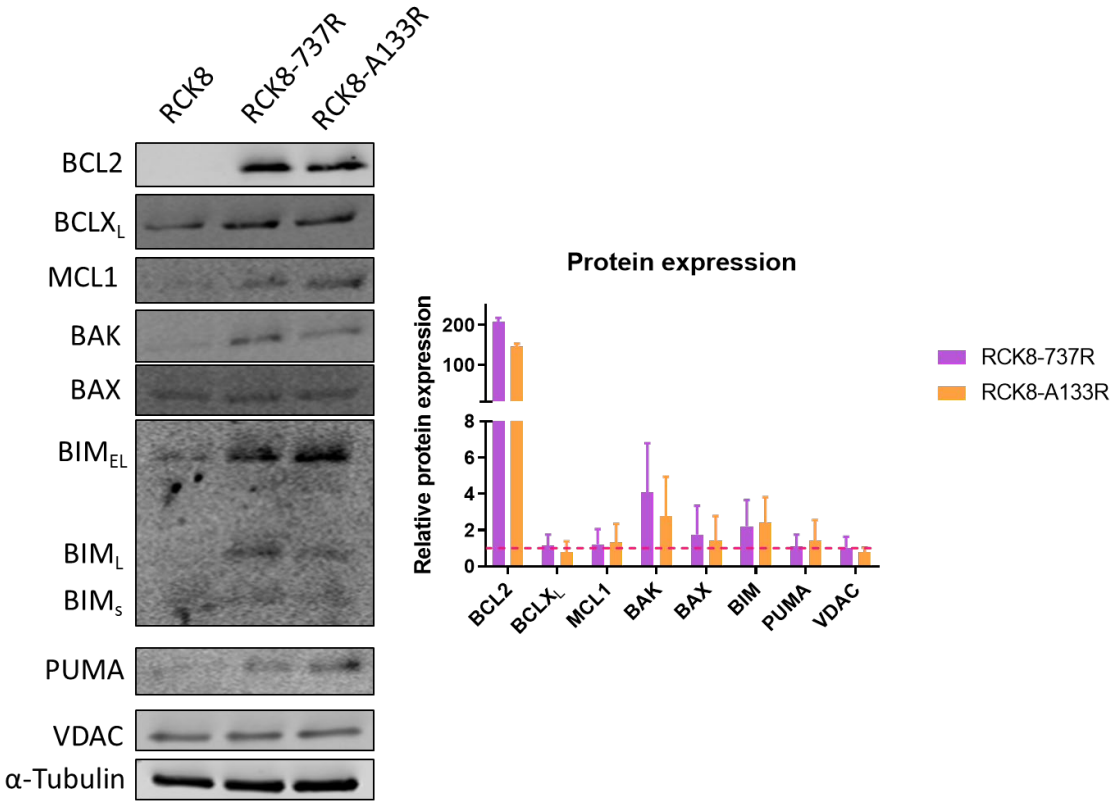

Figure 4-16 BCL2 family protein expression in RCK8 resistant cell lines
Whole cell lysates were prepared from RCK8 and derived resistant cell lines. 75µg of protein lysate was loaded in each lane. Expression of BCL2 family proteins were determined by immuno-blotting and a representative blot is shown. α-tubulin was used as a loading control and VDAC was used an indicator or mitochondrial mass. Bands were quantified using Image Studio Lite and normalised to α-tubulin expression. Data are expressed as mean + S.D (n=3-4). Multiple unpaired t-tests were performed on expression values relative to tubulin and p values were corrected for using the Holm-Sidak method; p <0.05*, p <0.005**, p <0.0005***.

Despite the resistance to BCLX$_L$ inhibition in both resistant cell lines, the abundance of BCLX$_L$ remained consistent to the parental cell line. However, interestingly, there was a large increase in BCL2 and BIM abundance in both of the resistant cell lines. This provides an insight into the mechanism of the shift in dependence from BCLX$_L$ to BCL2 in the RCK8-A133R cell line. However, the RCK8-737R had a similar level of BCL2 expression to ABT-A133R, but was not sensitive to ABT-199. As discussed, it is likely that the RCK8-737R cell line could not switch dependence to BCL2, as the cell line became resistant to the dual targeting of BCL2 and BCLX$_L$.

There was also an increase in protein expression of effector BAK in the resistant cell lines. This was increase is higher in the RCK8-737R cell line. Previous reports have suggested that BAK can be directly sequestered by MCL1 and BCLX$_L$ but not BCL2 (Willis, *et al* 2005), (Smith, *et al* 2019). This may partly explain why despite there being an

increase in BCL2, there was not an increase in ABT-199 sensitivity. If BAK is bound to and being kept in check by another anti-apoptotic protein, then the inhibition of BCL2 would not induce cell death. Alternatively, the RCK8-737R may acquire a BCL2 mutation rendering inhibitors ineffective. This would require further experiments such as co-immunoprecipitations and DNA sequencing to confirm.

The BCL2 family expression was also measured by RT-qPCR to assess if the deregulation of the proteins was at the level of transcription (Figure 4-17). The up-regulation of BCL2, BIM and BAK proteins were recapitulated at the level of mRNA in both resistant cell lines. The mRNA of BCLX was slightly reduced in the RCK8-A133R cell line, which would further provide rational for the development of resistance. However, this was not seen at protein level. This could be explained by the splice non-specific primers used or there could be a decrease in gene expression but an increase in protein stability. The RT-qPCR also suggested that there was a statistically significant reduction in *BAX* expression that was not seen at the protein level. This protein was expressed at a low level, therefore the small reduction in mRNA may be exaggerated. There was also an increase in *MCL1* mRNA which was not detected by immuno-blotting indicating there could be an increased transcription but equally increased degradation of the protein. Further experiments would be required to confirm this.

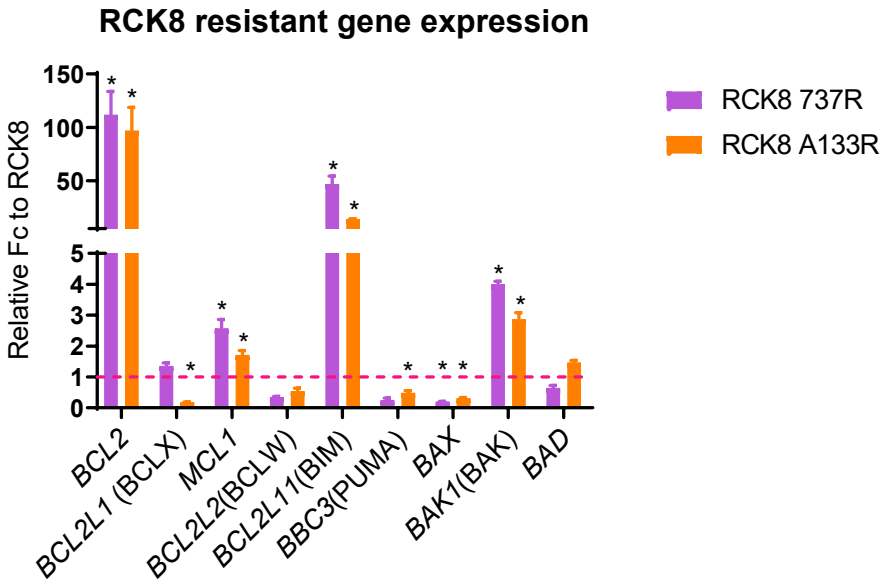

Figure 4-17 Gene expression of BCL2 family in RCK8 resistant cell lines
cDNA was synthesised from RNA extracted from the RCK8 resistant cell lines. qRT-PCR analysis was used to compare relative mRNA level of BCL2 family genes. GAPDH was used as to demonstrate equal cDNA loading. Resistant cell line data are shown as fold change relative to the parental cell line (pink dotted line).Data are expressed and mean +SD (n=2). Multiple unpaired t-tests were performed on the ΔCT values and p values were corrected for using the Holm-Sidak method; p <0.05*, p <0.005**, p <0.0005***.

4.2.4 Drug screen

The panel of drugs used in the drug screen for RIVA resistant cell lines were also assessed in the RCK8 resistant cell lines (Figure 4-18). Compared to the RIVA parental cell line, the RCK8 parental cell line was sensitive at much lower concentrations of CUDC-907. It is also sensitive to MG-132. As discussed, CUDC-907 may downregulate $BCLX_L$. This provides rationale for the exquisite sensitivity to CUDC-907 in the RCK8 parental cell lines. As with the effect of CUDC-907 in RIVA, the effect was likely independent of the PI3K pathway as the cell line was resistant to CAL-101.

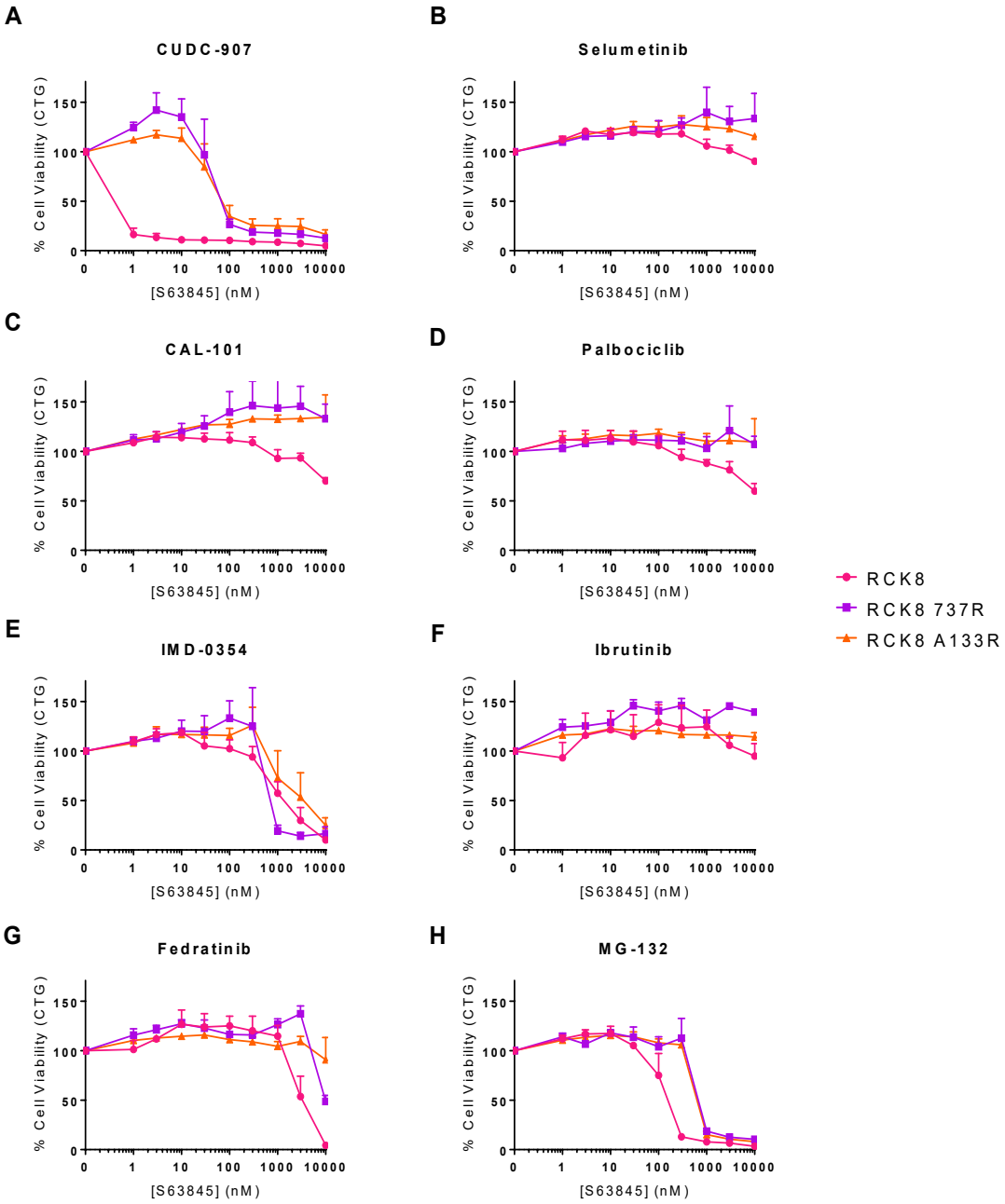

Figure 4-18 Drug screen in RCK8 resistant cell lines
RCK8 and derived resistant cell lines were plated and treated with 0-10,000nM of CUDC-907 **(A)**, selumetinib **(B)**, CAL-101 **(C)**, palbociclib **(D)**, IMD-0354 **(E)**, ibrutinib **(F)**, fedratinib **(G)** and MG-132 **(H)** for 72 hours. Cell viability was analysed by CellTiterGlo viability assay. Data were normalised to DMSO treated control. Data are expressed as mean + SD (n=3-6).

	EC_{50} (nM)		
	RCK8	RCK8-737R	RCK8-A133R
CUDC-907	**<1**	74.96	109.9
Selumetinib	N.C	N.C	N.C
CAL-101	>10,000	N.C	N.C
Palbociclib	>10,000	N.C	N.C
IMD-0354	1466	903.9	3488
Ibrutinib	N.C	N.C	N.C
Fedratinib	3025	9973	N.C
MG-132	150.6	950.2	874.6

Table 4-5 EC_{50} values for the drug screen in RCK8 resistant cell lines
The EC_{50} values for CUDC-907, selumetinib, CAL-101, Palbeciclib, IMD-0354, ibrutinib, fedratinib and MG-132 in RCK8 and resistant derived cell lines (presented in Figure 4-18) were calculated using Graphpad Prism. Values in red indicate the EC_{50} is less than 100nM and is therefore sensitive. Values in bold are less than 1nM indicating ultra-sensitivity. Values which could not be calculated due to the lack of convergence of the response with the x-axis are denoted as N.C, not converged.

Generally, the resistant cell lines responded similarly to the parental cell line. The resistant cell lines were less sensitive to CUDC-907 but still displayed a moderate response. The reduction in sensitivity was likely due to the reduced dependence on $BCLX_L$ in these cell lines and suggests the mechanism of CUDC-907 is $BCLX_L$ dependent. The resistant cell lines also became more resistant to the proteasome inhibitor MG-132. MG-132 has been reported to induce cell death via the intrinsic pathway, however the inhibition of the proteasome decreases the degradation of MCL1 which can inhibit apoptosis and MCL1 expression is therefore a negative marker for MG-132 sensitivity (Yuan*, et al* 2008). As neither of the resistant cell lines became more sensitive to the drugs used in this screen, it is likely that the cells did not activate one of these pathways.

4.2.5 Targeted combinations to overcome resistance

Combinations of the most effective drugs in the screen and BH3 mimetics were tested to look for synergistic interactions that could overcome the acquired resistance. As both resistant cell lines were resistant to A1331852, this drug was tested in combination with CUDC-907, IMD-0354 and MG-132 (Figure 4-19). The combinations were assessed using Calcusyn and the average CI values are indicated on each graph.

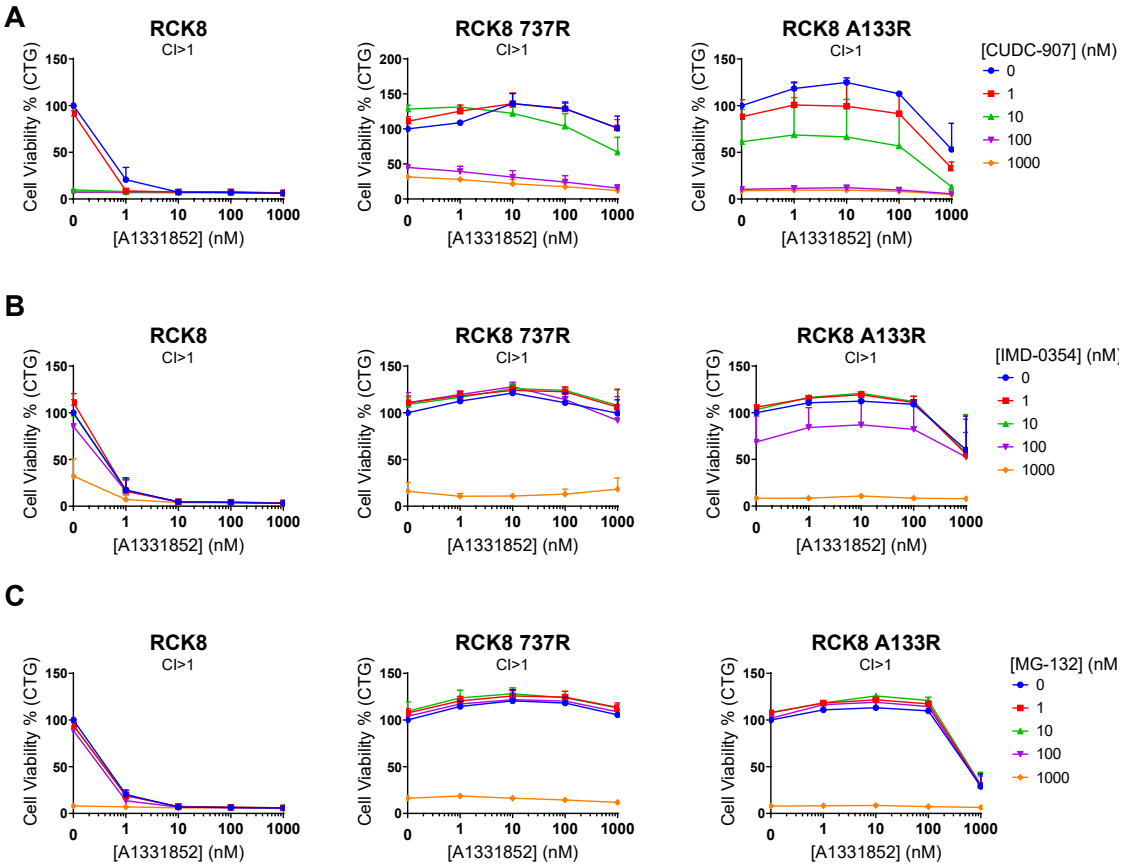

Figure 4-19 Drug combinations using A1331852 in the RCK8 resistant cell lines
RCK8 and derived resistant cell lines were treated with 0-1000nM of A1331852 in combination with 0-1000nM of CUDC-907 **(A)**, IMD-0354 **(B)** or MG-132 **(C)** for 72 hours. Cell viability was analysed by CellTiterGlo viability assay. Data were normalised to DMSO treated control. Data are expressed as mean +SD (n=2-3) .Combination index (CI) values were calculated for each cell line using Calcusyn and are shown. CI values <1 are indicative of synergy.

The RCK8 parental cell line was extremely sensitive to A1331852 mono-treatment, therefore the combinations were not effective, as the addition of another drug did not cause a further reduction in viability. The combinations in the resistant cell lines were all additive/antagonistic as indicated by average CI values >1.

Both resistant cell lines became more resistant to ABT-737. For this reason, resistant cell lines were tested for the effect of treatment with ABT-737 in combination with CUDC-907, IMD-0354 or MG-132 (Figure 4-20). The combinations were additive/ antagonistic for all three cell lines.

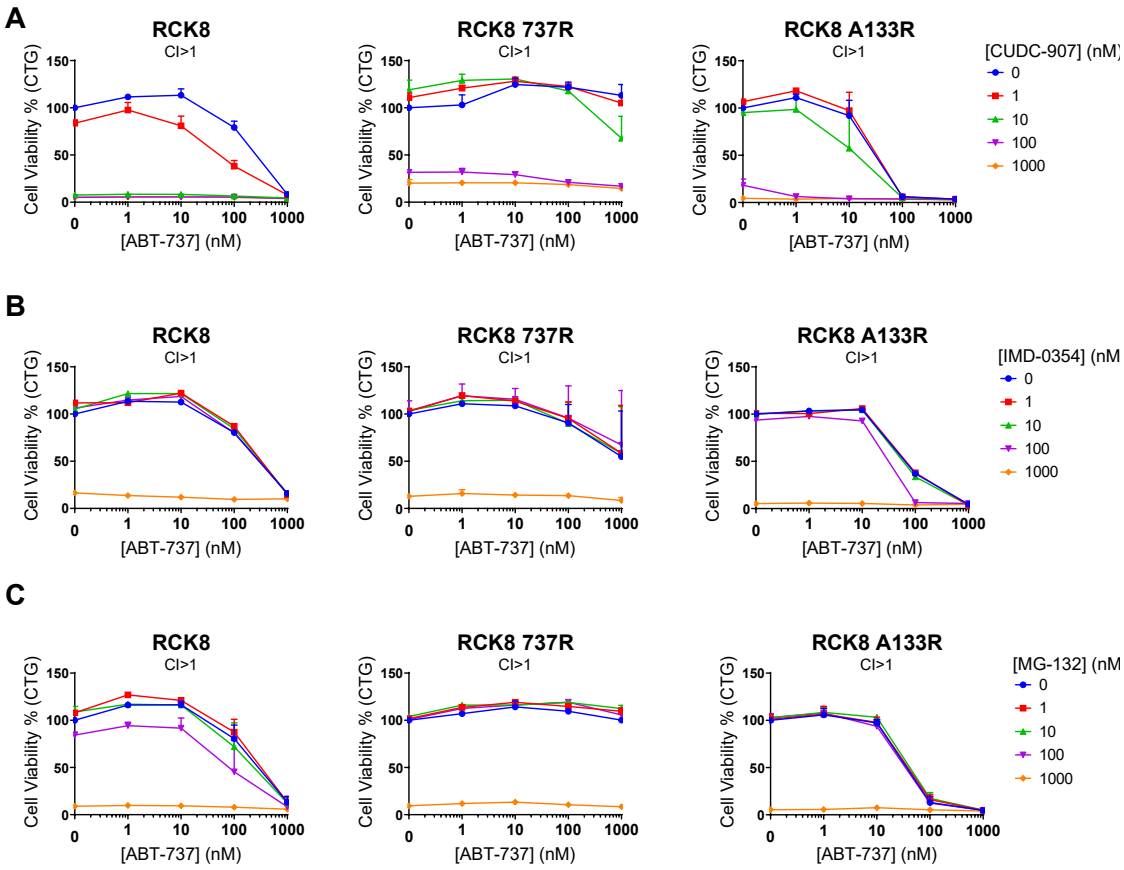

Figure 4-20 Drug combinations using ABT-737 in the RCK8 resistant cell lines
RCK8 and derived resistant cell lines were treated with 0-1000nM of ABT-737 in combination with 0-1000nM of CUDC-907 **(A)**, IMD-0354 **(B)** or MG-132 **(C)** for 72 hours. Cell viability was analysed by CellTiterGlo viability assay. Data were normalised to DMSO treated control. Data are expressed as mean +SD (n=2-3) .Combination index (CI) values were calculated for each cell line using Calcusyn and are shown. CI values <1 are indicative of synergy.

The RCK8-A133R cell line had an increased dependence on BCL2 and sensitivity to ABT-199. The RCK8-737R cell line also had increased BCL2 expression at both the mRNA and protein level. For this reason, the resistant cell lines were tested for the combination of ABT-199 and CUDC-907, IMD-0354 and MG-132 (Figure 4-21). The combinations were additive/ antagonistic for all three cell lines.

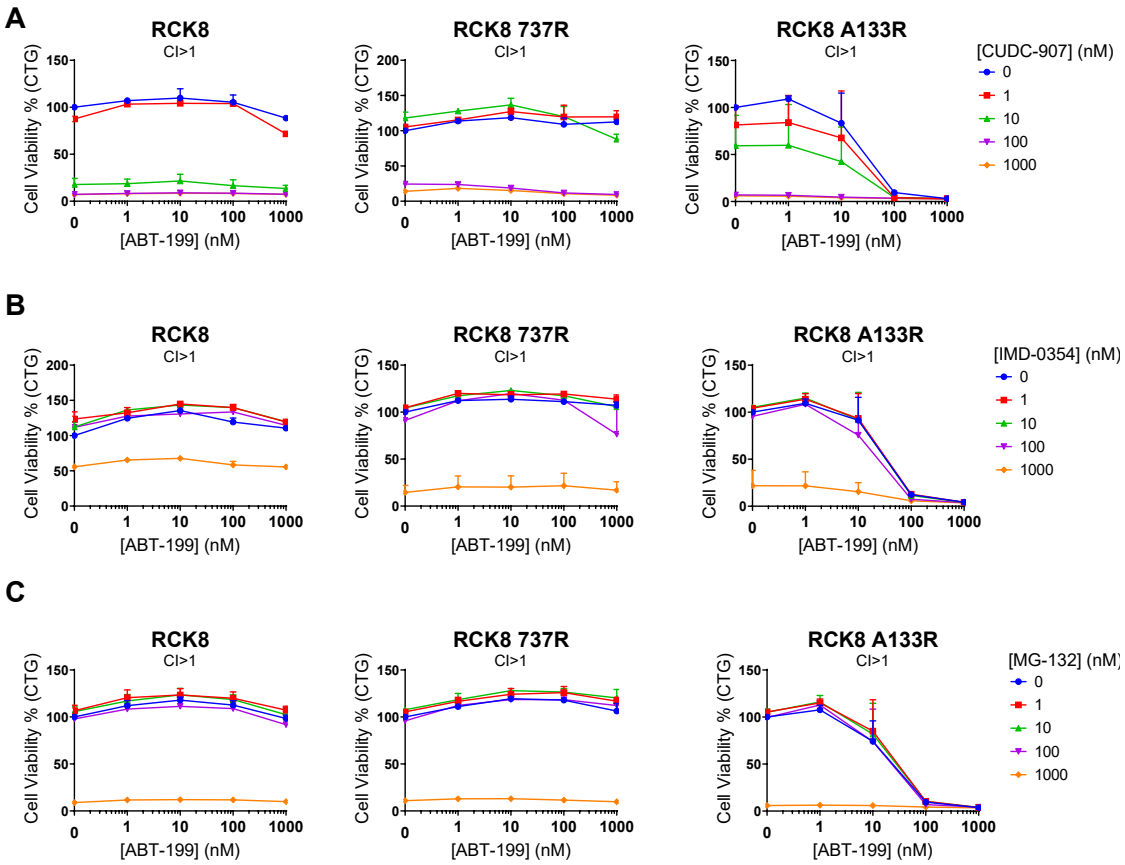

Figure 4-21 Drug combinations using ABT-199 in the RCK8 resistant cell lines
RCK8 and derived resistant cell lines were treated with 0-1000nM of ABT-199 in combination with 0-1000nM of CUDC-907 **(A)**, IMD-0354 **(B)** or MG-132 **(C)** for 72 hours. Cell viability was analysed by CellTiterGlo viability assay. Data were normalised to DMSO treated control. Data are expressed as mean +SD (n=2-3) .Combination index (CI) values were calculated for each cell line using Calcusyn and are shown. CI values <1 are indicative of synergy.

4.3 Discussion

To investigate mechanisms of acquired resistance to BH3 mimetics, resistant cell lines were generated from cell lines which exhibit extreme sensitivity to either ABT-199 or A1331852. CTG and annexinV-FITC /PI staining confirmed that resistant cell lines derived from BCL2 dependent RIVA (RIVA-737R and RIVA-199R) were over 6000x resistant to their respective mimetics. BH3 profiling of the resistant cell lines indicated that these cells were less primed and there was a decrease in dependence of the BCL2 protein. Furthermore, the profile did confirm the CTG data which suggested there was not a switch in dependence to $BCLX_L$ or MCL1. This is further supported by the lack of upregulation of other anti-apoptotic proteins at either the protein or RNA level.

The BH3 profiles of the RIVA resistant cell lines exhibited a reduced response after treatment with the BIM peptide indicating they are less primed for death. This was further supported by the reduction of BAK protein level suggesting there could be an apoptotic block in the resistant cell lines.

As there is little change in response to the drugs screened between the parental RIVA and resistant cell lines, it indicates there is not a dysregulation in one of these pathways inhibited. The resistant cell lines did not become more sensitive to the specific PI3K inhibitor, (CAL-101) and combinations with ABT-199 or ABT-737 were not synergistic. This is contradictory to previous reports which have implicated the PI3K pathway as a mediator of resistance to BCL2 inhibitor resistant by upregulating MCL1 (Pham*, et al* 2018). However, CAL-101 is specific to PI3K and does not inhibit other isoforms of PI3K. Another PI3K inhibitor such as duvelislib may have had a greater response. The response to other compounds which have been suggested to downregulate MCL1 such the CDK4/6 palbecicilib, suggest there was not a shift in dependence towards MCL1. With that said, the levels of anti-apoptotic proteins were not checked after the drug screen so we cannot be sure the compounds used are causing MCL1 downregulation.

The RIVA resistant cell lines remained sensitive to CUDC-907 which has been reported to reduce the expression of BCL2, $BCLX_L$ and MCL1 (Chen*, et al* 2019b). Therefore, it could be possible that that the cells are still primarily dependent on BCL2 but the drug is not effective at inhibiting the protein in these cells (perhaps due to a mutation). However, if BCL2 is down-regulated by CUDC-907 this would provide rationale for the decrease in viability. As the interaction is synergistic at some concentrations it would indicate that ABT-199 still has some effect on the cells so it is unlikely that there is a mutation present in every cell. These cells are multi-clonal and there may be multiple mechanisms of resistance within the cell line. Therefore, targeting the cells with two different ways of inhibiting BCL2 would increase the overall efficacy within the population. Alternatively, as CUDC-907 is understood to decrease the expression of $BCLX_L$ and MCL1 it is possible that the synergy could be caused by a decrease of multiple anti-apoptotic proteins. Previous data showed that the resistant cell lines do not become more sensitive to mono-treatment of A1331852 or S63845 indicating there is not a shift in dependence to $BCLX_L$ or MCL1. However, it is possible that the cells

become dependent on more than one anti-apoptotic protein which requires dual targeting. This could be further investigated using combinations of the BH3 mimetics in the resistant cell lines.

Similarly, the RCK8 resistant cell lines (RCK8-737R and RCK8-A133R) were confirmed to exhibit resistance to their respective drugs. RIVA-737R also became more resistant to $BCLX_L$ specific inhibition. This was not recapitulated with annexinV-FITC /PI staining but may be due to reduced viability of sample. Neither of the resistant cell lines became more sensitive to MCL1 inhibition and therefore do not become more dependent on this protein for survival. In support of this, the resistant cell lines' BH3 profiles have reduced response after treatment with the XXa1_Y4eK peptide. However, the RCK8-A133R cell line became more sensitive to ABT-199. Taken together with the upregulation of BCL2 at both the mRNA and protein level it suggests there is a switch in dependence from $BCLX_L$ to BCL2 in this cell line. Interestingly, the RCK8-737R cell line also had an upregulation of BCL2 but did not become more sensitive to ABT-199. The RCK8-737R is likely not to become sensitive to BCL2 inhibition as ABT-737 also targets BCL2. However, it is possible that the mediator of upregulation could be the same in both cells. Both cell lines also have an increase in BIM expression. These resistant cell lines also have an increased expression of BAK at both the protein and mRNA level. When considering the earlier immunoprecipitations performed previously, (3.10-Interactions of the BCL2 family members in DLBCL), this is unexpected as BAK was not shown to interact with BCL2 which these cell lines seem to become more dependent on. Immunoprecipitations would need to be performed in these cell lines to rule out a direct interaction but studies have indicated that BAX may be able to BAK (Smith*, et al* 2019) (Appendix 3). Nonetheless, this data could suggest a switch dependence of effector BCL2 family member.

The RCK8 resistant cell lines remain sensitive to CUDC-907 but the efficacy of the drug is reduced. The reduction in sensitivity was likely due to the reduced dependence on $BCLX_L$ in these cell lines and suggests the mechanism of CUDC-907 is $BCLX_L$ dependent. The partial response could be explained by the decrease in viability of subclones of the cells that are still dependent on $BCLX_L$ or due to the downregulation of other anti-apoptotic proteins, such as BCL2, which is depended upon in the RCK8-A133R cell line.

The resistant cell lines also became more resistant to the proteasome inhibitor MG-132. MG-132 has been reported to induce cell death via the intrinsic pathway, however the inhibition of the proteasome decreases the degradation of MCL1 which can inhibit apoptosis and MCL1 expression is therefore a negative marker for MG-132 sensitivity (Yuan*, et al* 2008). The resistant cell lines had an up-regulation of MCL1 RNA, which could provide rationale for the increased resistance to MG-132. Further experiments are required to ascertain the mechanism of resistance in these cell lines.

5 Final conclusions

DLBCL is an aggressive B-cell malignancy with a poor prognosis for patients who fail/ remit chemo-immunotherapy. ABT-199, the first specific BCL2 inhibitor, displays remarkable efficacy in some B-cell lymphomas and thus has received several FDA breakthrough designations for the treatment of chronic lymphocytic leukaemia (CLL), mantle cell lymphoma (MCL) and acute myeloid leukaemia. In contrast, in DLBCL, venetoclax monotherapy has been less successful, with one study observing a response rate in only 18% (Grecitano et al., 2015). Nevertheless, complete remissions can be obtained with single agent drug. Since the development of ABT-199, other specific mimetics targeting $BCLX_L$ and MCL1 have also been developed but there is yet to be any clinical data published on these compounds. This highlights the necessity to identify biomarkers which can stratify patients and allow the rational use of BH3 mimetics. However, acquired resistance is likely inevitable. This project sought to define the determinants of sensitivity to BH3 mimetics in DLBCL and ascertain the mechanism of acquired resistance.

DLBCL patient samples and cell lines exhibited heterogeneous BH3 mimetic responses and therefore anti-apoptotic protein dependence. These responses did not correlate with COO or BCL2 translocations. Although cell lines which were sensitive to a specific mimetic tended to have high expression of the respective anti-apoptotic protein, BCL2 family protein expression is a poor marker of response. The only statistically significant correlation was found between ABT-199 sensitivity and BCL2 protein expression. Correlations between mimetic sensitivity and target protein expression for A1331852 and S63845 were weak and without statistical significance. This poor correlation was also evident in the RCK8 resistant cell lines as both upregulated BCL2 expression but only RCK8-A133R became more sensitive to ABT-199.

The limitations of BH3 profiling notwithstanding, responses to XXa1_Y4eK peptide correlated with A1331852 sensitivity in a statistically significant manner for both the panel of cell lines and those generated with BH3 mimetic resistance. Dynamic profiling may be able to circumvent some of the pitfalls caused by not having a BCL2 specific peptide or a predictive MCL1 peptide. BH3 profiling has been reported to be able to

determine ABT-737 sensitivity in CLL primary samples (Del Gaizo Moore and Letai 2013). However, BH3 profiling was not able to be performed on the DLBCL patient samples used in this report as the assay requires samples to be of high viability. Unlike DLBCL, CLL samples can remain viable *ex vivo* (Chen*, et al* 2019b). Therefore, this assay may prove useful for CLL patients but would severely limit its use for other lymphomas clinically.

Immuno-precipitation in some specific BH3 mimetic sensitive cell lines indicates anti-apoptotic protein dependence is mediated by the direct sequestration of BIM, BAK and/or BAX. Immunoprecipitations of the resistant generated cell lines may provide an insight to the mechanism of resistance. As both RCK8 resistant cell lines upregulate BCL2 but have differential responses to ABT-199, and the RIVA resistant cell lines display similar protein expression to their parental yet they have different responses to the mimetics, it would be worthwhile investigating if the interactions between the pro and anti-apoptotic proteins are different. In the parental RCK8 cell line, BAK and BAX are sequestered by BCL2. It could be hypothesised that in the RCK8-A133R cell line BCL2 would sequester BAX, similar to the BCL2 dependent cell lines.

One possible explanation for the discordance between protein expression and BH3 mimetic sensitivity could be the localisation of the anti-apoptotic proteins. These proteins have other functions within the cell which can localise them to different compartments of the cell such as the ER. Therefore, BH3 mimetic sensitivity may correlate to the anti-apoptotic proteins available at the mitochondria as opposed to in whole cell lysates. It is anticipated that there will be major differences in the mitochondrial proteomes of ultrasensitive and resistant cell lines which could be investigated via mitochondrial isolation followed by immuno-blotting or mass spectrometry. The advantage of the latter being that it is unbiased and would allow detection of other proteins from outside the pathway. This would also be of interest in the resistant generated cell lines.

The drugs tested on the resistant generated cell lines were chosen as they target pathways which are often deregulated in DLBCL, plus most are either in clinical trials or FDA approved. Unbiased techniques such as RNA sequencing or genome wide

CRISPR/Cas9 screening may help elucidate the mechanisms of resistance plus may identify candidate pathways which could be targeted. Whole exome sequencing of the parental and derived resistant cell lines would also identify acquired mutations which were not assessed in this study.

It is likely that there are multiple causes of resistance to these mimetics both inter and intra cell line/ patient. This is supported by the reported identification of the $BCL2^{G101V}$ mutation and upregulation of $BCLX_L$ occurring in different subclones from one patient after relapsing to ABT-199 (Blombery*, et al* 2019a). For this reason, techniques such as single cell RNA sequencing and mutli-colour flow cytometry/ mass cytometry (CyTof) to assess changes of BCL2 family protein abundance may provide more insight into the heterogeneity of the samples and identify multiple mechanisms.

In order to assess mechanisms that might occur from different samples, more resistant cell lines could be derived from different parental cell lines. It would be interesting to see if the switch from $BCLX_L$ to BCL2 dependence is recapitulated in another A1331852 resistant cell line. Moreover, S63845 resistant cell lines were not developed/ assessed in this project. The mechanism of S63845 and MCL1 inhibitor resistance could be investigated via the same techniques performed in this report and described above. The identification of any biomarkers/ candidate drugs could then be confirmed in primary samples or patient derived xenografts.

There is an increasing plethora of small molecule inhibitors available for the treatment of DLBCL, which therefore requires careful matching of patients to molecules. The data presented here indicates that there is a correlation between BCL2 expression and ABT-199 sensitivity and BH3 profiling can predict sensitivity to A1331852 but there not a clear marker for sensitivity to S63845. Furthermore, anti-apoptotic protein dependence within DLBCL is caused by the direct sequestration of BIM, BAK and/or BAX. The need for subgrouping this disease based on anti-apoptotic protein dependence has been highlighted by this data, however further studies are required to elucidate better methods of doing this. Two models of BCL2 inhibitor resistance have been generated, for which the mechanisms are not fully understood. However, as there was not an increase in sensitivity to A133182, S63845 or CAL-101 it is independent of $BCLX_L$/MCL1

as has been previously reported (Konopleva*, et al* 2006, Lin*, et al* 2016, Tahir*, et al* 2017). Two models of $BCLX_L$ inhibitor resistance were also generated. There is currently no published data on the resistance to specific $BCLX_L$ inhibitors. Both the ABT-737 and A1331852 resistant cell line upregulated BCL2, however only RCK8-A133R became more sensitive to ABT-199 indicating a shift in dependence. Further studies are required to elucidate the mechanism behind this BCL2 upregulation. Understanding the mechanisms of resistance in these *in vitro* cell line models will become clinically relevant as BH3 mimetics are further developed and used to treat patients.

6 Bibliography

Abbvie (2018) AbbVie Receives US FDA Accelerated Approval for VENCLEXTA® (venetoclax) for Treatment of Newly-Diagnosed Acute Myeloid Leukemia Patients Ineligible for Intensive Chemotherapy. Abbvie, North Chicago, Illinois, U.S.A.

Abbvie (2019a) AbbVie Announces US FDA Approval of VENCLEXTA® (venetoclax) as a Chemotherapy-Free Combination Regimen for Previously Untreated Chronic Lymphocytic Leukemia Patients. Abbvie, North Chicago, Illinois, U.S.A.

Abbvie (2019b) AbbVie Announces US FDA Lifts Partial Clinical Hold on Phase 3 Study of Venetoclax in Patients with Multiple Myeloma Positive for the t(11;14) Genetic Abnormality. Abbvie, North Chicago, Illinois, U.S.A.

Abbvie (2019c) AbbVie Provides Update on VENCLEXTA®/VENCLYXTO® (venetoclax) Multiple Myeloma Program. Abbvie, North Chicago, Illinois, U.S.A.

Abulwerdi, F., Liao, C., Liu, M., Azmi, A.S., Aboukameel, A., Mady, A.S., Gulappa, T., Cierpicki, T., Owens, S., Zhang, T., Sun, D., Stuckey, J.A., Mohammad, R.M. & Nikolovska-Coleska, Z. (2014) A novel small-molecule inhibitor of mcl-1 blocks pancreatic cancer growth in vitro and in vivo. *Mol Cancer Ther,* **13,** 565-575.

Ackler, S., Mitten, M.J., Foster, K., Oleksijew, A., Refici, M., Tahir, S.K., Xiao, Y., Tse, C., Frost, D.J., Fesik, S.W., Rosenberg, S.H., Elmore, S.W. & Shoemaker, A.R. (2010) The Bcl-2 inhibitor ABT-263 enhances the response of multiple chemotherapeutic regimens in hematologic tumors in vivo. *Cancer Chemother Pharmacol,* **66,** 869-880.

Adam, A., Byth, K., Secrist, P., Schuller, A., Reimer, C., Lawson, D., MacIntyre, T. & Powell, F. (2014) A Dual Bcl-2/x_L Inhibitor Induces Tumor Cell Apoptosis in a Hematopoietic Xenograft Model. *Blood,* **124,** 5304-5304.

Adams, C.M., Kim, A.S., Mitra, R., Choi, J.K., Gong, J.Z. & Eischen, C.M. (2017) BCL-W has a fundamental role in B cell survival and lymphomagenesis. *J Clin Invest,* **127,** 635-650.

Adams, J.M. & Cory, S. (2018) The BCL-2 arbiters of apoptosis and their growing role as cancer targets. *Cell Death Differ,* **25,** 27-36.

Aguilar-Hernandez, M.M., Blunt, M.D., Dobson, R., Yeomans, A., Thirdborough, S., Larrayoz, M., Smith, L.D., Linley, A., Strefford, J.C., Davies, A., Johnson, P.M., Savelyeva, N., Cragg, M.S., Forconi, F., Packham, G., Stevenson, F.K. & Steele, A.J. (2016) IL-4 enhances expression and function of surface IgM in CLL cells. *Blood,* **127,** 3015-3025.

Aguilar, A., Zhou, H., Chen, J., Liu, L., Bai, L., McEachern, D., Yang, C.Y., Meagher, J., Stuckey, J. & Wang, S. (2013) A potent and highly efficacious Bcl-2/Bcl-xL inhibitor. *J Med Chem,* **56,** 3048-3067.

Albershardt, T.C., Salerni, B.L., Soderquist, R.S., Bates, D.J., Pletnev, A.A., Kisselev, A.F. & Eastman, A. (2011) Multiple BH3 mimetics antagonize antiapoptotic MCL1 protein by inducing the endoplasmic reticulum stress response and up-regulating BH3-only protein NOXA. *J Biol Chem,* **286,** 24882-24895.

Alizadeh, A.A., Eisen, M.B., Davis, R.E., Ma, C., Lossos, I.S., Rosenwald, A., Boldrick, J.C., Sabet, H., Tran, T., Yu, X., Powell, J.I., Yang, L., Marti, G.E., Moore, T., Hudson, J., Jr., Lu, L., Lewis, D.B., Tibshirani, R., Sherlock, G., Chan, W.C., Greiner, T.C., Weisenburger, D.D., Armitage, J.O., Warnke, R., Levy, R., Wilson, W., Grever, M.R., Byrd, J.C., Botstein, D., Brown, P.O. & Staudt, L.M. (2000) Distinct types of diffuse large B-cell lymphoma identified by gene expression profiling. *Nature,* **403,** 503-511.

Amundson, S.A., Myers, T.G., Scudiero, D., Kitada, S., Reed, J.C. & Fornace, A.J., Jr. (2000) An informatics approach identifying markers of chemosensitivity in human cancer cell lines. *Cancer Res,* **60,** 6101-6110.

Arbour, N., Vanderluit, J.L., Le Grand, J.N., Jahani-Asl, A., Ruzhynsky, V.A., Cheung, E.C., Kelly, M.A., MacKenzie, A.E., Park, D.S., Opferman, J.T. & Slack, R.S. (2008) Mcl-1 is a key regulator of apoptosis during CNS development and after DNA damage. *J Neurosci,* **28,** 6068-6078.

Bae, J., Leo, C.P., Hsu, S.Y. & Hsueh, A.J. (2000) MCL-1S, a splicing variant of the antiapoptotic BCL-2 family member MCL-1, encodes a proapoptotic protein possessing only the BH3 domain. *J Biol Chem,* **275,** 25255-25261.

Bai, L., Chen, J., McEachern, D., Liu, L., Zhou, H., Aguilar, A. & Wang, S. (2014) BM-1197: a novel and specific Bcl-2/Bcl-xL inhibitor inducing complete and long-lasting tumor regression in vivo. *PLoS One,* **9,** e99404.

Bajpai, U.D., Zhang, K., Teutsch, M., Sen, R. & Wortis, H.H. (2000) Bruton's tyrosine kinase links the B cell receptor to nuclear factor kappaB activation. *J Exp Med,* **191,** 1735-1744.

Becattini, B., Kitada, S., Leone, M., Monosov, E., Chandler, S., Zhai, D., Kipps, T.J., Reed, J.C. & Pellecchia, M. (2004) Rational design and real time, in-cell detection of the proapoptotic activity of a novel compound targeting Bcl-X(L). *Chem Biol,* **11,** 389-395.

Beham-Schmid, C. (2017) Aggressive lymphoma 2016: revision of the WHO classification. *Memo,* **10,** 248-254.

Beham, A., Marin, M.C., Fernandez, A., Herrmann, J., Brisbay, S., Tari, A.M., Lopez-Berestein, G., Lozano, G., Sarkiss, M. & McDonnell, T.J. (1997) Bcl-2 inhibits p53 nuclear import following DNA damage. *Oncogene,* **15,** 2767-2772.

Bergsbaken, T., Fink, S.L. & Cookson, B.T. (2009) Pyroptosis: host cell death and inflammation. *Nat Rev Microbiol,* **7,** 99-109.

Berman, S.B., Chen, Y.B., Qi, B., McCaffery, J.M., Rucker, E.B., 3rd, Goebbels, S., Nave, K.A., Arnold, B.A., Jonas, E.A., Pineda, F.J. & Hardwick, J.M. (2009) Bcl-x L increases mitochondrial fission, fusion, and biomass in neurons. *J Cell Biol,* **184,** 707-719.

Beroukhim, R., Mermel, C.H., Porter, D., Wei, G., Raychaudhuri, S., Donovan, J., Barretina, J., Boehm, J.S., Dobson, J., Urashima, M., Mc Henry, K.T., Pinchback, R.M., Ligon, A.H., Cho, Y.J., Haery, L., Greulich, H., Reich, M., Winckler, W., Lawrence, M.S., Weir, B.A., Tanaka, K.E., Chiang, D.Y., Bass, A.J., Loo, A., Hoffman, C., Prensner, J., Liefeld, T., Gao, Q., Yecies, D., Signoretti, S., Maher, E., Kaye, F.J., Sasaki, H., Tepper, J.E., Fletcher, J.A., Tabernero, J., Baselga, J., Tsao, M.S., Demichelis, F., Rubin, M.A., Janne, P.A., Daly, M.J., Nucera, C., Levine, R.L., Ebert, B.L., Gabriel, S., Rustgi, A.K., Antonescu, C.R., Ladanyi, M., Letai, A., Garraway, L.A., Loda, M., Beer, D.G., True, L.D., Okamoto, A., Pomeroy, S.L., Singer, S., Golub, T.R., Lander, E.S., Getz, G., Sellers, W.R. & Meyerson, M. (2010) The landscape of somatic copy-number alteration across human cancers. *Nature,* **463,** 899-905.

Beverly, L.J. & Varmus, H.E. (2009) MYC-induced myeloid leukemogenesis is accelerated by all six members of the antiapoptotic BCL family. *Oncogene,* **28,** 1274-1279.

Bharatham, N., Chi, S.W. & Yoon, H.S. (2011) Molecular basis of Bcl-X(L)-p53 interaction: insights from molecular dynamics simulations. *PLoS One,* **6,** e26014.

Billard, C. (2013) BH3 mimetics: status of the field and new developments. *Mol Cancer Ther,* **12,** 1691-1700.

Billen, L.P., Kokoski, C.L., Lovell, J.F., Leber, B. & Andrews, D.W. (2008) Bcl-XL inhibits membrane permeabilization by competing with Bax. *PLoS Biol,* **6,** e147.

Birkinshaw, R.W., Gong, J.N., Luo, C.S., Lio, D., White, C.A., Anderson, M.A., Blombery, P., Lessene, G., Majewski, I.J., Thijssen, R., Roberts, A.W., Huang, D.C.S., Colman, P.M. & Czabotar, P.E. (2019) Structures of BCL-2 in complex with venetoclax reveal the molecular basis of resistance mutations. *Nat Commun,* **10,** 2385.

Blombery, P., Anderson, M.A., Gong, J.N., Thijssen, R., Birkinshaw, R.W., Thompson, E.R., Teh, C.E., Nguyen, T., Xu, Z., Flensburg, C., Lew, T.E., Majewski, I.J., Gray, D.H.D., Westerman, D.A., Tam, C.S., Seymour, J.F., Czabotar, P.E., Huang, D.C.S. & Roberts, A.W. (2019a) Acquisition of the Recurrent Gly101Val Mutation in BCL2 Confers Resistance to Venetoclax in Patients with Progressive Chronic Lymphocytic Leukemia. *Cancer Discov,* **9,** 342-353.

Blombery, P., Birkinshaw, R.W., Nguyen, T., Gong, J.N., Thompson, E.R., Xu, Z., Westerman, D.A., Czabotar, P.E., Dickinson, M., Huang, D.C.S., Seymour, J.F. & Roberts, A.W. (2019b) Characterization of a novel venetoclax resistance mutation (BCL2 Phe104Ile) observed in follicular lymphoma. *Br J Haematol*.

Blunt, M.D., Koehrer, S., Dobson, R.C., Larrayoz, M., Wilmore, S., Hayman, A., Parnell, J., Smith, L.D., Davies, A., Johnson, P.W.M., Conley, P.B., Pandey, A., Strefford, J.C., Stevenson, F.K., Packham, G., Forconi, F., Coffey, G.P., Burger, J.A. & Steele, A.J. (2017) The Dual Syk/JAK Inhibitor Cerdulatinib Antagonizes B-cell Receptor and Microenvironmental Signaling in Chronic Lymphocytic Leukemia. *Clin Cancer Res,* **23,** 2313-2324.

Bodo, J., Zhao, X., Durkin, L., Souers, A.J., Phillips, D.C., Smith, M.R. & Hsi, E.D. (2016) Acquired resistance to venetoclax (ABT-199) in t(14;18) positive lymphoma cells. *Oncotarget,* **7,** 70000-70010.

Bogenberger, J., Whatcott, C., Hansen, N., Delman, D., Shi, C.X., Kim, W., Haws, H., Soh, K., Lee, Y.S., Peterson, P., Siddiqui-Jain, A., Weitman, S., Stewart, K., Bearss, D., Mesa, R., Warner, S. & Tibes, R. (2017) Combined venetoclax and alvocidib in acute myeloid leukemia. *Oncotarget,* **8,** 107206-107222.

Boise, L.H., Gonzalez-Garcia, M., Postema, C.E., Ding, L., Lindsten, T., Turka, L.A., Mao, X., Nunez, G. & Thompson, C.B. (1993) bcl-x, a bcl-2-related gene that functions as a dominant regulator of apoptotic cell death. *Cell,* **74,** 597-608.

Bojarczuk, K., Sasi, B.K., Gobessi, S., Innocenti, I., Pozzato, G., Laurenti, L. & Efremov, D.G. (2016) BCR signaling inhibitors differ in their ability to overcome Mcl-1-mediated resistance of CLL B cells to ABT-199. *Blood,* **127,** 3192-3201.

Borner, C., Martinou, I., Mattmann, C., Irmler, M., Schaerer, E., Martinou, J.C. & Tschopp, J. (1994) The protein bcl-2 alpha does not require membrane attachment, but two conserved domains to suppress apoptosis. *J Cell Biol,* **126,** 1059-1068.

Brien, G., Debaud, A.L., Robert, X., Oliver, L., Trescol-Biemont, M.C., Cauquil, N., Geneste, O., Aghajari, N., Vallette, F.M., Haser, R. & Bonnefoy-Berard, N. (2009) C-terminal residues regulate localization and function of the antiapoptotic protein Bfl-1. *J Biol Chem,* **284,** 30257-30263.

Bui, T.V. & Mendell, J.T. (2010) Myc: Maestro of MicroRNAs. *Genes Cancer,* **1,** 568-575.

Burke, J.P., Bian, Z., Shaw, S., Zhao, B., Goodwin, C.M., Belmar, J., Browning, C.F., Vigil, D., Friberg, A., Camper, D.V., Rossanese, O.W., Lee, T., Olejniczak, E.T. & Fesik, S.W. (2015) Discovery of tricyclic indoles that potently inhibit Mcl-1 using fragment-based methods and structure-based design. *J Med Chem,* **58,** 3794-3805.

Butterworth, M., Pettitt, A., Varadarajan, S. & Cohen, G.M. (2016) BH3 profiling and a toolkit of BH3-mimetic drugs predict anti-apoptotic dependence of cancer cells. *Br J Cancer,* **114,** 638-641.

Byrd, J.C., Furman, R.R., Coutre, S.E., Flinn, I.W., Burger, J.A., Blum, K.A., Grant, B., Sharman, J.P., Coleman, M., Wierda, W.G., Jones, J.A., Zhao, W., Heerema, N.A., Johnson, A.J., Sukbuntherng, J., Chang, B.Y., Clow, F., Hedrick, E., Buggy, J.J.,

James, D.F. & O'Brien, S. (2013) Targeting BTK with ibrutinib in relapsed chronic lymphocytic leukemia. *N Engl J Med,* **369,** 32-42.

Caenepeel, S., Brown, S.P., Belmontes, B., Moody, G., Keegan, K.S., Chui, D., Whittington, D.A., Huang, X., Poppe, L., Cheng, A.C., Cardozo, M., Houze, J., Li, Y., Lucas, B., Paras, N.A., Wang, X., Taygerly, J.P., Vimolratana, M., Zancanella, M., Zhu, L., Cajulis, E., Osgood, T., Sun, J., Damon, L., Egan, R.K., Greninger, P., McClanaghan, J.D., Gong, J., Moujalled, D., Pomilio, G., Beltran, P., Benes, C.H., Roberts, A.W., Huang, D.C., Wei, A., Canon, J., Coxon, A. & Hughes, P.E. (2018) AMG 176, a Selective MCL1 Inhibitor, Is Effective in Hematologic Cancer Models Alone and in Combination with Established Therapies. *Cancer Discov,* **8,** 1582-1597.

Calin, G.A., Dumitru, C.D., Shimizu, M., Bichi, R., Zupo, S., Noch, E., Aldler, H., Rattan, S., Keating, M., Rai, K., Rassenti, L., Kipps, T., Negrini, M., Bullrich, F. & Croce, C.M. (2002) Frequent deletions and down-regulation of micro- RNA genes miR15 and miR16 at 13q14 in chronic lymphocytic leukemia. *Proc Natl Acad Sci U S A,* **99,** 15524-15529.

Cao, K. & Tait, S.W.G. (2018) Apoptosis and Cancer: Force Awakens, Phantom Menace, or Both? *Int Rev Cell Mol Biol,* **337,** 135-152.

Casara, P., Davidson, J., Claperon, A., Le Toumelin-Braizat, G., Vogler, M., Bruno, A., Chanrion, M., Lysiak-Auvity, G., Le Diguarher, T., Starck, J.B., Chen, I., Whitehead, N., Graham, C., Matassova, N., Dokurno, P., Pedder, C., Wang, Y., Qiu, S., Girard, A.M., Schneider, E., Grave, F., Studeny, A., Guasconi, G., Rocchetti, F., Maiga, S., Henlin, J.M., Colland, F., Kraus-Berthier, L., Le Gouill, S., Dyer, M.J.S., Hubbard, R., Wood, M., Amiot, M., Cohen, G.M., Hickman, J.A., Morris, E., Murray, J. & Geneste, O. (2018) S55746 is a novel orally active BCL-2 selective and potent inhibitor that impairs hematological tumor growth. *Oncotarget,* **9,** 20075-20088.

Cerami, E., Gao, J., Dogrusoz, U., Gross, B.E., Sumer, S.O., Aksoy, B.A., Jacobsen, A., Byrne, C.J., Heuer, M.L., Larsson, E., Antipin, Y., Reva, B., Goldberg, A.P., Sander, C. & Schultz, N. (2012) The cBio cancer genomics portal: an open platform for exploring multidimensional cancer genomics data. *Cancer Discov,* **2,** 401-404.

Certo, M., Del Gaizo Moore, V., Nishino, M., Wei, G., Korsmeyer, S., Armstrong, S.A. & Letai, A. (2006) Mitochondria primed by death signals determine cellular addiction to antiapoptotic BCL-2 family members. *Cancer Cell,* **9,** 351-365.

Cervantes-Gomez, F., Lamothe, B., Woyach, J.A., Wierda, W.G., Keating, M.J., Balakrishnan, K. & Gandhi, V. (2015) Pharmacological and Protein Profiling Suggests Venetoclax (ABT-199) as Optimal Partner with Ibrutinib in Chronic Lymphocytic Leukemia. *Clin Cancer Res,* **21,** 3705-3715.

Chang, B.S., Kelekar, A., Harris, M.H., Harlan, J.E., Fesik, S.W. & Thompson, C.B. (1999) The BH3 domain of Bcl-x(S) is required for inhibition of the antiapoptotic function of Bcl-x(L). *Mol Cell Biol,* **19,** 6673-6681.

Chapuy, B., Stewart, C., Dunford, A.J., Kim, J., Kamburov, A., Redd, R.A., Lawrence, M.S., Roemer, M.G.M., Li, A.J., Ziepert, M., Staiger, A.M., Wala, J.A., Ducar, M.D., Leshchiner, I., Rheinbay, E., Taylor-Weiner, A., Coughlin, C.A., Hess, J.M., Pedamallu, C.S., Livitz, D., Rosebrock, D., Rosenberg, M., Tracy, A.A., Horn, H., van Hummelen, P., Feldman, A.L., Link, B.K., Novak, A.J., Cerhan, J.R., Habermann, T.M., Siebert, R., Rosenwald, A., Thorner, A.R., Meyerson, M.L., Golub, T.R., Beroukhim, R., Wulf, G.G., Ott, G., Rodig, S.J., Monti, S., Neuberg, D.S., Loeffler, M., Pfreundschuh, M., Trumper, L., Getz, G. & Shipp, M.A. (2018) Molecular subtypes of diffuse large B cell lymphoma are associated with distinct pathogenic mechanisms and outcomes. *Nat Med,* **24,** 679-690.

Chaurio, R., Janko, C., Schorn, C., Maueroder, C., Bilyy, R., Gaipl, U., Schett, G., Berens, C., Frey, B. & Munoz, L.E. (2013) UVB-irradiated apoptotic cells induce accelerated growth of co-implanted viable tumor cells in immune competent mice. *Autoimmunity,* **46,** 317-322.

Chen, J., Jin, S., Abraham, V., Huang, X., Liu, B., Mitten, M.J., Nimmer, P., Lin, X., Smith, M., Shen, Y., Shoemaker, A.R., Tahir, S.K., Zhang, H., Ackler, S.L., Rosenberg, S.H., Maecker, H., Sampath, D., Leverson, J.D., Tse, C. & Elmore, S.W. (2011) The Bcl-2/Bcl-X(L)/Bcl-w inhibitor, navitoclax, enhances the activity of chemotherapeutic agents in vitro and in vivo. *Mol Cancer Ther,* **10,** 2340-2349.

Chen, J., Jin, S., Tapang, P., Tahir, S.K., Smith, M., Xue, J., Zhang, H., Gao, W., Tong, Y., Clark, R., Ricker, J.L., Penning, T.D., Albert, D.H., Phillips, D.C., Souers, A.J. & Leverson, J.D. (2014) CDK9 Inhibition Reverses Resistance to ABT-199 (GDC-0199) By Down-Regulating MCL-1. *Blood,* **124,** 2161-2161.

Chen, L., Willis, S.N., Wei, A., Smith, B.J., Fletcher, J.I., Hinds, M.G., Colman, P.M., Day, C.L., Adams, J.M. & Huang, D.C. (2005) Differential targeting of prosurvival Bcl-2 proteins by their BH3-only ligands allows complementary apoptotic function. *Mol Cell,* **17,** 393-403.

Chen, W., Zhou, Z., Li, L., Zhong, C.Q., Zheng, X., Wu, X., Zhang, Y., Ma, H., Huang, D., Li, W., Xia, Z. & Han, J. (2013) Diverse sequence determinants control human and mouse receptor interacting protein 3 (RIP3) and mixed lineage kinase domain-like (MLKL) interaction in necroptotic signaling. *J Biol Chem,* **288,** 16247-16261.

Chen, X., Glytsou, C., Zhou, H., Narang, S., Reyna, D.E., Lopez, A., Sakellaropoulos, T., Gong, Y., Kloetgen, A., Yap, Y.S., Wang, E., Gavathiotis, E., Tsirigos, A., Tibes, R. & Aifantis, I. (2019a) Targeting Mitochondrial Structure Sensitizes Acute Myeloid Leukemia to Venetoclax Treatment. *Cancer Discov,* **9,** 890-909.

Chen, Y., Germano, S., Clements, C., Samuel, J., Shelmani, G., Jayne, S., Dyer, M.J. & Macip, S. (2016) Pro-survival signal inhibition by CDK inhibitor dinaciclib in Chronic Lymphocytic Leukaemia. *Br J Haematol,* **175,** 641-651.

Chen, Y., Peubez, C., Smith, V., Xiong, S., Kocsis-Fodor, G., Kennedy, B., Wagner, S., Balotis, C., Jayne, S., Dyer, M.J.S. & Macip, S. (2019b) CUDC-907 blocks multiple

pro-survival signals and abrogates microenvironment protection in CLL. *J Cell Mol Med,* **23,** 340-348.

Cheson, B.D., Heitner Enschede, S., Cerri, E., Desai, M., Potluri, J., Lamanna, N. & Tam, C. (2017) Tumor Lysis Syndrome in Chronic Lymphocytic Leukemia with Novel Targeted Agents. *Oncologist,* **22,** 1283-1291.

Chittenden, T., Harrington, E.A., O'Connor, R., Flemington, C., Lutz, R.J., Evan, G.I. & Guild, B.C. (1995) Induction of apoptosis by the Bcl-2 homologue Bak. *Nature,* **374,** 733-736.

Chou, T.C. (2008) Preclinical versus clinical drug combination studies. *Leuk Lymphoma,* **49,** 2059-2080.

Chou, T.C. (2010) Drug combination studies and their synergy quantification using the Chou-Talalay method. *Cancer Res,* **70,** 440-446.

Chou, T.C. & Talalay, P. (1984) Quantitative analysis of dose-effect relationships: the combined effects of multiple drugs or enzyme inhibitors. *Adv Enzyme Regul,* **22,** 27-55.

Choudhary, G.S., Al-Harbi, S., Mazumder, S., Hill, B.T., Smith, M.R., Bodo, J., Hsi, E.D. & Almasan, A. (2015a) MCL-1 and BCL-xL-dependent resistance to the BCL-2 inhibitor ABT-199 can be overcome by preventing PI3K/AKT/mTOR activation in lymphoid malignancies. *Cell Death Dis,* **6,** e1593.

Choudhary, G.S., Tat, T.T., Misra, S., Hill, B.T., Smith, M.R., Almasan, A. & Mazumder, S. (2015b) Cyclin E/Cdk2-dependent phosphorylation of Mcl-1 determines its stability and cellular sensitivity to BH3 mimetics. *Oncotarget,* **6,** 16912-16925.

Chuang, P.I., Morefield, S., Liu, C.Y., Chen, S., Harlan, J.M. & Willerford, D.M. (2002) Perturbation of B-cell development in mice overexpressing the Bcl-2 homolog A1. *Blood,* **99,** 3350-3359.

Cimmino, A., Calin, G.A., Fabbri, M., Iorio, M.V., Ferracin, M., Shimizu, M., Wojcik, S.E., Aqeilan, R.I., Zupo, S., Dono, M., Rassenti, L., Alder, H., Volinia, S., Liu, C.G., Kipps, T.J., Negrini, M. & Croce, C.M. (2005) miR-15 and miR-16 induce apoptosis by targeting BCL2. *Proc Natl Acad Sci U S A,* **102,** 13944-13949.

Cohen, N.A., Stewart, M.L., Gavathiotis, E., Tepper, J.L., Bruekner, S.R., Koss, B., Opferman, J.T. & Walensky, L.D. (2012) A competitive stapled peptide screen identifies a selective small molecule that overcomes MCL-1-dependent leukemia cell survival. *Chem Biol,* **19,** 1175-1186.

Correia, C., Lee, S.H., Meng, X.W., Vincelette, N.D., Knorr, K.L., Ding, H., Nowakowski, G.S., Dai, H. & Kaufmann, S.H. (2015) Emerging understanding of Bcl-2 biology: Implications for neoplastic progression and treatment. *Biochim Biophys Acta,* **1853,** 1658-1671.

Czabotar, P.E., Lessene, G., Strasser, A. & Adams, J.M. (2014) Control of apoptosis by the BCL-2 protein family: implications for physiology and therapy. *Nat Rev Mol Cell Biol,* **15,** 49-63.

Dai, H., Ding, H., Meng, X.W., Peterson, K.L., Schneider, P.A., Karp, J.E. & Kaufmann, S.H. (2015a) Constitutive BAK activation as a determinant of drug sensitivity in malignant lymphohematopoietic cells. *Genes Dev,* **29,** 2140-2152.

Dai, H., Ehrentraut, S., Nagel, S., Eberth, S., Pommerenke, C., Dirks, W.G., Geffers, R., Kalavalapalli, S., Kaufmann, M., Meyer, C., Faehnrich, S., Chen, S., Drexler, H.G. & MacLeod, R.A.F. (2015b) Genomic Landscape of Primary Mediastinal B-Cell Lymphoma Cell Lines. *PLoS One,* **10,** e0139663.

David, K.K., Sasaki, M., Yu, S.W., Dawson, T.M. & Dawson, V.L. (2006) EndoG is dispensable in embryogenesis and apoptosis. *Cell Death Differ,* **13,** 1147-1155.

Davids, M.S., Roberts, A.W., Seymour, J.F., Pagel, J.M., Kahl, B.S., Wierda, W.G., Puvvada, S., Kipps, T.J., Anderson, M.A., Salem, A.H., Dunbar, M., Zhu, M., Peale, F., Ross, J.A., Gressick, L., Desai, M., Kim, S.Y., Verdugo, M., Humerickhouse, R.A., Gordon, G.B. & Gerecitano, J.F. (2017) Phase I First-in-Human Study of Venetoclax in Patients With Relapsed or Refractory Non-Hodgkin Lymphoma. *J Clin Oncol,* **35,** 826-833.

Davis, R.E., Brown, K.D., Siebenlist, U. & Staudt, L.M. (2001) Constitutive nuclear factor kappaB activity is required for survival of activated B cell-like diffuse large B cell lymphoma cells. *J Exp Med,* **194,** 1861-1874.

Davis, R.E., Ngo, V.N., Lenz, G., Tolar, P., Young, R.M., Romesser, P.B., Kohlhammer, H., Lamy, L., Zhao, H., Yang, Y., Xu, W., Shaffer, A.L., Wright, G., Xiao, W., Powell, J., Jiang, J.K., Thomas, C.J., Rosenwald, A., Ott, G., Muller-Hermelink, H.K., Gascoyne, R.D., Connors, J.M., Johnson, N.A., Rimsza, L.M., Campo, E., Jaffe, E.S., Wilson, W.H., Delabie, J., Smeland, E.B., Fisher, R.I., Braziel, R.M., Tubbs, R.R., Cook, J.R., Weisenburger, D.D., Chan, W.C., Pierce, S.K. & Staudt, L.M. (2010) Chronic active B-cell-receptor signalling in diffuse large B-cell lymphoma. *Nature,* **463,** 88-92.

Day, C.L., Chen, L., Richardson, S.J., Harrison, P.J., Huang, D.C. & Hinds, M.G. (2005) Solution structure of prosurvival Mcl-1 and characterization of its binding by proapoptotic BH3-only ligands. *J Biol Chem,* **280,** 4738-4744.

Decuypere, J.P., Parys, J.B. & Bultynck, G. (2012) Regulation of the autophagic bcl-2/beclin 1 interaction. *Cells,* **1,** 284-312.

Degterev, A., Boyce, M. & Yuan, J. (2003) A decade of caspases. *Oncogene,* **22,** 8543-8567.

Del Gaizo Moore, V., Brown, J.R., Certo, M., Love, T.M., Novina, C.D. & Letai, A. (2007) Chronic lymphocytic leukemia requires BCL2 to sequester prodeath BIM, explaining sensitivity to BCL2 antagonist ABT-737. *J Clin Invest,* **117,** 112-121.

Del Gaizo Moore, V. & Letai, A. (2013) BH3 profiling--measuring integrated function of the mitochondrial apoptotic pathway to predict cell fate decisions. *Cancer Lett,* **332,** 202-205.

Deng, J., Carlson, N., Takeyama, K., Dal Cin, P., Shipp, M. & Letai, A. (2007) BH3 profiling identifies three distinct classes of apoptotic blocks to predict response to ABT-737 and conventional chemotherapeutic agents. *Cancer Cell,* **12,** 171-185.

Deng, J., Isik, E., Fernandes, S.M., Brown, J.R., Letai, A. & Davids, M.S. (2017) Bruton's tyrosine kinase inhibition increases BCL-2 dependence and enhances sensitivity to venetoclax in chronic lymphocytic leukemia. *Leukemia,* **31,** 2075-2084.

Deng, X., Ruvolo, P., Carr, B. & May, W.S., Jr. (2000) Survival function of ERK1/2 as IL-3-activated, staurosporine-resistant Bcl2 kinases. *Proc Natl Acad Sci U S A,* **97,** 1578-1583.

Dengler, M.A., Robin, A.Y., Gibson, L., Li, M.X., Sandow, J.J., Iyer, S., Webb, A.I., Westphal, D., Dewson, G. & Adams, J.M. (2019) BAX Activation: Mutations Near Its Proposed Non-canonical BH3 Binding Site Reveal Allosteric Changes Controlling Mitochondrial Association. *Cell Rep,* **27,** 359-373 e356.

Denisov, A.Y., Madiraju, M.S., Chen, G., Khadir, A., Beauparlant, P., Attardo, G., Shore, G.C. & Gehring, K. (2003) Solution structure of human BCL-w: modulation of ligand binding by the C-terminal helix. *J Biol Chem,* **278,** 21124-21128.

Deshmukh, M., Kuida, K. & Johnson, E.M., Jr. (2000) Caspase inhibition extends the commitment to neuronal death beyond cytochrome c release to the point of mitochondrial depolarization. *J Cell Biol,* **150,** 131-143.

Deveraux, Q.L., Leo, E., Stennicke, H.R., Welsh, K., Salvesen, G.S. & Reed, J.C. (1999) Cleavage of human inhibitor of apoptosis protein XIAP results in fragments with distinct specificities for caspases. *EMBO J,* **18,** 5242-5251.

Dewson, G., Kratina, T., Czabotar, P., Day, C.L., Adams, J.M. & Kluck, R.M. (2009) Bak activation for apoptosis involves oligomerization of dimers via their alpha6 helices. *Mol Cell,* **36,** 696-703.

Dewson, G., Kratina, T., Sim, H.W., Puthalakath, H., Adams, J.M., Colman, P.M. & Kluck, R.M. (2008) To trigger apoptosis, Bak exposes its BH3 domain and homodimerizes via BH3:groove interactions. *Mol Cell,* **30,** 369-380.

Dewson, G., Ma, S., Frederick, P., Hockings, C., Tan, I., Kratina, T. & Kluck, R.M. (2012) Bax dimerizes via a symmetric BH3:groove interface during apoptosis. *Cell Death Differ,* **19,** 661-670.

Dey, J., Deckwerth, T.L., Kerwin, W.S., Casalini, J.R., Merrell, A.J., Grenley, M.O., Burns, C., Ditzler, S.H., Dixon, C.P., Beirne, E., Gillespie, K.C., Kleinman, E.F. & Klinghoffer, R.A. (2017) Voruciclib, a clinical stage oral CDK9 inhibitor, represses

MCL-1 and sensitizes high-risk Diffuse Large B-cell Lymphoma to BCL2 inhibition. *Sci Rep,* **7,** 18007.

Dixon, S.J., Lemberg, K.M., Lamprecht, M.R., Skouta, R., Zaitsev, E.M., Gleason, C.E., Patel, D.N., Bauer, A.J., Cantley, A.M., Yang, W.S., Morrison, B., 3rd & Stockwell, B.R. (2012) Ferroptosis: an iron-dependent form of nonapoptotic cell death. *Cell,* **149,** 1060-1072.

Doi, K., Li, R., Sung, S.S., Wu, H., Liu, Y., Manieri, W., Krishnegowda, G., Awwad, A., Dewey, A., Liu, X., Amin, S., Cheng, C., Qin, Y., Schonbrunn, E., Daughdrill, G., Loughran, T.P., Jr., Sebti, S. & Wang, H.G. (2012) Discovery of marinopyrrole A (maritoclax) as a selective Mcl-1 antagonist that overcomes ABT-737 resistance by binding to and targeting Mcl-1 for proteasomal degradation. *J Biol Chem,* **287,** 10224-10235.

Drexler, H.G. (2010) *Guide to Leukemia-Lymphoma Cell Lines.* Braunschweig.

Drexler, H.G., Eberth, S., Nagel, S. & MacLeod, R.A. (2016) Malignant hematopoietic cell lines: in vitro models for double-hit B-cell lymphomas. *Leuk Lymphoma,* **57,** 1015-1020.

Du, C., Fang, M., Li, Y., Li, L. & Wang, X. (2000) Smac, a mitochondrial protein that promotes cytochrome c-dependent caspase activation by eliminating IAP inhibition. *Cell,* **102,** 33-42.

Du, H., Wolf, J., Schafer, B., Moldoveanu, T., Chipuk, J.E. & Kuwana, T. (2011) BH3 domains other than Bim and Bid can directly activate Bax/Bak. *J Biol Chem,* **286,** 491-501.

Dutta, S., Ryan, J., Chen, T.S., Kougentakis, C., Letai, A. & Keating, A.E. (2015) Potent and specific peptide inhibitors of human pro-survival protein Bcl-xL. *J Mol Biol,* **427,** 1241-1253.

Dyer, M.J., Zani, V.J., Lu, W.Z., O'Byrne, A., Mould, S., Chapman, R., Heward, J.M., Kayano, H., Jadayel, D., Matutes, E. & et al. (1994) BCL2 translocations in leukemias of mature B cells. *Blood,* **83,** 3682-3688.

Eckelman, B.P. & Salvesen, G.S. (2006) The human anti-apoptotic proteins cIAP1 and cIAP2 bind but do not inhibit caspases. *J Biol Chem,* **281,** 3254-3260.

Eckelman, B.P., Salvesen, G.S. & Scott, F.L. (2006) Human inhibitor of apoptosis proteins: why XIAP is the black sheep of the family. *EMBO Rep,* **7,** 988-994.

Edelmann, J., Holzmann, K., Miller, F., Winkler, D., Buhler, A., Zenz, T., Bullinger, L., Kuhn, M.W., Gerhardinger, A., Bloehdorn, J., Radtke, I., Su, X., Ma, J., Pounds, S., Hallek, M., Lichter, P., Korbel, J., Busch, R., Mertens, D., Downing, J.R., Stilgenbauer, S. & Dohner, H. (2012) High-resolution genomic profiling of chronic lymphocytic leukemia reveals new recurrent genomic alterations. *Blood,* **120,** 4783-4794.

Edlich, F., Banerjee, S., Suzuki, M., Cleland, M.M., Arnoult, D., Wang, C., Neutzner, A., Tjandra, N. & Youle, R.J. (2011) Bcl-x(L) retrotranslocates Bax from the mitochondria into the cytosol. *Cell,* **145,** 104-116.

Ellis, H.M. & Horvitz, H.R. (1986) Genetic control of programmed cell death in the nematode C. elegans. *Cell,* **44,** 817-829.

Eno, C.O., Eckenrode, E.F., Olberding, K.E., Zhao, G., White, C. & Li, C. (2012) Distinct roles of mitochondria- and ER-localized Bcl-xL in apoptosis resistance and Ca2+ homeostasis. *Mol Biol Cell,* **23,** 2605-2618.

Esteve-Arenys, A., Valero, J.G., Chamorro-Jorganes, A., Gonzalez, D., Rodriguez, V., Dlouhy, I., Salaverria, I., Campo, E., Colomer, D., Martinez, A., Rymkiewicz, G., Perez-Galan, P., Lopez-Guillermo, A. & Roue, G. (2018) The BET bromodomain inhibitor CPI203 overcomes resistance to ABT-199 (venetoclax) by downregulation of BFL-1/A1 in in vitro and in vivo models of MYC+/BCL2+ double hit lymphoma. *Oncogene,* **37,** 1830-1844.

Faia, K., White, K., Murphy, E., Proctor, J., Pink, M., Kosmider, N., McGovern, K. & Kutok, J. (2018) The phosphoinositide-3 kinase (PI3K)-delta,gamma inhibitor, duvelisib shows preclinical synergy with multiple targeted therapies in hematologic malignancies. *PLoS One,* **13,** e0200725.

Fatokun, A.A., Dawson, V.L. & Dawson, T.M. (2014) Parthanatos: mitochondrial-linked mechanisms and therapeutic opportunities. *Br J Pharmacol,* **171,** 2000-2016.

Fischer, K., Al-Sawaf, O., Bahlo, J., Fink, A.M., Tandon, M., Dixon, M., Robrecht, S., Warburton, S., Humphrey, K., Samoylova, O., Liberati, A.M., Pinilla-Ibarz, J., Opat, S., Sivcheva, L., Le Du, K., Fogliatto, L.M., Niemann, C.U., Weinkove, R., Robinson, S., Kipps, T.J., Boettcher, S., Tausch, E., Humerickhouse, R., Eichhorst, B., Wendtner, C.M., Langerak, A.W., Kreuzer, K.A., Ritgen, M., Goede, V., Stilgenbauer, S., Mobasher, M. & Hallek, M. (2019) Venetoclax and Obinutuzumab in Patients with CLL and Coexisting Conditions. *N Engl J Med,* **380,** 2225-2236.

Foight, G.W., Ryan, J.A., Gulla, S.V., Letai, A. & Keating, A.E. (2014) Designed BH3 peptides with high affinity and specificity for targeting Mcl-1 in cells. *ACS Chem Biol,* **9,** 1962-1968.

Frank, S., Gaume, B., Bergmann-Leitner, E.S., Leitner, W.W., Robert, E.G., Catez, F., Smith, C.L. & Youle, R.J. (2001) The role of dynamin-related protein 1, a mediator of mitochondrial fission, in apoptosis. *Dev Cell,* **1,** 515-525.

Fresquet, V., Rieger, M., Carolis, C., Garcia-Barchino, M.J. & Martinez-Climent, J.A. (2014) Acquired mutations in BCL2 family proteins conferring resistance to the BH3 mimetic ABT-199 in lymphoma. *Blood,* **123,** 4111-4119.

Furukawa, Y., Iwase, S., Kikuchi, J., Terui, Y., Nakamura, M., Yamada, H., Kano, Y. & Matsuda, M. (2000) Phosphorylation of Bcl-2 protein by CDC2 kinase during G2/M phases and its role in cell cycle regulation. *J Biol Chem,* **275,** 21661-21667.

Gao, J., Aksoy, B.A., Dogrusoz, U., Dresdner, G., Gross, B., Sumer, S.O., Sun, Y., Jacobsen, A., Sinha, R., Larsson, E., Cerami, E., Sander, C. & Schultz, N. (2013) Integrative analysis of complex cancer genomics and clinical profiles using the cBioPortal. *Sci Signal,* **6,** pl1.

Garcia-Saez, A.J., Ries, J., Orzaez, M., Perez-Paya, E. & Schwille, P. (2009) Membrane promotes tBID interaction with BCL(XL). *Nat Struct Mol Biol,* **16,** 1178-1185.

Garrison, S.P., Jeffers, J.R., Yang, C., Nilsson, J.A., Hall, M.A., Rehg, J.E., Yue, W., Yu, J., Zhang, L., Onciu, M., Sample, J.T., Cleveland, J.L. & Zambetti, G.P. (2008) Selection against PUMA gene expression in Myc-driven B-cell lymphomagenesis. *Mol Cell Biol,* **28,** 5391-5402.

Gavathiotis, E., Reyna, D.E., Davis, M.L., Bird, G.H. & Walensky, L.D. (2010) BH3-triggered structural reorganization drives the activation of proapoptotic BAX. *Mol Cell,* **40,** 481-492.

Gavathiotis, E., Suzuki, M., Davis, M.L., Pitter, K., Bird, G.H., Katz, S.G., Tu, H.C., Kim, H., Cheng, E.H., Tjandra, N. & Walensky, L.D. (2008) BAX activation is initiated at a novel interaction site. *Nature,* **455,** 1076-1081.

Giampazolias, E., Zunino, B., Dhayade, S., Bock, F., Cloix, C., Cao, K., Roca, A., Lopez, J., Ichim, G., Proics, E., Rubio-Patino, C., Fort, L., Yatim, N., Woodham, E., Orozco, S., Taraborrelli, L., Peltzer, N., Lecis, D., Machesky, L., Walczak, H., Albert, M.L., Milling, S., Oberst, A., Ricci, J.E., Ryan, K.M., Blyth, K. & Tait, S.W.G. (2017) Mitochondrial permeabilization engages NF-kappaB-dependent anti-tumour activity under caspase deficiency. *Nat Cell Biol,* **19,** 1116-1129.

Graninger, W.B., Seto, M., Boutain, B., Goldman, P. & Korsmeyer, S.J. (1987) Expression of Bcl-2 and Bcl-2-Ig fusion transcripts in normal and neoplastic cells. *J Clin Invest,* **80,** 1512-1515.

Greaves, G., Milani, M., Butterworth, M., Carter, R.J., Byrne, D.P., Eyers, P.A., Luo, X., Cohen, G.M. & Varadarajan, S. (2019) BH3-only proteins are dispensable for apoptosis induced by pharmacological inhibition of both MCL-1 and BCL-XL. *Cell Death Differ,* **26,** 1037-1047.

Greaves, M.F. (1986) Differentiation-linked leukemogenesis in lymphocytes. *Science,* **234,** 697-704.

Green, D.R. & Llambi, F. (2015) Cell Death Signaling. *Cold Spring Harb Perspect Biol,* **7**.

Griffiths, G.J., Dubrez, L., Morgan, C.P., Jones, N.A., Whitehouse, J., Corfe, B.M., Dive, C. & Hickman, J.A. (1999) Cell damage-induced conformational changes of the pro-

apoptotic protein Bak in vivo precede the onset of apoptosis. *J Cell Biol,* **144,** 903-914.

Hamasaki, A., Sendo, F., Nakayama, K., Ishida, N., Negishi, I., Nakayama, K. & Hatakeyama, S. (1998) Accelerated neutrophil apoptosis in mice lacking A1-a, a subtype of the bcl-2-related A1 gene. *J Exp Med,* **188,** 1985-1992.

Han, L., Zhang, Q., Dail, M., Shi, C., Cavazos, A., Ruvolo, V.R., Zhao, Y., Kim, E., Rahmani, M., Mak, D.H., Jin, S.S., Chen, J., Phillips, D.C., Bottecelli Koller, P., Jacamo, R., Burks, J.K., DiNardo, C., Daver, N., Jabbour, E., Wang, J., Kantarjian, H.M., Andreeff, M., Grant, S., Leverson, J.D., Sampath, D. & Konopleva, M. (2019) Concomitant targeting of BCL2 with venetoclax and MAPK signaling with cobimetinib in acute myeloid leukemia models. *Haematologica*.

Hanahan, D. & Weinberg, R.A. (2000) The hallmarks of cancer. *Cell,* **100,** 57-70.

Hanahan, D. & Weinberg, R.A. (2011) Hallmarks of cancer: the next generation. *Cell,* **144,** 646-674.

Happo, L., Strasser, A. & Cory, S. (2012) BH3-only proteins in apoptosis at a glance. *J Cell Sci,* **125,** 1081-1087.

Hatakeyama, S., Hamasaki, A., Negishi, I., Loh, D.Y., Sendo, F., Nakayama, K. & Nakayama, K. (1998) Multiple gene duplication and expression of mouse bcl-2-related genes, A1. *Int Immunol,* **10,** 631-637.

Hegde, R., Srinivasula, S.M., Zhang, Z., Wassell, R., Mukattash, R., Cilenti, L., DuBois, G., Lazebnik, Y., Zervos, A.S., Fernandes-Alnemri, T. & Alnemri, E.S. (2002) Identification of Omi/HtrA2 as a mitochondrial apoptotic serine protease that disrupts inhibitor of apoptosis protein-caspase interaction. *J Biol Chem,* **277,** 432-438.

Hengartner, M.O., Ellis, R.E. & Horvitz, H.R. (1992) Caenorhabditis elegans gene ced-9 protects cells from programmed cell death. *Nature,* **356,** 494-499.

Hengartner, M.O. & Horvitz, H.R. (1994) C. elegans cell survival gene ced-9 encodes a functional homolog of the mammalian proto-oncogene bcl-2. *Cell,* **76,** 665-676.

Henz, K., Al-Zebeeby, A., Basoglu, M., Fulda, S., Cohen, G.M., Varadarajan, S. & Vogler, M. (2019) Selective BH3-mimetics targeting BCL-2, BCL-XL or MCL-1 induce severe mitochondrial perturbations. *Biol Chem,* **400,** 181-185.

Herman, M.D., Nyman, T., Welin, M., Lehtio, L., Flodin, S., Tresaugues, L., Kotenyova, T., Flores, A. & Nordlund, P. (2008) Completing the family portrait of the anti-apoptotic Bcl-2 proteins: crystal structure of human Bfl-1 in complex with Bim. *FEBS Lett,* **582,** 3590-3594.

Hillmen, P., Rawstron, A.C., Brock, K., Munoz-Vicente, S., Yates, F.J., Bishop, R., Boucher, R., MacDonald, D., Fegan, C., McCaig, A., Schuh, A., Pettitt, A., Gribben, J.G.,

Patten, P.E.M., Devereux, S., Bloor, A., Fox, C.P., Forconi, F. & Munir, T. (2019) Ibrutinib Plus Venetoclax in Relapsed/Refractory Chronic Lymphocytic Leukemia: The CLARITY Study. *J Clin Oncol***,** JCO1900894.

Hinds, M.G., Lackmann, M., Skea, G.L., Harrison, P.J., Huang, D.C. & Day, C.L. (2003) The structure of Bcl-w reveals a role for the C-terminal residues in modulating biological activity. *EMBO J,* **22,** 1497-1507.

Hinds, M.G., Smits, C., Fredericks-Short, R., Risk, J.M., Bailey, M., Huang, D.C. & Day, C.L. (2007) Bim, Bad and Bmf: intrinsically unstructured BH3-only proteins that undergo a localized conformational change upon binding to prosurvival Bcl-2 targets. *Cell Death Differ,* **14,** 128-136.

Hirata, H., Takahashi, A., Kobayashi, S., Yonehara, S., Sawai, H., Okazaki, T., Yamamoto, K. & Sasada, M. (1998) Caspases are activated in a branched protease cascade and control distinct downstream processes in Fas-induced apoptosis. *J Exp Med,* **187,** 587-600.

Horvat, M., Zadnik, V., Juznic Setina, T., Boltezar, L., Pahole Golicnik, J., Novakovic, S. & Jezersek Novakovic, B. (2018) Diffuse large B-cell lymphoma: 10 years' real-world clinical experience with rituximab plus cyclophosphamide, doxorubicin, vincristine and prednisolone. *Oncol Lett,* **15,** 3602-3609.

Hou, Y., Gao, F., Wang, Q., Zhao, J., Flagg, T., Zhang, Y. & Deng, X. (2007) Bcl2 impedes DNA mismatch repair by directly regulating the hMSH2-hMSH6 heterodimeric complex. *J Biol Chem,* **282,** 9279-9287.

Huang, H., Hu, X., Eno, C.O., Zhao, G., Li, C. & White, C. (2013) An interaction between Bcl-xL and the voltage-dependent anion channel (VDAC) promotes mitochondrial Ca2+ uptake. *J Biol Chem,* **288,** 19870-19881.

Huh, J.R., Guo, M. & Hay, B.A. (2004) Compensatory proliferation induced by cell death in the Drosophila wing disc requires activity of the apical cell death caspase Dronc in a nonapoptotic role. *Curr Biol,* **14,** 1262-1266.

Ichim, G., Lopez, J., Ahmed, S.U., Muthalagu, N., Giampazolias, E., Delgado, M.E., Haller, M., Riley, J.S., Mason, S.M., Athineos, D., Parsons, M.J., van de Kooij, B., Bouchier-Hayes, L., Chalmers, A.J., Rooswinkel, R.W., Oberst, A., Blyth, K., Rehm, M., Murphy, D.J. & Tait, S.W.G. (2015) Limited mitochondrial permeabilization causes DNA damage and genomic instability in the absence of cell death. *Mol Cell,* **57,** 860-872.

Irvine, R.A., Adachi, N., Shibata, D.K., Cassell, G.D., Yu, K., Karanjawala, Z.E., Hsieh, C.L. & Lieber, M.R. (2005) Generation and characterization of endonuclease G null mice. *Mol Cell Biol,* **25,** 294-302.

Ito, D., Frantz, A.M., Williams, C., Thomas, R., Burnett, R.C., Avery, A.C., Breen, M., Mason, N.J., O'Brien, T.D. & Modiano, J.F. (2012) CD40 ligand is necessary and sufficient to support primary diffuse large B-cell lymphoma cells in culture: a tool

for in vitro preclinical studies with primary B-cell malignancies. *Leuk Lymphoma,* **53,** 1390-1398.

Jamil, S., Mojtabavi, S., Hojabrpour, P., Cheah, S. & Duronio, V. (2008) An essential role for MCL-1 in ATR-mediated CHK1 phosphorylation. *Mol Biol Cell,* **19,** 3212-3220.

Jamil, S., Sobouti, R., Hojabrpour, P., Raj, M., Kast, J. & Duronio, V. (2005) A proteolytic fragment of Mcl-1 exhibits nuclear localization and regulates cell growth by interaction with Cdk1. *Biochem J,* **387,** 659-667.

Jayappa, K.D., Portell, C.A., Gordon, V.L., Capaldo, B.J., Bekiranov, S., Axelrod, M.J., Brett, L.K., Wulfkuhle, J.D., Gallagher, R.I., Petricoin, E.F., Bender, T.P., Williams, M.E. & Weber, M.J. (2017) Microenvironmental agonists generate de novo phenotypic resistance to combined ibrutinib plus venetoclax in CLL and MCL. *Blood Adv,* **1,** 933-946.

Jenson, J.M., Ryan, J.A., Grant, R.A., Letai, A. & Keating, A.E. (2017) Epistatic mutations in PUMA BH3 drive an alternate binding mode to potently and selectively inhibit anti-apoptotic Bfl-1. *Elife,* **6**.

Jones, J., Choi, M.Y., Mato, A.R., Furman, R.R., Davids, M.S., Heffner, L.T., Cheson, B.D., Lamanna, N., Barr, P.M., Eradat, H., Halwani, A., Chyla, B., Zhu, M., Verdugo, M., Humerickhouse, R.A., Potluri, J., Wierda, W.G. & Coutre, S.E. (2016) Venetoclax (VEN) Monotherapy for Patients with Chronic Lymphocytic Leukemia (CLL) Who Relapsed after or Were Refractory to Ibrutinib or Idelalisib. *Blood,* **128,** 637-637.

Josefsson, E.C., James, C., Henley, K.J., Debrincat, M.A., Rogers, K.L., Dowling, M.R., White, M.J., Kruse, E.A., Lane, R.M., Ellis, S., Nurden, P., Mason, K.D., O'Reilly, L.A., Roberts, A.W., Metcalf, D., Huang, D.C. & Kile, B.T. (2011) Megakaryocytes possess a functional intrinsic apoptosis pathway that must be restrained to survive and produce platelets. *J Exp Med,* **208,** 2017-2031.

Juo, P., Kuo, C.J., Yuan, J. & Blenis, J. (1998) Essential requirement for caspase-8/FLICE in the initiation of the Fas-induced apoptotic cascade. *Curr Biol,* **8,** 1001-1008.

Kale, J., Osterlund, E.J. & Andrews, D.W. (2018) BCL-2 family proteins: changing partners in the dance towards death. *Cell Death Differ,* **25,** 65-80.

Karjalainen, R., Pemovska, T., Popa, M., Liu, M., Javarappa, K.K., Majumder, M.M., Yadav, B., Tamborero, D., Tang, J., Bychkov, D., Kontro, M., Parsons, A., Suvela, M., Mayoral Safont, M., Porkka, K., Aittokallio, T., Kallioniemi, O., McCormack, E., Gjertsen, B.T., Wennerberg, K., Knowles, J. & Heckman, C.A. (2017) JAK1/2 and BCL2 inhibitors synergize to counteract bone marrow stromal cell-induced protection of AML. *Blood,* **130,** 789-802.

Kawane, K., Fukuyama, H., Yoshida, H., Nagase, H., Ohsawa, Y., Uchiyama, Y., Okada, K., Iida, T. & Nagata, S. (2003) Impaired thymic development in mouse embryos deficient in apoptotic DNA degradation. *Nat Immunol,* **4,** 138-144.

Kawatani, M., Uchi, M., Simizu, S., Osada, H. & Imoto, M. (2003) Transmembrane domain of Bcl-2 is required for inhibition of ceramide synthesis, but not cytochrome c release in the pathway of inostamycin-induced apoptosis. *Exp Cell Res,* **286,** 57-66.

Kerr, J.F., Wyllie, A.H. & Currie, A.R. (1972) Apoptosis: a basic biological phenomenon with wide-ranging implications in tissue kinetics. *Br J Cancer,* **26,** 239-257.

Kim, H., Rafiuddin-Shah, M., Tu, H.C., Jeffers, J.R., Zambetti, G.P., Hsieh, J.J. & Cheng, E.H. (2006) Hierarchical regulation of mitochondrion-dependent apoptosis by BCL-2 subfamilies. *Nat Cell Biol,* **8,** 1348-1358.

Kim, H., Tu, H.C., Ren, D., Takeuchi, O., Jeffers, J.R., Zambetti, G.P., Hsieh, J.J. & Cheng, E.H. (2009a) Stepwise activation of BAX and BAK by tBID, BIM, and PUMA initiates mitochondrial apoptosis. *Mol Cell,* **36,** 487-499.

Kim, J.H., Sim, S.H., Ha, H.J., Ko, J.J., Lee, K. & Bae, J. (2009b) MCL-1ES, a novel variant of MCL-1, associates with MCL-1L and induces mitochondrial cell death. *FEBS Lett,* **583,** 2758-2764.

Kipps, T.J., Eradat, H., Grosicki, S., Catalano, J., Cosolo, W., Dyagil, I.S., Yalamanchili, S., Chai, A., Sahasranaman, S., Punnoose, E., Hurst, D. & Pylypenko, H. (2015) A phase 2 study of the BH3 mimetic BCL2 inhibitor navitoclax (ABT-263) with or without rituximab, in previously untreated B-cell chronic lymphocytic leukemia. *Leuk Lymphoma,* **56,** 2826-2833.

Kipps, T.J., Swinnen, L.J., Wierda, W.G., Jones, J.A., Coutre, S.E., Smith, M.R., Yang, J., Cui, Y., Busman, T., Enschede, S. & Humerickhouse, R. (2011) Navitoclax (ABT-263) Plus Fludarabine/Cyclophosphamide/Rituximab (FCR) or Bendamustine/Rituximab (BR): A Phase 1 Study in Patients with Relapsed/Refractory Chronic Lymphocytic Leukemia (CLL). *Blood,* **118,** 3904-3904.

Kitada, S., Leone, M., Sareth, S., Zhai, D., Reed, J.C. & Pellecchia, M. (2003) Discovery, characterization, and structure-activity relationships studies of proapoptotic polyphenols targeting B-cell lymphocyte/leukemia-2 proteins. *J Med Chem,* **46,** 4259-4264.

Klanova, M., Andera, L., Brazina, J., Svadlenka, J., Benesova, S., Soukup, J., Prukova, D., Vejmelkova, D., Jaksa, R., Helman, K., Vockova, P., Lateckova, L., Molinsky, J., Maswabi, B.C., Alam, M., Kodet, R., Pytlik, R., Trneny, M. & Klener, P. (2016) Targeting of BCL2 Family Proteins with ABT-199 and Homoharringtonine Reveals BCL2- and MCL1-Dependent Subgroups of Diffuse Large B-Cell Lymphoma. *Clin Cancer Res,* **22,** 1138-1149.

Knittel, G., Liedgens, P., Korovkina, D., Pallasch, C.P. & Reinhardt, H.C. (2016) Rewired NFkappaB signaling as a potentially actionable feature of activated B-cell-like diffuse large B-cell lymphoma. *Eur J Haematol,* **97,** 499-510.

Ko, J.K., Lee, M.J., Cho, S.H., Cho, J.A., Lee, B.Y., Koh, J.S., Lee, S.S., Shim, Y.H. & Kim, C.W. (2003) Bfl-1S, a novel alternative splice variant of Bfl-1, localizes in the nucleus via its C-terminus and prevents cell death. *Oncogene,* **22,** 2457-2465.

Konopleva, M., Contractor, R., Tsao, T., Samudio, I., Ruvolo, P.P., Kitada, S., Deng, X., Zhai, D., Shi, Y.X., Sneed, T., Verhaegen, M., Soengas, M., Ruvolo, V.R., McQueen, T., Schober, W.D., Watt, J.C., Jiffar, T., Ling, X., Marini, F.C., Harris, D., Dietrich, M., Estrov, Z., McCubrey, J., May, W.S., Reed, J.C. & Andreeff, M. (2006) Mechanisms of apoptosis sensitivity and resistance to the BH3 mimetic ABT-737 in acute myeloid leukemia. *Cancer Cell,* **10,** 375-388.

Korsmeyer, S.J., Wei, M.C., Saito, M., Weiler, S., Oh, K.J. & Schlesinger, P.H. (2000) Pro-apoptotic cascade activates BID, which oligomerizes BAK or BAX into pores that result in the release of cytochrome c. *Cell Death Differ,* **7,** 1166-1173.

Kotschy, A., Szlavik, Z., Murray, J., Davidson, J., Maragno, A.L., Le Toumelin-Braizat, G., Chanrion, M., Kelly, G.L., Gong, J.N., Moujalled, D.M., Bruno, A., Csekei, M., Paczal, A., Szabo, Z.B., Sipos, S., Radics, G., Proszenyak, A., Balint, B., Ondi, L., Blasko, G., Robertson, A., Surgenor, A., Dokurno, P., Chen, I., Matassova, N., Smith, J., Pedder, C., Graham, C., Studeny, A., Lysiak-Auvity, G., Girard, A.M., Grave, F., Segal, D., Riffkin, C.D., Pomilio, G., Galbraith, L.C., Aubrey, B.J., Brennan, M.S., Herold, M.J., Chang, C., Guasconi, G., Cauquil, N., Melchiore, F., Guigal-Stephan, N., Lockhart, B., Colland, F., Hickman, J.A., Roberts, A.W., Huang, D.C., Wei, A.H., Strasser, A., Lessene, G. & Geneste, O. (2016) The MCL1 inhibitor S63845 is tolerable and effective in diverse cancer models. *Nature,* **538,** 477-482.

Kozaki, R., Vogler, M., Walter, H.S., Jayne, S., Dinsdale, D., Siebert, R., Dyer, M.J.S. & Yoshizawa, T. (2018) Responses to the Selective Bruton's Tyrosine Kinase (BTK) Inhibitor Tirabrutinib (ONO/GS-4059) in Diffuse Large B-cell Lymphoma Cell Lines. *Cancers (Basel),* **10**.

Kozopas, K.M., Yang, T., Buchan, H.L., Zhou, P. & Craig, R.W. (1993) MCL1, a gene expressed in programmed myeloid cell differentiation, has sequence similarity to BCL2. *Proc Natl Acad Sci U S A,* **90,** 3516-3520.

Kraus, M., Alimzhanov, M.B., Rajewsky, N. & Rajewsky, K. (2004) Survival of resting mature B lymphocytes depends on BCR signaling via the Igalpha/beta heterodimer. *Cell,* **117,** 787-800.

Kumar, S., Kaufman, J.L., Gasparetto, C., Mikhael, J., Vij, R., Pegourie, B., Benboubker, L., Facon, T., Amiot, M., Moreau, P., Punnoose, E.A., Alzate, S., Dunbar, M., Xu, T., Agarwal, S.K., Enschede, S.H., Leverson, J.D., Ross, J.A., Maciag, P.C., Verdugo, M. & Touzeau, C. (2017) Efficacy of venetoclax as targeted therapy for relapsed/refractory t(11;14) multiple myeloma. *Blood,* **130,** 2401-2409.

Kuo, H.P., Ezell, S.A., Schweighofer, K.J., Cheung, L.W.K., Hsieh, S., Apatira, M., Sirisawad, M., Eckert, K., Hsu, S.J., Chen, C.T., Beaupre, D.M., Versele, M. &

Chang, B.Y. (2017) Combination of Ibrutinib and ABT-199 in Diffuse Large B-Cell Lymphoma and Follicular Lymphoma. *Mol Cancer Ther,* **16,** 1246-1256.

Kuppers, R. (2005) Mechanisms of B-cell lymphoma pathogenesis. *Nat Rev Cancer,* **5,** 251-262.

Kuwana, T., Bouchier-Hayes, L., Chipuk, J.E., Bonzon, C., Sullivan, B.A., Green, D.R. & Newmeyer, D.D. (2005) BH3 domains of BH3-only proteins differentially regulate Bax-mediated mitochondrial membrane permeabilization both directly and indirectly. *Mol Cell,* **17,** 525-535.

Lam, K.P., Kuhn, R. & Rajewsky, K. (1997) In vivo ablation of surface immunoglobulin on mature B cells by inducible gene targeting results in rapid cell death. *Cell,* **90,** 1073-1083.

Lam, L.T., Davis, R.E., Pierce, J., Hepperle, M., Xu, Y., Hottelet, M., Nong, Y., Wen, D., Adams, J., Dang, L. & Staudt, L.M. (2005) Small molecule inhibitors of IkappaB kinase are selectively toxic for subgroups of diffuse large B-cell lymphoma defined by gene expression profiling. *Clin Cancer Res,* **11,** 28-40.

Lam, L.T., Wright, G., Davis, R.E., Lenz, G., Farinha, P., Dang, L., Chan, J.W., Rosenwald, A., Gascoyne, R.D. & Staudt, L.M. (2008) Cooperative signaling through the signal transducer and activator of transcription 3 and nuclear factor-{kappa}B pathways in subtypes of diffuse large B-cell lymphoma. *Blood,* **111,** 3701-3713.

Lamy, L., Ngo, V.N., Emre, N.C., Shaffer, A.L., 3rd, Yang, Y., Tian, E., Nair, V., Kruhlak, M.J., Zingone, A., Landgren, O. & Staudt, L.M. (2013) Control of autophagic cell death by caspase-10 in multiple myeloma. *Cancer Cell,* **23,** 435-449.

Le Pen, J., Maillet, L., Sarosiek, K., Vuillier, C., Gautier, F., Montessuit, S., Martinou, J.C., Letai, A., Braun, F. & Juin, P.P. (2016) Constitutive p53 heightens mitochondrial apoptotic priming and favors cell death induction by BH3 mimetic inhibitors of BCL-xL. *Cell Death Dis,* **7,** e2083.

Leber, B., Lin, J. & Andrews, D.W. (2007) Embedded together: the life and death consequences of interaction of the Bcl-2 family with membranes. *Apoptosis,* **12,** 897-911.

LeBien, T.W. & Tedder, T.F. (2008) B lymphocytes: how they develop and function. *Blood,* **112,** 1570-1580.

Lee, J.S., Tang, S.S., Ortiz, V., Vo, T.T. & Fruman, D.A. (2015) MCL-1-independent mechanisms of synergy between dual PI3K/mTOR and BCL-2 inhibition in diffuse large B cell lymphoma. *Oncotarget,* **6,** 35202-35217.

Lehmann, C., Friess, T., Birzele, F., Kiialainen, A. & Dangl, M. (2016) Superior anti-tumor activity of the MDM2 antagonist idasanutlin and the Bcl-2 inhibitor venetoclax in p53 wild-type acute myeloid leukemia models. *J Hematol Oncol,* **9,** 50.

Lenz, G., Wright, G.W., Emre, N.C., Kohlhammer, H., Dave, S.S., Davis, R.E., Carty, S., Lam, L.T., Shaffer, A.L., Xiao, W., Powell, J., Rosenwald, A., Ott, G., Muller-Hermelink, H.K., Gascoyne, R.D., Connors, J.M., Campo, E., Jaffe, E.S., Delabie, J., Smeland, E.B., Rimsza, L.M., Fisher, R.I., Weisenburger, D.D., Chan, W.C. & Staudt, L.M. (2008) Molecular subtypes of diffuse large B-cell lymphoma arise by distinct genetic pathways. *Proc Natl Acad Sci U S A,* **105,** 13520-13525.

Lessene, G., Czabotar, P.E. & Colman, P.M. (2008) BCL-2 family antagonists for cancer therapy. *Nat Rev Drug Discov,* **7,** 989-1000.

Lessene, G., Czabotar, P.E., Sleebs, B.E., Zobel, K., Lowes, K.N., Adams, J.M., Baell, J.B., Colman, P.M., Deshayes, K., Fairbrother, W.J., Flygare, J.A., Gibbons, P., Kersten, W.J., Kulasegaram, S., Moss, R.M., Parisot, J.P., Smith, B.J., Street, I.P., Yang, H., Huang, D.C. & Watson, K.G. (2013) Structure-guided design of a selective BCL-X(L) inhibitor. *Nat Chem Biol,* **9,** 390-397.

Letai, A., Bassik, M.C., Walensky, L.D., Sorcinelli, M.D., Weiler, S. & Korsmeyer, S.J. (2002) Distinct BH3 domains either sensitize or activate mitochondrial apoptosis, serving as prototype cancer therapeutics. *Cancer Cell,* **2,** 183-192.

Leverson, J.D. & Cojocari, D. (2018) Hematologic Tumor Cell Resistance to the BCL-2 Inhibitor Venetoclax: A Product of Its Microenvironment? *Front Oncol,* **8,** 458.

Leverson, J.D., Phillips, D.C., Mitten, M.J., Boghaert, E.R., Diaz, D., Tahir, S.K., Belmont, L.D., Nimmer, P., Xiao, Y., Ma, X.M., Lowes, K.N., Kovar, P., Chen, J., Jin, S., Smith, M., Xue, J., Zhang, H., Oleksijew, A., Magoc, T.J., Vaidya, K.S., Albert, D.H., Tarrant, J.M., La, N., Wang, L., Tao, Z.F., Wendt, M.D., Sampath, D., Rosenberg, S.H., Tse, C., Huang, D.C., Fairbrother, W.J., Elmore, S.W. & Souers, A.J. (2015a) Exploiting selective BCL-2 family inhibitors to dissect cell survival dependencies and define improved strategies for cancer therapy. *Sci Transl Med,* **7,** 279ra240.

Leverson, J.D., Zhang, H., Chen, J., Tahir, S.K., Phillips, D.C., Xue, J., Nimmer, P., Jin, S., Smith, M., Xiao, Y., Kovar, P., Tanaka, A., Bruncko, M., Sheppard, G.S., Wang, L., Gierke, S., Kategaya, L., Anderson, D.J., Wong, C., Eastham-Anderson, J., Ludlam, M.J., Sampath, D., Fairbrother, W.J., Wertz, I., Rosenberg, S.H., Tse, C., Elmore, S.W. & Souers, A.J. (2015b) Potent and selective small-molecule MCL-1 inhibitors demonstrate on-target cancer cell killing activity as single agents and in combination with ABT-263 (navitoclax). *Cell Death Dis,* **6,** e1590.

Li, F., Huang, Q., Chen, J., Peng, Y., Roop, D.R., Bedford, J.S. & Li, C.Y. (2010) Apoptotic cells activate the "phoenix rising" pathway to promote wound healing and tissue regeneration. *Sci Signal,* **3,** ra13.

Li, H., Alavian, K.N., Lazrove, E., Mehta, N., Jones, A., Zhang, P., Licznerski, P., Graham, M., Uo, T., Guo, J., Rahner, C., Duman, R.S., Morrison, R.S. & Jonas, E.A. (2013) A Bcl-xL-Drp1 complex regulates synaptic vesicle membrane dynamics during endocytosis. *Nat Cell Biol,* **15,** 773-785.

Li, L., Pongtornpipat, P., Tiutan, T., Kendrick, S.L., Park, S., Persky, D.O., Rimsza, L.M., Puvvada, S.D. & Schatz, J.H. (2015) Synergistic induction of apoptosis in high-risk DLBCL by BCL2 inhibition with ABT-199 combined with pharmacologic loss of MCL1. *Leukemia,* **29,** 1702-1712.

Li, Z., He, S. & Look, A.T. (2019) The MCL1-specific inhibitor S63845 acts synergistically with venetoclax/ABT-199 to induce apoptosis in T-cell acute lymphoblastic leukemia cells. *Leukemia,* **33,** 262-266.

Liang, X.H., Kleeman, L.K., Jiang, H.H., Gordon, G., Goldman, J.E., Berry, G., Herman, B. & Levine, B. (1998) Protection against fatal Sindbis virus encephalitis by beclin, a novel Bcl-2-interacting protein. *J Virol,* **72,** 8586-8596.

Lin, E.Y., Orlofsky, A., Berger, M.S. & Prystowsky, M.B. (1993) Characterization of A1, a novel hemopoietic-specific early-response gene with sequence similarity to bcl-2. *J Immunol,* **151,** 1979-1988.

Lin, K.H., Winter, P.S., Xie, A., Roth, C., Martz, C.A., Stein, E.M., Anderson, G.R., Tingley, J.P. & Wood, K.C. (2016) Targeting MCL-1/BCL-XL Forestalls the Acquisition of Resistance to ABT-199 in Acute Myeloid Leukemia. *Sci Rep,* **6,** 27696.

Lindsten, T., Ross, A.J., King, A., Zong, W.X., Rathmell, J.C., Shiels, H.A., Ulrich, E., Waymire, K.G., Mahar, P., Frauwirth, K., Chen, Y., Wei, M., Eng, V.M., Adelman, D.M., Simon, M.C., Ma, A., Golden, J.A., Evan, G., Korsmeyer, S.J., MacGregor, G.R. & Thompson, C.B. (2000) The combined functions of proapoptotic Bcl-2 family members bak and bax are essential for normal development of multiple tissues. *Mol Cell,* **6,** 1389-1399.

Liston, P., Roy, N., Tamai, K., Lefebvre, C., Baird, S., Cherton-Horvat, G., Farahani, R., McLean, M., Ikeda, J.E., MacKenzie, A. & Korneluk, R.G. (1996) Suppression of apoptosis in mammalian cells by NAIP and a related family of IAP genes. *Nature,* **379,** 349-353.

Little, A.J., Matthews, A., Oettinger, M., Roth, D.B. & Schatz, D.G. (2015) The Mechanism of V(D)J Recombination. 13-34.

Liu, X., Dai, S., Zhu, Y., Marrack, P. & Kappler, J.W. (2003) The structure of a Bcl-xL/Bim fragment complex: implications for Bim function. *Immunity,* **19,** 341-352.

Liu, X., Kim, C.N., Yang, J., Jemmerson, R. & Wang, X. (1996) Induction of apoptotic program in cell-free extracts: requirement for dATP and cytochrome c. *Cell,* **86,** 147-157.

Liu, X., Li, F., Huang, Q., Zhang, Z., Zhou, L., Deng, Y., Zhou, M., Fleenor, D.E., Wang, H., Kastan, M.B. & Li, C.Y. (2017) Self-inflicted DNA double-strand breaks sustain tumorigenicity and stemness of cancer cells. *Cell Res,* **27,** 764-783.

Liu, Y., Mondello, P., Erazo, T., Tannan, N.B., Asgari, Z., de Stanchina, E., Nanjangud, G., Seshan, V.E., Wang, S., Wendel, H.G. & Younes, A. (2018) NOXA genetic

amplification or pharmacologic induction primes lymphoma cells to BCL2 inhibitor-induced cell death. *Proc Natl Acad Sci U S A,* **115,** 12034-12039.

Llambi, F., Moldoveanu, T., Tait, S.W., Bouchier-Hayes, L., Temirov, J., McCormick, L.L., Dillon, C.P. & Green, D.R. (2011) A unified model of mammalian BCL-2 protein family interactions at the mitochondria. *Mol Cell,* **44,** 517-531.

Lovell, J.F., Billen, L.P., Bindner, S., Shamas-Din, A., Fradin, C., Leber, B. & Andrews, D.W. (2008) Membrane binding by tBid initiates an ordered series of events culminating in membrane permeabilization by Bax. *Cell,* **135,** 1074-1084.

Luo, X., Budihardjo, I., Zou, H., Slaughter, C. & Wang, X. (1998) Bid, a Bcl2 interacting protein, mediates cytochrome c release from mitochondria in response to activation of cell surface death receptors. *Cell,* **94,** 481-490.

Maiuri, M.C., Criollo, A., Tasdemir, E., Vicencio, J.M., Tajeddine, N., Hickman, J.A., Geneste, O. & Kroemer, G. (2007) BH3-only proteins and BH3 mimetics induce autophagy by competitively disrupting the interaction between Beclin 1 and Bcl-2/Bcl-X(L). *Autophagy,* **3,** 374-376.

Mallick, D.J., Soderquist, R.S., Bates, D. & Eastman, A. (2019) Confounding off-target effects of BH3 mimetics at commonly used concentrations: MIM1, UMI-77, and A-1210477. *Cell death & disease,* **10,** 185-185.

Martinou, J.C. & Youle, R.J. (2011) Mitochondria in apoptosis: Bcl-2 family members and mitochondrial dynamics. *Dev Cell,* **21,** 92-101.

Masir, N., Campbell, L.J., Jones, M. & Mason, D.Y. (2010) Pseudonegative BCL2 protein expression in a t(14;18) translocation positive lymphoma cell line: a need for an alternative BCL2 antibody. *Pathology,* **42,** 212-216.

Massaad, C.A., Portier, B.P. & Taglialatela, G. (2004) Inhibition of transcription factor activity by nuclear compartment-associated Bcl-2. *J Biol Chem,* **279,** 54470-54478.

Mathews Griner, L.A., Guha, R., Shinn, P., Young, R.M., Keller, J.M., Liu, D., Goldlust, I.S., Yasgar, A., McKnight, C., Boxer, M.B., Duveau, D.Y., Jiang, J.K., Michael, S., Mierzwa, T., Huang, W., Walsh, M.J., Mott, B.T., Patel, P., Leister, W., Maloney, D.J., Leclair, C.A., Rai, G., Jadhav, A., Peyser, B.D., Austin, C.P., Martin, S.E., Simeonov, A., Ferrer, M., Staudt, L.M. & Thomas, C.J. (2014) High-throughput combinatorial screening identifies drugs that cooperate with ibrutinib to kill activated B-cell-like diffuse large B-cell lymphoma cells. *Proc Natl Acad Sci U S A,* **111,** 2349-2354.

Mato, A.R., Roeker, L.E., Eyre, T.A., Nabhan, C., Lamanna, N., Hill, B.T., Brander, D.M., Barr, P.M., Lansigan, F., Cheson, B.D., Singavi, A.K., Yazdy, M.S., Shah, N.N., Allan, J.N., Bhavsar, E.B., Rhodes, J., Kennard, K., Schuster, S.J., Williams, A.M., Skarbnik, A.P., Goy, A.H., Goodfriend, J.M., Dorsey, C., Coombs, C.C., Tuncer, H., Ujjani, C.S., Jacobs, R., Winter, A.M., Pagel, J.M., Bailey, N., Schuh, A., Shadman,

M., Sitlinger, A., Weissbrot, H., Muralikrishnan, S., Zelenetz, A., Kirkwood, A.A. & Fox, C.P. (2019) A retrospective comparison of venetoclax alone or in combination with an anti-CD20 monoclonal antibody in R/R CLL. *Blood Adv,* **3,** 1568-1573.

Mattoo, A.R., Pandita, R.K., Chakraborty, S., Charaka, V., Mujoo, K., Hunt, C.R. & Pandita, T.K. (2017) MCL-1 Depletion Impairs DNA Double-Strand Break Repair and Reinitiation of Stalled DNA Replication Forks. *Mol Cell Biol,* **37**.

Mazel, S., Burtrum, D. & Petrie, H.T. (1996) Regulation of cell division cycle progression by bcl-2 expression: a potential mechanism for inhibition of programmed cell death. *J Exp Med,* **183,** 2219-2226.

McDonnell, J.M., Fushman, D., Milliman, C.L., Korsmeyer, S.J. & Cowburn, D. (1999) Solution structure of the proapoptotic molecule BID: a structural basis for apoptotic agonists and antagonists. *Cell,* **96,** 625-634.

Miao, E.A., Leaf, I.A., Treuting, P.M., Mao, D.P., Dors, M., Sarkar, A., Warren, S.E., Wewers, M.D. & Aderem, A. (2010) Caspase-1-induced pyroptosis is an innate immune effector mechanism against intracellular bacteria. *Nat Immunol,* **11,** 1136-1142.

Miramar, M.D., Costantini, P., Ravagnan, L., Saraiva, L.M., Haouzi, D., Brothers, G., Penninger, J.M., Peleato, M.L., Kroemer, G. & Susin, S.A. (2001) NADH oxidase activity of mitochondrial apoptosis-inducing factor. *J Biol Chem,* **276,** 16391-16398.

Moldoveanu, T., Grace, C.R., Llambi, F., Nourse, A., Fitzgerald, P., Gehring, K., Kriwacki, R.W. & Green, D.R. (2013) BID-induced structural changes in BAK promote apoptosis. *Nat Struct Mol Biol,* **20,** 589-597.

Moldoveanu, T., Liu, Q., Tocilj, A., Watson, M., Shore, G. & Gehring, K. (2006) The X-ray structure of a BAK homodimer reveals an inhibitory zinc binding site. *Mol Cell,* **24,** 677-688.

Montero, J., Sarosiek, K.A., DeAngelo, J.D., Maertens, O., Ryan, J., Ercan, D., Piao, H., Horowitz, N.S., Berkowitz, R.S., Matulonis, U., Janne, P.A., Amrein, P.C., Cichowski, K., Drapkin, R. & Letai, A. (2015) Drug-induced death signaling strategy rapidly predicts cancer response to chemotherapy. *Cell,* **160,** 977-989.

Motoyama, N., Wang, F., Roth, K.A., Sawa, H., Nakayama, K., Nakayama, K., Negishi, I., Senju, S., Zhang, Q., Fujii, S. & et al. (1995) Massive cell death of immature hematopoietic cells and neurons in Bcl-x-deficient mice. *Science,* **267,** 1506-1510.

Mott, J.L., Kobayashi, S., Bronk, S.F. & Gores, G.J. (2007) mir-29 regulates Mcl-1 protein expression and apoptosis. *Oncogene,* **26,** 6133-6140.

Mou, Y., Wang, J., Wu, J., He, D., Zhang, C., Duan, C. & Li, B. (2019) Ferroptosis, a new form of cell death: opportunities and challenges in cancer. *J Hematol Oncol,* **12,** 34.

Moujalled, D.M., Pomilio, G., Ghiurau, C., Ivey, A., Salmon, J., Rijal, S., Macraild, S., Zhang, L., Teh, T.C., Tiong, I.S., Lan, P., Chanrion, M., Claperon, A., Rocchetti, F., Zichi, A., Kraus-Berthier, L., Wang, Y., Halilovic, E., Morris, E., Colland, F., Segal, D., Huang, D., Roberts, A.W., Maragno, A.L., Lessene, G., Geneste, O. & Wei, A.H. (2019) Combining BH3-mimetics to target both BCL-2 and MCL1 has potent activity in pre-clinical models of acute myeloid leukemia. *Leukemia,* **33,** 905-917.

Muchmore, S.W., Sattler, M., Liang, H., Meadows, R.P., Harlan, J.E., Yoon, H.S., Nettesheim, D., Chang, B.S., Thompson, C.B., Wong, S.L., Ng, S.L. & Fesik, S.W. (1996) X-ray and NMR structure of human Bcl-xL, an inhibitor of programmed cell death. *Nature,* **381,** 335-341.

Muramatsu, M., Kinoshita, K., Fagarasan, S., Yamada, S., Shinkai, Y. & Honjo, T. (2000) Class switch recombination and hypermutation require activation-induced cytidine deaminase (AID), a potential RNA editing enzyme. *Cell,* **102,** 553-563.

Nagata, S. (2000) Apoptotic DNA fragmentation. *Exp Cell Res,* **256,** 12-18.

Naik, E., Michalak, E.M., Villunger, A., Adams, J.M. & Strasser, A. (2007) Ultraviolet radiation triggers apoptosis of fibroblasts and skin keratinocytes mainly via the BH3-only protein Noxa. *J Cell Biol,* **176,** 415-424.

Nemati, F., de Montrion, C., Lang, G., Kraus-Berthier, L., Carita, G., Sastre-Garau, X., Berniard, A., Vallerand, D., Geneste, O., de Plater, L., Pierre, A., Lockhart, B., Desjardins, L., Piperno-Neumann, S., Depil, S. & Decaudin, D. (2014) Targeting Bcl-2/Bcl-XL induces antitumor activity in uveal melanoma patient-derived xenografts. *PLoS One,* **9,** e80836.

Ngo, V.N., Davis, R.E., Lamy, L., Yu, X., Zhao, H., Lenz, G., Lam, L.T., Dave, S., Yang, L., Powell, J. & Staudt, L.M. (2006) A loss-of-function RNA interference screen for molecular targets in cancer. *Nature,* **441,** 106-110.

Nguyen, M., Marcellus, R.C., Roulston, A., Watson, M., Serfass, L., Murthy Madiraju, S.R., Goulet, D., Viallet, J., Belec, L., Billot, X., Acoca, S., Purisima, E., Wiegmans, A., Cluse, L., Johnstone, R.W., Beauparlant, P. & Shore, G.C. (2007) Small molecule obatoclax (GX15-070) antagonizes MCL-1 and overcomes MCL-1-mediated resistance to apoptosis. *Proc Natl Acad Sci U S A,* **104,** 19512-19517.

Oberstein, A., Jeffrey, P.D. & Shi, Y. (2007) Crystal structure of the Bcl-XL-Beclin 1 peptide complex: Beclin 1 is a novel BH3-only protein. *J Biol Chem,* **282,** 13123-13132.

Oltersdorf, T., Elmore, S.W., Shoemaker, A.R., Armstrong, R.C., Augeri, D.J., Belli, B.A., Bruncko, M., Deckwerth, T.L., Dinges, J., Hajduk, P.J., Joseph, M.K., Kitada, S., Korsmeyer, S.J., Kunzer, A.R., Letai, A., Li, C., Mitten, M.J., Nettesheim, D.G., Ng,

S., Nimmer, P.M., O'Connor, J.M., Oleksijew, A., Petros, A.M., Reed, J.C., Shen, W., Tahir, S.K., Thompson, C.B., Tomaselli, K.J., Wang, B., Wendt, M.D., Zhang, H., Fesik, S.W. & Rosenberg, S.H. (2005) An inhibitor of Bcl-2 family proteins induces regression of solid tumours. *Nature,* **435,** 677-681.

Oltvai, Z.N., Milliman, C.L. & Korsmeyer, S.J. (1993) Bcl-2 heterodimerizes in vivo with a conserved homolog, Bax, that accelerates programmed cell death. *Cell,* **74,** 609-619.

Opferman, J.T., Iwasaki, H., Ong, C.C., Suh, H., Mizuno, S., Akashi, K. & Korsmeyer, S.J. (2005) Obligate role of anti-apoptotic MCL-1 in the survival of hematopoietic stem cells. *Science,* **307,** 1101-1104.

Opferman, J.T., Letai, A., Beard, C., Sorcinelli, M.D., Ong, C.C. & Korsmeyer, S.J. (2003) Development and maintenance of B and T lymphocytes requires antiapoptotic MCL-1. *Nature,* **426,** 671-676.

Pan, R., Ruvolo, V., Mu, H., Leverson, J.D., Nichols, G., Reed, J.C., Konopleva, M. & Andreeff, M. (2017) Synthetic Lethality of Combined Bcl-2 Inhibition and p53 Activation in AML: Mechanisms and Superior Antileukemic Efficacy. *Cancer Cell,* **32,** 748-760 e746.

Park, D., Magis, A.T., Li, R., Owonikoko, T.K., Sica, G.L., Sun, S.Y., Ramalingam, S.S., Khuri, F.R., Curran, W.J. & Deng, X. (2013) Novel small-molecule inhibitors of Bcl-XL to treat lung cancer. *Cancer Res,* **73,** 5485-5496.

Pasqualucci, L., Migliazza, A., Fracchiolla, N., William, C., Neri, A., Baldini, L., Chaganti, R.S., Klein, U., Kuppers, R., Rajewsky, K. & Dalla-Favera, R. (1998) BCL-6 mutations in normal germinal center B cells: evidence of somatic hypermutation acting outside Ig loci. *Proc Natl Acad Sci U S A,* **95,** 11816-11821.

Pasqualucci, L., Neumeister, P., Goossens, T., Nanjangud, G., Chaganti, R.S., Kuppers, R. & Dalla-Favera, R. (2001) Hypermutation of multiple proto-oncogenes in B-cell diffuse large-cell lymphomas. *Nature,* **412,** 341-346.

Patel, V.M., Balakrishnan, K., Douglas, M., Tibbitts, T., Xu, E.Y., Kutok, J.L., Ayers, M., Sarkar, A., Guerrieri, R., Wierda, W.G., O'Brien, S., Jain, N., Stern, H.M. & Gandhi, V. (2017) Duvelisib treatment is associated with altered expression of apoptotic regulators that helps in sensitization of chronic lymphocytic leukemia cells to venetoclax (ABT-199). *Leukemia,* **31,** 1872-1881.

Pattingre, S., Tassa, A., Qu, X., Garuti, R., Liang, X.H., Mizushima, N., Packer, M., Schneider, M.D. & Levine, B. (2005) Bcl-2 antiapoptotic proteins inhibit Beclin 1-dependent autophagy. *Cell,* **122,** 927-939.

Peng, R., Tong, J.S., Li, H., Yue, B., Zou, F., Yu, J. & Zhang, L. (2013) Targeting Bax interaction sites reveals that only homo-oligomerization sites are essential for its activation. *Cell Death Differ,* **20,** 744-754.

Perri, F., Pisconti, S. & Della Vittoria Scarpati, G. (2016) P53 mutations and cancer: a tight linkage. *Ann Transl Med,* **4,** 522.

Petros, A.M., Medek, A., Nettesheim, D.G., Kim, D.H., Yoon, H.S., Swift, K., Matayoshi, E.D., Oltersdorf, T. & Fesik, S.W. (2001) Solution structure of the antiapoptotic protein bcl-2. *Proc Natl Acad Sci U S A,* **98,** 3012-3017.

Pfreundschuh, M., Trumper, L., Osterborg, A., Pettengell, R., Trneny, M., Imrie, K., Ma, D., Gill, D., Walewski, J., Zinzani, P.L., Stahel, R., Kvaloy, S., Shpilberg, O., Jaeger, U., Hansen, M., Lehtinen, T., Lopez-Guillermo, A., Corrado, C., Scheliga, A., Milpied, N., Mendila, M., Rashford, M., Kuhnt, E., Loeffler, M. & MabThera International Trial, G. (2006) CHOP-like chemotherapy plus rituximab versus CHOP-like chemotherapy alone in young patients with good-prognosis diffuse large-B-cell lymphoma: a randomised controlled trial by the MabThera International Trial (MInT) Group. *Lancet Oncol,* **7,** 379-391.

Pham, L.V., Huang, S., Zhang, H., Zhang, J., Bell, T., Zhou, S., Pogue, E., Ding, Z., Lam, L., Westin, J., Davis, R.E., Young, K.H., Medeiros, L.J., Ford, R.J., Nomie, K., Zhang, L. & Wang, M. (2018) Strategic Therapeutic Targeting to Overcome Venetoclax Resistance in Aggressive B-cell Lymphomas. *Clin Cancer Res,* **24,** 3967-3980.

Phillips, D.C., Xiao, Y., Lam, L.T., Litvinovich, E., Roberts-Rapp, L., Souers, A.J. & Leverson, J.D. (2015) Loss in MCL-1 function sensitizes non-Hodgkin's lymphoma cell lines to the BCL-2-selective inhibitor venetoclax (ABT-199). *Blood Cancer J,* **5,** e368.

Pieper, K., Grimbacher, B. & Eibel, H. (2013) B-cell biology and development. *J Allergy Clin Immunol,* **131,** 959-971.

Plotz, M., Gillissen, B., Hossini, A.M., Daniel, P.T. & Eberle, J. (2012) Disruption of the VDAC2-Bak interaction by Bcl-x(S) mediates efficient induction of apoptosis in melanoma cells. *Cell Death Differ,* **19,** 1928-1938.

Promega (2015) CellTiter-Glo® Luminescent

Cell Viability Assay. p. 4. Promega Corporation, Madison, USA.

Proskuryakov, S.Y., Konoplyannikov, A.G. & Gabai, V.L. (2003) Necrosis: a specific form of programmed cell death? *Exp Cell Res,* **283,** 1-16.

Prukova, D., Andera, L., Nahacka, Z., Karolova, J., Svaton, M., Klanova, M., Havranek, O., Soukup, J., Svobodova, K., Zemanova, Z., Tuskova, D., Pokorna, E., Helman, K., Forsterova, K., Pacheco-Blanco, M., Vockova, P., Berkova, A., Fronkova, E., Trneny, M. & Klener, P. (2019) Cotargeting of BCL2 with Venetoclax and MCL1 with S63845 Is Synthetically Lethal In Vivo in Relapsed Mantle Cell Lymphoma. *Clin Cancer Res,* **25,** 4455-4465.

Punnoose, E.A., Leverson, J.D., Peale, F., Boghaert, E.R., Belmont, L.D., Tan, N., Young, A., Mitten, M., Ingalla, E., Darbonne, W.C., Oleksijew, A., Tapang, P., Yue, P., Oeh, J., Lee, L., Maiga, S., Fairbrother, W.J., Amiot, M., Souers, A.J. & Sampath, D.

(2016) Expression Profile of BCL-2, BCL-XL, and MCL-1 Predicts Pharmacological Response to the BCL-2 Selective Antagonist Venetoclax in Multiple Myeloma Models. *Mol Cancer Ther,* **15,** 1132-1144.

Quentmeier, H., Drexler, H.G., Hauer, V., MacLeod, R.A.F., Pommerenke, C., Uphoff, C.C., Zaborski, M., Berglund, M., Enblad, G. & Amini, R.-M. (2016) Diffuse Large B Cell Lymphoma Cell Line U-2946: Model for MCL1 Inhibitor Testing. *PLoS One,* **11,** e0167599.

Rahmani, M., Nkwocha, J., Hawkins, E., Pei, X., Parker, R.E., Kmieciak, M., Leverson, J.D., Sampath, D., Ferreira-Gonzalez, A. & Grant, S. (2018) Cotargeting BCL-2 and PI3K Induces BAX-Dependent Mitochondrial Apoptosis in AML Cells. *Cancer Res,* **78,** 3075-3086.

Raut, L.S. & Chakrabarti, P.P. (2014) Management of relapsed-refractory diffuse large B cell lymphoma. *South Asian J Cancer,* **3,** 66-70.

Reed, J.C., Cuddy, M., Slabiak, T., Croce, C.M. & Nowell, P.C. (1988) Oncogenic potential of bcl-2 demonstrated by gene transfer. *Nature,* **336,** 259-261.

Reed, J.C., Zha, H., Aime-Sempe, C., Takayama, S. & Wang, H.G. (1996) Structure-function analysis of Bcl-2 family proteins. Regulators of programmed cell death. *Adv Exp Med Biol,* **406,** 99-112.

Ricci, J.E., Gottlieb, R.A. & Green, D.R. (2003) Caspase-mediated loss of mitochondrial function and generation of reactive oxygen species during apoptosis. *J Cell Biol,* **160,** 65-75.

Richard, D.J., Lena, R., Bannister, T., Blake, N., Pierceall, W.E., Carlson, N.E., Keller, C.E., Koenig, M., He, Y., Minond, D., Mishra, J., Cameron, M., Spicer, T., Hodder, P. & Cardone, M.H. (2013) Hydroxyquinoline-derived compounds and analoguing of selective Mcl-1 inhibitors using a functional biomarker. *Bioorg Med Chem,* **21,** 6642-6649.

Richter-Larrea, J.A., Robles, E.F., Fresquet, V., Beltran, E., Rullan, A.J., Agirre, X., Calasanz, M.J., Panizo, C., Richter, J.A., Hernandez, J.M., Roman-Gomez, J., Prosper, F. & Martinez-Climent, J.A. (2010) Reversion of epigenetically mediated BIM silencing overcomes chemoresistance in Burkitt lymphoma. *Blood,* **116,** 2531-2542.

Rinkenberger, J.L., Horning, S., Klocke, B., Roth, K. & Korsmeyer, S.J. (2000) Mcl-1 deficiency results in peri-implantation embryonic lethality. *Genes Dev,* **14,** 23-27.

Roberts, A.W., Advani, R.H., Kahl, B.S., Persky, D., Sweetenham, J.W., Carney, D.A., Yang, J., Busman, T.B., Enschede, S.H., Humerickhouse, R.A. & Seymour, J.F. (2015) Phase 1 study of the safety, pharmacokinetics, and antitumour activity of the BCL2 inhibitor navitoclax in combination with rituximab in patients with

relapsed or refractory CD20+ lymphoid malignancies. *Br J Haematol,* **170,** 669-678.

Roberts, A.W., Davids, M.S., Pagel, J.M., Kahl, B.S., Puvvada, S.D., Gerecitano, J.F., Kipps, T.J., Anderson, M.A., Brown, J.R., Gressick, L., Wong, S., Dunbar, M., Zhu, M., Desai, M.B., Cerri, E., Heitner Enschede, S., Humerickhouse, R.A., Wierda, W.G. & Seymour, J.F. (2016) Targeting BCL2 with Venetoclax in Relapsed Chronic Lymphocytic Leukemia. *N Engl J Med,* **374,** 311-322.

Roberts, A.W., Seymour, J.F., Brown, J.R., Wierda, W.G., Kipps, T.J., Khaw, S.L., Carney, D.A., He, S.Z., Huang, D.C., Xiong, H., Cui, Y., Busman, T.A., McKeegan, E.M., Krivoshik, A.P., Enschede, S.H. & Humerickhouse, R. (2012) Substantial susceptibility of chronic lymphocytic leukemia to BCL2 inhibition: results of a phase I study of navitoclax in patients with relapsed or refractory disease. *J Clin Oncol,* **30,** 488-496.

Roberts, A.W., Stilgenbauer, S., Seymour, J.F. & Huang, D.C.S. (2017) Venetoclax in Patients with Previously Treated Chronic Lymphocytic Leukemia. *Clin Cancer Res,* **23,** 4527-4533.

Roumane, A., Berthenet, K., El Fassi, C. & Ichim, G. (2018) Caspase-independent cell death does not elicit a proliferative response in melanoma cancer cells. *BMC Cell Biol,* **19,** 11.

Roy, N., Deveraux, Q.L., Takahashi, R., Salvesen, G.S. & Reed, J.C. (1997) The c-IAP-1 and c-IAP-2 proteins are direct inhibitors of specific caspases. *EMBO J,* **16,** 6914-6925.

Rudel, T. & Bokoch, G.M. (1997) Membrane and morphological changes in apoptotic cells regulated by caspase-mediated activation of PAK2. *Science,* **276,** 1571-1574.

Ryan, J. (2017) A guide to BH3 profiling. In: *BH3 profiling*, Vol. 2019. The Letai Lab, Dana-Farber Cancer Institute.

Ryan, J. & Letai, A. (2013) BH3 profiling in whole cells by fluorimeter or FACS. *Methods,* **61,** 156-164.

Ryoo, H.D., Gorenc, T. & Steller, H. (2004) Apoptotic cells can induce compensatory cell proliferation through the JNK and the Wingless signaling pathways. *Dev Cell,* **7,** 491-501.

Saelens, X., Festjens, N., Vande Walle, L., van Gurp, M., van Loo, G. & Vandenabeele, P. (2004) Toxic proteins released from mitochondria in cell death. *Oncogene,* **23,** 2861-2874.

Salvador-Gallego, R., Mund, M., Cosentino, K., Schneider, J., Unsay, J., Schraermeyer, U., Engelhardt, J., Ries, J. & Garcia-Saez, A.J. (2016) Bax assembly into rings and

arcs in apoptotic mitochondria is linked to membrane pores. *EMBO J,* **35,** 389-401.

Sattler, M., Liang, H., Nettesheim, D., Meadows, R.P., Harlan, J.E., Eberstadt, M., Yoon, H.S., Shuker, S.B., Chang, B.S., Minn, A.J., Thompson, C.B. & Fesik, S.W. (1997) Structure of Bcl-xL-Bak peptide complex: recognition between regulators of apoptosis. *Science,* **275,** 983-986.

Scaffidi, C., Fulda, S., Srinivasan, A., Friesen, C., Li, F., Tomaselli, K.J., Debatin, K.M., Krammer, P.H. & Peter, M.E. (1998) Two CD95 (APO-1/Fas) signaling pathways. *EMBO J,* **17,** 1675-1687.

Schellenberg, B., Wang, P., Keeble, J.A., Rodriguez-Enriquez, R., Walker, S., Owens, T.W., Foster, F., Tanianis-Hughes, J., Brennan, K., Streuli, C.H. & Gilmore, A.P. (2013) Bax exists in a dynamic equilibrium between the cytosol and mitochondria to control apoptotic priming. *Mol Cell,* **49,** 959-971.

Schenk, R.L., Tuzlak, S., Carrington, E.M., Zhan, Y., Heinzel, S., Teh, C.E., Gray, D.H., Tai, L., Lew, A.M., Villunger, A., Strasser, A. & Herold, M.J. (2017) Characterisation of mice lacking all functional isoforms of the pro-survival BCL-2 family member A1 reveals minor defects in the haematopoietic compartment. *Cell Death Differ,* **24,** 534-545.

Schinkothe, T., Leistert, C. & Staib, P. (2006) Functional characterization of the Bcl-2 splice variant beta. *Blood,* **108,** 420a-420a.

Schmitz, R., Wright, G.W., Huang, D.W., Johnson, C.A., Phelan, J.D., Wang, J.Q., Roulland, S., Kasbekar, M., Young, R.M., Shaffer, A.L., Hodson, D.J., Xiao, W., Yu, X., Yang, Y., Zhao, H., Xu, W., Liu, X., Zhou, B., Du, W., Chan, W.C., Jaffe, E.S., Gascoyne, R.D., Connors, J.M., Campo, E., Lopez-Guillermo, A., Rosenwald, A., Ott, G., Delabie, J., Rimsza, L.M., Tay Kuang Wei, K., Zelenetz, A.D., Leonard, J.P., Bartlett, N.L., Tran, B., Shetty, J., Zhao, Y., Soppet, D.R., Pittaluga, S., Wilson, W.H. & Staudt, L.M. (2018) Genetics and Pathogenesis of Diffuse Large B-Cell Lymphoma. *N Engl J Med,* **378,** 1396-1407.

Schuetz, J.M., Johnson, N.A., Morin, R.D., Scott, D.W., Tan, K., Ben-Nierah, S., Boyle, M., Slack, G.W., Marra, M.A., Connors, J.M., Brooks-Wilson, A.R. & Gascoyne, R.D. (2012) BCL2 mutations in diffuse large B-cell lymphoma. *Leukemia,* **26,** 1383-1390.

Sentman, C.L., Shutter, J.R., Hockenbery, D., Kanagawa, O. & Korsmeyer, S.J. (1991) bcl-2 inhibits multiple forms of apoptosis but not negative selection in thymocytes. *Cell,* **67,** 879-888.

Seymour, J.F., Ma, S., Brander, D.M., Choi, M.Y., Barrientos, J., Davids, M.S., Anderson, M.A., Beaven, A.W., Rosen, S.T., Tam, C.S., Prine, B., Agarwal, S.K., Munasinghe, W., Zhu, M., Lash, L.L., Desai, M., Cerri, E., Verdugo, M., Kim, S.Y., Humerickhouse, R.A., Gordon, G.B., Kipps, T.J. & Roberts, A.W. (2017)

Venetoclax plus rituximab in relapsed or refractory chronic lymphocytic leukaemia: a phase 1b study. *Lancet Oncol,* **18,** 230-240.

Shaffer, A.L., 3rd, Young, R.M. & Staudt, L.M. (2012) Pathogenesis of human B cell lymphomas. *Annu Rev Immunol,* **30,** 565-610.

Shamas-Din, A., Kale, J., Leber, B. & Andrews, D.W. (2013) Mechanisms of action of Bcl-2 family proteins. *Cold Spring Harb Perspect Biol,* **5,** a008714.

Shao, L., Sun, Y., Zhang, Z., Feng, W., Gao, Y., Cai, Z., Wang, Z.Z., Look, A.T. & Wu, W.S. (2010) Deletion of proapoptotic Puma selectively protects hematopoietic stem and progenitor cells against high-dose radiation. *Blood,* **115,** 4707-4714.

Shimizu, S., Kanaseki, T., Mizushima, N., Mizuta, T., Arakawa-Kobayashi, S., Thompson, C.B. & Tsujimoto, Y. (2004) Role of Bcl-2 family proteins in a non-apoptotic programmed cell death dependent on autophagy genes. *Nat Cell Biol,* **6,** 1221-1228.

Shiozaki, E.N., Chai, J., Rigotti, D.J., Riedl, S.J., Li, P., Srinivasula, S.M., Alnemri, E.S., Fairman, R. & Shi, Y. (2003) Mechanism of XIAP-mediated inhibition of caspase-9. *Mol Cell,* **11,** 519-527.

Shkreta, L., Michelle, L., Toutant, J., Tremblay, M.L. & Chabot, B. (2011) The DNA damage response pathway regulates the alternative splicing of the apoptotic mediator Bcl-x. *J Biol Chem,* **286,** 331-340.

Singh, K. & Briggs, J.M. (2016) Functional Implications of the spectrum of BCL2 mutations in Lymphoma. *Mutat Res Rev Mutat Res,* **769,** 1-18.

Smith, G.L., Benfield, C.T., Maluquer de Motes, C., Mazzon, M., Ember, S.W., Ferguson, B.J. & Sumner, R.P. (2013) Vaccinia virus immune evasion: mechanisms, virulence and immunogenicity. *J Gen Virol,* **94,** 2367-2392.

Smith, V.M., Dietz, A., Henz, K., Bruecher, D., Jackson, R., Kowald, L., van Wijk, S.J.L., Jayne, S., Macip, S., Fulda, S., Dyer, M.J.S. & Vogler, M. (2019) Specific interactions of BCL-2 family proteins mediate sensitivity to BH3-mimetics in diffuse large B-cell lymphoma. *Haematologica,* **In press**.

Snyder, A.G., Hubbard, N.W., Messmer, M.N., Kofman, S.B., Hagan, C.E., Orozco, S.L., Chiang, K., Daniels, B.P., Baker, D. & Oberst, A. (2019) Intratumoral activation of the necroptotic pathway components RIPK1 and RIPK3 potentiates antitumor immunity. *Sci Immunol,* **4**.

Sochalska, M., Ottina, E., Tuzlak, S., Herzog, S., Herold, M. & Villunger, A. (2016) Conditional knockdown of BCL2A1 reveals rate-limiting roles in BCR-dependent B-cell survival. *Cell Death Differ,* **23,** 628-639.

Soderquist, R., Pletnev, A.A., Danilov, A.V. & Eastman, A. (2014a) The putative BH3 mimetic S1 sensitizes leukemia to ABT-737 by increasing reactive oxygen

species, inducing endoplasmic reticulum stress, and upregulating the BH3-only protein NOXA. *Apoptosis,* **19,** 201-209.

Soderquist, R.S., Danilov, A.V. & Eastman, A. (2014b) Gossypol increases expression of the pro-apoptotic BH3-only protein NOXA through a novel mechanism involving phospholipase A2, cytoplasmic calcium, and endoplasmic reticulum stress. *J Biol Chem,* **289,** 16190-16199.

Soderquist, R.S. & Eastman, A. (2016) BCL2 Inhibitors as Anticancer Drugs: A Plethora of Misleading BH3 Mimetics. *Molecular Cancer Therapeutics,* **15,** 2011-2017.

Song, T., Chai, G., Liu, Y., Yu, X., Wang, Z. & Zhang, Z. (2016) Bcl-2 phosphorylation confers resistance on chronic lymphocytic leukaemia cells to the BH3 mimetics ABT-737, ABT-263 and ABT-199 by impeding direct binding. *Br J Pharmacol,* **173,** 471-483.

Souers, A.J., Leverson, J.D., Boghaert, E.R., Ackler, S.L., Catron, N.D., Chen, J., Dayton, B.D., Ding, H., Enschede, S.H., Fairbrother, W.J., Huang, D.C., Hymowitz, S.G., Jin, S., Khaw, S.L., Kovar, P.J., Lam, L.T., Lee, J., Maecker, H.L., Marsh, K.C., Mason, K.D., Mitten, M.J., Nimmer, P.M., Oleksijew, A., Park, C.H., Park, C.M., Phillips, D.C., Roberts, A.W., Sampath, D., Seymour, J.F., Smith, M.L., Sullivan, G.M., Tahir, S.K., Tse, C., Wendt, M.D., Xiao, Y., Xue, J.C., Zhang, H., Humerickhouse, R.A., Rosenberg, S.H. & Elmore, S.W. (2013) ABT-199, a potent and selective BCL-2 inhibitor, achieves antitumor activity while sparing platelets. *Nat Med,* **19,** 202-208.

Srinivasan, L., Sasaki, Y., Calado, D.P., Zhang, B., Paik, J.H., DePinho, R.A., Kutok, J.L., Kearney, J.F., Otipoby, K.L. & Rajewsky, K. (2009) PI3 kinase signals BCR-dependent mature B cell survival. *Cell,* **139,** 573-586.

Steimer, D.A., Boyd, K., Takeuchi, O., Fisher, J.K., Zambetti, G.P. & Opferman, J.T. (2009) Selective roles for antiapoptotic MCL-1 during granulocyte development and macrophage effector function. *Blood,* **113,** 2805-2815.

Stennicke, H.R. & Salvesen, G.S. (1999) Catalytic properties of the caspases. *Cell Death Differ,* **6,** 1054-1059.

Stilgenbauer, S., Eichhorst, B., Schetelig, J., Coutre, S., Seymour, J.F., Munir, T., Puvvada, S.D., Wendtner, C.M., Roberts, A.W., Jurczak, W., Mulligan, S.P., Bottcher, S., Mobasher, M., Zhu, M., Desai, M., Chyla, B., Verdugo, M., Enschede, S.H., Cerri, E., Humerickhouse, R., Gordon, G., Hallek, M. & Wierda, W.G. (2016) Venetoclax in relapsed or refractory chronic lymphocytic leukaemia with 17p deletion: a multicentre, open-label, phase 2 study. *Lancet Oncol,* **17,** 768-778.

Strasser, A. & Vaux, D.L. (2018) Viewing BCL2 and cell death control from an evolutionary perspective. *Cell Death Differ,* **25,** 13-20.

Suzuki, M., Youle, R.J. & Tjandra, N. (2000) Structure of Bax: coregulation of dimer formation and intracellular localization. *Cell,* **103,** 645-654.

Suzuki, Y., Imai, Y., Nakayama, H., Takahashi, K., Takio, K. & Takahashi, R. (2001) A serine protease, HtrA2, is released from the mitochondria and interacts with XIAP, inducing cell death. *Mol Cell,* **8,** 613-621.

Swerdlow, S.H., Campo, E., Pileri, S.A., Harris, N.L., Stein, H., Siebert, R., Advani, R., Ghielmini, M., Salles, G.A., Zelenetz, A.D. & Jaffe, E.S. (2016) The 2016 revision of the World Health Organization classification of lymphoid neoplasms. *Blood,* **127,** 2375-2390.

Tagawa, H., Karnan, S., Suzuki, R., Matsuo, K., Zhang, X., Ota, A., Morishima, Y., Nakamura, S. & Seto, M. (2005) Genome-wide array-based CGH for mantle cell lymphoma: identification of homozygous deletions of the proapoptotic gene BIM. *Oncogene,* **24,** 1348-1358.

Tahir, S.K., Smith, M.L., Hessler, P., Rapp, L.R., Idler, K.B., Park, C.H., Leverson, J.D. & Lam, L.T. (2017) Potential mechanisms of resistance to venetoclax and strategies to circumvent it. *BMC Cancer,* **17,** 399.

Tait, S.W., Ichim, G. & Green, D.R. (2014) Die another way--non-apoptotic mechanisms of cell death. *J Cell Sci,* **127,** 2135-2144.

Tait, S.W., Oberst, A., Quarato, G., Milasta, S., Haller, M., Wang, R., Karvela, M., Ichim, G., Yatim, N., Albert, M.L., Kidd, G., Wakefield, R., Frase, S., Krautwald, S., Linkermann, A. & Green, D.R. (2013) Widespread mitochondrial depletion via mitophagy does not compromise necroptosis. *Cell Rep,* **5,** 878-885.

Tanaka, S., Saito, K. & Reed, J.C. (1993) Structure-function analysis of the Bcl-2 oncoprotein. Addition of a heterologous transmembrane domain to portions of the Bcl-2 beta protein restores function as a regulator of cell survival. *J Biol Chem,* **268,** 10920-10926.

Tao, Z.F., Hasvold, L., Wang, L., Wang, X., Petros, A.M., Park, C.H., Boghaert, E.R., Catron, N.D., Chen, J., Colman, P.M., Czabotar, P.E., Deshayes, K., Fairbrother, W.J., Flygare, J.A., Hymowitz, S.G., Jin, S., Judge, R.A., Koehler, M.F., Kovar, P.J., Lessene, G., Mitten, M.J., Ndubaku, C.O., Nimmer, P., Purkey, H.E., Oleksijew, A., Phillips, D.C., Sleebs, B.E., Smith, B.J., Smith, M.L., Tahir, S.K., Watson, K.G., Xiao, Y., Xue, J., Zhang, H., Zobel, K., Rosenberg, S.H., Tse, C., Leverson, J.D., Elmore, S.W. & Souers, A.J. (2014) Discovery of a Potent and Selective BCL-XL Inhibitor with in Vivo Activity. *ACS Med Chem Lett,* **5,** 1088-1093.

Tate, J.G., Bamford, S., Jubb, H.C., Sondka, Z., Beare, D.M., Bindal, N., Boutselakis, H., Cole, C.G., Creatore, C., Dawson, E., Fish, P., Harsha, B., Hathaway, C., Jupe, S.C., Kok, C.Y., Noble, K., Ponting, L., Ramshaw, C.C., Rye, C.E., Speedy, H.E., Stefancsik, R., Thompson, S.L., Wang, S., Ward, S., Campbell, P.J. & Forbes, S.A. (2019) COSMIC: the Catalogue Of Somatic Mutations In Cancer. *Nucleic Acids Res,* **47,** D941-D947.

Tausch, E., Close, W., Dolnik, A., Bloehdorn, J., Chyla, B., Bullinger, L., Dohner, H., Mertens, D. & Stilgenbauer, S. (2019) Venetoclax resistance and acquired BCL2 mutations in chronic lymphocytic leukemia. *Haematologica*.

Tessoulin, B., Papin, A., Gomez-Bougie, P., Bellanger, C., Amiot, M., Pellat-Deceunynck, C. & Chiron, D. (2018) BCL2-Family Dysregulation in B-Cell Malignancies: From Gene Expression Regulation to a Targeted Therapy Biomarker. *Front Oncol,* **8,** 645.

Thomas, L.W., Lam, C. & Edwards, S.W. (2010) Mcl-1; the molecular regulation of protein function. *FEBS Lett,* **584,** 2981-2989.

Tonegawa, S. (1987) [Molecular biology of immunologic recognition]. *Tanpakushitsu Kakusan Koso,* **32,** 239-250.

Trescol-Biemont, M.C., Verschelde, C., Cottalorda, A. & Bonnefoy-Berard, N. (2004) Regulation of A1/Bfl-1 expression in peripheral splenic B cells. *Biochimie,* **86,** 287-294.

Tron, A.E., Belmonte, M.A., Adam, A., Aquila, B.M., Boise, L.H., Chiarparin, E., Cidado, J., Embrey, K.J., Gangl, E., Gibbons, F.D., Gregory, G.P., Hargreaves, D., Hendricks, J.A., Johannes, J.W., Johnstone, R.W., Kazmirski, S.L., Kettle, J.G., Lamb, M.L., Matulis, S.M., Nooka, A.K., Packer, M.J., Peng, B., Rawlins, P.B., Robbins, D.W., Schuller, A.G., Su, N., Yang, W., Ye, Q., Zheng, X., Secrist, J.P., Clark, E.A., Wilson, D.M., Fawell, S.E. & Hird, A.W. (2018) Discovery of Mcl-1-specific inhibitor AZD5991 and preclinical activity in multiple myeloma and acute myeloid leukemia. *Nat Commun,* **9,** 5341.

Tse, C., Shoemaker, A.R., Adickes, J., Anderson, M.G., Chen, J., Jin, S., Johnson, E.F., Marsh, K.C., Mitten, M.J., Nimmer, P., Roberts, L., Tahir, S.K., Xiao, Y., Yang, X., Zhang, H., Fesik, S., Rosenberg, S.H. & Elmore, S.W. (2008) ABT-263: a potent and orally bioavailable Bcl-2 family inhibitor. *Cancer Res,* **68,** 3421-3428.

Tsujimoto, Y. (1989) Stress-resistance conferred by high level of bcl-2 alpha protein in human B lymphoblastoid cell. *Oncogene,* **4,** 1331-1336.

Tsujimoto, Y., Finger, L.R., Yunis, J., Nowell, P.C. & Croce, C.M. (1984) Cloning of the chromosome breakpoint of neoplastic B cells with the t(14;18) chromosome translocation. *Science,* **226,** 1097-1099.

Tsujimoto, Y., Gorham, J., Cossman, J., Jaffe, E. & Croce, C.M. (1985) The t(14;18) chromosome translocations involved in B-cell neoplasms result from mistakes in VDJ joining. *Science,* **229,** 1390-1393.

Tzung, S.P., Kim, K.M., Basanez, G., Giedt, C.D., Simon, J., Zimmerberg, J., Zhang, K.Y. & Hockenbery, D.M. (2001) Antimycin A mimics a cell-death-inducing Bcl-2 homology domain 3. *Nat Cell Biol,* **3,** 183-191.

van Delft, M.F., Wei, A.H., Mason, K.D., Vandenberg, C.J., Chen, L., Czabotar, P.E., Willis, S.N., Scott, C.L., Day, C.L., Cory, S., Adams, J.M., Roberts, A.W. & Huang, D.C. (2006) The BH3 mimetic ABT-737 targets selective Bcl-2 proteins and efficiently induces apoptosis via Bak/Bax if Mcl-1 is neutralized. *Cancer Cell,* **10,** 389-399.

Varadarajan, S., Poornima, P., Milani, M., Gowda, K., Amin, S., Wang, H.G. & Cohen, G.M. (2015) Maritoclax and dinaciclib inhibit MCL-1 activity and induce apoptosis in both a MCL-1-dependent and -independent manner. *Oncotarget,* **6,** 12668-12681.

Varadarajan, S., Vogler, M., Butterworth, M., Dinsdale, D., Walensky, L.D. & Cohen, G.M. (2013) Evaluation and critical assessment of putative MCL-1 inhibitors. *Cell Death Differ,* **20,** 1475-1484.

Vaux, D.L., Cory, S. & Adams, J.M. (1988) Bcl-2 gene promotes haemopoietic cell survival and cooperates with c-myc to immortalize pre-B cells. *Nature,* **335,** 440-442.

Verhaegen, M., Bauer, J.A., Martin de la Vega, C., Wang, G., Wolter, K.G., Brenner, J.C., Nikolovska-Coleska, Z., Bengtson, A., Nair, R., Elder, J.T., Van Brocklin, M., Carey, T.E., Bradford, C.R., Wang, S. & Soengas, M.S. (2006) A novel BH3 mimetic reveals a mitogen-activated protein kinase-dependent mechanism of melanoma cell death controlled by p53 and reactive oxygen species. *Cancer Res,* **66,** 11348-11359.

Verhagen, A.M., Ekert, P.G., Pakusch, M., Silke, J., Connolly, L.M., Reid, G.E., Moritz, R.L., Simpson, R.J. & Vaux, D.L. (2000) Identification of DIABLO, a mammalian protein that promotes apoptosis by binding to and antagonizing IAP proteins. *Cell,* **102,** 43-53.

Verschelde, C., Walzer, T., Galia, P., Biemont, M.C., Quemeneur, L., Revillard, J.P., Marvel, J. & Bonnefoy-Berard, N. (2003) A1/Bfl-1 expression is restricted to TCR engagement in T lymphocytes. *Cell Death Differ,* **10,** 1059-1067.

Vikstrom, I.B., Slomp, A., Carrington, E.M., Moesbergen, L.M., Chang, C., Kelly, G.L., Glaser, S.P., Jansen, J.H., Leusen, J.H., Strasser, A., Huang, D.C., Lew, A.M., Peperzak, V. & Tarlinton, D.M. (2016) MCL-1 is required throughout B-cell development and its loss sensitizes specific B-cell subsets to inhibition of BCL-2 or BCL-XL. *Cell Death Dis,* **7,** e2345.

Villunger, A., Michalak, E.M., Coultas, L., Mullauer, F., Bock, G., Ausserlechner, M.J., Adams, J.M. & Strasser, A. (2003) p53- and drug-induced apoptotic responses mediated by BH3-only proteins puma and noxa. *Science,* **302,** 1036-1038.

Vogler, M. (2012) BCL2A1: the underdog in the BCL2 family. *Cell Death Differ,* **19,** 67-74.

Vogler, M. (2014) Targeting BCL2-Proteins for the Treatment of Solid Tumours. *Adv Med,* **2014,** 943648.

Vogler, M., Butterworth, M., Majid, A., Walewska, R.J., Sun, X.M., Dyer, M.J. & Cohen, G.M. (2009a) Concurrent up-regulation of BCL-XL and BCL2A1 induces approximately 1000-fold resistance to ABT-737 in chronic lymphocytic leukemia. *Blood,* **113,** 4403-4413.

Vogler, M., Furdas, S.D., Jung, M., Kuwana, T., Dyer, M.J. & Cohen, G.M. (2010) Diminished sensitivity of chronic lymphocytic leukemia cells to ABT-737 and ABT-263 due to albumin binding in blood. *Clin Cancer Res,* **16,** 4217-4225.

Vogler, M., Walter, H.S. & Dyer, M.J.S. (2017) Targeting anti-apoptotic BCL2 family proteins in haematological malignancies - from pathogenesis to treatment. *Br J Haematol,* **178,** 364-379.

Vogler, M., Weber, K., Dinsdale, D., Schmitz, I., Schulze-Osthoff, K., Dyer, M.J. & Cohen, G.M. (2009b) Different forms of cell death induced by putative BCL2 inhibitors. *Cell Death Differ,* **16,** 1030-1039.

Walensky, L.D., Pitter, K., Morash, J., Oh, K.J., Barbuto, S., Fisher, J., Smith, E., Verdine, G.L. & Korsmeyer, S.J. (2006) A stapled BID BH3 helix directly binds and activates BAX. *Mol Cell,* **24,** 199-210.

Walter, H.S., Trethewey, C.S., Ahearne, M.J., Jackson, R., Jayne, S., Wagner, S.D., Saldanha, G. & Dyer, M.J.S. (2019) Successful Treatment of Primary Cutaneous Diffuse Large B-Cell Lymphoma Leg Type With Single-Agent Venetoclax. *JCO Precision Oncology***,** 1-5.

Wang, C. & Youle, R.J. (2009) The role of mitochondria in apoptosis*. *Annu Rev Genet,* **43,** 95-118.

Wang, J.L., Liu, D., Zhang, Z.J., Shan, S., Han, X., Srinivasula, S.M., Croce, C.M., Alnemri, E.S. & Huang, Z. (2000) Structure-based discovery of an organic compound that binds Bcl-2 protein and induces apoptosis of tumor cells. *Proc Natl Acad Sci U S A,* **97,** 7124-7129.

Wang, P., Wang, P., Liu, B., Zhao, J., Pang, Q., Agrawal, S.G., Jia, L. & Liu, F.T. (2015) Dynamin-related protein Drp1 is required for Bax translocation to mitochondria in response to irradiation-induced apoptosis. *Oncotarget,* **6,** 22598-22612.

Wang, Q., Gao, F., May, W.S., Zhang, Y., Flagg, T. & Deng, X. (2008) Bcl2 negatively regulates DNA double-strand-break repair through a nonhomologous end-joining pathway. *Mol Cell,* **29,** 488-498.

Wang, X., Bathina, M., Lynch, J., Koss, B., Calabrese, C., Frase, S., Schuetz, J.D., Rehg, J.E. & Opferman, J.T. (2013) Deletion of MCL-1 causes lethal cardiac failure and mitochondrial dysfunction. *Genes Dev,* **27,** 1351-1364.

Wang, Z., Jiang, H., Chen, S., Du, F. & Wang, X. (2012) The mitochondrial phosphatase PGAM5 functions at the convergence point of multiple necrotic death pathways. *Cell,* **148,** 228-243.

Warren, C.F.A., Wong-Brown, M.W. & Bowden, N.A. (2019) BCL-2 family isoforms in apoptosis and cancer. *Cell Death Dis,* **10,** 177.

Wei, D., Zhang, Q., Schreiber, J.S., Parsels, L.A., Abulwerdi, F.A., Kausar, T., Lawrence, T.S., Sun, Y., Nikolovska-Coleska, Z. & Morgan, M.A. (2015) Targeting mcl-1 for radiosensitization of pancreatic cancers. *Transl Oncol,* **8,** 47-54.

Wei, M.C., Zong, W.X., Cheng, E.H., Lindsten, T., Panoutsakopoulou, V., Ross, A.J., Roth, K.A., MacGregor, G.R., Thompson, C.B. & Korsmeyer, S.J. (2001) Proapoptotic BAX and BAK: a requisite gateway to mitochondrial dysfunction and death. *Science,* **292,** 727-730.

Wei, Y., Sinha, S. & Levine, B. (2008) Dual role of JNK1-mediated phosphorylation of Bcl-2 in autophagy and apoptosis regulation. *Autophagy,* **4,** 949-951.

Wenzel, S.S., Grau, M., Mavis, C., Hailfinger, S., Wolf, A., Madle, H., Deeb, G., Dorken, B., Thome, M., Lenz, P., Dirnhofer, S., Hernandez-Ilizaliturri, F.J., Tzankov, A. & Lenz, G. (2013) MCL1 is deregulated in subgroups of diffuse large B-cell lymphoma. *Leukemia,* **27,** 1381-1390.

Westphal, D., Dewson, G., Menard, M., Frederick, P., Iyer, S., Bartolo, R., Gibson, L., Czabotar, P.E., Smith, B.J., Adams, J.M. & Kluck, R.M. (2014) Apoptotic pore formation is associated with in-plane insertion of Bak or Bax central helices into the mitochondrial outer membrane. *Proc Natl Acad Sci U S A,* **111,** E4076-4085.

Widlak, P., Li, L.Y., Wang, X. & Garrard, W.T. (2001) Action of recombinant human apoptotic endonuclease G on naked DNA and chromatin substrates: cooperation with exonuclease and DNase I. *J Biol Chem,* **276,** 48404-48409.

Wilfling, F., Weber, A., Potthoff, S., Vogtle, F.N., Meisinger, C., Paschen, S.A. & Hacker, G. (2012) BH3-only proteins are tail-anchored in the outer mitochondrial membrane and can initiate the activation of Bax. *Cell Death Differ,* **19,** 1328-1336.

Willis, S.N., Chen, L., Dewson, G., Wei, A., Naik, E., Fletcher, J.I., Adams, J.M. & Huang, D.C. (2005) Proapoptotic Bak is sequestered by Mcl-1 and Bcl-xL, but not Bcl-2, until displaced by BH3-only proteins. *Genes Dev,* **19,** 1294-1305.

Wilson, W.H., O'Connor, O.A., Czuczman, M.S., LaCasce, A.S., Gerecitano, J.F., Leonard, J.P., Tulpule, A., Dunleavy, K., Xiong, H., Chiu, Y.L., Cui, Y., Busman, T., Elmore, S.W., Rosenberg, S.H., Krivoshik, A.P., Enschede, S.H. & Humerickhouse, R.A. (2010) Navitoclax, a targeted high-affinity inhibitor of BCL-2, in lymphoid malignancies: a phase 1 dose-escalation study of safety, pharmacokinetics, pharmacodynamics, and antitumour activity. *Lancet Oncol,* **11,** 1149-1159.

Wilson, W.H., Young, R.M., Schmitz, R., Yang, Y., Pittaluga, S., Wright, G., Lih, C.J., Williams, P.M., Shaffer, A.L., Gerecitano, J., de Vos, S., Goy, A., Kenkre, V.P., Barr, P.M., Blum, K.A., Shustov, A., Advani, R., Fowler, N.H., Vose, J.M., Elstrom, R.L., Habermann, T.M., Barrientos, J.C., McGreivy, J., Fardis, M., Chang, B.Y., Clow, F.,

Munneke, B., Moussa, D., Beaupre, D.M. & Staudt, L.M. (2015) Targeting B cell receptor signaling with ibrutinib in diffuse large B cell lymphoma. *Nat Med,* **21,** 922-926.

Wolter, K.G., Hsu, Y.T., Smith, C.L., Nechushtan, A., Xi, X.G. & Youle, R.J. (1997) Movement of Bax from the cytosol to mitochondria during apoptosis. *J Cell Biol,* **139,** 1281-1292.

www.fda.gov/ (2019) https://www.fda.gov/. US Government.

Wyllie, A.H., Kerr, J.F. & Currie, A.R. (1980) Cell death: the significance of apoptosis. *Int Rev Cytol,* **68,** 251-306.

Yamin, T.T., Ayala, J.M. & Miller, D.K. (1996) Activation of the native 45-kDa precursor form of interleukin-1-converting enzyme. *J Biol Chem,* **271,** 13273-13282.

Yang, L., Cao, Z., Yan, H. & Wood, W.C. (2003a) Coexistence of high levels of apoptotic signaling and inhibitor of apoptosis proteins in human tumor cells: implication for cancer specific therapy. *Cancer Res,* **63,** 6815-6824.

Yang, Q.H., Church-Hajduk, R., Ren, J., Newton, M.L. & Du, C. (2003b) Omi/HtrA2 catalytic cleavage of inhibitor of apoptosis (IAP) irreversibly inactivates IAPs and facilitates caspase activity in apoptosis. *Genes Dev,* **17,** 1487-1496.

Yang, T., Thakur, A., Chen, T., Yang, L., Lei, G., Liang, Y., Zhang, S., Ren, H. & Chen, M. (2015) MicroRNA-15a induces cell apoptosis and inhibits metastasis by targeting BCL2L2 in non-small cell lung cancer. *Tumour Biol,* **36,** 4357-4365.

Yao, Y., Fujimoto, L.M., Hirshman, N., Bobkov, A.A., Antignani, A., Youle, R.J. & Marassi, F.M. (2015) Conformation of BCL-XL upon Membrane Integration. *J Mol Biol,* **427,** 2262-2270.

Ye, H., Cande, C., Stephanou, N.C., Jiang, S., Gurbuxani, S., Larochette, N., Daugas, E., Garrido, C., Kroemer, G. & Wu, H. (2002) DNA binding is required for the apoptogenic action of apoptosis inducing factor. *Nat Struct Biol,* **9,** 680-684.

Yu, L., Alva, A., Su, H., Dutt, P., Freundt, E., Welsh, S., Baehrecke, E.H. & Lenardo, M.J. (2004) Regulation of an ATG7-beclin 1 program of autophagic cell death by caspase-8. *Science,* **304,** 1500-1502.

Yu, L., Wan, F., Dutta, S., Welsh, S., Liu, Z., Freundt, E., Baehrecke, E.H. & Lenardo, M. (2006) Autophagic programmed cell death by selective catalase degradation. *Proc Natl Acad Sci U S A,* **103,** 4952-4957.

Yu, S.W., Wang, H., Poitras, M.F., Coombs, C., Bowers, W.J., Federoff, H.J., Poirier, G.G., Dawson, T.M. & Dawson, V.L. (2002) Mediation of poly(ADP-ribose) polymerase-1-dependent cell death by apoptosis-inducing factor. *Science,* **297,** 259-263.

Yuan, B.-Z., Chapman, J.A. & Reynolds, S.H. (2008) Proteasome Inhibitor MG132 Induces Apoptosis and Inhibits Invasion of Human Malignant Pleural Mesothelioma Cells. *Translational oncology,* **1,** 129-140.

Yuan, J., Shaham, S., Ledoux, S., Ellis, H.M. & Horvitz, H.R. (1993) The C. elegans cell death gene ced-3 encodes a protein similar to mammalian interleukin-1 beta-converting enzyme. *Cell,* **75,** 641-652.

Zelenetz, A.D., Salles, G., Mason, K.D., Casulo, C., Le Gouill, S., Sehn, L.H., Tilly, H., Cartron, G., Chamuleau, M.E.D., Goy, A., Tam, C.S., Lugtenburg, P.J., Petrich, A.M., Sinha, A., Samineni, D., Herter, S., Ingalla, E., Szafer-Glusman, E., Klein, C., Sampath, D., Kornacker, M., Mobasher, M. & Morschhauser, F. (2019) Venetoclax plus R- or G-CHOP in non-Hodgkin lymphoma: results from the CAVALLI phase 1b trial. *Blood,* **133,** 1964-1976.

Zhang, D.W., Shao, J., Lin, J., Zhang, N., Lu, B.J., Lin, S.C., Dong, M.Q. & Han, J. (2009) RIP3, an energy metabolism regulator that switches TNF-induced cell death from apoptosis to necrosis. *Science,* **325,** 332-336.

Zhang, J., Huang, K., O'Neill, K.L., Pang, X. & Luo, X. (2016) Bax/Bak activation in the absence of Bid, Bim, Puma, and p53. *Cell Death Dis,* **7,** e2266.

Zhang, Z., Jin, L., Qian, X., Wei, M., Wang, Y., Wang, J., Yang, Y., Xu, Q., Xu, Y. & Liu, F. (2007) Novel Bcl-2 inhibitors: Discovery and mechanism study of small organic apoptosis-inducing agents. *Chembiochem,* **8,** 113-121.

Zhang, Z., Zhu, W., Lapolla, S.M., Miao, Y., Shao, Y., Falcone, M., Boreham, D., McFarlane, N., Ding, J., Johnson, A.E., Zhang, X.C., Andrews, D.W. & Lin, J. (2010) Bax forms an oligomer via separate, yet interdependent, surfaces. *J Biol Chem,* **285,** 17614-17627.

Zhao, J., Niu, X., Li, X., Edwards, H., Wang, G., Wang, Y., Taub, J.W., Lin, H. & Ge, Y. (2016) Inhibition of CHK1 enhances cell death induced by the Bcl-2-selective inhibitor ABT-199 in acute myeloid leukemia cells. *Oncotarget,* **7,** 34785-34799.

Zhou, L., Zhang, Y., Sampath, D., Leverson, J., Dai, Y., Kmieciak, M., Nguyen, M., Orlowski, R.Z. & Grant, S. (2018) Flavopiridol enhances ABT-199 sensitivity in unfavourable-risk multiple myeloma cells in vitro and in vivo. *Br J Cancer,* **118,** 388-397.

Zou, H., Yang, R., Hao, J., Wang, J., Sun, C., Fesik, S.W., Wu, J.C., Tomaselli, K.J. & Armstrong, R.C. (2003) Regulation of the Apaf-1/caspase-9 apoptosome by caspase-3 and XIAP. *J Biol Chem,* **278,** 8091-8098.

7 Appendix

7.1 Table indicating DLBCL cell line characteristics

Cell line	Age	Sex	Subtype	Genetic modifications	
				Driver mutations	Chromosomal alterations of BCL2 genes
UOL-AME*	56	F	GCB		t(14;18)(q32;q21) → IGH-BCL2 genes altered
BJAB	5	F	GCB	p53 mutation	
CTB-1	70	M		t(3;14;8) involving the genes BCL6, IGH and MYC	
Farage	70	F	GCB	t(3;22)(q27;q11)BCL6 p53, CREBBP mutations	
HBL-1	65	M	ABC	CD79b, MYD88 mutations	
KIS1	53	M		t(9;14)(p13;q32) → *PAX5/BSAP-IGH* genes altered	
MedB1	27	M	PMBL	SOCS1 deletion, TNFAIP3 mutation	
MD901	Unknown		ABC	t(8;22)(q24;q11) MYC t(3;22)(q27;q11)BCL6	
OCI-LY1	44	M	GCB	MYC amplification p53, EZH2, CREBBP, KMT2D mutations	t(14;18)(q32;q21) → *IGH-BCL2* genes altered

OCI-LY3	52	M	ABC	CARD11, MYD88 , HLA-A , IRF4, PIM1, PRDM1 mutations	t(14;18)(q32;q21) → *IGH-BCL2* genes altered
OCI-LY10	27	F	ABC	CARD11, CD79a, MYD88 mutations	BCL2 amplification
OCI-LY19	27	F	GCB	CREBBP	t(14;18)(q32;q21) → IGH-BCL2 genes altered
Pfeiffer			GCB	EZH2, KMT2D	t(14;18)(q32;q21) → *IGH-BCL2* genes altered
UOL-RAD*	56	M	ABC		
RCK8	55	M	GCB	REL/NFkB mutation (chimeric protein REL-NRG) t(11;14)(q23;q32) → *DDX6-IGH* genes altered BCL6 translocation, TNFAIP3 mutation	
RIVA	57	M	ABC	P15INK4B del, P16INK4A del, RB1 del/mut p53 mutationbja	BCL2 amplification, NOXA amplification
SU-DHL6	43	M	GCB	p53, EZH2, KMT2D, CREBBP, RELN mutations	t(14;18)(q32;q21) → *IGH-BCL2* genes altered
SU-DHL8	59	M	GCB	t(8;22)(q24;q11) → *MYC-IGH* P53, KMT2D, CREBBP, EP300, SOCS1 mutations	
SU-DHL10	25	M	GCB	*P15INK4B* deletion, *P53,* EZH2, PTEN, EP300 mutations, t(8;14)(q24;q32) → *MYC-IGH* genes altered	t(14;18)(q32;q21) → *IGH-BCL2*
TMD-8	62	M	ABC	CD79b, MYD88, PIM1 mutations	

TMD-8 RO*	See TMD-8				
TMD-8 RI*	See TMD-8				
U2932	29	F	ABC	p53 mutation	BCL2 amplification, NOXA amplification
U2946	52	M	ABC	t(8;14)(q24;q32) → *MYC-IGH* genes altered	MCL1 amplification

Appendix 1 Characterisation of DLBCL cell lines used in this study

Characteristics of DLBCL cell lines are displayed including derived patient age, sex (male; M, F; female), the subtype of DLBCL (Activated B-cell; ABC, Germinal Center B-Cell; GC), and known driver and BCL-2 family mutations. * denotes cell lines which have been generated by the Dyer lab. (Dai*, et al* 2015b, Drexler 2010, Quentmeier*, et al* 2016, Smith*, et al* 2013, Tate*, et al* 2019)

7.2 BH3 profiles of DLBCL cell lines alongside their BH3 mimetic responses

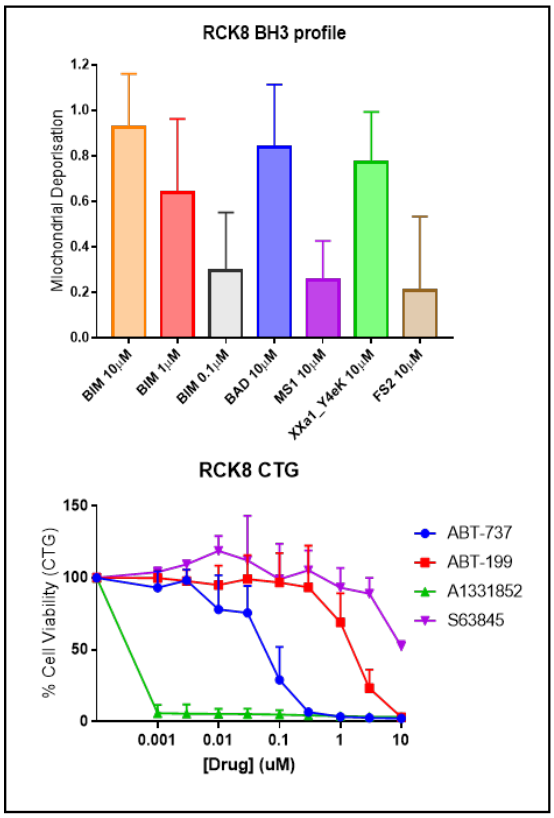

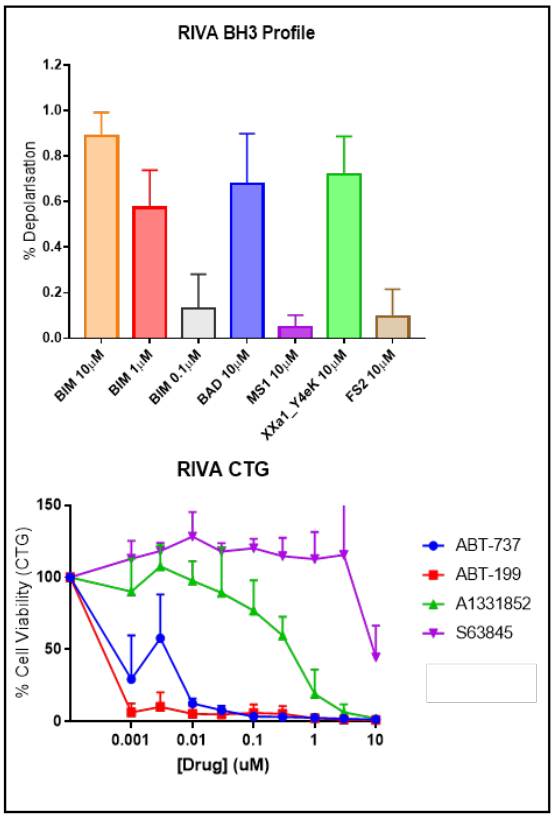

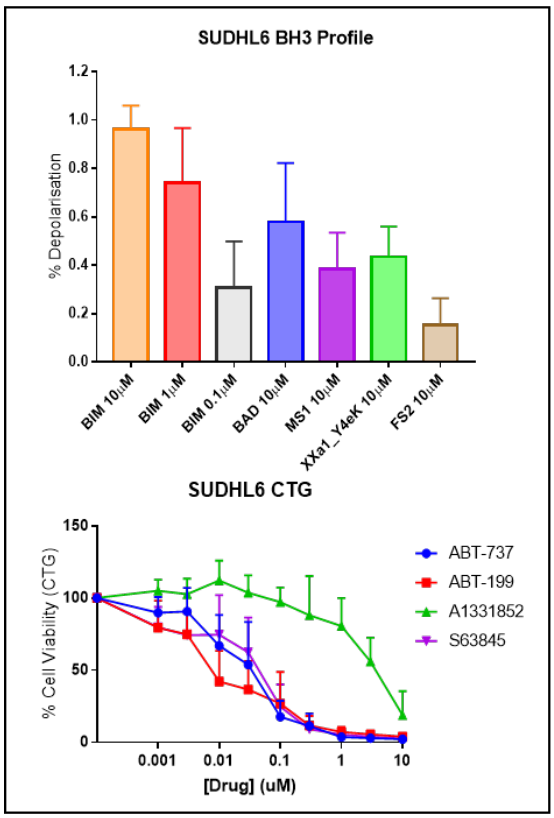

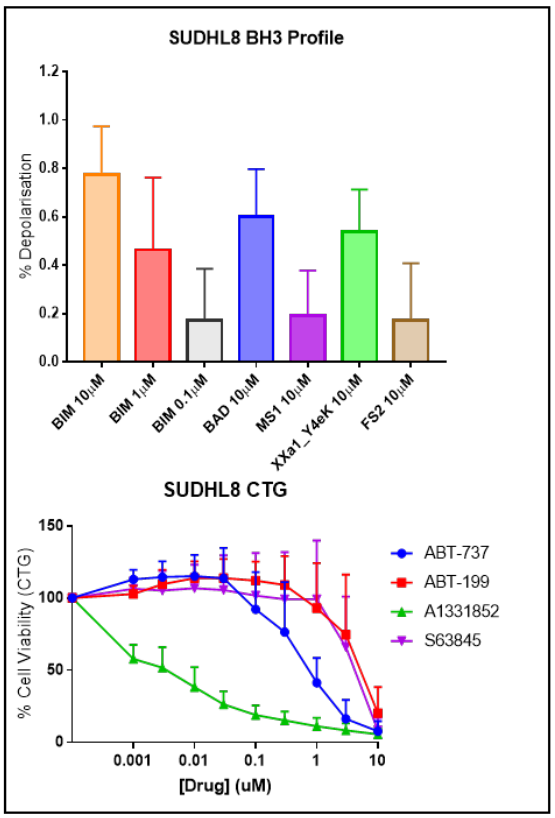

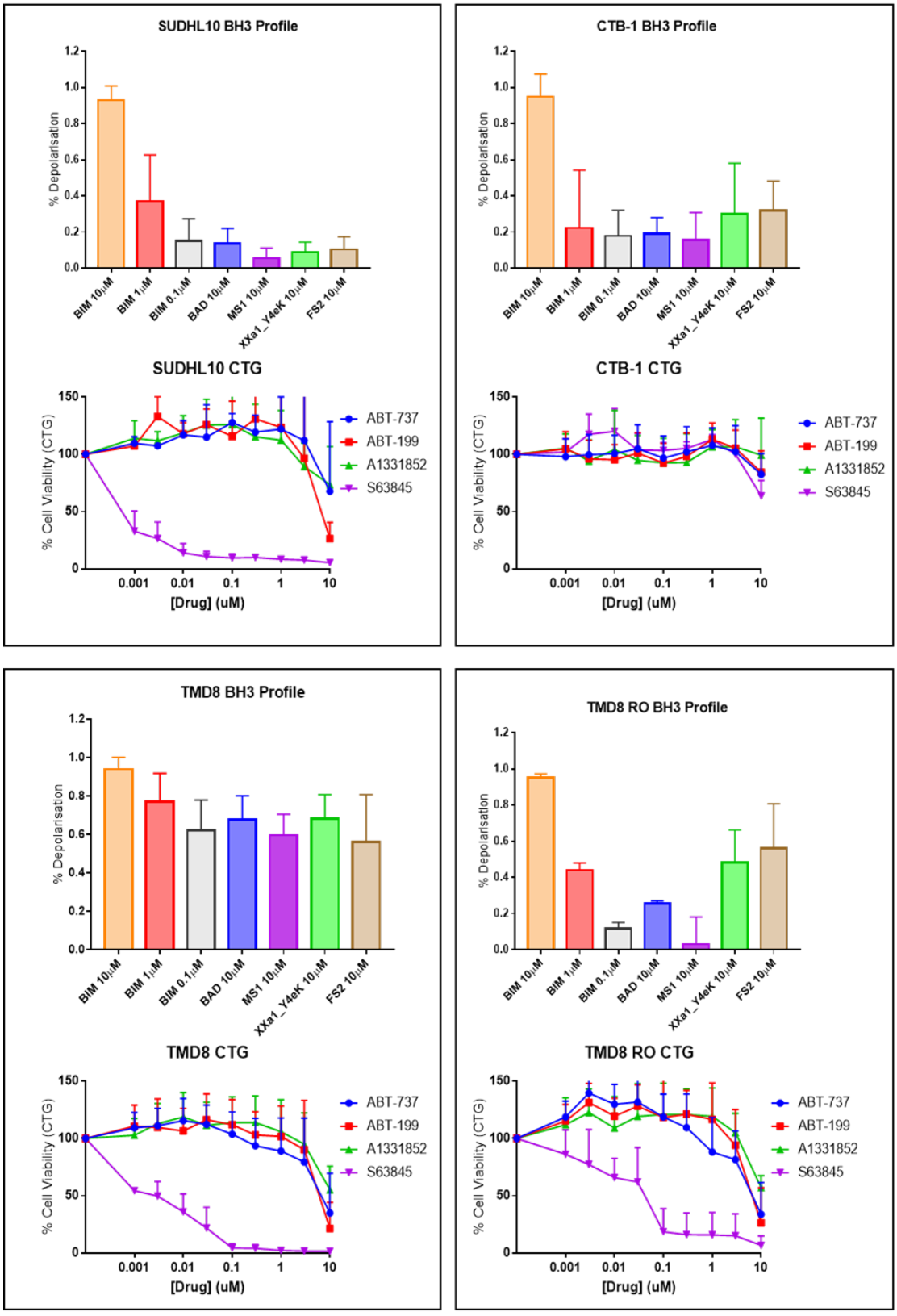
SUDHL10 BH3 Profile
% Depolarisation
BIM 10μM
BIM 1μM
BIM 0.1μM
BAD 10μM
MS1 10μM
XXa1_Y4eK 10μM
FS2 10μM
SUDHL10 CTG
% Cell Viability (CTG)
[Drug] (uM)
ABT-737
ABT-199
A1331852
S63845
CTB-1 BH3 Profile
CTB-1 CTG
TMD8 BH3 Profile
TMD8 CTG
TMD8 RO BH3 Profile
TMD8 RO CTG

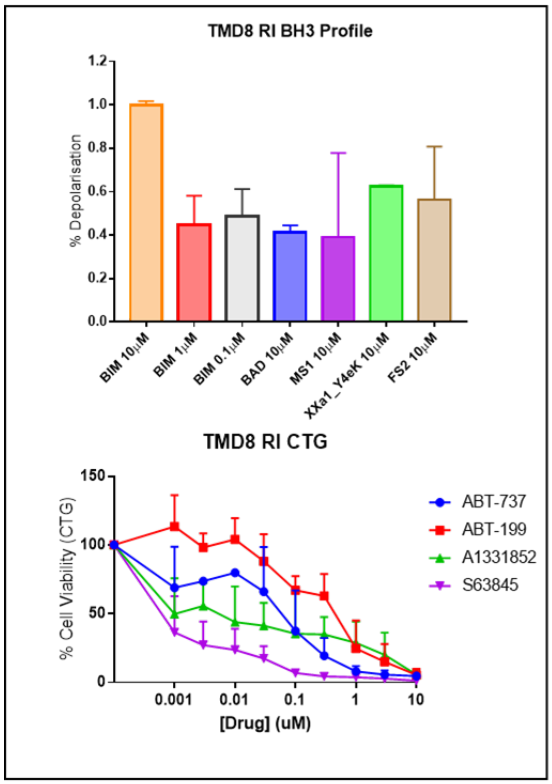
TMD8 RI BH3 Profile
% Depolarisation
BIM 10μM
BIM 1μM
BIM 0.1μM
BAD 10μM
MS1 10μM
XXa1_Y4eK 10μM
FS2 10μM

TMD8 RI CTG
% Cell Viability (CTG)
[Drug] (uM)
ABT-737
ABT-199
A1331852
S63845

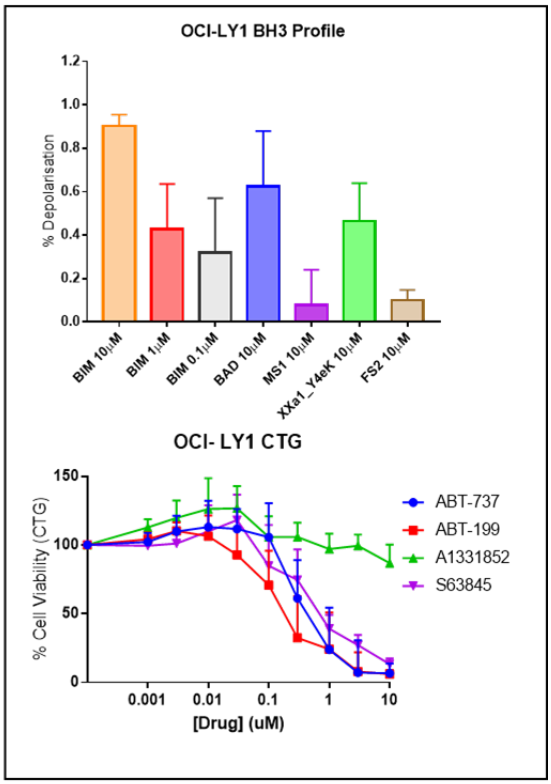
OCI-LY1 BH3 Profile
% Depolarisation
BIM 10μM
BIM 1μM
BIM 0.1μM
BAD 10μM
MS1 10μM
XXa1_Y4eK 10μM
FS2 10μM

OCI- LY1 CTG
% Cell Viability (CTG)
[Drug] (uM)
ABT-737
ABT-199
A1331852
S63845

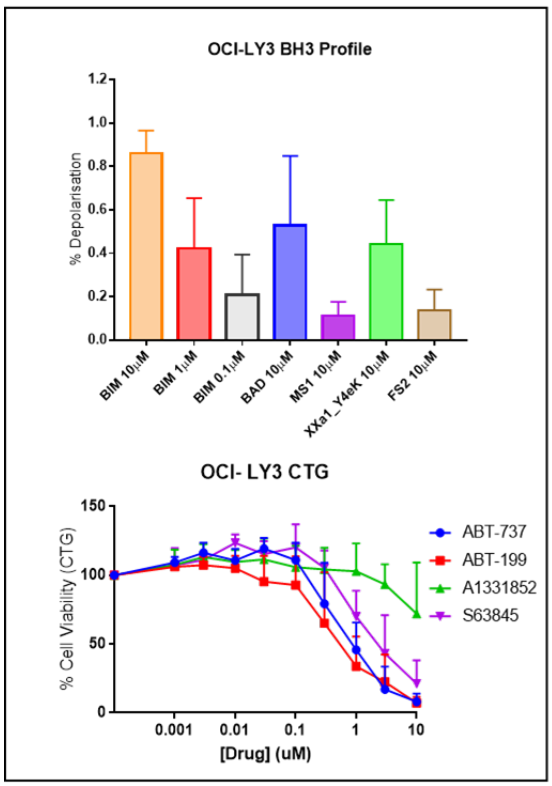
OCI-LY3 BH3 Profile
% Depolarisation
BIM 10μM
BIM 1μM
BIM 0.1μM
BAD 10μM
MS1 10μM
XXa1_Y4eK 10μM
FS2 10μM

OCI- LY3 CTG
% Cell Viability (CTG)
[Drug] (uM)
ABT-737
ABT-199
A1331852
S63845

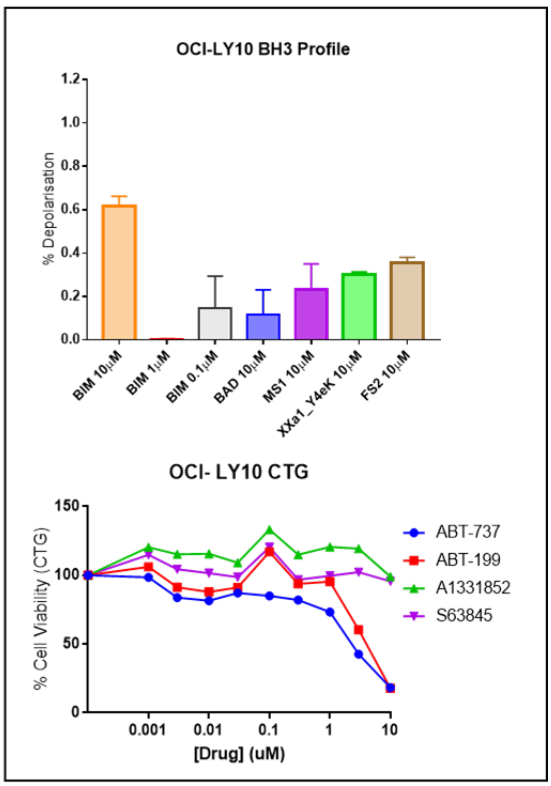
OCI-LY10 BH3 Profile
% Depolarisation
BIM 10μM
BIM 1μM
BIM 0.1μM
BAD 10μM
MS1 10μM
XXa1_Y4eK 10μM
FS2 10μM

OCI- LY10 CTG
% Cell Viability (CTG)
[Drug] (uM)
ABT-737
ABT-199
A1331852
S63845

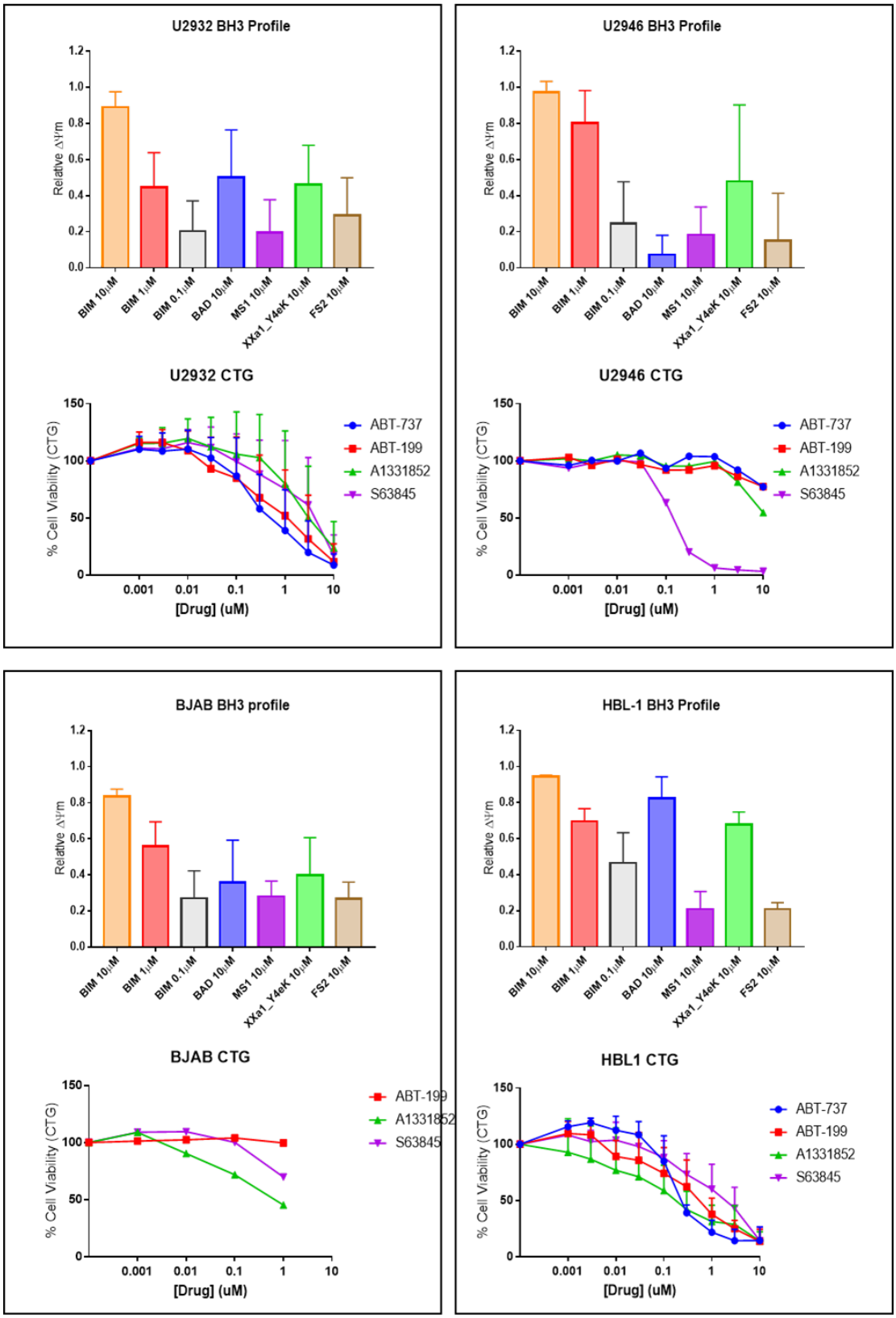
U2932 BH3 Profile
Relative ΔΨm
1.2
1.0
0.8
0.6
0.4
0.2
0.0
BIM 10μM
BIM 1μM
BIM 0.1μM
BAD 10μM
MS1 10μM
XXa1_Y4eK 10μM
FS2 10μM
U2946 BH3 Profile
Relative ΔΨm
1.2
1.0
0.8
0.6
0.4
0.2
0.0
BIM 10μM
BIM 1μM
BIM 0.1μM
BAD 10μM
MS1 10μM
XXa1_Y4eK 10μM
FS2 10μM
U2932 CTG
% Cell Viability (CTG)
150
100
50
0
0.001
0.01
0.1
1
10
[Drug] (uM)
ABT-737
ABT-199
A1331852
S63845
U2946 CTG
% Cell Viability (CTG)
150
100
50
0
0.001
0.01
0.1
1
10
[Drug] (uM)
ABT-737
ABT-199
A1331852
S63845
BJAB BH3 profile
Relative ΔΨm
1.2
1.0
0.8
0.6
0.4
0.2
0.0
BIM 10μM
BIM 1μM
BIM 0.1μM
BAD 10μM
MS1 10μM
XXa1_Y4eK 10μM
FS2 10μM
HBL-1 BH3 Profile
Relative ΔΨm
1.2
1.0
0.8
0.6
0.4
0.2
0.0
BIM 10μM
BIM 1μM
BIM 0.1μM
BAD 10μM
MS1 10μM
XXa1_Y4eK 10μM
FS2 10μM
BJAB CTG
% Cell Viability (CTG)
150
100
50
0
0.001
0.01
0.1
1
10
[Drug] (uM)
ABT-199
A1331852
S63845
HBL1 CTG
% Cell Viability (CTG)
150
100
50
0
0.001
0.01
0.1
1
10
[Drug] (uM)
ABT-737
ABT-199
A1331852
S63845

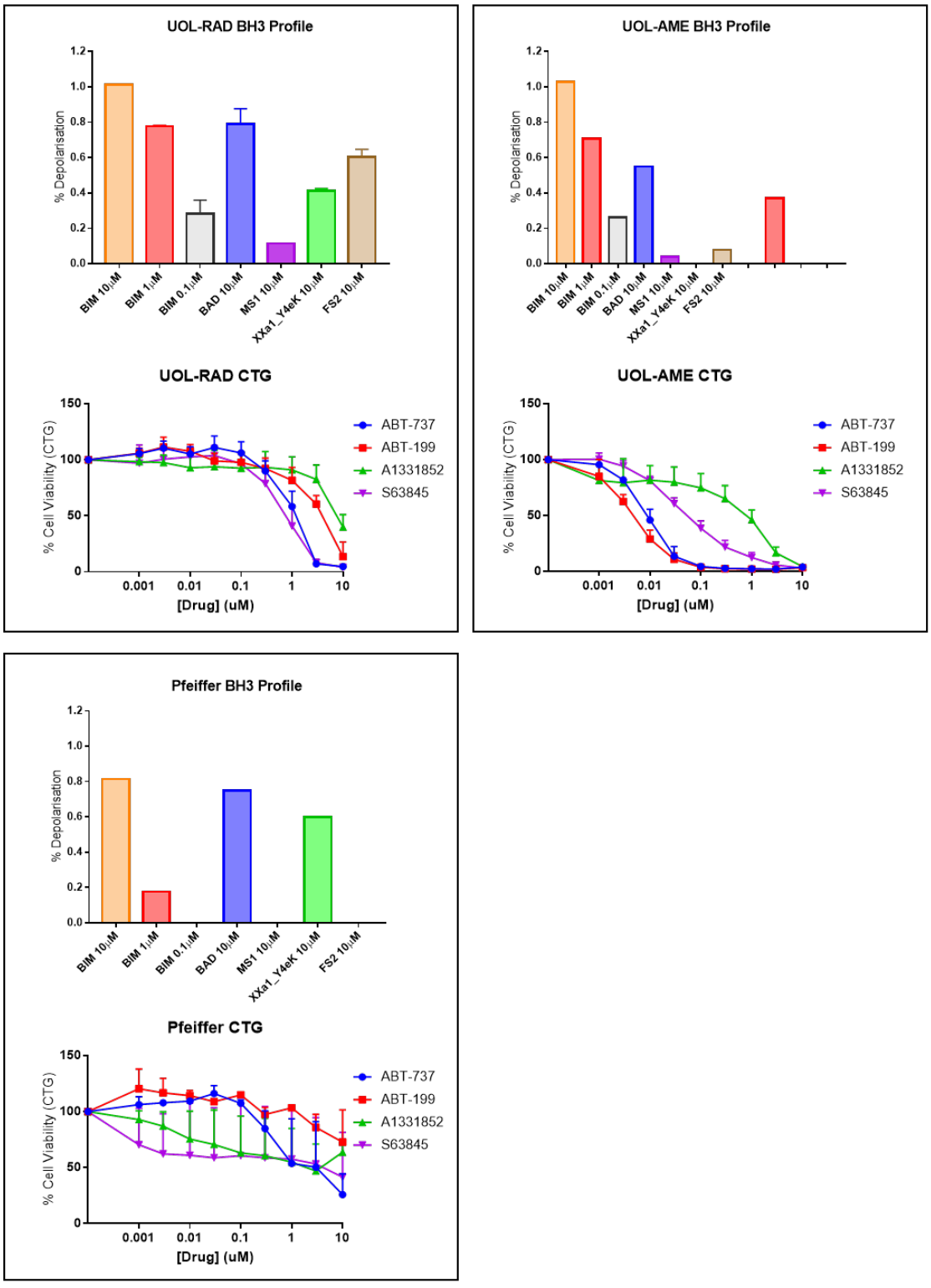

Appendix 2 BH3 profiles of DLBCL cell lines alongside their BH3 mimetic responses

The BH3 profile results are shown for DLBCL cell lines alongside their cell viability assays using the specific BH3 mimetics. Mimetics and peptides with the same target protein/s are shown in the same colour. Data are expressed as mean +SD.

7.3 Manuscript (ePub ahead of print)

Published Ahead of Print on October 10, 2019, as doi:10.3324/haematol.2019.220525.

haematologica
Journal of The Ferrata Storti Foundation

Specific interactions of BCL-2 family proteins mediate sensitivity to BH3-mimetics in diffuse large B-cell lymphoma

by Victoria M. Smith, Anna Dietz, Kristina Henz, Daniela Bruecher, Ross Jackson, Lisa Kowald, Sjoerd J.L. van Wijk, Sandrine Jayne, Salvador Macip, Simone Fulda, Martin J.S. Dyer, and Meike Vogler

Haematologica 2019 [Epub ahead of print]

Citation: Victoria M. Smith, Anna Dietz, Kristina Henz, Daniela Bruecher, Ross Jackson, Lisa Kowald, Sjoerd J.L. van Wijk, Sandrine Jayne, Salvador Macip, Simone Fulda, Martin J.S. Dyer, and Meike Vogler. Specific interactions of BCL-2 family proteins mediate sensitivity to BH3-mimetics in diffuse large B-cell lymphoma.
Haematologica. 2019; 104:xxx
doi:10.3324/haematol.2019.220525

Appendix 3 Manuscript
Smith, V.M., Dietz, A., Henz, K., Bruecher, D., Jackson, R., Kowald, L., van Wijk, S.J.L., Jayne, S., Macip, S., Fulda, S., Dyer, M.J.S. & Vogler, M. (2019) Specific interactions of BCL-2 family proteins mediate sensitivity to BH3-mimetics in diffuse large B-cell lymphoma. Haematologica, In press.

Specific interactions of BCL-2 family proteins mediate sensitivity to BH3-mimetics in diffuse large B-cell lymphoma

Victoria M Smith[1,2], Anna Dietz[3], Kristina Henz[3], Daniela Bruecher[3], Ross Jackson[1,2], Lisa Kowald[3], Sjoerd JL van Wijk[3], Sandrine Jayne[1,2], Salvador Macip[1], Simone Fulda[3,4,5], Martin JS Dyer[1,2], Meike Vogler[1,3]

[1] Department of Molecular and Cell Biology, University of Leicester, UK

[2] Ernest and Helen Scott Haematological Research Institute, University of Leicester, UK

[3] Institute for Experimental Cancer Research in Pediatrics, Goethe-University Frankfurt, Germany

[4] German Cancer Consortium (DKTK), Heidelberg, Germany

[5] German Cancer Research Center (DKFZ), Heidelberg, Germany

Running heads: Apoptosis induced by selective BH3-mimetics

To whom correspondence and reprint requests should be addressed:

Dr. Meike Vogler

Email: m.vogler@kinderkrebsstiftung-frankfurt.de

Word count: 3964

Acknowledgments

The authors would like to thank C. Hugenberg for expert secretarial assistance and Sandeep Dave for providing us with OCI-LY10 cells. This work has been partially supported by the Else Kröner-Fresenius-Stiftung (to MV), the Experimental Cancer Medicine Center (ECMC) Leicester and funding from the Scott Waudby Trust (to SJ and MJSD).

Abstract

The BCL-2 specific inhibitor, venetoclax/ABT-199 has exhibited remarkable clinical activity in nearly all cases of chronic lymphocytic leukemia. In contrast, responses are usually much less in diffuse large B-cell lymphoma, despite high level expression of BCL-2 in over 40% of cases, indicating that co-expression of related anti-apoptotic BCL-2 family proteins may limit activity. We have investigated the roles of the BCL-2 proteins in diffuse large B-cell lymphoma cells using a panel of specific BCL-2 Homology 3 mimetics and identified subgroups of diffuse large B-cell lymphoma cells that exhibited marked and specific dependency on either BCL-2, BCL-X_L or MCL-1 for survival. Dependency was associated with a sequestration of the pro-apoptotic proteins BIM, BAX and BAK selectively by the specific anti-apoptotic BCL-2 protein that was important for cellular survival. Sensitivity to BCL-2 Homology 3 mimetics was independent of genetic alterations involving the BCL-2 family and only partially correlated with protein expression levels. Treatment with ABT-199 displaced BAX and BIM from BCL-2, leading subsequently to BAK activation and apoptosis. In contrast, apoptosis induced by inhibiting BCL-X_L with A1331852 was associated with a displacement of both BAX and BAK from BCL-X_L and occurred independently of BIM. Finally, the MCL-1 inhibitor S63845 induced mainly BAX-dependent apoptosis mediated by a displacement of BAK, BIM and NOXA from MCL-1. In conclusion, our study indicates that in diffuse large B-cell lymphoma, the heterogeneous response to BCL-2 Homology 3 mimetics is mediated by selective interactions between BAX, BAK and anti-apoptotic BCL-2 proteins.

Introduction

Deregulated apoptosis is a key hallmark of cancer, and high expression of anti-apoptotic proteins is frequently observed in cancer cells. Apoptosis is initiated by ligation of death receptors on the cell surface or by the release of cytochrome c into cytosol followed by formation of the apoptosome (intrinsic apoptosis). Amongst the most important regulators of apoptosis is the BCL-2 protein family, which consists of both pro- and anti-apoptotic proteins[1]. The pro-apoptotic BCL-2 proteins BAX and BAK are essential for the execution of intrinsic apoptosis, as they mediate the release of cytochrome c from the mitochondrial intermembrane space. The anti-apoptotic proteins (BCL-2, BCL-X_L, MCL-1, BCL-w, BCL2A1 and BCL-B) inhibit the activation of BAX and BAK, thus preventing the release of cytochrome c. BAX and BAK can either be bound and inhibited directly by the anti-apoptotic BCL-2 proteins, or alternatively, their activation can be inhibited by a sequestration of BIM or related BCL-2 homology domain 3 (BH3)-only proteins. In this latter model, the release of BH3-only proteins from anti-apoptotic BCL-2 proteins is required in order to allow the BH3-only proteins to interact and directly activate BAX/BAK.

BCL-2 was identified as the target for the t(14;18)(q32.3;q21.3) chromosomal translocation involving the *BCL2* gene with the immunoglobulin heavy chain transcriptional enhancer in follicular lymphoma and related B-cell malignancies including diffuse large B-cell lymphoma (DLBCL)[2]. This chromosomal translocation results in constitutive expression of BCL-2 and increased resistance to apoptosis. About 40% of DLBCL display high expression of BCL-2, not only due to t(14;18)(q32.3;q21.3) but also gene copy number alterations and amplifications[3]. These genetic changes are associated with poor prognosis, particularly when combined with those affecting *MYC* in double hit lymphomas[4, 5]. Apart from these genetic changes *BCL2* is also amongst the most commonly mutated genes in DLBCL[6], with 91/393 cases reported as mutated in the COSMIC database (cancer.sanger.ac.uk/cosmic). In comparison, mutations involving MCL-1 (3/391) or BCL-X_L (0/391) are rare in DLBCL. A recent study has analyzed the protein expression of BCL-2, BCL-X_L and MCL-1 in a large set

of DLBCL cell lines and patient tissues and confirmed high expression of these anti-apoptotic proteins[7]. Also, RNA sequencing data obtained from a large cohort of DLBCL patients (n=584) indicates high expression of all main anti-apoptotic BCL-2 proteins in DLBCL[8].

Elevated expression of the anti-apoptotic BCL-2 proteins in cancer makes them promising targets for the development of novel therapeutics. The first clinical inhibitor, ABT-199/venetoclax, selectively targets BCL-2 and has been approved for the treatment of chronic lymphocytic leukemia (CLL) and Acute Myeloid Leukemia[9-11]. CLL cells display uniform sensitivity to ABT-199 and clinical responses are observed irrespective of genotype, demonstrating that in CLL, the most important anti-apoptotic protein is BCL-2[12].

In this study, we hypothesized that in DLBCL other BCL-2 family proteins like BCL-X_L and MCL-1 are important therapeutic targets. Here for the first time directly comparing specific BH3-mimetics that target either BCL-2 (ABT-199)[13], BCL-X_L (A1331852)[14] or MCL-1 (S63845)[15] in an extensive panel of DLBCL cell lines and primary cells, we identified subgroups of DLBCL that depended on individual BCL-2 family proteins for survival. Dependency was associated with the presence of preformed complexes of the respective anti-apoptotic BCL-2 protein with BIM, BAX and BAK, indicating that sensitive cells were highly primed and that the sequestration of BAX/BAK by the anti-apoptotic BCL-2 proteins was necessary for cellular survival.

Methods

Material

All chemicals apart from ABT-199, A1331852, A1155463, A1210477 (Selleck Chemicals, Houston, TX), or S63845 (ApexBio, Taiwan) were from Sigma (Deisenhofen, Germany). Most cell lines used in this study were obtained from Deutsche Sammlung von Mikroorganismen und Zellkulturen (DSMZ, Braunschweig, Germany) except Pfeiffer and SUDHL2 cells (American Type Culture Collection, Manassas, VA), OCI-LY10 (Sandeep Dave, Duke University, Durham), MedB1[16] (Peter Moeller, University of Ulm, Ulm, Germany) or Karpas-1106[17] (Abraham Karpas, University of Cambridge, Cambridge, UK). All cell lines were authenticated by Short Tandem Repeat profiling and routinely tested for mycoplasma contamination. Primary patient-derived samples were obtained from patients attending the University Hospital of Leicester, UK. Local ethical approval (Leicestershire, Northamptonshire and Rutland REC06/Q2501/122) and patient consent was obtained through the Haematological Tissue Bank of the Ernest and Helen Scott Haematological Research Institute, Leicester, UK. Peripheral blood mononuclear cells were isolated from the blood of patients presenting in leukemic phase and CellTiterGlo assay (Promega, Mannheim, Germany) was used to assess viability.

Western blotting and immunoprecipitation

For Western blotting, proteins were obtained using Tris-lysis buffer containing 1% TritonX. Western blotting was performed using the following antibodies: mouse anti-BCL-2 (Dako (Agilent), M088701-2, Hamburg, Germany), rabbit anti-BCL-X_L (Cell Signaling, 2762S, Beverly, MA), rabbit anti-MCL-1 (Enzo, ADI-AAP-240F, Farmindale, NY), rabbit anti-BIM (Cell Signaling, 3183S), mouse anti-NOXA (Enzo, ALX-804-408), rabbit anti-BAK (Upstate/ Merck, 06-536), mouse anti-BAX (Cell Signaling, 2772S) and mouse anti-GAPDH (BioTrend (Hy Test Ltd), 5G4-6C5, Turku, Finland). Immunoprecipitation was performed using the following antibodies: hamster anti-BCL-2 (BD Bioscience, 551051, Heidelberg, Germany), rabbit anti-BCL-X_L (Abcam, ab32370), rabbit anti-MCL-1 (Enzo, ADI-AAP-240F), mouse anti-

BAX (BD Bioscience, 610983) rabbit anti-BAK (Abcam, ab32371). Antibodies were crosslinked to Protein G dynabeads (Invitrogen, Karlsruhe, Germany). CHAPS containing lysates were incubated overnight at 4°C with the antibody-Protein G complexes before washing of precipitates in lysis buffer and analysis by Western blotting.

BH3-profiling

Cells were gently permeabilized with 0.0025% digitonin before exposure to 0.1, 1 or 10µM of synthetic peptides (BIM, BAD, XXa1_Y4eK [18]). Loss of mitochondrial membrane potential (MMP) was measured using 1 µM JC-1 via a Hidex Sense plate reader as described previously[19]. Results were normalized to DMSO and FCCP controls.

Genetic modifications

For silencing of individual genes cells were electroporated using Neon transfection system (ThermoFisher) using two pulses of 20 ms at 1200 V. The following silencer select siRNAs (ThermoFisher) were used at 100 nM: BAX (#1s1888, #3s1890), BAK (#1s1880, #2s1881), BIM (#1s195011, #2s195012, #3s223065), BCL-X_L (s1921), MCL-1 (s8583), NOXA (s10709, s10710). CRISPR/Cas9 engineering was done as described previously[20]. Briefly, three gRNAs against human BAK (GGTAGACGTGTAGGGCCAGA, TCACCTGCTAGGTTGCAG, AAGACCCTTACCAGAAGCAG) or against GFP (NHT; GGAGCGCACCATCTTCTTCA , GCCACAAGTTCAGCGTGTC, GGGCGAGGAGCTGTTCACCG) were cloned in pLentiCRISPRv2 (Addgene # 52961). Lentiviral particles were generated by co-transfecting pLenti-CRISPRv2 NHT and BAK with pPAX2 (Addgene # 12260) and pMD2.G (Addgene # 12259) in HEK293T cells and used to transduce U2946 or SUDHL8 target cells using spin transduction followed by puromycin selection and isolation of BAK-deleted single-clones using limited dilution. The BAK expression status was assessed using Western blotting.

Results

BCL-2, BCL-X_L and MCL-1 are important therapeutic targets in DLBCL

To investigate the roles of the main anti-apoptotic BCL-2 proteins in DLBCL, we assessed the effects of selective BH3-mimetics in DLBCL cells. We focussed on commercially available inhibitors that target BCL-2 (ABT-199), BCL-X_L (A1331852, A1155463) or MCL-1 (A1210477[21], S63845). Primary cells isolated from patient tissues were exposed to different concentrations of BH3-mimetics before analysis of viability using CellTiterGlo Assay (Figure 1A). The direct comparison of ABT-199, A1331852 and S63845 revealed that the response to BH3-mimetics was highly heterogeneous, with 3/7 samples (#1, 2, and 3) responding to low nanomolar concentrations of S63845, sample #4 responding best to ABT-199, and samples #5, 6 and 7 being more resistant to all three BH3-mimetics. Notably, sample #3 displayed a better response to A1331852 than to ABT-199, indicating that although none of these primary samples displayed highest sensitivity to A1331852, all three main anti-apoptotic BCL-2 proteins may be relevant therapeutic targets in DLBCL.

As primary patient-derived DLBCL cells are limited and freshly isolated malignant B-cells rapidly lose viability *ex vivo*, we continued our investigations in a panel of 18 DLBCL cell lines comprising the main subtypes of DLBCL defined by gene expression profiling[22], namely Activated B-cell (ABC), Germinal Center (GC) and Primary Mediastinal B-cell Lymphoma (PMBL) like cells (Table 1). In addition, we characterized the cell lines based on the mutation/translocation signature derived from public databases according to their genetic drivers MCD (*MYD88* and *CD79b* mutations), BN2 (*BCL6* fusion and *NOTCH2* mutations), N1 (*NOTCH1* mutations) and EZB (*EZH2* mutations and *BCL2* translocations) as recently described[8]. An initial comparison of different selective BH3-mimetics indicated that A1331852 was more potent than A1155463, and S63845 displayed significantly higher potency than A1210477 (Figure 1B-D, Supplementary Figure 1 and Table 1).

DLBCL cell lines displayed highly heterogeneous responses to BH3-mimetics (Figure 1 B-D). RIVA, U2932 and OCI-LY1 cells responded primarily to ABT-199, indicating a dependency on BCL-2 for survival. In contrast, RCK8, SUDHL8 and MedB1 cells were highly sensitive to A1331852 demonstrating BCL-X_L dependency. Notably, these three cell lines displayed sensitivity to low nanomolar/picomolar concentrations of A1331852 (EC_{50} 0.0006, 0.005 and 0.002 μM respectively), highlighting its potency in cellular systems. Susceptibility to S63845 was more homogeneous than the responses to ABT-199 or A1331852, with 10/18 cell lines responding to less than 3 μM. The most sensitive cell line in our panel was SUDHL10 (EC_{50} 0.006 μM), which have previously been described to be resistant to BH3-mimetics[23].

Most cell lines were primarily sensitive to one specific BH3-mimetic, indicating that firstly, in each cell line one particular BCL-2 family protein was functionally most dominant, and secondly and unexpectedly, that expression of the other anti-apoptotic BCL-2 proteins could not prevent apoptosis induction. However, four cell lines (OCI-LY1, RIVA, SUDHL8 and TMD8) showed sensitivity to multiple inhibitors. Notably, 5/18 cell lines did not respond to any inhibitor at submicromolar concentrations (OCI-LY10, Pfeiffer, OCI-LY3, Karpas-1106 and HBL1 (Table 1).

BH3-profiling using XXa1_Y4eK may predict sensitivity to A1331852

To confirm that BCL-X_L and MCL-1 are important therapeutic targets in DLBCL, we utilized a genetic approach to silence BCL-X_L and MCL-1, respectively. Knockdown of BCL-X_L by siRNA was sufficient to induce apoptosis in RCK8, SUDHL8 and MedB1 cells but not in BCL-2 dependent RIVA or U2932 cells, whereas knockdown of MCL-1 was sufficient to induce apoptosis in SUDHL10, TMD8 and U2946 cells but not in BCL-X_L dependent MedB1 cells, which correlated with susceptibility to A1331852 and S63845, respectively (Figure 2 A-D). BH3-profiling may serve as a surrogate assay to investigate priming in tumour samples[24]. To examine whether BH3-profiling may predict the sensitivity to BH3-mimetics in DLBCL, permeabilized cells were exposed to BH3-peptides from BIM, which binds to all anti-

apoptotic BCL-2 proteins, BAD, which binds to BCL-2 and BCL-X_L, and the engineered peptide XXa1_Y4eK, which binds with high affinity selectively to BCL-X_L[18]. All tested cell lines displayed a dose-dependency towards BIM (Figure 2E). Both RIVA and RCK8 cells also responded to BAD and XXa1_Y4eK, in line with a dependency on BCL-2 and/or BCL-X_L for survival. In contrast, the MCL-1 dependent cell line SUDHL10 did not respond to BAD or XXa1_Y4eK, as observed in previous studies[23]. Next, we asked whether the response to XXa1_Y4eK may correlate with the sensitivity to A1331852 in a larger panel of cell lines. The EC_{50} for A1331852 displayed a significant correlation with the response to XXa1_Y4eK ($p<0.001$), indicating that BH3-profiling could serve as a biomarker to predict responses to BH3-mimetics provided that specific and potent peptides like XXa1_Y4eK are available (Figure 2F).

BCL-2 protein expression was highly variable but only partially associated with sensitivity to BH3-mimetics

Next, we aimed to understand the heterogeneity in the response to BH3-mimetics in the panel of DLBCL cell lines. Western blot analysis revealed that the expression of BCL-2 proteins was highly variable (Figure 2G and Supplementary Figure 2A). Amongst the cell lines, several contain genetic alterations involving *BCL2* e.g. t(14;18)(q32.3;q21.3) chromosomal translocation or gene amplifications (Table 1). Quantification of protein expression indicated that gene alterations of *BCL2* correlated partially with high protein expression (Supplementary Figure 2B). Although there was a tendency that cells with genetic alterations of *BCL2* were more sensitive to ABT-199, as reported previously[25], this difference was not significant (Supplementary Figure 2C). Of note, although the SUDHL4 and SUDHL6 cells are reported to contain missense mutations of *BCL2* which may prevent antibody recognition[26], BCL-2 protein expression was detectable with the antibody used in our study.

Highest expression of BCL-X_L was detected in RCK8, SUDHL8 and MedB1 cells, which were most sensitive to A1331852. Expression of MCL-1 was more homogeneous, with all cell lines

expressing detectable MCL-1 protein and highest expression in the *MCL1* amplified U2946 cells[27]. The pore-forming BCL-2 proteins BAK and BAX were expressed in all cell lines while BH3-only protein expression was highly variable (Figure 2G).

To test whether susceptibility to BH3-mimetics was associated with expression levels of their targeted BCL-2 proteins, the EC_{50} values were correlated with BCL-2 protein expression. Linear regression analysis showed a significant correlation between the response to ABT-199 and expression of BCL-2, but this appeared to be driven by the very high or very low BCL-2 expressing cell lines. Sensitivity to ABT-199 also significantly correlated with the ratio of BCL-2 to MCL-1 expression (Supplementary Figure 3A). Although the cell lines with highest sensitivity to A1331852 expressed high BCL-X_L, the correlation of BCL-X_L expression and sensitivity to A1331852 was not significant, which may be explained by several cell lines expressing high BCL-X_L but nevertheless being resistant to A1331852 (HBL1, Pfeiffer and Karpas-1106). Susceptibility to A1331852 was more strongly correlated with the ratio of BCL-X_L expression to a combined expression of the other anti-apoptotic proteins BCL-2 and MCL-1, although the resistant Pfeiffer and Karpas-1106 cells still displayed a high ratio and made this correlation weak (R^2=0.23) (Supplementary Figure 3B). Sensitivity to S63845 did not correlate with expression of its target MCL-1 (Supplementary Figure 3C) but as described previously[15] did to some extent inversely correlate with expression of BCL-X_L. In addition, we found a significant correlation of S63845 sensitivity to the ratio of MCL-1 to BIM expression.

Sensitivity to BH3-mimetics correlated with a sequestration of pro-apoptotic BCL-2 proteins

To interrogate whether the interactions of anti- and pro-apoptotic BCL-2 proteins might influence susceptibility towards BH3-mimetics, we selected ten representative cell lines and performed immunoprecipitation of the main anti-apoptotic proteins (Figure 3). In the BCL-2 dependent cell lines (RIVA, U2932 and OCI-LY1), BIM was highly bound to BCL-2, with no detectable binding of BIM to BCL-X_L or MCL-1, despite high protein expression of BCL-X_L

and MCL-1. In contrast, BIM was highly bound by MCL-1 in the MCL-1 dependent cell lines SUDHL10 and U2946. These two cell lines expressed low levels of BCL-2 and BCL-X_L, which may explain why BIM was bound to MCL-1. In the BCL-X_L dependent SUDHL8 and RCK8 cells, BIM expression was comparatively low, and some BIM appeared bound to BCL-X_L but not to BCL-2 or MCL-1. Collectively, these data suggest a relationship between the sequestration of BIM by the different anti-apoptotic BCL-2 proteins and a dependency on the respective anti-apoptotic BCL-2 protein for survival. However, the resistant cells OCI-LY3 and Pfeiffer, which did not respond to any BH3-mimetic, also displayed binding of BIM to BCL-2 and/or BCL-X_L and MCL-1. The Pfeiffer cells have been reported to contain a missense mutation in BIM (S10C), but this mutation did not prevent binding of BIM to its anti-apoptotic binding partners. In line with its published binding profile[28], the BH3-only protein NOXA was exclusively bound by MCL-1 but not by BCL-2 or BCL-X_L in all cell lines.

Besides binding BH3-only proteins, the anti-apoptotic BCL-2 proteins can also sequester BAX and BAK[29]. Intriguingly, we found that both BAX and BAK are bound by the anti-apoptotic BCL-2 proteins, highlighting that in DLBCL the anti-apoptotic BCL-2 proteins may act by inhibiting already partially activated BAX and BAK, where the BH3-domain is exposed and accessible for interaction with the anti-apoptotic BCL-2 proteins[30]. Thus, BAX was sequestered by BCL-2 predominantly in the BCL-2 dependent cell lines, and predominantly sequestered by BCL-X_L in the BCL-X_L dependent cell lines, indicating that the binding of BAX by the respective anti-apoptotic BCL-2 protein was associated with sensitivity to specific inhibitors (Figure 3). Besides BAX, also BAK was bound by BCL-X_L in the BCL-X_L dependent cell lines and by MCL-1 in the MCL-1 dependent cell lines. Taken together, our investigations show that sensitive DLBCL cell lines were highly primed and that a direct sequestration of BAX and BAK by the anti-apoptotic BCL-2 proteins could be the last step preventing apoptosis in these cells.

BH3-mimetics induced cell death by displacing and activating BAX and BAK

Next, we asked how BH3-mimetics induced cell death in DLBCL cell lines. Exposure to BH3-mimetics induced caspase-3 cleavage, caspase-dependent phosphatidylserine-externalization and loss of MMP (Supplementary Figure 4). The activation and oligomerization of BAX and/or BAK are key events in the intrinsic apoptotic pathway and require conformational changes. Treatment with BH3-mimetics induced conformational changes associated with activation and oligomerization of BAX and BAK in all sensitive cell lines (Supplementary Figure 5 A-C). Of note, some active BAK was detectable in untreated cells, but the amount of constitutively active BAK did not correlate with sensitivity (Supplementary Figure 5D).

To investigate how BH3-mimetics induced the activation of BAX and BAK we interrogated how the interaction of pro- and anti-apoptotic proteins changed upon exposure to BH3-mimetics (Figure 4). In the BCL-2 dependent cell lines RIVA and U2932, the recently described displacement of BIM from BCL-2[31] was difficult to detect but some reduction in binding of BIM to BCL-2 was found in U2932 cells. In RIVA cells, a minor amount of BIM appeared bound to BCL-X_L following treatment with ABT-199, which may indicate a low level of BIM displacement from BCL-2. In both cell lines, less BAX was bound to BCL-2 following treatment with ABT-199, indicating a direct displacement of BAX from BCL-2 (Figure 4A). Similarly, in the BCL-X_L dependent cell lines, BIM binding to BCL-X_L was reduced upon treatment with A1331852. Strikingly, both BAX and BAK were less bound by BCL-X_L upon A1331852 treatment, supporting the hypothesis that BH3-mimetics can directly displace BAX and BAK (Figure 4B). Treatment with S63845 in the MCL-1 dependent cell lines resulted in less binding of BIM and BAK to MCL-1 (Figure 4C). In summary, these studies demonstrate that treatment with BH3-mimetics resulted in reduced binding of pro-apoptotic BCL-2 proteins.

The displacement of BIM could be functionally important for apoptosis induction, as released BIM could initiate apoptosis by directly binding to and activating BAX and BAK. To

investigate whether BIM is necessary, we performed siRNA mediated knockdown of BIM followed by treatment with BH3-mimetics. Combined use of two distinct siRNAs partially inhibited BH3-mimetic induced cell death in a treatment and cell-line dependent manner, as BIM knockdown reduced cell death in RIVA, SUDHL10 and to a lesser extend in U2946 cells (Figure 5 A-C, Supplementary Figure 6), although efficient knockdown was achieved in all cell lines (Figure 5D). As the RIVA cells also expressed high levels of the BH3-only protein BMF we asked whether BMF could be functionally important, but silencing of BMF did not affect ABT-199 induced apoptosis (Supplementary Figure 7).

BAX and BAK were required to mediate ABT-199 induced apoptosis

Next, we explored the role of BAX in BH3-mimetic induced cell death. Silencing of BAX using siRNAs indicated that BAX was essential for BH3-mimetic induced cell death, as cell death was significantly reduced in RIVA, U2932, RCK8, SUDHL10 and U2946 cells (Figure 6 A-D). In contrast, knockdown of BAK only reduced apoptosis upon treatment with ABT-199 but not upon treatment with A1331852 or S63845, highlighting a prominent role for BAK only in ABT-199 induced apoptosis (Supplementary Figure 8).

Further, we investigated how BAK was involved in ABT-199 induced apoptosis. As no direct inhibition of BAK by BCL-2 was observed, we hypothesized that BAX inhibition by BCL-2 is the initial target of ABT-199, and that once BAX is released, BAK is also activated and accelerates cell death. To test this hypothesis, the activation of BAK was assessed upon silencing of BAX and treatment with ABT-199. In both RIVA and U2932 cells, silencing of BAX resulted in significantly less active BAK induced by ABT-199, suggesting that BAX contributed to an activation of BAK (Figure 6E). To investigate whether BAX could directly activate BAK, the interaction between BAK and BAX was investigated. Treatment with ABT-199 induced complex formation between BAX and BAK in both RIVA and U2932 cells (Figure 6F).

BAX rather than BAK is functionally required for A1331852 or S63845 induced apoptosis

To exclude that the absence of an influence of BAK silencing on A1331852 or S63845 induced apoptosis may be caused by insufficient knockdown, we performed genetic deletion of BAK using CRISPR/Cas9. Deletion of BAK in SUDHL8 cells had only a minor effect on A1331852 induced cell death as compared to cells transduced with NHT control gRNAs (Supplementary Figure 9 A-B). To investigate whether BAX could be activated in the absence of BAK, BAX activation was quantified upon treatment with A1331852 using a conformation specific antibody and flow cytometry. Although the deletion of BAK had a minor influence on the activation of BAX, BAX could clearly still be activated even though BAK was deleted (Supplementary Figure 9C).

To interrogate the role of BAK in S63845 induced apoptosis, BAK was deleted in U2946 cells. In contrast to the data obtained by siRNA mediated knockdown, genetic deletion of BAK had a significant influence on S63845 induced apoptosis in all BAK-deleted clones investigated (Figure 7A). However, S63845 induced apoptosis was not completely inhibited, suggesting that BAX may play a prominent role also upon S63845 treatment. To confirm that S63845-mediated apoptosis involved BAX, knockdown of BAX was performed in BAK-deleted cells (Figure 7B). Knockdown of BAX by siRNAs had a stronger influence on S63845 induced apoptosis than BAK deletion. Combined deletion of BAK and depletion of BAX resulted in complete inhibition of S63845 induced apoptosis (Figure 7C). To investigate how BAX may be activated upon inhibition of MCL-1, we first asked whether BAK was essential in activating BAX. Analysis of BAX activation in BAK-deleted cells indicated that BAK may be involved in activating BAX, as BAX activation was significantly reduced in BAK-deleted cells. However, some active BAX was still present in BAK-deleted cells, indicating that other factors may be involved in activating BAX. To explore a role of the BH3-only proteins BIM and NOXA, siRNA mediated knockdown of BIM and NOXA was performed in BAK-deleted

cells. In line with the minor reduction of S63845 induced apoptosis by BIM knockdown (Figure 5C), BIM knockdown also reduced S63845 induced apoptosis in NHT or BAK-deleted U2946 cells (Figure 7 E-F). In addition to BIM also NOXA may be involved in S63845 induced cell death, as knockdown of NOXA partially reduced S63845 induced apoptosis (Figure 7 G-H). These data indicate that NOXA may participate in activating BAX upon S63845 treatment. To explore how NOXA may be activating BAK we next investigated the binding of NOXA to MCL-1 and observed a prominent displacement of NOXA from MCL-1 by S63845 (Figure 7I). Taken together, these data indicate that BH3-only proteins displaced from MCL-1 by S63845 may contribute to an activation of BAX which primarily mediates S63845 induced apoptosis.

Discussion

By investigating the response to selective BH3-mimetics we have identified subgroups of DLBCL cells that depend on either BCL-2, BCL-X_L or MCL-1 for survival. Our side by side comparison of selective BH3-mimetics targeting the main anti-apoptotic proteins suggests that BCL-2, BCL-X_L and MCL-1 are all important therapeutic targets in DLBCL. However, we have not investigated the role of other BCL-2 family proteins such as BCL2A1 or BCLw due to the lack of specific inhibitors.

In line with previous studies, our data indicate a correlation of ABT-199 sensitivity with high BCL-2 protein expression[7, 25]. However, in our study sensitivity to ABT-199 was independent of genetic alterations of BCL-2 and not all cells expressing high BCL-2 levels were sensitive to ABT-199, highlighting the need to better understand the mechanisms of resistance in BCL-2 high expressing cells like HBL1 or OCI-LY3. Although RIVA and U2932 also expressed high levels of BCL-X_L and MCL-1, BAX and BIM were exclusively sequestered by BCL-2, indicating that in these cells BCL-2 is the preferred binding partner for the pro-apoptotic proteins. The molecular basis for this preferential binding is not known. Increased binding to BCL-2 instead of the related protein BCL-X_L cannot be explained by different binding affinities, as BIM BH3-peptides bind more strongly to BCL-X_L than to BCL-2[28, 32], but may be explained by the amount of accessible protein at the mitochondria or enhanced protein stability[33]. Our data indicate that ABT-199 released pro-apoptotic BAX and BIM and that the released BAX induced an activation of BAK, as knockdown of BAX significantly reduced BAK activation (Figure 6E). The involvement of BIM in ABT-199 induced apoptosis appears to be cell type dependent, as BIM knockdown reduced apoptosis in RIVA but not in U2932 cells (Figure 5).

In contrast, in the BCL-X_L dependent cell lines RCK8 and SUDHL8, BAX and BAK were exclusively bound to BCL-X_L. These cell lines expressed high levels of BCL-X_L but low levels of BCL-2 and MCL-1, which may explain why BCL-X_L was the preferred binding partner. Treatment with A1331852 displaced both BAX, BAK and BIM from BCL-X_L. Knockdown

experiments indicated that although BIM was displaced, it did not contribute to A1331852 induced apoptosis, whereas both BAX and BAK were involved. Taken together, these experiments indicate that the high sensitivity of RCK8 and SUDHL8 cells reflected the high levels of BAX and BAK bound by BCL-X_L and that their displacement by A1331852 was sufficient to induce apoptosis. Another study has shown a requirement for BH3-only proteins for A1331852 induced apoptosis in HCT-116 cells[34], highlighting important differences with DLBCL.

In terms of S63845 induced apoptosis, the MCL-1 dependent cell lines SUDHL10 and U2946 did not express especially high levels of MCL-1, but both cell lines expressed only little BCL-2 or BCL-X_L. BIM and BAK were predominantly sequestered by MCL-1 in these cells. BAK has previously been identified as an essential mediator of S63845 induced cell death in breast cancer cells[35], but our data demonstrate that BAX may be more important for MCL-1 inhibition in DLBCL. Thereby, BAK and/or BH3-only proteins displaced from MCL-1 contributed to the activation of BAX and apoptosis. Besides BIM, our data also indicate NOXA as potential mediator of S63845 induced apoptosis. NOXA is highly bound by MCL-1 and displaced by S63845, which may enable NOXA to act as a direct activator for BAX, as suggested previously[36,37].

Taken together, our study demonstrates that the sensitivity to BH3-mimetics is underlined by a sequestration of BIM, BAX and/or BAK by the anti-apoptotic BCL-2 proteins which is disrupted by BH3-mimetics, leading to predominantly BAX mediated apoptosis. Therefore, our data support a model in which the major function of the anti-apoptotic BCL-2 proteins in DLBCL cells is to directly sequester or inhibit BAX. Dependent on the abundance of the different anti-apoptotic BCL-2 proteins, the pro-apoptotic proteins preferentially bind to either BCL-2, BCL-X_L or MCL-1 which renders these cells highly sensitive to selective BH3-mimetics. However, our data also highlight that besides BCL-2, BCL-X_L or MCL-1 additional anti-apoptotic BCL-2 proteins like BCL2A1[38] or BCL-w[39] may play an important role in DLBCL, as some cell lines like Pfeiffer and OCI-LY3 display high priming but are

nevertheless not responsive to an inhibition of BCL-2, BCL-X_L or MCL-1. A more detailed understanding of the molecular mechanisms of resistance in these cell is required to enable the best use of these potent BCL-2 family inhibitors in clinical practice.

References

1. Adams JM, Cory S. The Bcl-2 apoptotic switch in cancer development and therapy. Oncogene. 2007;26(9):1324-1337.

2. Tsujimoto Y, Ikegaki N, Croce CM. Characterization of the protein product of bcl-2, the gene involved in human follicular lymphoma. Oncogene. 1987;2(1):3-7.

3. Aukema SM, Siebert R, Schuuring E, et al. Double-hit B-cell lymphomas. Blood. 2011;117(8):2319-2331.

4. Sarkozy C, Traverse-Glehen A, Coiffier B. Double-hit and double-protein-expression lymphomas: aggressive and refractory lymphomas. Lancet Oncol. 2015;16(15):e555-e567.

5. Horn H, Ziepert M, Becher C, et al. MYC status in concert with BCL2 and BCL6 expression predicts outcome in diffuse large B-cell lymphoma. Blood. 2013;121(12):2253-2263.

6. Schuetz JM, Johnson NA, Morin RD, et al. BCL2 mutations in diffuse large B-cell lymphoma. Leukemia. 2012;26(6):1383-1390.

7. Klanova M, Andera L, Brazina J, et al. Targeting of BCL2 family proteins with ABT-199 and homoharringtonine reveals BCL2- and MCL1-dependent subgroups of diffuse large B-cell lymphoma. Clin Cancer Res. 2016;22(5):1138-1149.

8. Schmitz R, Wright GW, Huang DW, et al. Genetics and Pathogenesis of Diffuse Large B-Cell Lymphoma. N Engl J Med. 2018;378(15):1396-1407.

9. Vogler M, Walter HS, Dyer MJS. Targeting anti-apoptotic BCL2 family proteins in haematological malignancies - from pathogenesis to treatment. Br J Haematol. 2017;178(3):364-379.

10. Davids MS, Roberts AW, Seymour JF, et al. Phase I First-in-Human Study of Venetoclax in Patients With Relapsed or Refractory Non-Hodgkin Lymphoma. J Clin Oncol. 2017;35(8):826-833.

11. DiNardo CD, Pratz K, Pullarkat V, et al. Venetoclax combined with decitabine or azacitidine in treatment-naive, elderly patients with acute myeloid leukemia. Blood. 2019;133(1):7-17.

12. Anderson MA, Tam C, Lew TE, et al. Clinicopathological features and outcomes of progression of CLL on the BCL2 inhibitor venetoclax. Blood. 2017;129(25):3362-3370.

13. Souers AJ, Leverson JD, Boghaert ER, et al. ABT-199, a potent and selective BCL-2 inhibitor, achieves antitumor activity while sparing platelets. Nat Med 2013;19(2):202-208.

14. Leverson JD, Phillips DC, Mitten MJ, et al. Exploiting selective BCL-2 family inhibitors to dissect cell survival dependencies and define improved strategies for cancer therapy. Sci Transl Med. 2015;7(279):279ra240.

15. Kotschy A, Szlavik Z, Murray J, et al. The MCL1 inhibitor S63845 is tolerable and effective in diverse cancer models. Nature. 2016;538(7626):477-482.

16. Moller P, Bruderlein S, Strater J, et al. MedB-1, a human tumor cell line derived from a primary mediastinal large B-cell lymphoma. Int J Cancer. 2001;92(3):348-353.

17. Nacheva E, Dyer MJ, Metivier C, et al. B-cell non-Hodgkin's lymphoma cell line (Karpas 1106) with complex translocation involving 18q21.3 but lacking BCL2 rearrangement and expression. Blood. 1994;84(10):3422-3428.

18. Dutta S, Ryan J, Chen TS, Kougentakis C, Letai A, Keating AE. Potent and specific peptide inhibitors of human pro-survival protein Bcl-xL. J Mol Biol. 2015;427(6 Pt B):1241-1253.

19. Ryan J, Letai A. BH3 profiling in whole cells by fluorimeter or FACS. Methods. 2013;61(2):156-164.

20. van Wijk SJL, Fricke F, Herhaus L, et al. Linear ubiquitination of cytosolic Salmonella Typhimurium activates NF-kappaB and restricts bacterial proliferation. Nat Microbiol. 2017;2(17066.

21. Leverson JD, Zhang H, Chen J, et al. Potent and selective small-molecule MCL-1 inhibitors demonstrate on-target cancer cell killing activity as single agents and in combination with ABT-263 (navitoclax). Cell Death Dis. 2015;6:e1590.

22. Alizadeh AA, Eisen MB, Davis RE, et al. Distinct types of diffuse large B-cell lymphoma identified by gene expression profiling. Nature. 2000;403(6769):503-511.

23. Deng J, Carlson N, Takeyama K, Dal Cin P, Shipp M, Letai A. BH3 profiling identifies three distinct classes of apoptotic blocks to predict response to ABT-737 and conventional chemotherapeutic agents. Cancer Cell. 2007;12(2):171-185.

24. Del Gaizo Moore V, Letai A. BH3 profiling--measuring integrated function of the mitochondrial apoptotic pathway to predict cell fate decisions. Cancer Lett. 2013;332(2):202-205.

25. Pham LV, Huang S, Zhang H, et al. Strategic Therapeutic Targeting to Overcome Venetoclax Resistance in Aggressive B-cell Lymphomas. Clin Cancer Res. 2018;24(16):3967-3980.

26. Masir N, Campbell LJ, Jones M, Mason DY. Pseudonegative BCL2 protein expression in a t(14;18) translocation positive lymphoma cell line: a need for an alternative BCL2 antibody. Pathology. 2010;42(3):212-216.

27. Quentmeier H, Drexler HG, Hauer V, et al. Diffuse Large B Cell Lymphoma Cell Line U-2946: Model for MCL1 Inhibitor Testing. PLoS One. 2016;11(12):e0167599.

28. Chen L, Willis SN, Wei A, et al. Differential targeting of prosurvival Bcl-2 proteins by their BH3-only ligands allows complementary apoptotic function. Mol Cell. 2005;17(3):393-403.

29. Willis SN, Chen L, Dewson G, et al. Proapoptotic Bak is sequestered by Mcl-1 and Bcl-xL, but not Bcl-2, until displaced by BH3-only proteins. Genes Develop. 2005;19(11):1294-1305.

30. Westphal D, Kluck RM, Dewson G. Building blocks of the apoptotic pore: how Bax and Bak are activated and oligomerize during apoptosis. Cell Death Diff. 2014;21(2):196-205.

31. Liu Y, Mondello P, Erazo T, et al. NOXA genetic amplification or pharmacologic induction primes lymphoma cells to BCL2 inhibitor-induced cell death. Proc Natl Acad Sci U S A. 2018;115(47):12034-12039.

32. Kong W, Zhou M, Li Q, Fan W, Lin H, Wang R. Experimental Characterization of the Binding Affinities between Proapoptotic BH3 Peptides and Antiapoptotic Bcl-2 Proteins. ChemMedChem. 2018;13(17):1763-1770.

33. Rooswinkel RW, van de Kooij B, de Vries E, et al. Antiapoptotic potency of Bcl-2 proteins primarily relies on their stability, not binding selectivity. Blood. 2014;123(18):2806-2815.

34. Greaves G, Milani M, Butterworth M, et al. BH3-only proteins are dispensable for apoptosis induced by pharmacological inhibition of both MCL-1 and BCL-XL. Cell Death Diff. 2019;26(6):1037-1047.

35. Merino D, Whittle JR, Vaillant F, et al. Synergistic action of the MCL-1 inhibitor S63845 with current therapies in preclinical models of triple-negative and HER2-amplified breast cancer. Science translational medicine. 2017;9(401).

36. Chen HC, Kanai M, Inoue-Yamauchi A, et al. An interconnected hierarchical model of cell death regulation by the BCL-2 family. Nat Cell Biol. 2015;17(10):1270-1281.

37. Du H, Wolf J, Schafer B, Moldoveanu T, Chipuk JE, Kuwana T. BH3 domains other than Bim and Bid can directly activate Bax/Bak. J Biol Chem. 2011;286(1):491-501.

38. Vogler M. BCL2A1: the underdog in the BCL2 family. Cell Death Diff. 2012;19(1):67-74.

39. Adams CM, Mitra R, Gong JZ, Eischen CM. Non-Hodgkin and Hodgkin Lymphomas Select for Overexpression of BCLW. Clin Cancer Res. 2017;23(22):7119-7129.

40. Th'ng KH, Garewal G, Kearney L, et al. Establishment and characterization of three new malignant lymphoid cell lines. Int J Cancer. 1987;39(1):89-93.

41. Amini RM, Berglund M, Rosenquist R, et al. A novel B-cell line (U-2932) established from a patient with diffuse large B-cell lymphoma following Hodgkin lymphoma. Leuk Lymphoma. 2002;43(11):2179-2189.

42. Tweeddale ME, Lim B, Jamal N, et al. The presence of clonogenic cells in high-grade malignant lymphoma: a prognostic factor. Blood. 1987;69(5):1307-1314.

43. Epstein AL, Levy R, Kim H, Henle W, Henle G, Kaplan HS. Biology of the human malignant lymphomas. IV. Functional characterization of ten diffuse histiocytic lymphoma cell lines. Cancer. 1978;42(5):2379-2391.

44. Kubonishi I, Niiya K, Miyoshi I. Establishment of a new human lymphoma line that secretes plasminogen activator. Jpn J Cancer Res. 1985;76(1):12-15.

45. Tohda S, Sato T, Kogoshi H, Fu L, Sakano S, Nara N. Establishment of a novel B-cell lymphoma cell line with suppressed growth by gamma-secretase inhibitors. Leuk Res. 2006;30(11):1385-1390.

46. Epstein AL, Variakojis D, Berger C, Hecht BK. Use of novel chemical supplements in the establishment of three human malignant lymphoma cell lines (NU-DHL-1, NU-DUL-1, and NU-AMB-1) with chromosome 14 translocations. Int J Cancer. 1985;35(5):619-627.

47. Fridberg M, Servin A, Anagnostaki L, et al. Protein expression and cellular localization in two prognostic subgroups of diffuse large B-cell lymphoma: higher expression of ZAP70 and PKC-beta II in the non-germinal center group and poor survival in patients deficient in nuclear PTEN. Leuk Lymphoma. 2007;48(11):2221-2232.

48. Epstein AL, Kaplan HS. Biology of the human malignant lymphomas. I. Establishment in continuous cell culture and heterotransplantation of diffuse histiocytic lymphomas. Cancer. 1974;34(6):1851-1872.

49. Abe M, Nozawa Y, Wakasa H, Ohno H, Fukuhara S. Characterization and comparison of two newly established Epstein-Barr virus-negative lymphoma B-cell lines. Surface markers, growth characteristics, cytogenetics, and transplantability. Cancer. 1988;61(3):483-490.

50. Gabay C, Ben-Bassat H, Schlesinger M, Laskov R. Somatic mutations and intraclonal variations in the rearranged Vkappa genes of B-non-Hodgkin's lymphoma cell lines. Eur J Haematol. 1999;63(3):180-191.

Table 1 Characteristics of cell lines

			Genetic modifications			Targeting BCL-2	Targeting BCL-X_L		Targeting MCL-1			
Cell Line	**Gene Expression Subtype**	**Genetic Driver Subtype**	**Driver Mutations**	**Alterations of *BCL2* Genes**	***BCL2* Family Mutations**	**ABT-199**	**A1331852**	**A115463**	**S63845**	**A1210477**	**OR**	**Mutation Reference**
RIVA/Ri-1	ABC	Other ABC		BCL2 amp, PMAIP1 amp		0,008	1,127	7,500	5,500	>10	40	31
U2932	ABC	Other ABC		BCL2 amp, PMAIP1 amp		1,439	4,520	ND	5,260	5,466	41	31
OCI-LY1	GC	EZB	EZH2, CREBBP, KMT2D	t(14;18)	BCL2	0,245	6,0390	ND	0,170	>10	42	Cosmic
SUDHL4	GC	EZB	EZH2	t(14;18)	BCL2	5,000	2,224	ND	0,470	>10	43	Cosmic
OCI-LY10	ABC	MCD	CARD11, CD79a, MYD88		BCL2 (silent)	5,625	5,740	ND	2,320	>10	42	CCLE
RC-K8	GC	BN2	BCL6 translocation, RELN, TNFAIP3, SPEN			>10	0,0006	0,005	4,870	>10	44	Cosmic
SUDHL8	GC	Other GC	KMT2D, CREBBP, EP300, SOCS1			6,170	0,005	0,012	0,530	>10	43	Cosmic
MedB1	PMBL	Other GC	SOCS1			>10	0,002	0,067	>10	>10	16	Cosmic
SUDHL6	GC	EZB	EZH2, KMT2D, CREBBP, RELN	t(14;18)	BCL2	3,016	>10	>10	0,160	>10	43	Cosmic
TMD8	ABC	MCD	CD79b, MYD88, PIM1			1,635	3,598	>10	0,330	4,253	45	unpublished
NU-DUL-1	GC	Other GC	KMT2D			9,846	3,603	ND	0,320	6,973	46	Cosmic
U2946	GC	Other GC		MCL1 amp		>10	>10	ND	0,140	>10	47	27
SUDHL10	GC	EZB	EZH2, PTEN, EP300	t(14;18)		>10	>10	>10	0,006	1,723	43	Cosmic
Karpas-1106	PMBL	EZB	EZH2, KMT2D, TNFAIP3, NFKBIE, RELT			>10	>10	ND	>10	>10	17	Cosmic
SUDHL2	ABC	BN2	TNFAIP3, MYD88 , EP300			2,740	1,824	ND	not calc	3,666	48	Cosmic
HBL-1	ABC	MCD	CD79b, MYD88			8,742	>10	4,000	5,900	>10	49	Cosmic
OCI-LY3	ABC	MCD	CARD11, MYD88 , HLA-A ,IRF4, PIM1, PRDM1	BCL2 amp	BCL2 (silent)	4,127	6,653	ND	1,850	>10	42	CCLE
Pfeiffer	GC	EZB	EZH2, KMT2D	t(14;18)	BIM, BCL2 (silent)	>10	>10	ND	3,430	>10	50	Cosmic

Characteristics of DLBCL cell lines are displayed including the subtype of DLBCL (Activated B-cell; ABC, Germinal Center B-Cell; GC, or Primary Mediastinal B-cell like; PMBL, *MYD88* and *CD79b* mutations, MCD, *BCL6* fusion and *NOTCH2* mutations, BN2, *EZH2* mutations and *BCL2* translocations, EZB), and genetic modifications affecting the BCL-2 proteins. EC_{50} for the five BH3-mimetics used in this study is shown as calculated from the CellTiterGlo data displayed in Figure 1 B-D and Supplementary Figure 1 A-B (in μM). OR; Original reference.

Figure Legends

Figure 1 DLBCL cells display a heterogeneous sensitivity to selective BH3-mimetics

A) Primary cells isolated from patient tissues were incubated with different concentrations of ABT-199, A1331852 or S63845 for 24h before analysis of cell viability using CellTiterGlo. Experiments were performed in triplicate and data shown are mean and standard deviation (S.D.) for each individual sample (n=7). B-D) DLBCL cell lines were exposed to different concentrations of ABT-199 (B), A1331852 (C) or S63845 (D) before analysis of cell viability using CellTiterGlo at 72h. Data shown are mean and S.D. (n=4-6). EC_{50} values as displayed in Table 1 are indicated for highly sensitive cell lines.

Figure 2 BH3-profiling and genetic silencing of BCL-X_L and MCL-1 confirms these proteins as important therapeutic targets independent of protein expression

A-D) The importance of the anti-apoptotic proteins BCL-X_L (A, C) or MCL-1 (B, D) in DLBCL was confirmed using siRNA mediated knockdown. A) Apoptosis was investigated 48h after siRNA mediated knockdown of BCL-X_L. Data shown are mean and S.D. (n=3). B) Apoptosis was investigated 24h after siRNA mediated knockdown of MCL-1. Data shown are mean and S.D. (n=3). C-D) Representative Western blots showing knockdown efficiency are displayed for BCL-X_L (C) or MCL-1 (D). GAPDH or α-tubulin were used as loading controls. E-F) BH3-profiling was performed using selected cell lines and exposure of permeabilized cells to BIM (10, 1 or 0.1 μM), BAD (10 μM) or XXa1_Y4eK (10 μM) peptides before staining with JC-1 and fluorescence reading over time. Data shown are mean and S.D. (n=4-5). F) The response to XXa1_Y4eK was correlated with the EC_{50} for A1331852. Cell lines corresponding to the data points are indicated. G) Expression of BCL-2 proteins in DLBCL cells was analyzed by Western blotting. As this was done on two independent gels (*, #) two GAPDH loading controls are shown. A representative example of 5 independent experiments is shown. Quantification is shown in Supplementary Figure 2A.

Figure 3 Priming correlates with sensitivity to BH3-mimetics

The interaction of anti- and pro-apoptotic BCL-2 proteins was investigated in a selection of 10 cell lines with varying sensitivities to BH3-mimetics. Immunoprecipitation of BCL-2, BCL-X_L and MCL-1 was performed in untreated cell lysates followed by analysis of binding of pro-apoptotic BCL-2 proteins (BIM, NOXA, BAX and BAK) using Western blotting. Protein G beads without primary antibody were used to control for unspecific binding. Staining with BCL-2, BCL-X_L, MCL-1 and GAPDH was performed to demonstrate efficient immunoprecipitation and equal protein loading, respectively. Representative Western blots of 2 independent experiments are shown.

Figure 4 On-target binding of BH3-mimetics displaces pro-apoptotic BCL-2 proteins

A-C) The interaction of anti- and pro-apoptotic BCL-2 proteins (BIM, BAX and BAK) was studied upon treatment with the BH3-mimetics ABT-199 (A; RIVA, 3 nM; U2932, 10 nM), A1331852 (B, RCK8, 3 nM; SUDHL8, 10 nM) or S63845 (C; SUDHL10, 100 nM; U2946, 300 nM) for 4h. In order to exclude downstream caspase-mediated effects on protein expression, the broad range caspase inhibitor zVAD.fmk was added to the cells. Input lanes show the presence of overall protein in the lysate, and IP lanes show interaction with BCL-2, BCL-X_L or MCL-1. Protein G beads without primary antibody were used to control for unspecific binding. Staining with BCL-2, BCL-X_L, MCL-1 and GAPDH was performed to demonstrate efficient immunoprecipitation and equal protein loading, respectively. Representative Western blots of 2-5 independent experiments are shown.

Figure 5 BH3-mimetic induced cell death is partially dependent on BIM

A-C) Depletion of BIM was achieved using a combination of two distinct siRNA oligonucleotides (siBIM#1 and siBIM#2). Data on individual BIM siRNAs are provided in Supplementary Figure 6. Upon transfection, cells were treated with indicated concentrations

of ABT-199 (A) in RIVA or U2932 cells, upon treatment with A1331852 (B) in RCK8 or SUDHL8 cells, or upon treatment with S63845 (C) in SUDHL10 or U2946 for 4 or 6h and analysis of PS-exposure by staining with AnnexinV-FITC and flow cytometry. Non-targeting siRNA (siCtrl) was used as control. Mean and S.D. are shown (n=3-4). D). Knockdown efficiency was controlled by Western blotting at 48h after transfection. *p< 0.05;**p< 0.01; ***p< 0.001.

Figure 6 BH3-mimetic induced cell death is mediated by BAX

A-D) Knockdown of BAX using siRNA mediated gene silencing was performed before treatment with ABT-199 (A) in RIVA (3 nM) or U2932 (10 nM) cells, upon treatment with A1331852 (B) in RCK8 (3 nM) or SUDHL8 (10 nM) cells, or upon treatment with S63845 (C) in SUDHL10 (100 nM) or U2946 (300 nM) cells for 4h and analysis of PS-exposure by staining with AnnexinV-FITC and flow cytometry. Untransfected cells and non-targeting siRNA (siCtrl) were used as controls. Mean and S.D. are shown (n=3-4). D) Knockdown efficiency was assessed by Western blotting. E) Knockdown of BAX with siRNA constructs #1 and #3 combined was followed by treatment with ABT-199 in RIVA (10 nM) or U2932 (30 nM) cells for 4h and analysis of BAK activation by flow cytometry. Mean and S.D. are shown (n=3 for RIVA and n=2 for U2932). F) Interaction between BAK and BAX was assessed by immunoprecipitation (IP) in RIVA or U2932 with or without treatment with ABT-199 (-;+). Input lanes show the presence of overall protein in the lysate, and IP lanes show interaction between BAX and BAK upon treatment with ABT-199. Protein G beads without primary antibody were used to control for unspecific binding. * indicates IgG band. GAPDH was used as loading control. *p< 0.05;**p< 0.01; ***p< 0.001.

Figure 7 S63845 induced apoptosis is mainly independent of BAK

A) Deletion of BAK was performed in U2946 using CRISPR/Cas9. Cells were transduced with pLentiCRISPRv2 either carrying non-human target (NHT) control gRNAs or BAK gRNAs (BAK) followed by selection of stable clones with BAK deletion. NHT or BAK-deleted clones were exposed to different concentrations of S63845 for 4h before analysis of PS-exposure by staining with AnnexinV-FITC and flow cytometry. Mean and S.D. are shown (n=3). B-C) To achieve efficient knockdown, silencing of BAX was performed in U2946 NHT control or BAK-deleted cells (clone 12) using siRNA#1 and #3 combined. B) Knockdown of BAX and genetic deletion of BAK was confirmed by Western blotting. C) Cells were exposed to different concentrations of S63845 for 4h before analysis of PS-exposure by staining with AnnexinV-FITC and flow cytometry. Mean and S.D. are shown (n=4). D) NHT or BAK-deleted cells were treated with 100 nM S63845 for 4h before analysis of BAX activation using intracellular staining with an active conformation specific BAX antibody and flow cytometry. Mean and S.D. are shown (n=3). E-F) Silencing of BIM using siRNA was performed in U2946 NHT control or BAK-deleted cells (clone 12). E) Knockdown of BIM was confirmed by Western blotting. F) Cells were exposed to different concentrations of S63845 for 4h before analysis of PS-exposure by staining with AnnexinV-FITC and flow cytometry. Mean and S.D. are shown (n=4). G-H) Silencing of NOXA using siRNA was performed in U2946 NHT control or BAK-deleted cells (clone 12). G) Knockdown of NOXA was confirmed by Western blotting. H) Cells were exposed to different concentrations of S63845 for 4h before analysis of PS-exposure by staining with AnnexinV-FITC and flow cytometry. Mean and S.D. are shown (n=4). I) NHT or BAK-deleted clones were exposed to S63845 (100 nM) for 4h before lysis in CHAPS-containing buffer and immunoprecipitation (IP) of MCL-1. Interaction with NOXA is shown by Western blotting. Input lanes show the presence of overall protein in the lysate, and IP lanes show interaction with MCL-1. Protein G beads without primary antibody were used to control for unspecific binding. Representative Blot of two independent experiments is shown. *p< 0.05;**p< 0.01; ***p< 0.001.

Figure 1

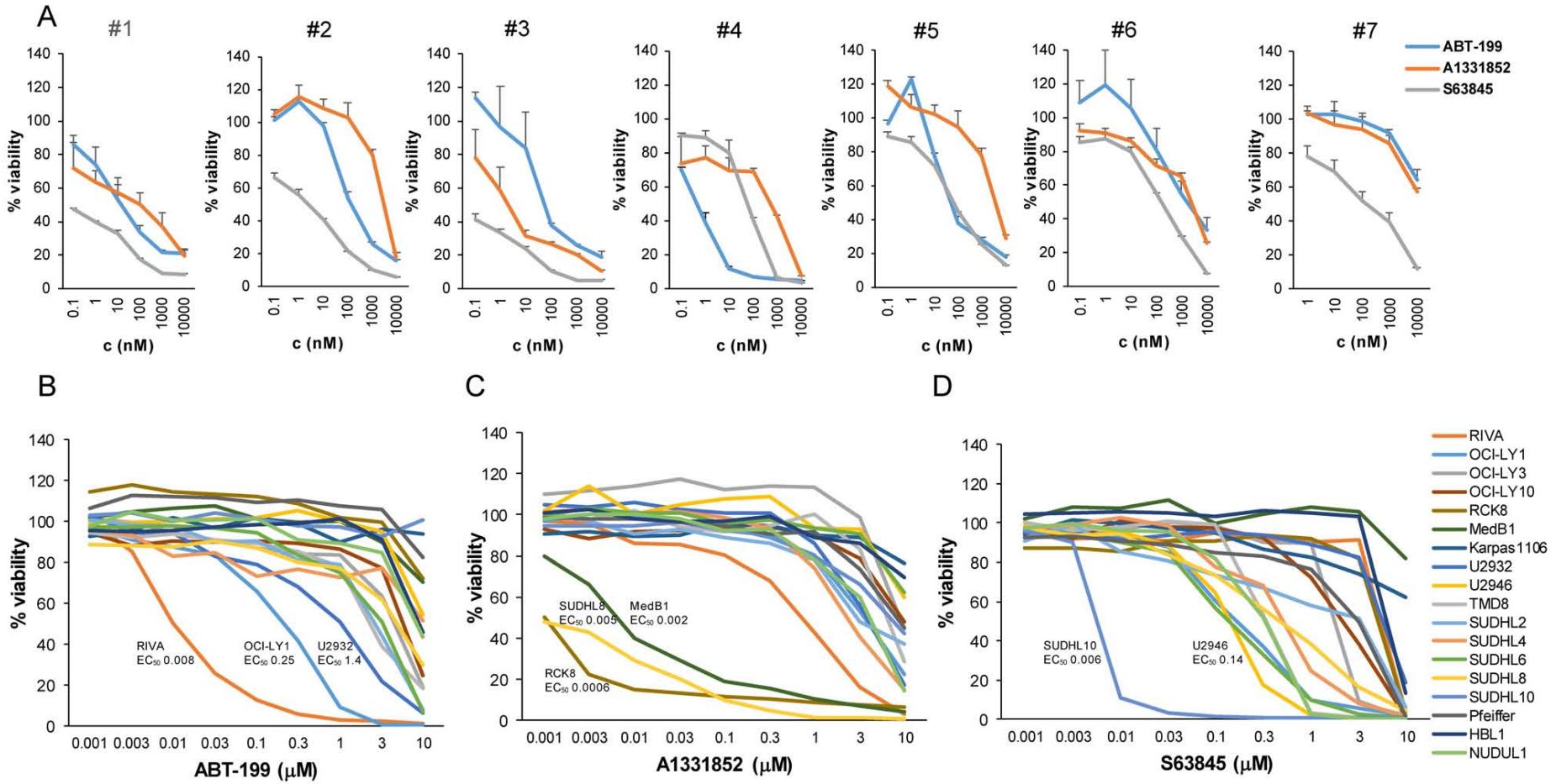
A
#1
#2
#3
#4
#5
#6
#7
% viability
c (nM)
ABT-199
A1331852
S63845
B
ABT-199 (μM)
RIVA EC50 0.008
OCI-LY1 EC50 0.25
U2932 EC50 1.4
C
A1331852 (μM)
SUDHL8 EC50 0.005
MedB1 EC50 0.002
RCK8 EC50 0.0006
D
S63845 (μM)
SUDHL10 EC50 0.006
U2946 EC50 0.14
RIVA
OCI-LY1
OCI-LY3
OCI-LY10
RCK8
MedB1
Karpas1106
U2932
U2946
TMD8
SUDHL2
SUDHL4
SUDHL6
SUDHL8
SUDHL10
Pfeiffer
HBL1
NUDUL1

Figure 2

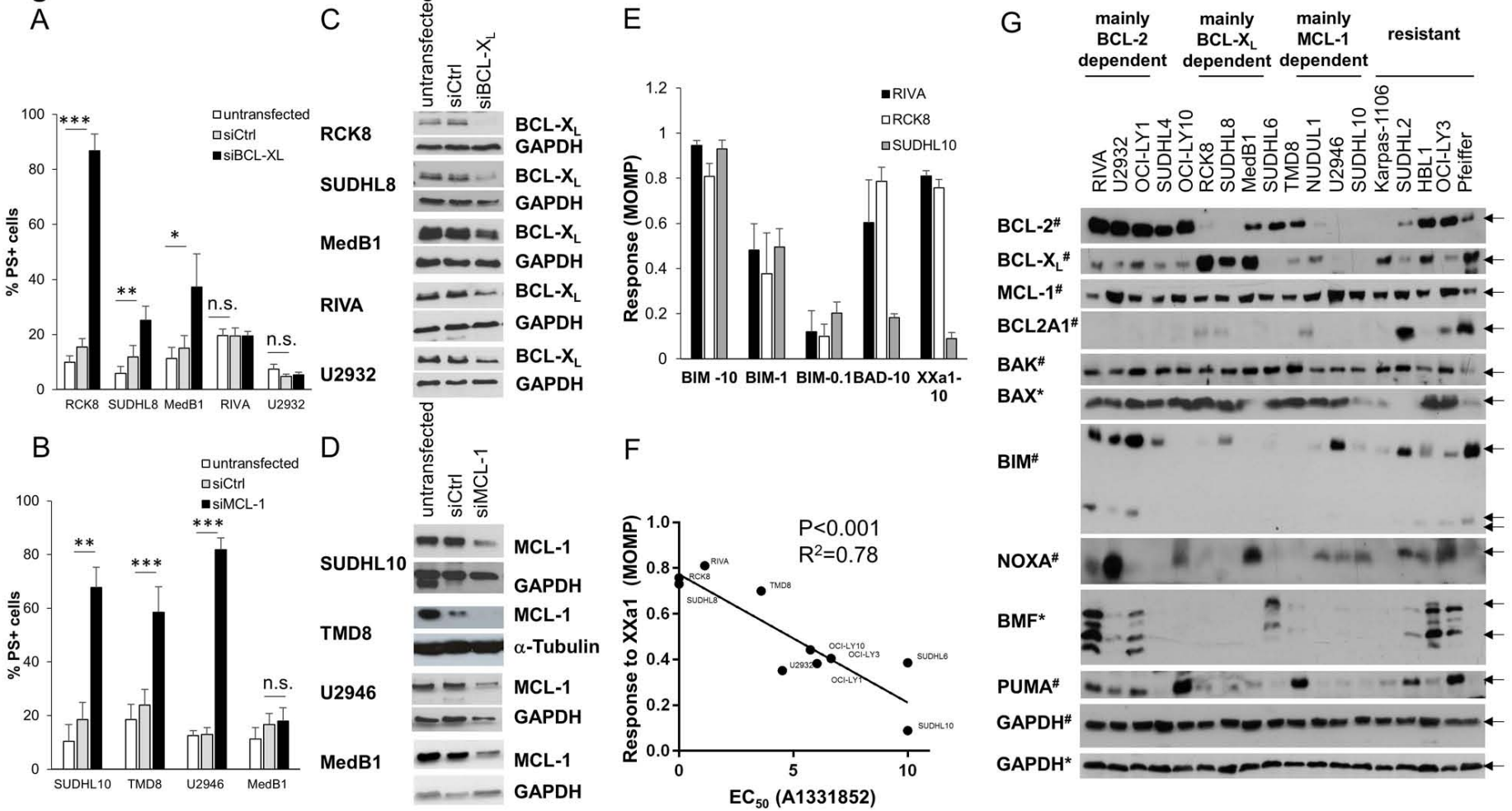
A
untransfected
siCtrl
siBCL-XL
% PS+ cells
RCK8
SUDHL8
MedB1
RIVA
U2932
***
**
*
n.s.
n.s.
B
untransfected
siCtrl
siMCL-1
% PS+ cells
SUDHL10
TMD8
U2946
MedB1
**
***
***
n.s.
C
untransfected
siCtrl
siBCL-XL
RCK8
SUDHL8
MedB1
RIVA
U2932
BCL-XL
GAPDH
D
untransfected
siCtrl
siMCL-1
SUDHL10
TMD8
U2946
MedB1
MCL-1
GAPDH
α-Tubulin
E
RIVA
RCK8
SUDHL10
Response (MOMP)
BIM -10
BIM-1
BIM-0.1
BAD-10
XXa1-10
F
P<0.001
R2=0.78
Response to XXa1 (MOMP)
EC50 (A1331852)
RIVA
RCK8
SUDHL8
TMD8
OCI-LY10
OCI-LY3
U2932
OCI-LY1
SUDHL6
SUDHL10
G
mainly BCL-2 dependent
mainly BCL-XL dependent
mainly MCL-1 dependent
resistant
RIVA
U2932
OCI-LY1
SUDHL4
OCI-LY10
RCK8
SUDHL8
MedB1
SUDHL6
TMD8
NUDUL1
U2946
SUDHL10
Karpas-1106
SUDHL2
HBL1
OCI-LY3
Pfeiffer
BCL-2#
BCL-XL#
MCL-1#
BCL2A1#
BAK#
BAX*
BIM#
NOXA#
BMF*
PUMA#
GAPDH#
GAPDH*

Figure 3

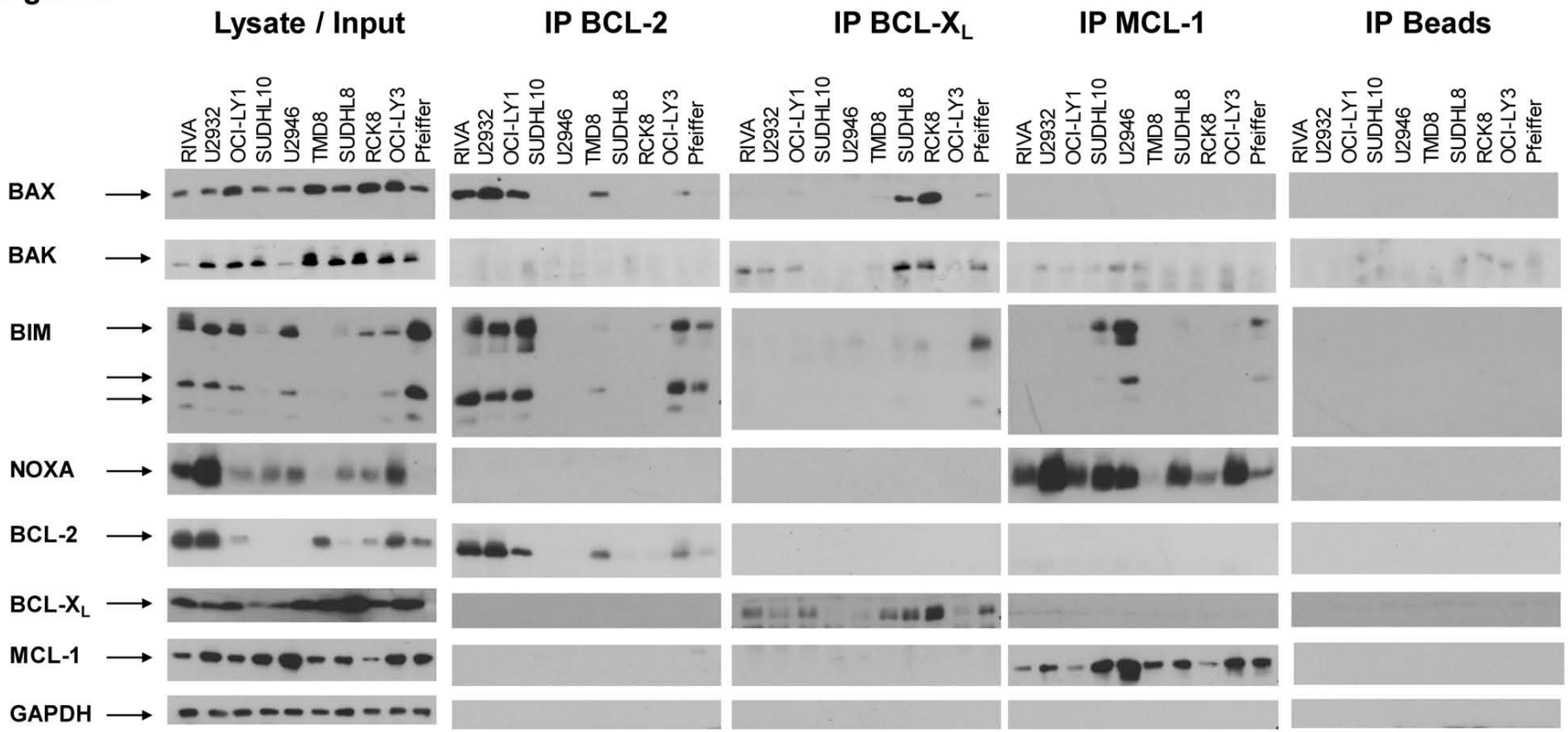
Lysate / Input
IP BCL-2
IP BCL-X$_L$
IP MCL-1
IP Beads
RIVA
U2932
OCI-LY1
SUDHL10
U2946
TMD8
SUDHL8
RCK8
OCI-LY3
Pfeiffer
BAX
BAK
BIM
NOXA
BCL-2
BCL-X$_L$
MCL-1
GAPDH

Figure 4

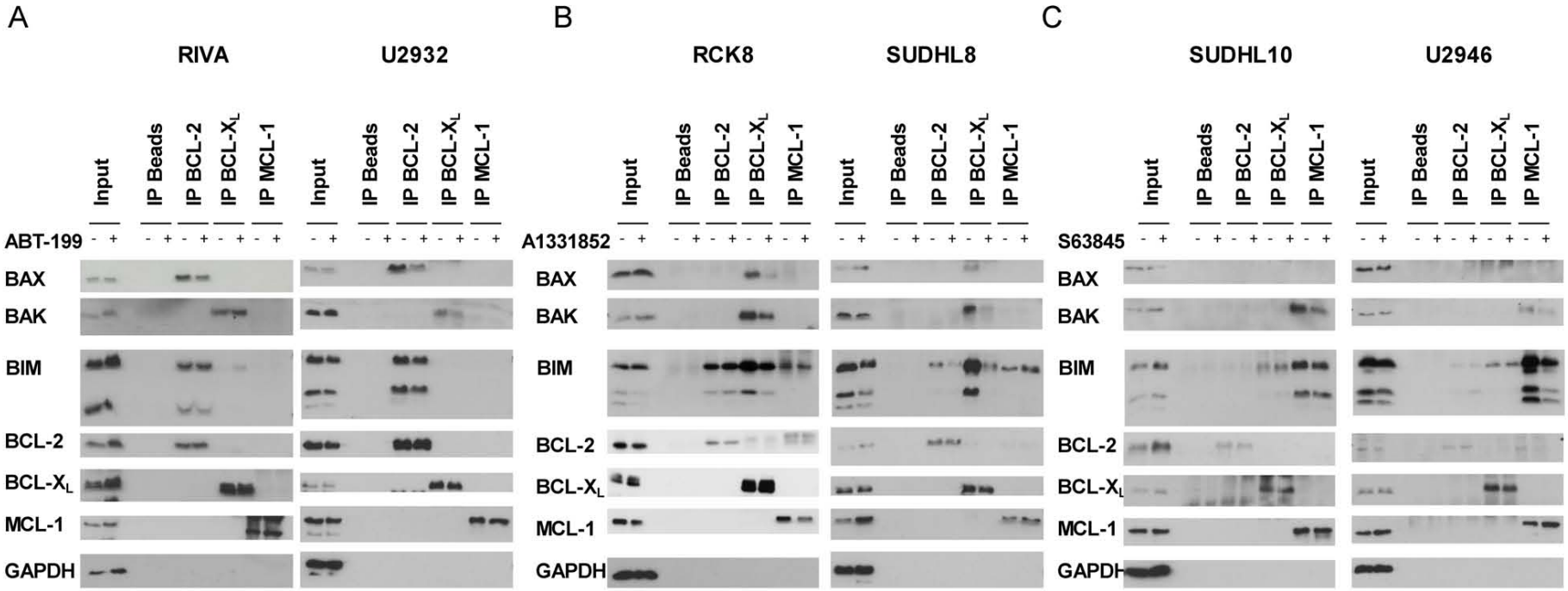
A
RIVA
U2932
B
RCK8
SUDHL8
C
SUDHL10
U2946
Input
IP Beads
IP BCL-2
IP BCL-XL
IP MCL-1
ABT-199
A1331852
S63845
BAX
BAK
BIM
BCL-2
BCL-XL
MCL-1
GAPDH

Figure 5

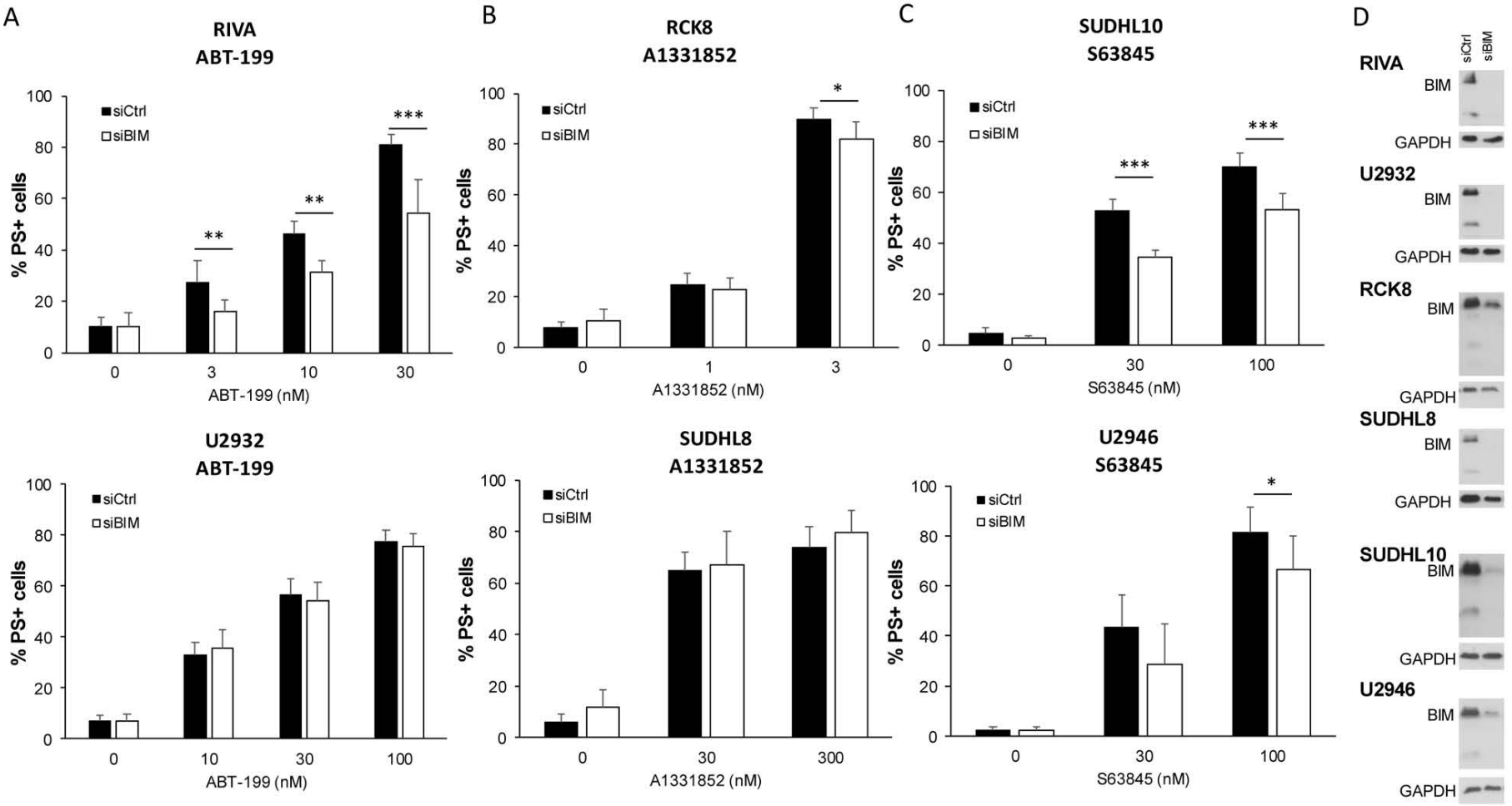
A
RIVA
ABT-199
siCtrl
siBIM
% PS+ cells
ABT-199 (nM)
U2932
ABT-199
B
RCK8
A1331852
A1331852 (nM)
SUDHL8
A1331852
C
SUDHL10
S63845
S63845 (nM)
U2946
S63845
D
siCtrl
siBIM
RIVA
BIM
GAPDH
U2932
RCK8
SUDHL8
SUDHL10
U2946

Figure 6

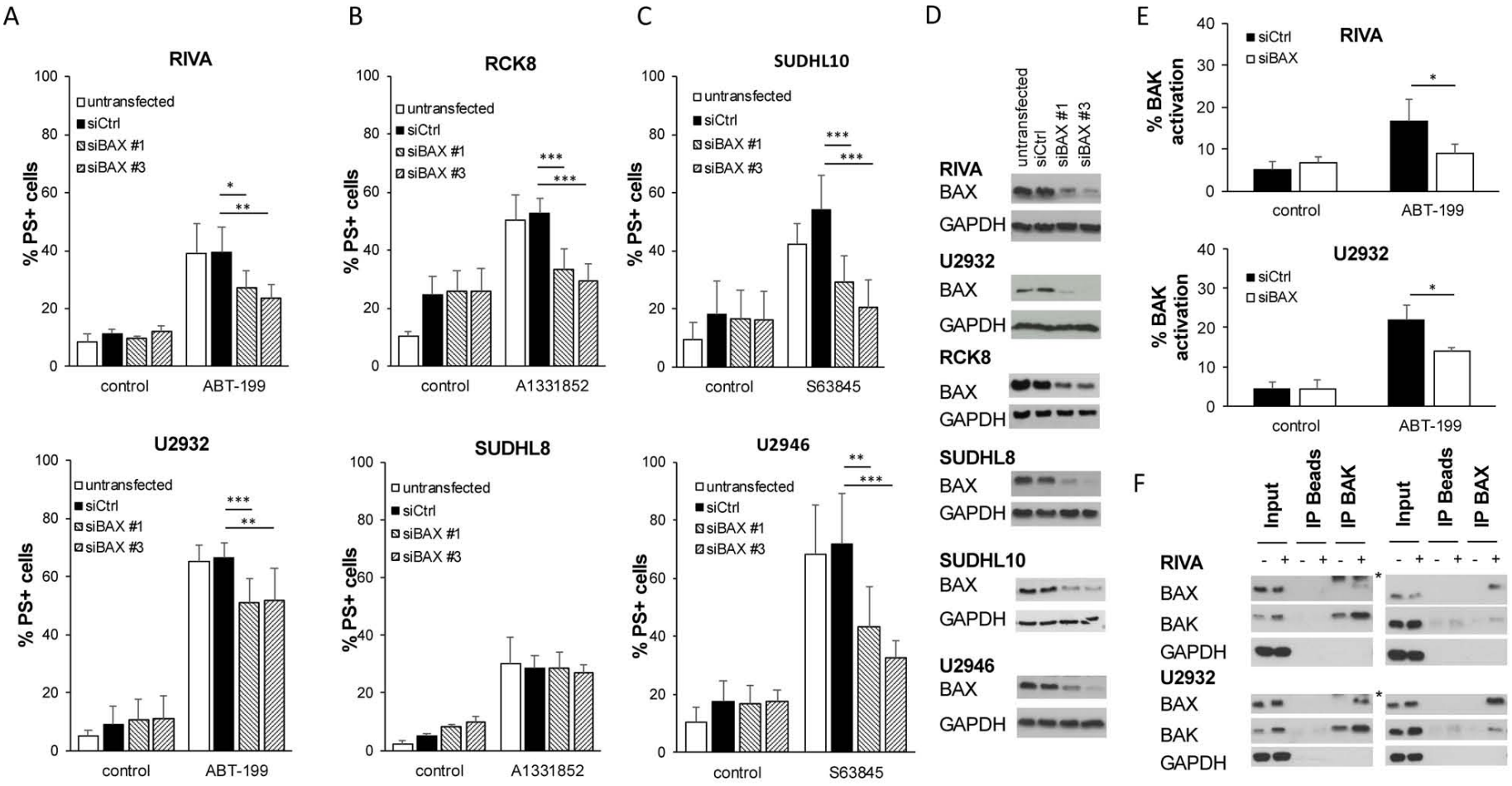
A
RIVA
U2932
B
RCK8
SUDHL8
C
SUDHL10
U2946
untransfected
siCtrl
siBAX #1
siBAX #3
% PS+ cells
control
ABT-199
A1331852
S63845
D
RIVA
BAX
GAPDH
U2932
RCK8
SUDHL8
SUDHL10
U2946
E
siCtrl
siBAX
% BAK activation
F
Input
IP Beads
IP BAK
IP BAX
BAK

Figure 7

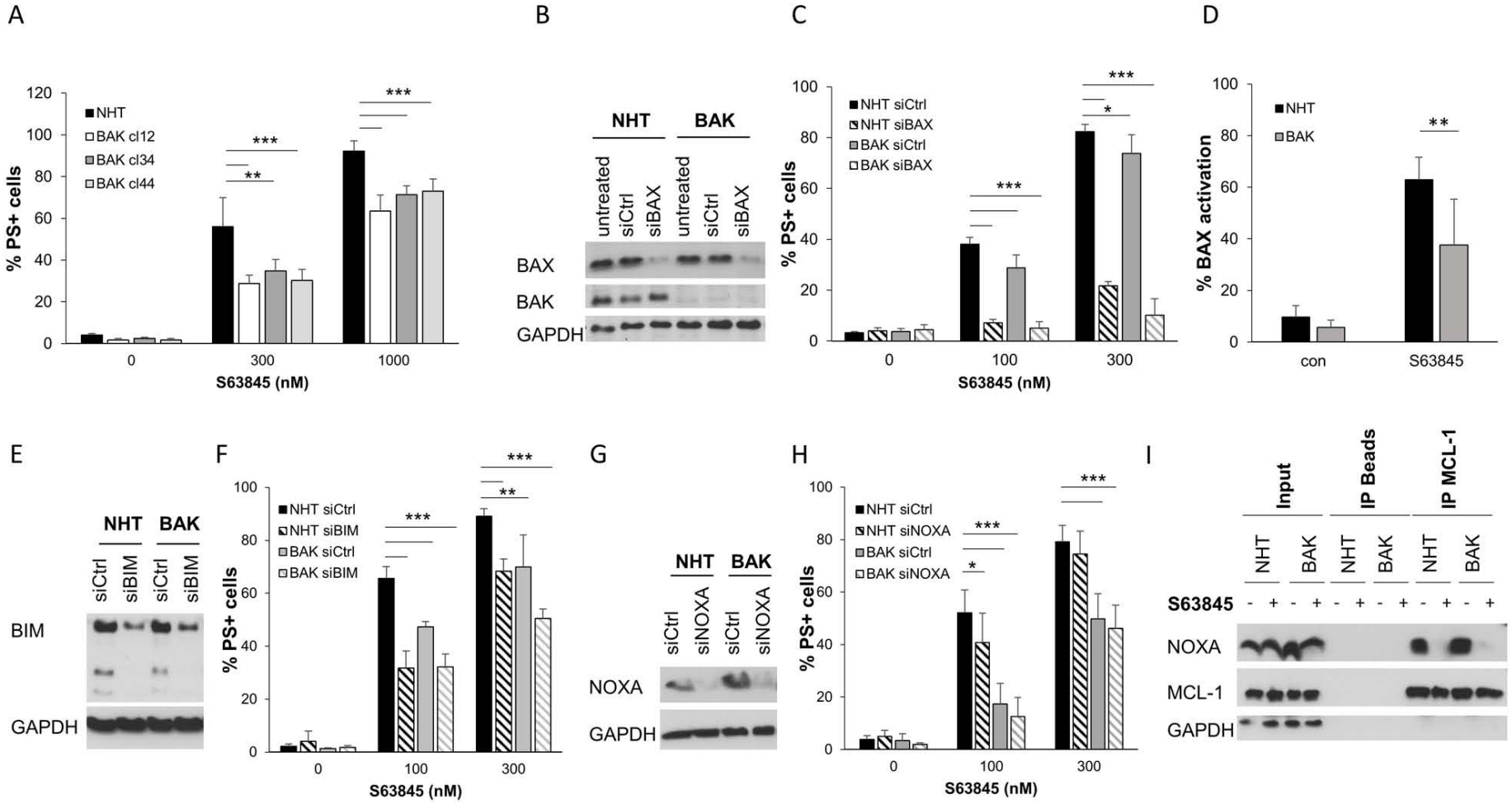
A
% PS+ cells
NHT
BAK cl12
BAK cl34
BAK cl44
S63845 (nM)
B
NHT
BAK
untreated
siCtrl
siBAX
BAX
BAK
GAPDH
C
% PS+ cells
NHT siCtrl
NHT siBAX
BAK siCtrl
BAK siBAX
S63845 (nM)
D
% BAX activation
NHT
BAK
con
S63845
E
NHT
BAK
siCtrl
siBIM
BIM
GAPDH
F
% PS+ cells
NHT siCtrl
NHT siBIM
BAK siCtrl
BAK siBIM
S63845 (nM)
G
NHT
BAK
siCtrl
siNOXA
NOXA
GAPDH
H
% PS+ cells
NHT siCtrl
NHT siNOXA
BAK siCtrl
BAK siNOXA
S63845 (nM)
I
Input
IP Beads
IP MCL-1
NHT
BAK
S63845
NOXA
MCL-1
GAPDH

Supplementary Methods

Immunoprecipitation and flow cytometry to detect active BAX and BAK

For analysis of BAX and BAK activation, immunoprecipitation was performed with antibodies (mouse anti-BAX clone 6A7, Sigma; mouse anti-BAK Ab-1, Calbiochem) that recognize an N-terminal epitope which is usually buried within the protein and only becomes accessible for antibody binding upon the conformational change associated with activation of BAX and BAK. CHAPS-containing lysates were incubated with 2 μl of antibody and 10 μl of anti-mouse IgG Dynabeads (Invitrogen) overnight before washing of the precipitate and analysis of bound proteins by Western blotting. To quantify the amount of cells with active BAX or BAK, cells were fixed in 2% paraformaldehyde followed by gentle permeabilization in 0.1% saponin and staining with mouse anti-BAX (BD Biosciences, Cat 610983) or mouse anti-BAK Ab-1. Staining was visualized by addition of anti-mouse-IgG-PE and flow cytometry.

Knockdown of BMF

For silencing of individual genes cells were electroporated using Neon transfection system (ThermoFisher) using two pulses of 20 ms at 1200 V. The following silencer select siRNAs (ThermoFisher) were used at 100 nM: BMF (#1 s40385, #2 s40386, #3 s40387).

TMRM staining

For analysis of mitochondrial membrane potential, cells were stained with 50 nM tetramethylrhodamine methyl ester (TMRM) for 10 min at 37°C before analysis by flow cytometry.

Statistical analysis

The half-maximal response (EC_{50}) to BH3-mimetics was calculated in GraphPad Prism using a sigmoidal dose response curve (unequal variance). Correlation analysis of drug or BH3-profiling responses and protein expression was done in GraphPad Prism using linear regression analysis. For statistical significance, student's t-test or One-way ANOVA was used.

Supplementary Figure Legends

Supplementary Figure 1. Response of DLBCL cells to BH3-mimetics

A-B) DLBCL cell lines were exposed to different concentrations of A1155463 (A) or A1210477 (B) before analysis of cell viability using CellTiterGlo at 72h. Data shown are mean and S.D. (n=4-6).

Supplementary Figure 2. Quantification of BCL-2 protein levels

A) Protein expression relative to GAPDH loading control was quantified using Licor Image Studio Lite from 5 independent Western blots. Heatmap was created using Microsoft Excel to visualize high (red) or low (green) protein expression. B) Genetic alterations of *BCL2* in this panel of DLBCL cell lines as outlined in Table 1 (mt) are associated with higher BCL-2 protein expression as compared to the expression in wildtype (wt) cells without genetic alteration of BCL-2. Scatter blot displays individual values and mean plus S.D. $*p < 0.05$. C) Genetic alterations of *BCL2* in this panel of DLBCL cell lines are not significantly associated with sensitivity to ABT-199. Scatter blot displays individual values and mean and S.D. (n.s.; not significant).

Supplementary Figure 3. Correlation of BCL-2 protein expression and response to BH3-mimetics

BCL-2 protein expression relative to GAPDH loading control was correlated with the EC_{50} values for ABT-199 (A), A1331852 (B) or S63845 (C). Sensitivity to ABT-199 correlated with expression of BCL-2 and the ratio of BCL-2 versus MCL-1 or combined BCL-X_L and MCL-1 expression. B) Sensitivity to A1331852 did not significantly correlate with the expression of BCL-X_L but the ratio of BCL-X_L versus combined BCL-2 and MCL-1 expression. C) Sensitivity to S63845 did not significantly correlate with the expression of MCL-1 but did inversely correlate with BCL-X_L expression or the ratio of MCL-1 to BIM expression (n.s.; not significant).

Supplementary Figure 4. Molecular mechanism of BH3-mimetic induced cell death

A) DLBCL cells were exposed to BH3-mimetics (RIVA: 3 nM ABT-199, RCK8: 3 nM A1331852, SUDHL10: 100 nM S63845) for 2, 4, or 8h before analysis of capase-3 cleavage by Western blotting. GAPDH was used as loading control. Representative Western blots of 3 independent experiments are shown. B) DLBCL cells were exposed to BH3-mimetics (RIVA: 3 nM ABT-199, RCK8: 3 nM A1331852, SUDHL10: 100 nM S63845) with or without the caspase inhibitor zVAD.fmk (50 μM) for 24h before analysis of apoptosis by staining with AnnexinV-FITC and flow cytometry. Mean and S.D. are shown (n=3). C) DLBCL cells were exposed to BH3-mimetics (RIVA: 3 nM ABT-199, RCK8: 3 nM A1331852, SUDHL10: 100 nM S63845) for the indicated time points before analysis of mitochondrial membrane potential using staining with TMRE and flow cytometry. Mean and S.D. are shown (n=3).

Supplementary Figure 5. BAX and BAK activation in DLBCL

A-C). BAX and BAK conformational change was detected upon treatment of cells with ABT-199 (A) in RIVA (3 nM) or U2932 (10 nM) cells, upon treatment with A1331852 (B) in RCK8 (3 nM) or SUDHL8 (10 nM) cells, or upon treatment with S63845 (C) in SUDHL10 (100 nM) or U2946 (300 nM) for 4h. Input lanes show presence of overall BAX and BAK in the CHAPS-containing lysates. Immunoprecipitation (IP) samples show the presence of conformationally active BAX or BAK, which was detected using IP with active conformation specific antibodies. D) Conformationally active BAK was assessed in untreated CHAPS-

containing lysates of 18 DLBCL cells lines. Input blot (lower panel) shows presence of overall BAK in the CHAPS lysates. BAK Immunoprecipitation (IP) blot (upper panel) shows the presence of conformationally active BAK, which was detected using IP with active conformation specific antibody. RIVA, U2932 and OCI-LY1 input lysate was loaded in the first three lanes as control on the BAK IP blot. GAPDH is shown as loading control.

Supplementary Figure 6. Silencing of BIM using distinct siRNA oligonucleotides has little effect on apoptosis

A-C) Depletion of BIM using three distinct siRNAs (#1,2,3) was performed before treatment with ABT-199 (A) in RIVA (3 nM) or U2932 (10 nM) cells, upon treatment with A1331852 (B) in RCK8 (3 nM) or SUDHL8 (10 nM) cells, or upon treatment with S63845 (C) in SUDHL10 (100 nM) or U2946 (300 nM) for 4h and analysis of PS-exposure by staining with AnnexinV-FITC and flow cytometry. Untransfected cells and non-targeting siRNA (siCtrl) were used as controls. Mean and S.D. are shown (n=3-4). *p< 0.05;**p< 0.01; ***p< 0.001. D). Knockdown efficiency was controlled by Western blotting at 48h after transfection.

Supplementary Figure 7. BMF does not play a role in ABT-199 induced cell death

A) Depletion of BMF using siRNA mediated gene silencing was performed in RIVA cells before treatment with 3 nM ABT-199 and analysis of PS-externalization. Mean and S.D. are shown (n=3). B) Knockdown efficiency was assessed by Western blotting. GAPDH is shown as loading control.

Supplementary Figure 8. Knockdown of BAK is only able to prevent ABT-199 induced apoptosis, but does not inhibit A1331852 or S63845 induced apoptosis.

A-D) Depletion of BAK using siRNA mediated gene silencing was performed before treatment with ABT-199 (A) in RIVA (3 nM) or U2932 (10 nM) cells, upon treatment with A1331852 (B) in RCK8 (3 nM) or SUDHL8 (10 nM) cells, or upon treatment with S63845 (C) in SUDHL10 (100 nM) or U2946 (300 nM) cells for 4h and analysis of PS-exposure by staining with AnnexinV-FITC and flow cytometry. Untransfected cells and non-targeting siRNA (siCtrl) were used as controls. Mean and S.D. are shown (n=3-4). *p< 0.05;**p< 0.01; ***p< 0.001. D) Knockdown efficiency was assessed by Western blotting. *p< 0.05;**p< 0.01; ***p< 0.001.

Supplementary Figure 9. Knockout of BAK using CRISPR/Cas9 has little effect on A1331852 induced apoptosis.

A) Deletion of BAK was performed in SUDHL8 using CRISPR/Cas9. Cells were transduced with pLentiCRISPRv2 either carrying non-human target (NHT) control gRNAs or BAK gRNAs (BAK) followed by selection of a stable clone with BAK deletion. Western blotting was performed to confirm deletion of BAK. B) NHT or BAK deleted cells were exposed to different concentrations of A1331852 for 4h before analysis of PS-exposure by staining with AnnexinV-FITC and flow cytometry. Mean and S.D. are shown (n=3).C) NHT or BAK deleted cells were treated with 100 nM A1331852 for 4h before analysis of BAX activation using intracellular staining with an active conformation specific BAX antibody and flow cytometry. Mean and S.D. are shown (n=3). *p< 0.05;**p< 0.01; ***p< 0.001.

Supplementary Figure 1

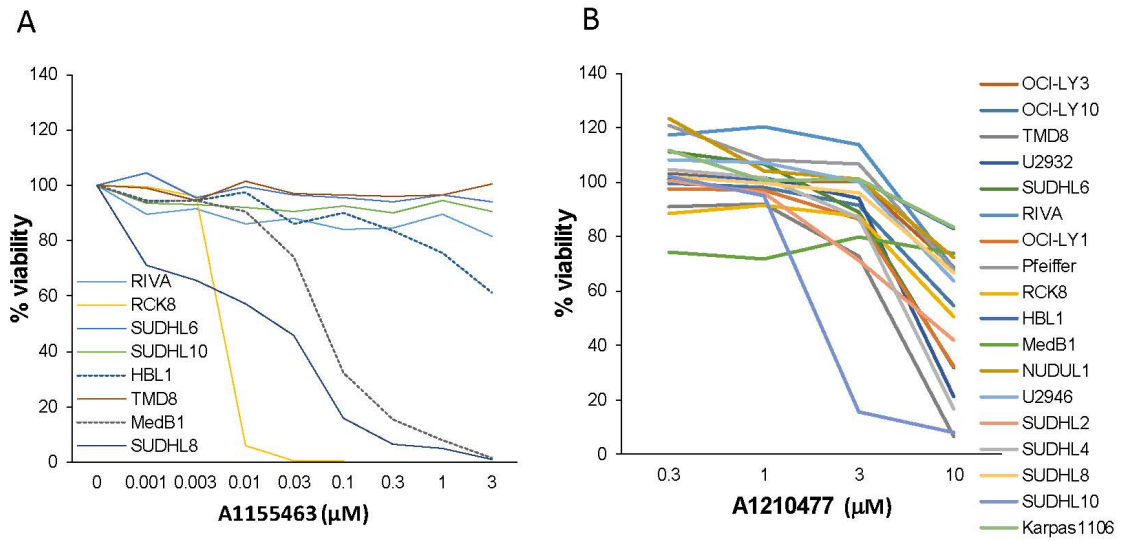

Supplementary Figure 2

A

	BCL-2	BCL-Xl	MCL-1	BCL2A1	BAX	BAK	BIM	NOXA	BMF	PUMA
RIVA	1,4	0,4	0,3	0,1	0,2	0,3	2,9	0,3	1,1	0,2
U2932	1,4	0,1	1,1	0,3	0,3	0,4	2,4	1,2	0,1	0,1
OCI-LY1	1,3	0,4	0,4	0,0	0,5	0,5	3,0	0,1	0,8	0,1
SUDHL4	0,7	0,2	0,2	0,1	0,3	0,3	1,5	0,1	0,0	0,0
OCI-LY10	0,9	0,1	0,5	0,4	0,8	0,4	0,1	0,5	0,0	0,5
RCK8	0,1	1,7	0,3	0,3	0,7	0,5	0,6	0,5	0,0	0,1
SUDHL8	0,0	1,1	0,3	0,0	0,3	0,3	1,9	0,1	0,0	0,0
MedB1	0,3	1,2	0,4	0,0	0,3	0,5	0,0	1,1	0,0	0,1
SUDHL6	0,8	0,0	0,6	0,2	0,5	0,6	0,7	0,3	0,5	0,0
TMD8	0,6	0,4	0,5	0,8	0,7	0,7	0,3	0,0	0,1	0,4
NUDUL1	0,1	0,4	0,6	0,0	0,4	0,3	0,8	0,3	0,0	0,0
U2946	0,0	0,1	1,4	0,1	0,4	0,3	2,6	0,5	0,0	0,0
SUDHL10	0,0	0,0	0,7	0,1	0,1	0,2	0,9	0,4	0,0	0,0
Karpas1106	0,0	0,7	0,6	0,4	0,4	0,6	1,2	0,0	0,0	0,0
SUDHL2	0,2	0,2	0,5	1,3	0,1	0,7	2,1	0,4	0,1	0,1
HBL1	0,7	0,7	0,3	0,2	0,5	0,3	2,0	0,3	0,8	0,0
OCI-LY3	1,0	0,4	1,0	0,9	0,6	0,7	2,5	0,5	0,6	0,4
Pfeiffer	0,2	0,8	0,5	1,0	0,2	0,3	3,5	0,0	0,0	0,1

B

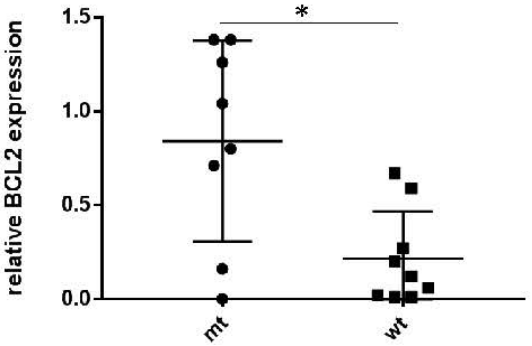

C

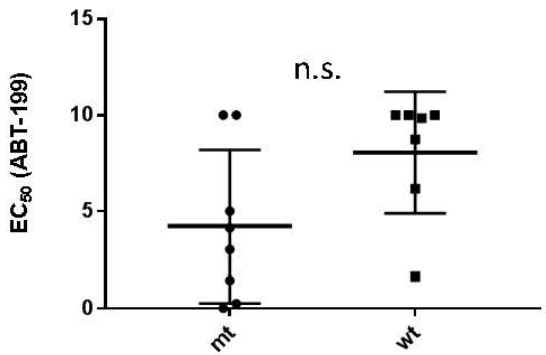

Supplementary Figure 3

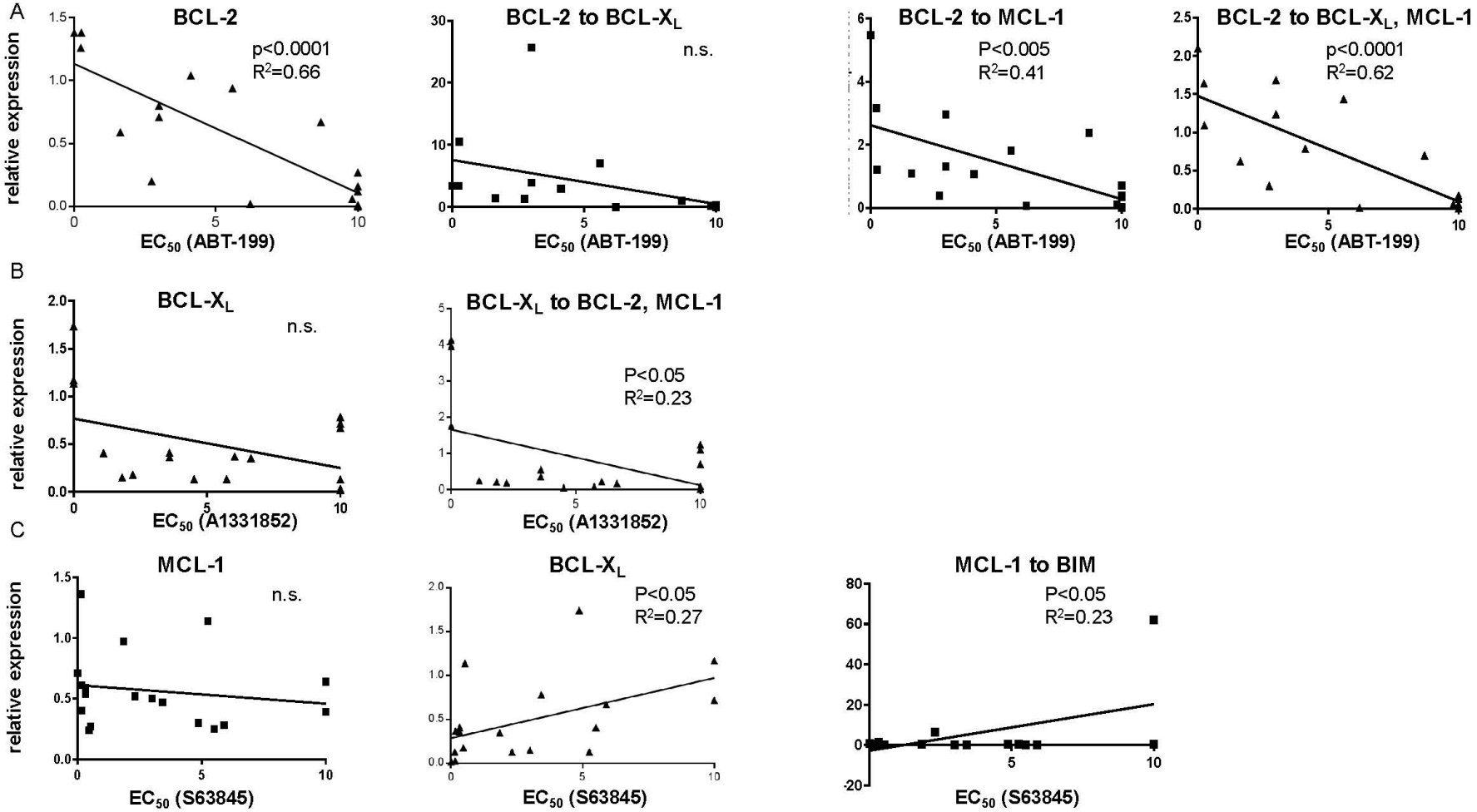

Supplementary Figure 4

A

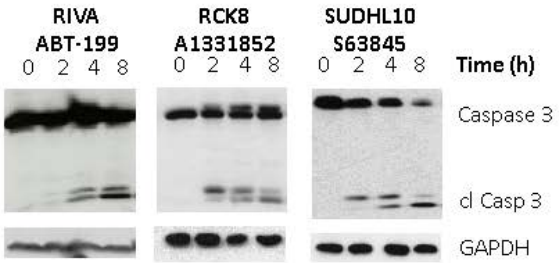

B

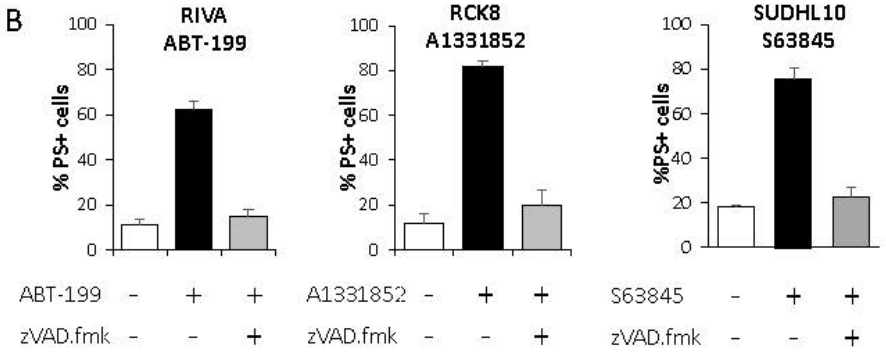

C

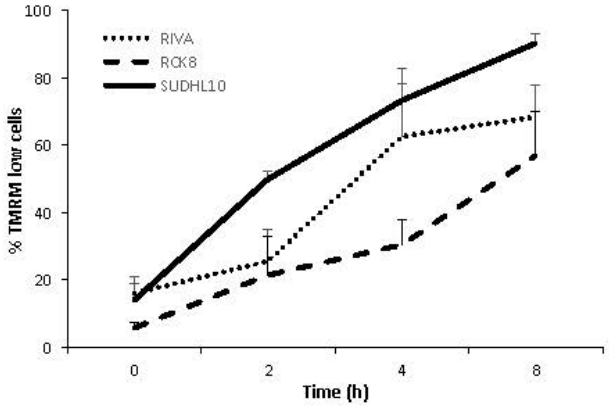

Supplementary Figure 5

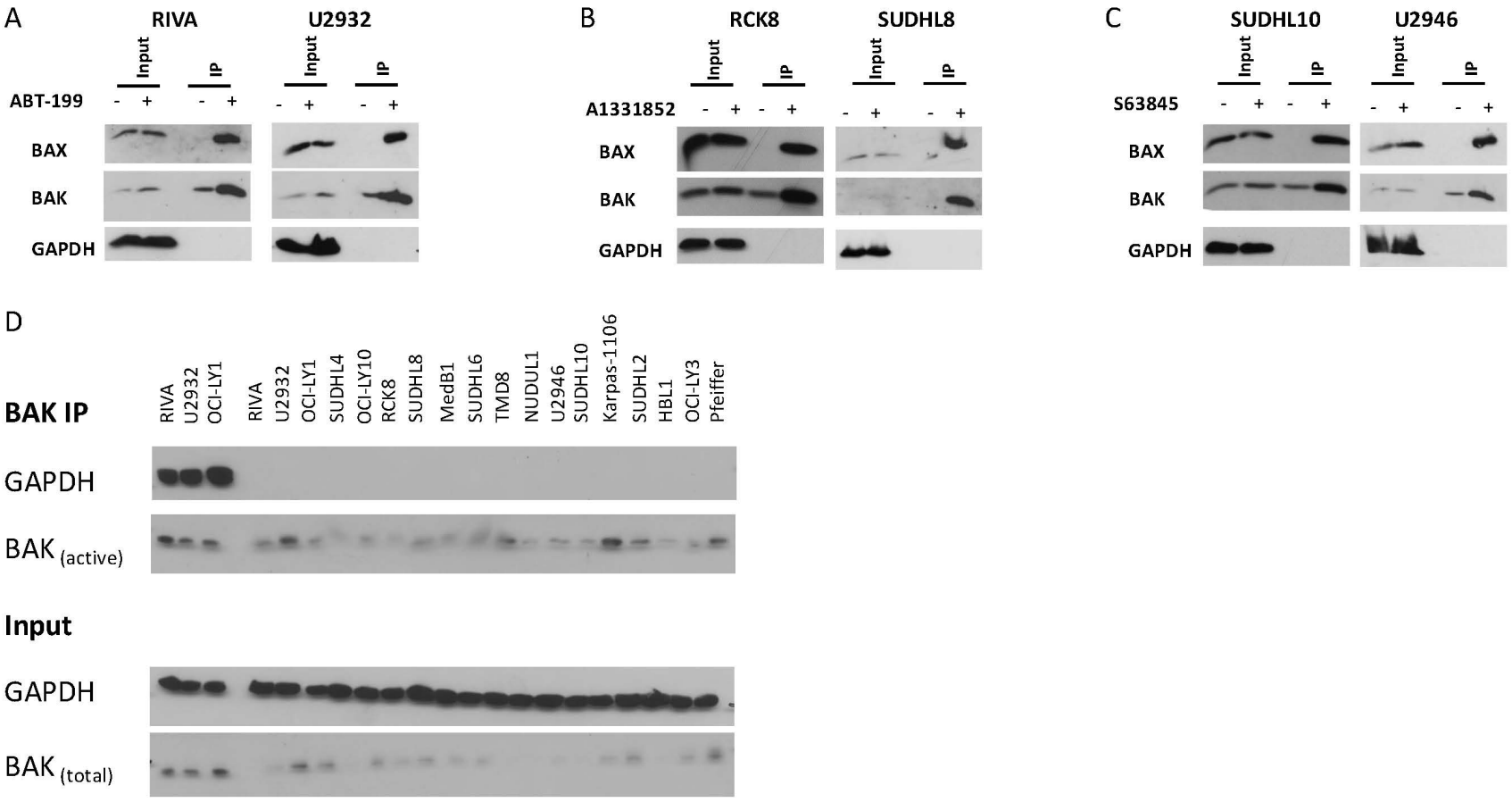

Supplementary Figure 6

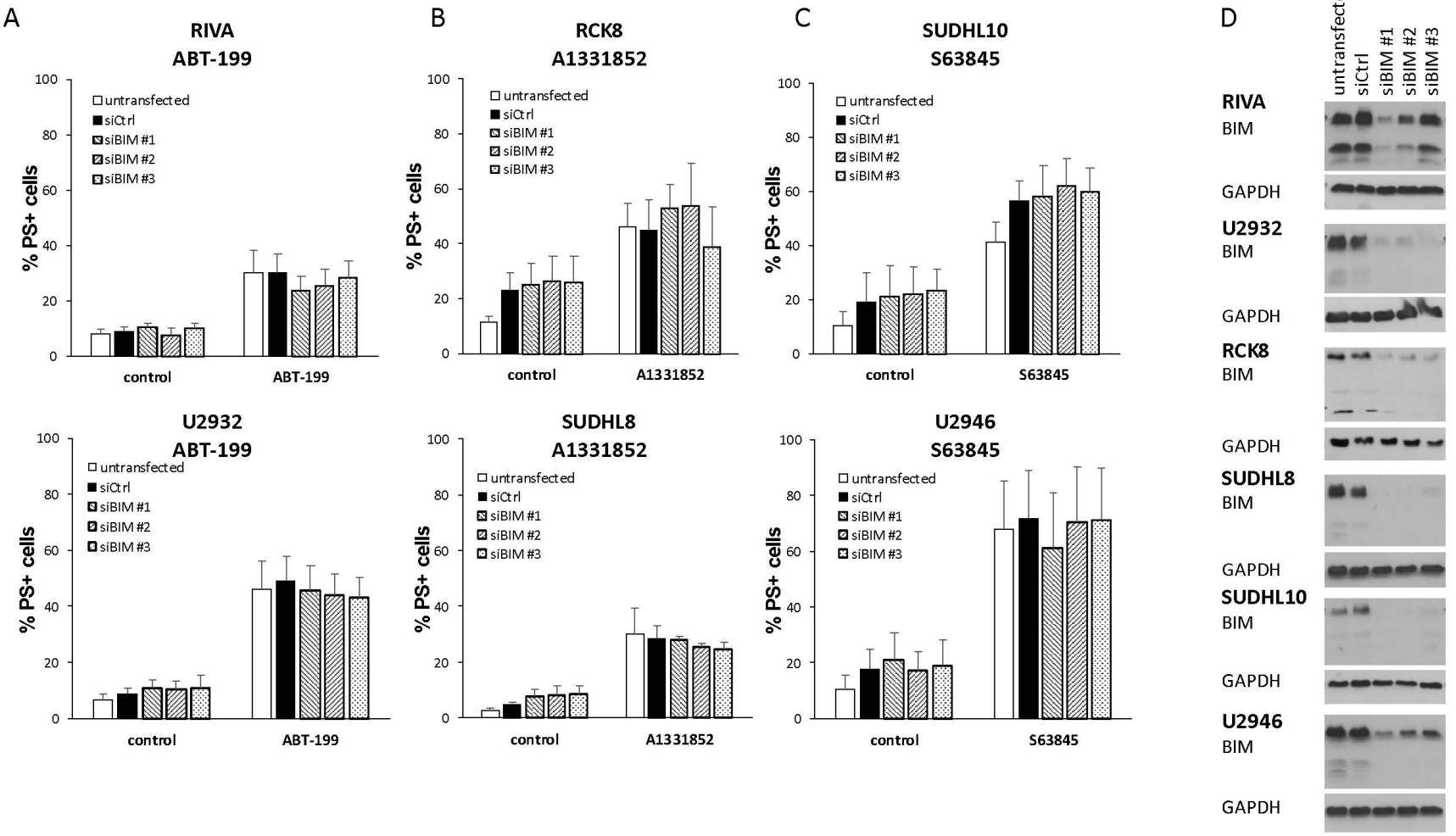

Supplementary Figure 7

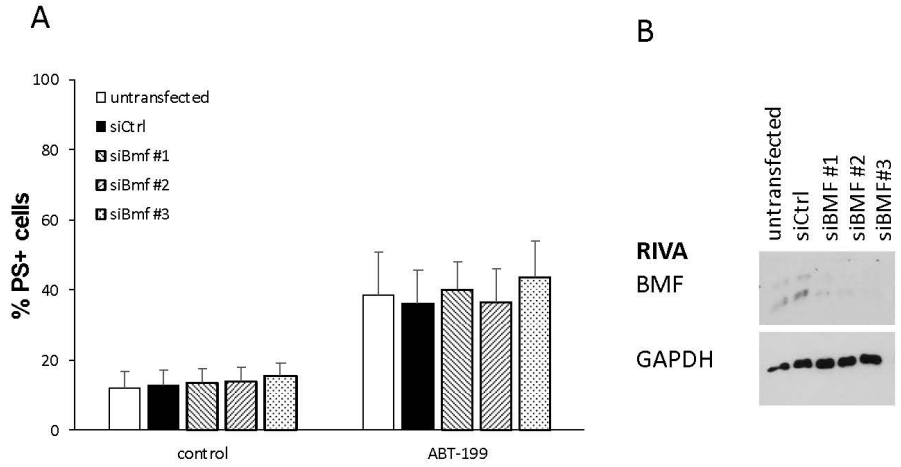

Supplementary Figure 8

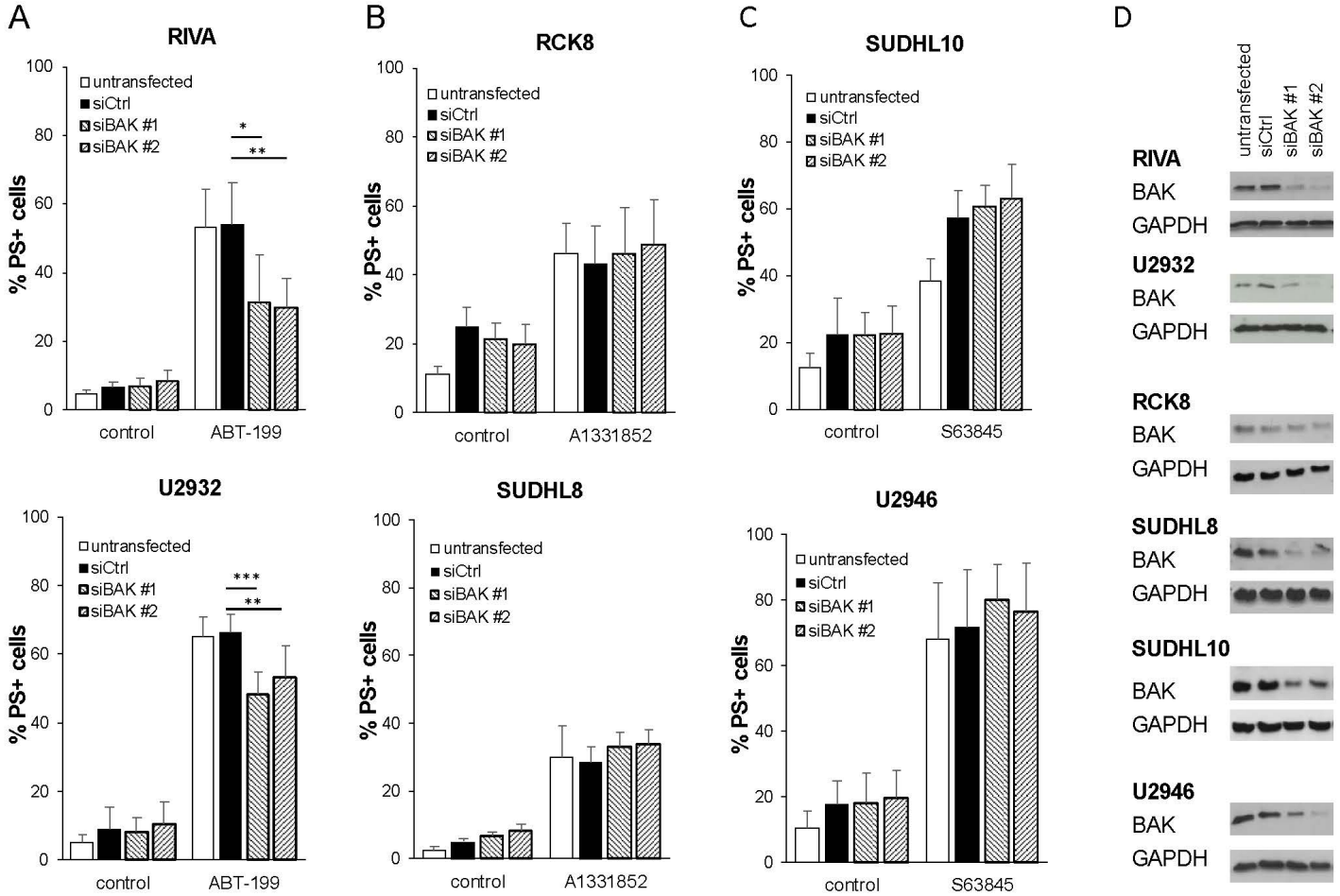

Supplementary Figure 9